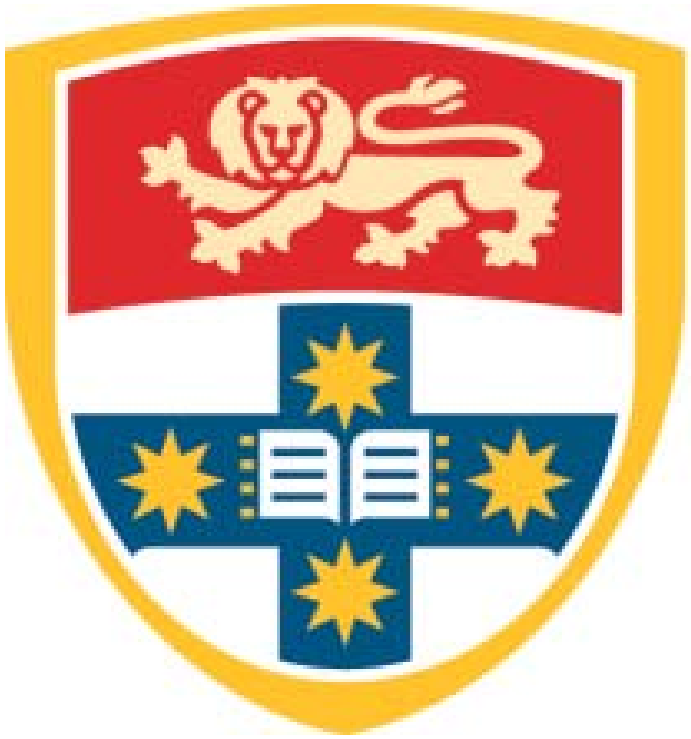

The effect of high-frequency, low-magnitude, mechanical stimuli on the rat condyle during mandibular protrusion.

A Micro-CT Study

Olivia Rogers BDSc Hons

A thesis submitted in partial fulfilment of the requirements for the Doctor of Clinical Dentistry in Orthodontics

Discipline of Orthodontics, Faculty of Dentistry

University of Sydney

Dedication

To my husband Craig for all of your love, support and encouragement.

To Coco Rogers for sitting next to me for every word of this thesis.

To my Mum, Anne and Dad, Frank for always picking up the phone.

To my sister Kirsten, a breath of fresh air.

To all my dear friends who went out of their way to make my life easier through this journey – you know who you are!

Here's to seeing things for what they are. After all, it is what it is.

Acknowledgements

Sincere gratitude is expressed to the following:

Professor M Ali Darendeliler, Head of Department, Discipline of Orthodontics, University of Sydney for his supervision and support throughout this thesis.

Professor William Walsh, Surgical & Orthopaedic Laboratories, Prince of Wales Hospital, for the collaboration and providing the facilities for the experimentation.

Associate Professor Allan Jones, Australian Centre for Microscopy and Microanalysis, University of Sydney, for his help with the micro-CT, VG Studio Max and CTAn and for his supervision and support with the project.

Dr Carmen Gonzales, Senior Lecturer, Discipline of Orthodontics, University of Sydney for her supervision of the project.

Dr Oyku Dalci, Lecturer, Discipline of Orthodontics, University of Sydney for her supervision of the project.

Dr Peter Petocz, Department of Mathematical Sciences, Macquarie University for his assistance with the statistical analysis.

Mr Dennis Dwarte, Australian Centre for Microscopy and Microanalysis, University of Sydney, for his help with the micro-CT and CTAn.

Mr John Rawlinson and Mr Greg Mitchell, Surgical & Orthopaedic Research laboratories, Prince of Wlaes Hospital for their assistance and support during the animal experimentation period.

Ms Marcel Dugo, St George Hospital animal facility for her help during the animal experimentation period.

To my colleagues, Drs Vanessa Jimenez, Angie Phelan and Tiffany Huang for their continuous support and friendship over the last three years.

To Drs Lam Cheng, Kerem Dalci, Ersan Karadeniz, Adrian Tan, Gosia Barley, Navin Michael Sequiera, Jude Aarthi Joseph Antoniraj and Wiraya Mongkolsawan who helped with various aspects of this work.

Declaration

CANDIDATE CERTIFICATION

This is to certify that the candidate carried out the work in this thesis in the Orthodontic Department at the University of Sydney, and this work has not been submitted to any other university or institution for a higher degree.

Contents

Dedication....2

Acknowledgements.... 3

Declaration....5

Table of Contents....6

Abbreviations....10

1 Introduction 14
2 Mandibular Growth 16
2.1 Prenatal Development of the Human Mandible....16
2.2 Postnatal Development of the Human Mandible....17
2.2.1 Mandibular Growth by Surface Remodelling....18
2.2.2 Mandibular Growth Rotations....19
2.2.3 Mandibular Condylar Cartilage....20
2.2.3.1 Histomorphology of the Mandibular Condylar Cartilage....22
2.2.3.2 Expression of Regulating Factors during Chondrogenesis....23
2.2.3.3 Osteogenesis....25
3 Class II malocclusion....26
3.1 Definition and Demographics....26
3.2 Class II Growth....26
3.3 Treatment Options for Class II Malocclusions....30
3.4 Functional Appliances....31
3.5 Functional Jaw Orthopaedics....33
3.5.1 Functional Appliance Studies in Animals....34
3.5.2 Functional Appliance Studies in Humans....44
3.5.3 Functional Jaw Orthopaedics in Adolescent Humans....54
3.5.3.1 Patient Factors....54
3.5.3.2 Treatment Factors....57
3.5.3.3 Stability of Orthopaedic Class II correction....57
4 Bone....58
4.1 Definition, Function and Categories....58
4.2 Cellular Composition of Bone....58
4.2.1 Osteoblasts....59
4.2.2 Bone Lining Cells....59
4.2.3 Osteocytes....60

4.2.4 Osteoclasts 60
4.2.5 Osteoblast – Osteoclast Interactions During Bone Remodelling 61
4.3 Extracellular Composition of Bone 61
4.3.1 Organic Bone Matrix 61
4.3.1.1 Collagen 61
4.3.1.2 Proteoglycans 62
4.3.1.3 Osteocalcin 62
4.3.1.4 Osteonectin 62
4.3.1.5 Osteopontin 62
4.3.2 Inorganic Bone Matrix 63
4.3.2.1 Mineralisation 63
4.4 Gross Bone Structure 63
4.4.1 Cortical Bone 63
4.4.2 Cancellous Bone 64
4.5 Microscopic Bone Structure 64
4.5.1 Woven Bone 64
4.5.2 Lamellar Bone 64
4.5.3 Periosteum 65
4.5.4 Endosteum 65
4.6 Osteogenesis 65
4.6.1 Endochondral Ossification 65
4.6.2 Intramembranous Ossification 66
4.7 Physical Properties of Bone 66
4.7.1 Stress 66
4.7.2 Strain 67
4.7.3 Anisotrophy 67
4.7.4 Viscoelasticity 67
4.8 Bone Modelling and Remodelling 67
4.8.1 Bone Modelling 67
4.8.2 Bone Remodelling 67
4.9 Structural Adaption of Bone 68
4.9.1 The Optimal Strain Environment 69
4.9.2 The Cellular Basis of Structural Bone Adaption 70
5 The Evolution of High-Frequency, Low-Magnitude Mechanical Stimulation as a Therapeutic Means 71

5.1 Mechanical Loading 72
5.1.1 Observational Studies 72
5.1.2 Experimental Studies 72
5.2 Studies on the Mechanical Milieu 74
5.2.1 Parameters of the Mechanical Milieu 75
5.2.1.1 Character of the Load 75
5.2.1.2 Strain Duration 76
5.2.1.3 Strain Magnitude 77
5.2.1.4 Strain Frequency 77
5.2.1.5 Strain History 78
6 High-frequency, Low-magnitude Mechanical Stimuli for Therapeutic Use 83
6.1 Whole Body Vibration 84
6.1.1 Development of the Whole Body Vibration Device 84
6.1.2 Transmissibility of Whole Body Vibration to the Skeleton 84
6.2 Whole Body Vibration and Bone 85
6.2.1 Disuse 85
6.2.2 Anabolism 86
6.2.3 Pathological States and Bone Healing 90
6.2.3.1 Children with Disabling Conditions 90
6.2.3.2 Young Women with Low Bone Mineral Density 90
6.2.3.3 Postmenopausal Osteoporosis 91
6.2.3.4 Bone Healing 92
6.3 Vibration and Cartilage 93
6.3.1 In Vitro Studies 93
6.3.2 In Vivo Study 95
6.4 Vibration in Dentistry and Orthodontics 95
6.4.1 Vibration and the Rate of Orthodontic Tooth Movement 95
6.4.2 Vibration and Pain Control 97
7 X-Ray Microtomography 97
7.1 Cartilage Imaging 99
7.2 X-Ray Microtomography of Bone 100
8 Conclusion 101
9 References 103
10 Manuscript 117
11 Abstract 118
12 Introduction 120
13 Aims and Objectives 121

14 Materials and Methods 122
14.1 Animal Grouping and Housing 122
14.2 Functional Appliance Placement 123
14.3 Vibration 124
14.4 Animal Monitoring 124
14.5 Study Design 125
14.6 Specimen Preparation 125
14.7 Specimen Imaging 126
14.8 Sample analysis 127
14.8.1 Qualitative Analysis of the Condyle 127
14.8.2 Quantitative Analysis of Mandibular Condylar Cartilage 127
14.8.3 Quantitative Bone Analysis: Bone Morphometry 128
14.9 Statistical Analysis 130
15 Results 131
15.1 Animal Weight 131
15.2 Quantitative Analysis 131
15.2.1 Changes in Total Cartilage Volume 132
15.2.2 Changes in Bone parameters 132
15.2.2.1 Bone Surface (BS) 133
15.2.2.2 Bone Surface to Bone Volume Ratio (BS/BV) 133
15.2.2.3 Bone Surface density (BS/TV) 134
15.2.2.4 Trabecular Bone Pattern Factor (Tb.Pf) 134
15.2.2.5 Structure Model Index (SMI) 135
15.2.2.6 Trabecular Thickness (Tb.Th) 135
15.2.2.7 Trabecular Number (Tb.N) 135
15.2.2.8 Trabecular Separation (Tb.Sp) 136
15.2.3 Qualitative Changes 136
15.2.3.1 Normal Growth 136
15.2.3.2 Vibration only 136
15.2.3.3 Functional appliance only 137
15.2.3.4 Functional appliance with vibration 137
16 Discussion 138
16.1 Study design 139
16.1.1 Animal Selection and Housing 139
16.1.2 Appliance Design 140
16.1.3 Vibration 141
16.1.4 Experimental Duration 142

16.2 Image analysis 143
16.2.1 Condylar Cartilage 143
16.2.2 Bone Morphometric Analysis 144
16.3 Results 144
16.3.1 Animal weights 144
16.3.2 Qualitative Analysis 145
16.3.3 Quantitative Analysis 148
16.3.3.1 Functional Appliance Only 149
16.3.3.2 Vibration Only 151
16.3.3.3 Functional Appliance with Vibration 152
17 Conclusions 155
18 References 157
19 Appendix One Literature Review 193
19.1 Appendix 1a 193
19.2 Appendix 1b 194
19.3 Appendix 1c 195
19.4 Appendix 1d 197
19.5 Appendix 1e 198
19.6 Appendix 1f 200
20 Appendix 2 Manuscript 208
20.1 Appendix 2a 208
20.2 Appendix 2b 208
20.3 209
20.4 209
20.5 209
20.6 Appendix 2c 209
20.7 Appendix 2d 209
20.8 210
20.9 Appendix 2e 210
20.10 210
20.11 Appendix 2f – description of box plot 211
21.1 Appendix References 212
21.2 Future Directions 214

Abbreviations

2D	Two dimensional
3D	Three dimensional
BFR	Bone forming rate
BMD	Bone mineral density
BMP	Bitemap
BS	Bone surface
BS/BV	Bone surface to bone volume ratio
BS/TV	Bone surface density
BV	Bone volume
BV/TV	Bone volume to tissue volume ratio
cAMP	Cyclic adenosine monophosphate
Cbfa	Core binding factor alpha
CCT	Controlled clinical trial
Co	Condylion
CRO	Condylar ramus occlusal angle
CS	Cervical Stage
CT	Computed tomography
CVM	Cervical vertebral maturation
DACM	Dentoalveolar compensatory mechanism
DNA	Deoxyribose nucleic acid
e.g.	For example
EMG	Electromyography
F	Female
FGF	Fibroblast Growth Factor
g	Grams; $9.8x10^{-2}$ gravity
Gd	Gadolinium
$GdCl_3$	Gadolinium chloride
Gd-DTPA^{2-}	Gadopentetate
Gn	Gnathion
HA	Hydroxyapatite
Hif-1	Hypoxia-inducible factor 1
Hz	Hertz
IGF	Insulin-like Growth Factor
Ihh	Indian hedgehog
Kg	Kilogram
kV	Kilo volts
M	Male
mA	Milliamps
Me	Menton
Micro-CT	Micro computed tomography
MRI	Magnetic Resonance Imaging
N	Newton
OPG	Osteoprotegrin
PCNA	Proliferating cell nuclear antigen
PCR	Polymerase chain reaction
PEMF	Pulsed electromagnetic fields
Pog	Pogonion

PTHrP	Parathyroid Hormone related Peptide
rAAV	Recombinant adeno-associated virus
rAAV-eGFP	Recombinant adeno-associated virus mediated enhanced green fluorescence protein
rAAV-VEGF	Recombinant adeno-associated virus mediated vascular endothelial growth factor
RANK	Receptor activator nuclear factor kappa receptor
RANKL	Receptor activator of nuclear factor kappa ligand
RCT	Randomised controlled trial
RT-PCR	Reverse transcriptase polymerase chain reaction
SMI	Structure model index
SNA	Sella-Nasion-APoint
SNB	Sella-Nasion-Bpoint
Tb.N	Trabecular number
Tb.Pf	Trabecular bone pattern factor
Tb.Sp	Trabecular separation
Tb.Th	Trabecular thickness
TGF	Transforming Growth Factor
TIFF	Tagged image file format
TMJ	Temporomandibular joint
TNF	Tumour necrosis factor
TRAP	Tartrate resistant acid phosphatase
TS	Tissue surface
TV	Tissue volume
VEGF	Vascular endothelial growth factor
Vib	Vibration
WBV	Whole body vibration
με	Micro strain

1 Introduction

Class II malocclusion is one of the most common orthodontic problems, occurring in about 20-30% of the population [1]. Dentally, a Class II malocclusion is defined as distal occlusion whereby the mandibular first molars occlude distal to the normal relationship with the maxillary first molars [2]. It is further divided into Class II Division 1, whereby the upper incisors are proclined, and Class II Division 2, whereby the upper incisors are retroclined [3]. Skeletally, the Class II pattern can manifest across a range of morphologies owing to maxillary and mandibular components, however it is more likely to arise from a retruded mandible [1]. The Class II malocclusion is believed to establish early [4,5] and is expected to worsen during the pubertal growth period due to increasing deficiency in mandibular length and ramus height at this time [6-8]. Therefore, without orthodontic intervention, the Class II malocclusion will not self correct. In growing Class II, mandibular retrognathic patients, mandibular growth modification is indicated and achieved with the use of functional appliances.

The aims of mandibular growth modification are to correct the Class II dental malocclusion and achieve an improvement in balance of the facial profile. The action of functional appliances is believed to be multifactorial, exerting effects in the mandible, maxilla and dentoalveolus [9]. The effect of functional appliances on the temporomandibular joint (TMJ) has been widely reported in the literature, however remains controversial.

The adaptive nature of the mandibular condylar cartilage is suggestive of its possible participation in achieving positive results in response to functional appliance treatment [10,11]. The mandibular condylar cartilage is a unique type of articular cartilage, able to respond and adapt to the external environment throughout life [11,12]. It is a secondary cartilage and is characterised by its unique histomorphology that typifies its function of chondrogenesis and endochondral ossification during normal growth and adaption.

Condylar and glenoid fossa adaption to mandibular protrusion has been reported in the literature since the early 1940's based on histological studies conducted on monkeys [13,14]. Subsequent to this, consistently similar reports have been made [15-20]. These studies observed that, in response to mandibular protrusion, growth of the condyle is redirected posteriorly, with the glenoid fossa relocating anteriorly, thereby contributing to the class II correction. Histological studies on rats [21] and monkeys [22] show that there is an initial increase in posterior condylar cartilage thickness, followed by thinning to baseline levels as endochondral ossification ensues . A similar temporal change in cartilage thickness has been observed in human studies investigating the effects of the Herbst appliance on the TMJ using magnetic resonance imaging (MRI) [23,24].

The use of high-frequency, low-magnitude mechanical stimuli for therapeutic purposes has evolved from a long history of studies investigating the relationship between bone and the external environment. The original concept of 'form follows function' was introduced by Wollf [25] however this did not explain the specific parameters of the osteogenic stimulus responsible for functional bone adaption. Extensive subsequent experimental investigations [26-28] found that the frequency of the applied load is important in functional bone adaption, such that, as the frequency of the applied load increased, the strain required to maintain bone was dramatically reduced. Fritton *et al.* [29] and Rubin *et al.* [30] have shown that loading frequency is also of prime importance in defining bone morphology in the natural state. Fritton *et al.* [29] showed that very small strains occur many times a day (hundreds of times in the order of 100με and thousands of times in the order of 10με), whereas peak strains occur only a few times per day. The continual barrage of high-frequency stimuli in the range of 20Hz to 40Hz that engender small but continual strains in bone are therefore considered important in the organisation of bone tissue. It was therefore concluded from these studies that extremely high frequencies, engendering extremely low strain magnitudes for a sufficient period of time may be used therapeutically to maintain bone or promote osteogenesis [26,30].

In order to administer high-frequency, low-magnitude stimuli to the skeleton, a whole body vibration (WBV) device was invented [31] and proven effective in transmitting the vibratory stimuli to the skeleton in humans [32]. This means of vibration has been shown to induce positive bone changes in small experimental animals [33-39]. Using whole body vibration, Sriram *et al.* found enhanced endochondral ossification in the condyles of adult mice through bone analysis with X-ray microtomography (micro-CT) and morphometry. Xiong *et al.* [40] also used micro-CT and bone morphometry to show new bone formation in the adult rat condyle in response to mechanical strain produced by mandibular advancement. The concomitant use of functional appliances and vibration had not been studied to date.

The following literature review aims to provide information on the history behind functional appliance treatment and the rationale for their use in orthodontics based on growth and the morphology of the Class II pattern. Controversies in the literature will be discussed as well as the history and rationale behind the use of high-frequency, low-magnitude mechanical stimuli for therapeutic purposes. The prospect of vibration enhancing the effect of the functional appliance has provided the motivation behind this investigation.

2 Mandibular Growth

2.1 Prenatal Development of the Human Mandible

The human mandible is a membranous bone that develops from condensations of fibrocellular covered cartilage on either side of Meckel's cartilage at 6 weeks in utero [41-43]. Such condensations develop on the right and left sides from the ear down toward the midline where they lie in close proximity separated by a thin region of mesenchyme. At week 7 in utero, intra-membranous ossification begins at an ossification centre from which ossification radiates anteriorly, superiorly and posteriorly to form the processes of the mandible namely the symphysis, coronoid process and

condyle respectively [42,43]. During the ossification process, the mandibular branch of the trigeminal nerve, lying in close association with Meckel's cartilage, is incorporated within the bone. By 10 weeks, a rudimentary mandible is seen and pre-natal mandibular growth thereafter depends on four secondary growth cartilages and muscular attachments[42,43].

The secondary cartilages of the mandible are the symphyseal, coronoid, gonial and condylar cartilages. During pre-natal week 12, the condylar cartilage forms as a mass on a large area of the mandibular ramus. After several weeks of rapid endochondral ossification, the condylar head forms and the condylar cartilage is limited to only a thin layer of over this area. This cartilage persists throughout life [42].

The coronoid cartilage appears at four months prenatal and disappears prior to birth[42].

The two symphyseal cartilages form in the connective tissue separating the two Meckel's cartilages but are independent of it. The symphyseal cartilages ceases to exist within the first year after birth[42].

Unlike other primitive vertebrates, the human mandible does not develop from Meckel's cartilage although has a close positional relationship to it [41-43]. Meckel's cartilage forms the scaffold upon which nerves, blood vessels and muscles are located and are incorporated from that location into the bone of the mandible[42,43]. Aside from forming the malleus of the inner ear and the sphenomandibular ligament, Meckel's cartilage is completely resorbed, a process beginning at 12 weeks in utero [41-43].

2.2 Postnatal Development of the Human Mandible

The mandible grows in three planes of space, transversely, sagitally and vertically, this being achieved by surface remodelling and endochondral ossification. The direction of mandibular growth is up and back in response to soft tissue pull from the front [41] such that the bone remodels and displaces in a downward and forward movement. The rate of growth of the mandible is constant

until puberty when ramal height increases on average 1-2mm per year and body length increases 2-3mm per year [41]. Bjork's longitudinal study of mandibular growth by the implant method revealed that the rate of condylar growth increases from on average 3mm per year during the juvenile period to 5mm per year during the pubertal period [44]. The timing, peak velocity and duration of peak condylar growth is variable amongst individuals [44] and generally occurs earlier in females than in males [41,44].

2.2.1 Mandibular Growth by Surface Remodelling

The mandible grows in part by surface remodelling via bone apposition and resorption [41]. This has been described qualitatively by Enlow and qualitatively by Bjork.

Enlow describes a unique pattern of surface remodelling called the V-Principle. Bones in the shape of a 'V' show simultaneous growth movement and enlargement in the direction of the wide part of the 'V', by apposition at the inner surface of and resorption along the outer surface of the bone [45]. Areas in the mandible exhibiting growth via the V-Principle contribute to its growth in all planes of space.

Enlow's qualitative histological studies show that the major sites of surface remodelling in the mandible occur at the mandibular ramus, condyle and coronoid process with less remodelling occurring at the chin [44,45]. Enlow reports a resorptive area at the reversal line of the chin where the concave curvature becomes convex. Contrary to this, Bjork's studies show that the chin is stable in most cases with apposition or resorption occurring in only a few cases [44].

Remodelling of the mandibular ramus is instrumental in positioning the lower dentition with the upper dentition and adapting to growth changes in the maxilla as they occur [45]. Deposition of bone along the posterior surface of the ramus accompanied by resorption along its anterior surface, relocate the entire ramus posteriorly, effectively lengthening the corpus of the mandible. Lengthening of the mandible is also achieved by deposition of bone at the lingual tuberosity -that is,

the junction between the ramus and corpus of the mandible and by surface remodelling in line with the V-Principle in the posterior direction at the coronoid process.

As the ramus relocates posteriorly, there is an increase in the transverse dimension of both the entire mandible and the coronoid process which takes place in accordance with the V-Principle [45].

Surface remodelling contributes to vertical mandibular growth via the V-Principle occurring at the condylar and coronoid processes [45].

Through the remodelling process, the ramus uprights to a more vertical orientation over the growth period [45].

The direction of condylar growth was documented quantitatively by Bjork using the implant method on a sample of 45 Danish boys [44]. Yearly radiographs were taken between the ages of 4 and 24 years and the first and last radiographs in the series were compared. The average direction of condylar growth with respect to posterior border of the ramus was negative 6, ranging from -26 to +16. The growth was not linear and individual variation was great and symmetrically distributed. On average, the condyle was at a mean tangent of 123 to the lower border of the mandible which was less than the first radiograph, in essence showing a decrease in the gonial angle with growth due to surface remodelling along the mandibular border.

2.2.2 Mandibular Growth Rotations

Early longitudinal cephalometric studies have documented the preservation of facial shape during growth [46,47]. Bjork [44] used tantalum pins in longitudinal radiographic studies to investigate the growth of the mandible. He found that the forward and downward displacement of the mandible had a component of rotation.

Strategic placement of four tantalum pin implants in the body of the mandible was used by Bjork [44] to create a stable landmark called the implant line which represented the core of the mandible.

Bjork observed that that the total rotation (the rotation of the stable implant line in the mandibular corpus relative to the cranial base) was greater than matrix rotation (the rotation of the mandibular plane relative to the cranial base) [48,49]. This evidenced that despite rotation of the core of the mandible, the facial pattern is predominantly preserved during growth due to considerable surface remodelling and condylar adaption taking place during the peak growth period [44,48].

Bjork [50] described mandibular rotation as either forward or backward with sub-types for both. A typical forward rotator has vertical condylar growth with a decreased gonial angle, marked by increased resorption at the mandibular angle and hence presents as a short face type. A typical backward rotator has sagittal condylar growth with an increased gonial angle marked by less resorption, and in some cases, even apposition at the mandibular angle, and therefore presents as a long face type [41,44,50].

Through mandibular growth rotations and surface remodelling, the mandible is able to interact favourably with the rest of the cranio-maxillary complex in order to achieve harmonious facial proportions [51]. The individual growth of the cranial base, middle cranial fossa, maxilla and mandible is matched with, and compensated for, by the growth of other structures. When skeletal compensations are inadequate, the dentoalveolar structures compensate in an attempt to maintain normal inter-arch dental relationships in the presence of disproportionate jaw relationships. This is called the dentoalveolar compensatory mechanism (DACM) [52]. Inadequate function of the DACM will manifest as a more severe malocclusion [52].

2.2.3 Mandibular Condylar Cartilage

The mandibular condylar cartilage is a type of articular cartilage that persists throughout postnatal life. Unlike other articular cartilages, the mandibular condylar cartilage has the unique ability to undergo both adaptive responses to external stimuli and endochondral ossification throughout life. This is of interest in the field of orthodontics in that it may form the basis of functional jaw

orthopaedics. In contrast, epiphyseal cartilages persist only until puberty at which time profound phenotypic changes occur during endochondral ossification [11].

According to Shen and Darendeliler [11], the mandibular condylar cartilage can be classified as a secondary cartilage based on the following reasons. Developmentally, the mandibular condylar cartilage occurs later in prenatal development than the primary cartilages and does not form from the mesenchymal blastema as primary cartilages do [12,53,54]. Anatomically, the primary cartilages are covered by a thin layer of periosteum in contrast to the mandibular condylar cartilage, which is covered by a mesenchymal cell layer continuous with the periosteum of the mandibular ramus reflective of its function [55]. Finally, growth of the primary cartilage, is controlled by systemic factors such as hormonal stimuli [12,42]. The mandibular condylar cartilage is only responsive to such systemic factors after their modulation by local growth factors and condylar remodelling can occur in response to external environmental stimuli both during and after natural growth [11,55].

The cartilage of the mandibular condyle is an important growth site, however it does not control mandibular growth as once thought [56]. Endochondral ossification is the growth process whereby formed cartilage is replaced by bone and involves the progression from chondrogenesis to osteogenesis [11,41]. There are two types of endochondral ossification, appositional and interstitial. Appositional endochondral ossification takes place in the mandibular condyle and does not involve mitosis of existing cartilage progenitor cells. Rather, the mode of growth involves addition of new cells to the cartilage from the exterior, through mitosis of undifferentiated mesenchymal cells. In response to signals controlling growth, mesenchymal cells in the articular layer duplicate and migrate into the cartilage where they differentiate into chondrocytes. In contrast, interstitial endochondral ossification in the primary cartilage starts with growth of cartilage cells within the central layer of the epiphyseal plate cartilage followed by normal mitosis [11].

The distinct histological arrangement of the cartilage typifies the process of appositional endochondral ossification, during condylar growth [11].

2.2.3.1 Histomorphology of the Mandibular Condylar Cartilage

The histomorphology of the mandibular condylar cartilage is unique and typifies the progression of chondrogenesis and mineralisation during condylar growth [11].The mandibular condylar cartilage is arranged in five distinct layers as summarised by Shen and Darendeliler [11]. (Appendix 1a)

1. Articular Zone. The condyle is covered by a dense layer of fibrous connective tissue that is continuous with periosteum of the mandibular ramus. A layer of mesenchymal cells is located beneath the superficial layer of fibroblasts and densely packed collagenous fibres.
2. Resting zone. This is the start of the condylar cartilage and consists of small immature chondrocytes with high mitotic potential reflected by a high nuclei- to- cytoplasmic ratio.
3. Proliferative Zone. This zone occupies large mature chondrocytes enclosed in lacunae in a random non-columnar arrangement. The mandibular condylar cartilage is structurally different from the primary cartilages showing an absence of ordered columns of chondrocytes that allows multi-directional growth.
4. Hypertrophic Zone. Highly mature chondrocytes amongst an intercellular matrix containing dense collagen fibres form this zone. While cells in this zone can still proliferate, chondrocytes with pyknotic appearances indicate the start chondrocyte degeneration. This is timely with the initiation of calcification in this zone. The chondrocytic lacunae increase in size.
5. Erosive Zone. Chondrogenesis ends and osteogenesis begins in this zone. The cartilage is directly adjacent to the connective tissue of the marrow cavity. Hydroxyapetite crystals deposit on cartilage spicules remnant from cell death and cartilage breakdown and blood vessel invasion is noted. The random arrangement of the bony trabeculae reflects new bone formation.

2.2.3.2 Expression of Regulating Factors during Chondrogenesis

Chondrogenesis is defined as a biological and biomolecular process in which chondrocytes undergo phenotypic and morphologic changes manifested histologically as progressive maturation. Chondrogenesis is highly regulated by the factors described below and can be represented diagrammatically as indicated in [57]. (Appendix 1b)

2.2.3.2.1 Sox 9

Sox9 is a transcription factor belonging to the Sry-related family of HMG- box DNA binding proteins and controls the differentiation of mesenchymal cells into immature chondrocytes [58,59]. Inactivation of Sox9 inhibits the differentiation process [60]. In addition, Sox9 directly activates gene expression for the synthesis of type II collagen [61], the main component of the condylar cartilage matrix required for cartilage synthesis and subsequent condylar growth [10]. Sox9 is thought to use a cAMP-response element binding protein as a co-activator to exert its effect [62]. Rabie *et al.*[57] noted the expression of Sox9 in the proliferative layer of chondrocytes in the condylar cartilage.

2.2.3.2.2 Fibroblast Growth Factor

Fibroblast growth factor (FGF-2) most likely targets mesenchymal cells and promotes their proliferation in the aim of stimulating and expanding the chondroprogenitor population [63]. Hiraki *et al.* [63] showed that local administration of FGF-2 into defective articular cartilage increased the proliferation of chondroprogenitor cells.

2.2.3.2.3 Insulin-like Growth Factor and Transforming Growth Factor

Insulin-like growth factor (IGF) and transforming growth factor (TGF) enhance chondrocyte proliferation. IGF I and II are important local factors involved in proliferation and differentiation of several tissues including cartilage [64] and have been located in rat articular cartilage [65]. IGF-I administration to the condylar cartilage in rats resulted in thickening of the cartilage at this site [66]. Wildemann *et al.* [67] showed that IGF-I and TGF-β1 delivered locally at fracture sites was followed by

more rapid appearance of cartilage and chondrocyte proliferation as indicated by cell proliferation markers. TGF-betas have been found to initiate intracellular signalling cascades leading to cartilage specific gene expression [68].

2.2.3.2.4 Proliferating Cell Nuclear Antigen

Proliferating cell nuclear antigen (PCNA) is an essential component for eukaryotic chromosomal DNA replication and is therefore used as a marker for cell proliferation. PCNA expression increases in condylar cartilage during chondrocyte proliferation and therefore is thought to have a regulatory role in mandibular condylar cartilage growth [69].

2.2.3.2.5 D-Type Cyclins

Several molecular cascades control the entry and progression of cells through the cell cycle during mitosis, and therefore play an important role in cell replication during chondrogenesis. For instance, D-type cyclins bind to and activate cyclin dependant kinases, which in turn activate the expression of S-phase genes, further committing the cell through the cell cycle [11].

2.2.3.2.6 Wnt

Certain analogues of Wnt co-ordinate chondrocyte proliferation and early differentiation by regulating the D-type cyclins as well as chondrocyte expression, while others impede differentiation[11]. Certain Wnt signalling molecules may also accelerate terminal chondrocyte differentiation [11].

2.2.3.2.7 Parathyroid Hormone Related Protein

The pace of chondrocyte maturation and differentiation in the condyle is controlled by parathyroid hormone related protein (PTHrP). Parathyroid hormone related protein slows down the rate at which proliferating chondrocytes further differentiate into hypertrophic inactive chondrocytes, thereby prolonging cartilage growth at point in the chondrogenesis pathway [11]. In the absence of PTHrP, premature maturation of the chondrocytes is seen [70].

2.2.3.2.8 Indian Hedgehog (Ihh)

Indian hedgehog (Ihh) is a mechanotransduction mediator that converts the mechanical stimuli into biochemical signals leading to chondrocyte proliferation in the condyle [71].

2.2.3.2.9 Core Binding Factor Alpha

Core binding factor alpha - 1, (Cbfa-1) is a transcription factor that regulates chondrocyte maturation and terminal differentiation in both embryonic and post-natal growth of the mandibular condyle [72]. In addition, it is involved in osteoblast differentiation by up-regulating all the major osteoblast specific genes [73] and also facilitates osteoblast invasion in endochondral ossification in the condyle [72]. Cbfa-1 is an essential factor for mediating VEGF functions during endochondral ossification [74]. Cbfa is therefore important in post-natal regulation of condylar growth by coupling the processes of chondrocyte maturation and degradation during endochondral bone formation [11]. Cbfa and RunX2 are interchangeable terms.

2.2.3.2.10 Vascular Endothelial Growth Factor

Vascular endothelial growth factor (VEGF) is a potent regulator of neovascularisation and is expressed in the condyle and glenoid fossa of growing rats [57]. Osteogenesis and angiogenesis are closely coupled, such that angiogenesis is essential for the replacement of cartilage by bone. During normal growth of the condyle in rats, the maximum level of VEGF precedes the maximum level of bone formation.

2.2.3.3 Osteogenesis

Osteogenesis is the terminal event of appositional endochondral ossification, occurring during growth of the mandibular condyle. The mature remaining chondrocytes produce alkaline phosphatase, a precursor to calcification. Calcification hinders the delivery of nutrients to the chondrocytes leading to cell death, breakdown of the matrix and therefore an increase in the lacunae size. This makes space for vascular invasion which carries osteogenic progenitor and bone

marrow stem cells to the site for osteogenesis [11]. Type X collagen has been used as a marker for endochondral ossification in the mandibular condyle. Hypertrophic chondrocytes express type X collagen just prior to the onset of endochondral ossification [21,57,75,76].

3 Class II malocclusion

3.1 Definition and Demographics

Class II malocclusion is one of the most common orthodontic problems and although is variable between race, occurs in about 20-30% of the population [1]. The aetiology of the Class II malocclusion is multifactorial and can be attributed to genetic, racial, environmental and functional causes [1,41]. Edward H. Angle was the first to describe malocclusion in 1899 and defined the Class II malocclusion as a distal occlusion whereby the mandibular first molars occlude distal to the normal relationship with the maxillary first molars [2]. He further differentiated the Class II malocclusion into Division 1, where the upper incisors are proclined and Division 2, where the upper incisors are retroclined [2]. This definition was an oversimplification of the Class II dentofacial pattern due to exclusion of the skeletal contribution to the dentofacial disharmony. Class II patterns can manifest across a range of morphologies owing to maxillary and mandibular dental and skeletal components. Skeletally, the Class II pattern is more likely to arise from a retruded mandible [77], although a protrusive maxilla or a combination of the two, may define the Class II morphology. Further, a more obtuse cranial base angle in Class II subjects (owing to a more posteriorly located glenoid fossa) also contributes to the Class II skeletal pattern [78].

3.2 Class II Growth

Broadbent in 1937 [46] followed by Brodie in 1941 [47], introduced the concept of 'the constancy of the facial pattern' during growth from birth to adulthood. Moore in 1959 [79] clarifies that this does not mean a proportionate enlargement with all skeletal points maintaining a constant relationship to

each other, but rather that the general conformation of the average face remains the same. A retrognathic face in childhood will be retrognathic in adulthood and a prognathic face in childhood will be prognathic in adulthood.

Several studies have compared the growth of Class II subjects with that of normal Class I subjects. An early study by Buschang *et al.* [80] reported less mandibular growth in 41 untreated female and 71 untreated male Class II Division 1 subjects, compared with Class I subjects from age 6-15 years. Since then, Baccetti and co-workers have conducted two key studies that have described in detail Class II growth at the circum-pubertal periods.

The first study by Baccetti *et al.* [4] compared the dentofacial pattern of 22 Class II patients in the deciduous dentition (characterised by a distal step, Class II canines and an increased overjet) with that of 20 Class I controls (characterised by a flush terminal plane, Class I canines and normal overbite and overjet) from the deciduous to the mixed dentition over a period of 2.5 years. Consistent with the findings of Bishara *et al* [5], Baccetti *et al.* found that Class II occlusal relations were maintained or worsened during the study. In addition, Baccetti *et al.* noted that the early presence of the Class II skeletal pattern indicated by a significantly retruded mandible and shorter mandibular length. Over the duration of the study, Baccetti *et al.* observed greater maxillary growth increments and smaller mandibular growth increments in the Class II subjects. This occurred together with greater downward and backward inclination of the condylar axis resulting in smaller decrements of the gonial angle. This indicated a posterior morphogenetic rotation of the condyle. In conclusion, the results indicate that the Class II dental and skeletal patterns are established early in life and are never self correcting in the transition from the deciduous to the mixed dentition.

In collaboration with Baccetti, Stahl *et al.* [6] examined the craniofacial growth of 17 Class II Division 1 male and female subjects, against 17 subjects with a Class I occlusion from pre-pubertal to post pubertal stages of development using the records from the University of Michigan Growth Study and

the Denver Growth Study. The cervical vertebral maturation (CVM) method [81] was used in this study. The CVM serves as a biological indicator of skeletal maturity by correlating the stage of mandibular growth with the maturation of the cervical vertebrae. Six clearly defined cervical vertebral maturation stages (CS1-CS6) correlating with a particular morphology of the cervical spine form the basis of this method, with the peak in mandibular growth occurring during cervical stages (CS) 3 and 4.The subjects in both groups were analysed longitudinally at six consecutive observations from CS1 to CS6. When compared to the controls, the untreated Class II Division 1 subjects showed significantly smaller increases in mandibular length at the pubertal growth spurt, that is, at CS3 and CS4, as well as during the entire observation period from CS1 to CS6. The deficiency of mandibular growth during the pubertal growth spurt was 2mm and the cumulative difference over the six stages was 2.9mm. In addition, the cranial base angle was found to be more obtuse in the Class II group thereby contributing to the Class II pattern. This remained constant over the pubertal growth period. The maxillary growth of the Class II subjects was essentially the same as the Class I subjects [6,82]. Based on these findings, Stahl *et al.* concluded that the Class II malocclusion is present early and without orthodontic treatment will worsen during the growth period due to increasing deficiency in mandibular length (2.9mm) and ramus height (1.5mm) [6].

These findings are consistent with Kerr and Hirst [7] and Ngan *et al.* [8] who also reported less mandibular growth in Class II subjects when compared to Class I subjects. Owing to differences in study design, the reported values of mandibular growth deficiency were variable, however all were statistically significant.

In contrast, Bishara *et al.* [83,84] reported no significant difference in mandibular growth trends between Class II and Class I subjects when studied longitudinally from age 5 to 12.2 years. Cross-sectional studies revealed that at earlier stages the mandibular length differed between Class I and Class II subjects, however the difference was not significant at later stages of development. Bishara

attributed this to 'catch-up' growth of the mandible. Stahl *et al.* [6] ascribe Bishara's conflicting results to i) the use of age rather than skeletal maturation as selection criteria such that that the pubertal growth spurt and therefore the completion of growth had not yet been reached during the observation period ii) the exclusion of severe Class II malocclusions from the study and iii) the use of articulare, a non-anatomical cephalometric landmark, to measure mandibular length.

More recently, Baccetti *et al.* [85] investigated the dentofacial changes in subjects with untreated Class II malocclusion from late puberty CS6, to young adulthood on average 3.5 years later. Twenty three Class II Division 1 subjects from the University of Michigan Growth Study and the Denver Growth Study were compared against Class I subjects from the same sources. It was found that there is no significant difference between Class I and Class II growth following late puberty into young adulthood. This plays an important role in conferring stability of Class II treatment following functional jaw orthopaedics.

Glenoid fossa displacement during childhood and adolescence in males and females has been evaluated by Buschang and Santos-Pinto [86]. Serial lateral cephalograms from the Human Growth Research Centre at the University of Montreal were used for the study. Cephalometric evaluation showed that relative to the cranial base reference structures, the glenoid fossa was displaced between 1.8 and 2.1mm posteriorly and between 1.0 and 1.8mm inferiorly. Prior to this, Bjork [87], in his study on the growth of the cranial base, found that growth at the spheno-occipital synchondrosis influences the backward and downward translation of the temporal bone and therefore the glenoid fossa, and that the distance between the glenoid fossa and nasion increases 7.5mm between 12 and 20 years of age.

Baccetti *et al.* [78] conducted a cephalometric study to analyse the position of the glenoid fossa in subjects with different sagittal skeletal facial patterns. One hundred and eighty subjects were divided equally into three groups according to their skeletal sagittal relationships. Cephalometric

comparisons of the three groups showed that the position of the temporomandibular joint was more posterior in skeletal Class II when compared with skeletal Class III In the vertical plane indicating a relationship between the position of the glenoid fossa and the type of malocclusion.

3.3 Treatment Options for Class II Malocclusions

Several treatment options exist for the treatment of Class II anomalies. Appropriate treatment selection is based on sound clinical and radiographic diagnosis, the type Class II morphological pattern and the stage of growth.

In the absence of skeletal disharmony, the Class II malocclusion can be treated by orthodontics alone, with or without extractions.

In the absence of growth, a mild skeletal Class II malocclusion can be camouflaged by extractions and orthodontics whereas the more severe skeletal discrepancies require a combined orthodontic-surgical approach. Growing patients with Class II skeletal patterns can be managed with orthopaedic treatment prescribed to suit the Class II dysplasia whether it be maxillary protrusion, mandibular retrusion or a combination of both [1]. Essentially, maxillary growth modification is achieved by the headgear appliance which applies heavy forces to the maxillary sutures changing the magnitude and direction of their growth, allowing catch-up growth of the mandible [41,88,89] This is therefore indicated in cases with maxillary protrusion. Where the Class II pattern is due to mandibular retrusion, mandibular growth modification is indicated and achieved with the use of functional appliances. In essence, functional appliances orthopaedically enhance mandibular growth and redirect maxillary growth, as well as induce dentoalveolar effects and eruption guidance favourable in Class II correction.

Several prospective and retrospective studies [90-93] have compared the dentoskeletal effects of headgear therapy with mandibular growth modification. These studies all showed that there is

slightly greater maxillary restriction in the headgear samples, and slightly greater mandibular growth or advancement with mandibular growth modification. In a more recent study, Baccetti *et al.* [94] compared the dental, skeletal and soft tissue effects of head gear and functional appliances by conducting a double blind study on 28 bonded Herbst patients and 28 headgear-full fixed appliance-Class II elastics patients. Distinguishing it from other studies, both groups were treated consecutively during the peak pubertal growth spurt and were compared against a matched sample of untreated Class II controls. Both treatment modalities were successful in achieving normal occlusal parameters. Greater dento-alveolar changes were observed in the headgear group due to the use of Class II elastics, as seen by upper incisor retroclination, lower incisor proclination and significant mesio-vertical movements of the lower molars. Both treatment modalities achieved a significant increase in mandibular length and about equal amounts of maxillary restriction. The differentiating observation between the two treatment regimens was a greater favourable change in the position of the soft tissue chin point, measured as the distance from soft tissue pogonion to nasion vertical in the functional appliance group. This was 2mm more anterior than in the headgear group and 2.5mm more anterior than the control group. The authors concluded that functional jaw orthopaedics is indicated as the preferred treatment modality during the pubertal growth spurt when mandibular retrusion is greater than 7mm behind nasion perpendicular [94] with a gonial angle less than 123^{o} [95].

3.4 Functional Appliances

Bishara [96] defines functional appliance as “an appliance that alters the arrangement of various muscle groups that influence the function and position of the mandible in order to transmit forces to the dentition and basal bone. These muscle forces are generated by altering the mandibular position sagitally and vertically resulting in orthodontic and orthopaedic changes.”

Functional appliances may be fixed (e.g. Herbst appliance) or removable (e.g. Twin Block); tissue borne, passive tooth borne or active tooth borne appliances [41].

The development of functional appliances began in Europe owing to their ease of use and the philosophy of providing limited treatment to high volumes of patients under the social welfare system. Functional appliances were introduced globally in the 1960's and were common place in orthodontic practice in both Europe and the United States of America by the 1970's [41].

The first functional appliance was introduced by Robin in 1902. His monobloc appliance was indicated to prevent glossoptosis in children with undersized mandibles. The activator however was better received and more widely used after its introduction by Adreassen in Norway in the 1920's [41]. The modified activator design that incorporated high pull headgear was named the Teusher appliance [97]. Several modifications to the design have been made such as, torquing spurs on the incisors to control root torque, Sved capping on the incisors to limit incisor tipping and expansion screws for maxillary transverse correction [1]. Haupl was instrumental in introducing the activator to Germany [41].

The Bionator was introduced by Wilhelm Balters of Germany in the 1950's [98]. In contrast to the Activator, there was minimal acrylic with a wire frame and no occlusal acrylic coverage on the upper permanent first molars conferring patient comfort and enhancing day time wear [1].

The Frankel Functional Regulator, designed by Rolf Frankel in the 1970's, is the only tissue borne functional appliance [99]. The design incorporates lingual acrylic pads to posture the mandible forwards, and acrylic buccal shields, joined by a wire framework, to remove lip and cheek pressure from the teeth. This appliance aims to reduce the degree of unwanted tooth movement during functional appliance treatment, and eliminate abnormal muscle function.

Clark in 1982 introduced the Twin Block appliance [100]. This appliance consists of upper and lower components that incorporate stepped inclined bite planes that serve as the active component to posture the mandible forward. This appliance can incorporate in its design a sagittal expansion

screw, sved capping, headgear tubes [1] and magnets to facilitate mandibular posturing [101,102]. It can be removable or bonded.

The Herbst appliance was first introduced by Emil Herbst in 1905 [1]. This appliance was not widely accepted at the time and therefore fell into disuse after the 1930's. Hans Pancherz reintroduced the appliance in the 1970's [103] and it has gained increasing popularity since. This is a fixed functional appliance and therefore compliance free. The active components are telescopic arms soldered to rigid maxillary and mandibular frameworks via stainless steel crowns on the teeth. The mechanism of Class II correction by the Herbst appliance is due to skeletal and dental changes occurring in the maxilla and mandible [104]. The molar correction is achieved predominantly by an increase in mandibular length and posterior movement of the maxillary molars whereas overjet correction is achieved by an increase in mandibular length and lower incisor proclination [104]. A systematic review by Cozza *et al.* [105] revealed that the Herbst appliance showed the highest co-efficient of efficiency (0.28mm increase in mandibular length per month) of all functional appliances.

3.5 Functional Jaw Orthopaedics

The aim of functional jaw orthopaedics in Class II mandibular retrognathic patients is to correct the Class II dental malocclusion and achieve a balance in profile by achieving a more anterior mandibular position.

The way in which functional appliances exert their therapeutic effects is believed to be multifactorial and not confined to changes occurring in the mandible alone. According to Woodside *et al*.[9], the mandibular effects of functional appliances include induction of mandibular growth, redirection of condylar growth, deflection of ramal form and horizontal expression of mandibular growth. The other effects of functional appliances include dentoalveolar changes, midface restriction, changes in neuromuscular activity and anterior relocation of the glenoid fossa [9].

Therefore, a combination of orthopaedic and orthodontic effects contribute to the movements necessary for Class II correction with function appliances [41,106,107].

The response of the temporomandibular joint to functional protrusion of the mandible is controversial in the orthodontic literature. Numerous animal and human studies have been conducted to determine the response of the temporomandibular joint to functional appliance therapy. Some studies support the notion that functional appliances induce condylar remodelling and growth, while others claim that the changes are due to remodelling of the glenoid fossa. Other researchers discount the involvement of the temporomandibular joint in class II correction, believing that functional appliances only induce dentoalveolar change.

3.5.1 Functional Appliance Studies in Animals

Breitner in 1940 and 1941,[13,14] pioneered studies on the effects of functional protrusion on the temporomandibular joint in non-human primates reporting convincing histological evidence of condylar and glenoid fossa remodelling. It was noted that the mandibular condylar cartilage is capable of exhibiting compensatory tissue responses after anterior repositioning of the mandible and that the glenoid fossa relocates anteriorly. Similar non-human primate studies conducted subsequently by Baume and Derichsweiler [16], Hiniker and Ramfjord [17], Stokli and Wilert [19], Meikle (Meikle, 1970), Adams *et al.*[15] and Voudouris *et al.* [20] yielded comparable results.

Charlier *et al.* [108] and Petrovic *et al.* [109] observed histologically, additional growth of the mandibular condylar cartilage in rats during forward mandibular displacement by stimulating the cells of the proliferative zone to undergo mitosis. In addition, they found an increase in the intensity of condylar growth and amount of periosteal bone apposition on the posterior border and rear inferior border of the mandible.

The Michigan group [110], observed the condyles of juvenile *Macaca mulatta* on cephalograms using the implant method whilst in functional protrusion. Tantalum pins were strategically inserted into

the maxilla and mandible of sixteen animals, six of which also wore a protrusive appliance. Radiographs were taken monthly. A statistically significant increase in both the rate and extent of condylar growth was observed over the first three months of the experimental period. The increments over the last two months of the experiment were equivalent to those observed in the control group. It was concluded that the action of functional appliances was time related and that functional appliances possibly needed reactivation after the initial three months.

The sequence of condylar cartilage adaption following anterior mandibular displacement was studied further by McNamara and Carlson [22], using histological methods. Twenty eight juvenile *Macaca mulatta* were used in the study, fourteen of which were fitted with cast occlusal splints to facilitate functional protrusion and were compared to controls that had no appliance. The animals were sacrificed at time points 2 weeks, 4 weeks, 6 weeks, 8 weeks, 10 weeks, 12 weeks and 24 weeks and the temporomandibular joints prepared for histological examination. At two weeks, adaptive responses in the condylar cartilage were seen particularly at the posterior border of the cartilage evidenced by an increase in thickness to three and a half times that in the control group. At four weeks, a more profound effect was seen across the cartilage reaching the peak response at six weeks along with an increase in new bone formation beneath the cartilage. By eight weeks, the thickness of the cartilage was comparable to the matched controls except at the posterior region that remained thicker until week twelve. At twenty four weeks, the cartilage in the experimental and control groups were indistinguishable in thickness, however the experimental group showed a greater cell density in the prechondroblastic layer. This can be explained not as a decrease in cartilage proliferation but rather the initiation of endochondral bone formation that increases and matches the rate of cartilage proliferation. This observation was noted previously by Stokli *et al.* [19] and subsequently in studies investigating forced mandibular protrusion using the Herbst appliance [9,20,111] and in histological studies on rats [21].

Considering that normal glenoid fossa growth direction is downward and backward [86], the finding of an anterior-inferior relocation of the glenoid fossa during forward mandibular repositioning is consistent in the literature. After continuous forward positioning of the condyles in juvenile, adolescent and adult in monkeys using a Herbst type appliance, Woodside *et al.* [9] documented continuous deposition of bone along the anterior border of the postglenoid spine and resorption along the posterior border of the postglenoid spine culminating in anterior reposition of the glenoid fossa. This in turn contributes to Class II correction. The result was found in all subjects but was more dramatic in the adolescent subjects. Other monkey studies by Hinton and McNamara [112], Peterson and McNamara [111] and Voudouris *et al.* [20] mirror these findings.

In the study by Voudouris *et al.,* [20] fifteen monkeys across juvenile, adolescent and adult stages of development were treated with a Herbst like functional appliance and compared to control animals. The implant technique was used to facilitate accurate cephalometric analysis of dental and skeletal changes. All experimental subjects had statistically significant additional condylar extension, mostly in a superior-posterior direction, and an increase in gonial angle. Histologically at six weeks, an increase in the proliferation of the prechondroblastic and chondroblastic cartilage layers was observed in a posterior superior direction. This was accompanied by endochondral bone deposition seen as multi-directional, finger like processes in a starburst pattern. By 12 and 18 weeks, there was thinning of the prechondroblastic and chondroblastic cell layers of the cartilage which was explained by a faster rate of endochondral bone formation. At the glenoid fossa, there was new bone formation on the anterior border of the post-glenoid spine and bone resorption along the posterior border indicative of downward and forward displacement. Voudouris *et al.* [113] explained their findings using the growth relativity theory. Growth relativity refers to growth that is relative to the displaced condyles from the actively relocating fossae and is dependent on viscoelastic tissues. In this paper, viscoelastic tissues are defined as non-muscular tissues and include synovial fluid, retrodiscal tissues, perimysium of the lateral pterygoid muscle, tendons, ligaments, other soft tissues

and body fluid. It is theorised that following displacement of the condyle from the fossa, forces are produced from the stretched retrodiscal tissues, flow of synovium and alteration in joint capsule morphology. Such forces are referred on to the glenoid fossa and the condyle resulting in remodelling at these sites. Condylar remodelling is redirected posteriorly and the glenoid fossa remodelling (also termed glenoid fossa restriction) occurs in an anterior inferior direction accounting for 22-46% and 6-32% of the Class II correction respectively. Voudouris *et al.* also apply this theory to relapse following Class II treatment.

Animal studies have also been conducted to investigate the craniofacial adaptations associated with forward mandibular positioning. McNamara and Bryan [114] conducted a cephalometric study to investigate the changes that occur in mandibular growth rate and direction in animals wearing a protrusive appliance from the juvenile age period to adulthood. Twenty three male juvenile rhesus monkeys were used over an experimental period of 144 weeks and the changes in mandibular length and morphology were investigated. At the end of the experimental period it was noted that condylar cartilage proliferation was followed by increased bone deposition leading to lengthening of the mandible. The mandibular lengths of the experimental animals were 5-6mm longer than the matched controls with the most increase in mandibular length occurring during the peak of the growth spurt. The angle formed between the posterior border of the mandible and the occlusal plane increased in the experimental subjects and decreased in the control animals. The increase in the mandibular length in the monkeys was 6-7% which correlates to the 6-8% increase seen in rats reported by Petrovic [115]. Applied to humans, McNamara and Bryan[114] hypothesised that an 8-9mm increase in mandibular length may be possible following the use of a functional appliance. McNamara and Bryan [114] also looked at the changes between the ramus and the body of the mandible, measured by the condylar-ramus-occlusal (CRO) angle. This angle decreased in the control group indicating a forward growth rotation whereas it increased in the experimental group showing that the effect of the functional appliance was to reverse the pattern of closure of the CRO angle.

Meikle [116] interprets McNamara's [114] findings based on the normal age dependent changes in growth direction of the condyle as described by Bjork [44] and Bjork and Skieller [117]. He explains that forward positioning of the mandible induces remodelling of the condyle in a more posterior direction resulting in reversal of the forward rotation of the mandible and accounting for increased length of the mandible. For this reason, Meikle does not see the effects of functional appliances as growth stimulation but rather prefers the term growth remodelling.

Early studies supported the role of the lateral pterygoid muscle in promoting condylar growth. McNamara conducted electromyographic (EMG) studies to investigate the pattern and sequence of muscle adaption in response to functional protrusion in infant, juvenile, adolescent and adult *Macaca mulatta* [118]. An increase in lateral pterygoid activity was associated with forward repositioning of the lower jaw and was noted initially during phasic activities such as, swallowing and subsequently during tonic functions such as, maintaining the jaw position. By the end of the experiment, the activity of the muscle reduced to the pre-appliance levels. This change in activity was concomitant with skeletal and dentoalveolar adaptations seen in the same animals. They concluded that the growth of the temporomandibular joints is adaptive in young animals and the condylar cartilage is responsive to changes in function.

In 1990, Stutzmann and Petrovic [119] reported on the role of the lateral pterygoid muscle and the temporomandibular frenum on condylar growth during functional protrusion in rats. Following resection of these structures, they found that even though the condylar cartilage growth continued, it was significantly diminished. Based on their work, Petrovic *et al.* considered the lateral pterygoid muscle to be of critical importance in functional appliance therapy and one of the various regulatory factors affecting the growth of the condylar cartilage [120].

Easton and Carlson [121] used rats to ascertain whether, if any, functional changes occurred in the lateral pterygoid muscles in association with chronically altered mandibular posture. Thirty juvenile

male Sprague-Dawley rats were divided into a control group and experimental group that wore bonded protrusive appliances for two weeks. Histochemical analysis of the lateral pterygoid muscle showed that the percentage of type I fibres increased significantly and the percentage of type IIb fibres decreased significantly in the experimental animals, indicating the muscles ability to undergo an increase in postural activity in response to chronic mandibular protrusion. These findings were consistent with those of McNamara [118] and Stutzmann and Petrovic [119].

In contrast, several studies have shown a decrease in the postural activity of the lateral pterygoid muscle. Whetten and Johnston [122] conducted a radiographic study using metallic implants placed in the condyle, ramus and glenoid fossa of rats. Following resection of the lateral pterygoid muscle on one side of the mandible, the growth of the condyles was compared over the six week experimental period. The presence or absence of the lateral pterygoid muscle had no significance on the anterio-posterior position of the condylar implants and only a slight transitory effect on their vertical position. They concluded that the lateral pterygoid muscle did not have any pronounced effect on condylar growth.

A later study by the Toronto group [123] revealed a similar finding when investigating the effect forced-protrusive and functional-protrusive appliances on the postural EMG activity of the masticatory muscles in six juvenile *Macaca fascicularis*. EMG activity was monitored longitudinally for twelve weeks using chronically implanted EMG electrodes. A significant decrease in the postural EMG activity was found in the superior and inferior heads of the lateral pterygoid muscles and the masseter muscle for the first six weeks following appliance placement. The following six weeks saw a gradual increase in the EMG activity to the pre-appliance levels. The forced protrusive appliance was activated incrementally, however did not prevent the decrease in postural EMG activity.

The adaptive nature of the mandibular condylar cartilage has lead to investigation of its role in enhancing condylar growth during functional protrusion on a cellular level. Rabie and co workers have conducted a series of experiments on Sprague-Dawley rats and have shown that the factors

regulating chondrogenesis and endochondral ossification during normal condylar growth are enhanced during condylar unloading through functional protrusion. The regulatory growth factors and transcription factors are up-regulated in a molecular cascade to increase mesenchymal cell proliferation, chondrocyte proliferation and maturation, neovascularisation and osteogenesis - resulting in enhanced bone formation by appositional endochondral ossification. (Appendix 1b)

The studies described below used Sprague-Dawley rats in their juvenile growth period. In the rat model, the growth spurt starts at day 31.5 and ends by day 135 [124]. Following sacrifice at the designated time points, the specimens were prepared for histological examination. These studies are described in detail in Appendix 1c.

Rabie *et al.* [10] quantitatively assessed the temporal pattern of expression of Sox9 during functional protrusion against its expression in normal growth. Sox9 is a transcription factor that regulates mesenchymal cell differentiation into chondrocytes and directly activates the gene expression for type II collagen. The earlier and increased expression of both Sox9 and collagen type II in the functional protrusion group indicated enhancement of chondrocyte differentiation and chondroid matrix formation. During functional protrusion in rats, Rabie *et al.* [125] also showed an increase in the number of replicating mesenchymal cells in the condyle. The number of replicating mesenchymal cells is genetically controlled and determines the growth potential of the condyle. Rabie *et al.*[10,125] concluded that the genetically predetermined level of mesenchymal cells in the condyle could influence the response to functional appliance therapy for each individual.

Up-regulation of SOX9 and Type II collagen expression in the glenoid fossa has also been documented by Rabie *et al.* [126].

The increase in mesenchymal cell proliferation [125] during functional protrusion coincides with up-regulation of the Indian hedgehog gene expression [127]. Indian hedgehog is believed to be a mediator of mechanotransduction - the process of converting mechanical stimuli into cellular responses. In

the condyle, this results in a stimulation of cell proliferation in the condylar cartilage. This process occurs via integrins [128]. Integrins are heterodimeric trans-membrane receptors formed by α and β subunits. Marques *et al.* [128] were able to show that the force delivered through functional protrusion modulates the growth of the rat condylar cartilage and that RGD-binding integrins participate in mechanotransduction.

As the chondrocytes mature during normal growth, parathyroid hormone related protein slows down the transformation of differentiating chondrocytes into hypertrophic inactive chondrocytes thereby prolonging growth at this point in the pathway [71]. Rabie *et al.* [71] conducted a histological investigation to determine the effect of functional protrusion on the expression of PTHrP in rats. They found higher levels of PTHrP expression in the experimental animals indicative of retardation of chondrocyte maturation, thereby sustaining highly productive chondrocytes, enhancing growth of the condylar cartilage.

Mature chondrocytes produce type X collagen, thus the synthesis of type X collagen indicates terminal stages of chondrocyte maturation and thus chondrogenesis [129]. Several studies [21,75,76] have shown that when the mandible is set forward there is a significant increase in type X collagen compared with that of natural condylar growth. Interestingly, Shen *et al.* [21] noted that type X collagen is expressed in the same temporal pattern seen during natural condylar cartilage growth. They concluded that the transition from chondrogenesis to osteogenesis is not in fact accelerated during functional appliance therapy but rather it is enhanced to encourage bone formation in the condyle. A thinning of condylar cartilage in the functional appliance group was observed in this study. This was representative of aggressive enhancement of endochondral bone formation replacing the cartilage during adaptive remodelling. In contrast, the control groups showed a thicker cartilage with distinct hypertrophic and erosive zones suggestive of a moderate rate of osteogenesis.

Core binding factor alpha-1 (Cbfa or RunX2) is a transcription factor that regulates chondrocyte maturation and terminal differentiation; extracellular matrix mineralisation and degradation; and osteoblast invasion during post natal growth of the mandibular condyle [72]. Over a thirty day experimental period [130], it was shown that mandibular advancement elicited Cbfa-1 expression in the condylar cartilage with subsequent expansion of the type X collagen domain in the hypertrophic layer. Increased expression of Cbfa-1 in the sub-chondral bone corresponded with an increased recruitment of chondroclasts and osteoblasts that preceded new bone formation in the condyle. Cbfa-1 facilitates osteoblast invasion for endochondral ossification in the condyle and up-regulates VEGF. It was therefore concluded that Cbfa-1 mediates chondrocyte terminal maturation and plays a central role in endochondral ossification in the mandibular condyle in response to functional protrusion [130].

Vascular endothelial growth factor is responsible for vascularisation during appositional endochondral ossification in normal mandibular condylar cartilage growth [57,131]. Several studies on rats investigated the temporal pattern of VEGF expression and new bone formation in the condyle and glenoid fossa during forward mandibular positioning. Rabie *et al.* [131] showed that there was a significant increase in both vascularisation and mandibular bone growth during forward mandibular positioning, the highest amount of both being expressed in the posterior part of the condyle. In addition, peak levels of VEGF preceded maximum bone formation. A similar finding was noted in the glenoid fossa of experimental animals [132]. It can therefore be concluded that forward mandibular positioning causes significant increases in vascularisation and new bone formation in the condyle and glenoid fossa, resulting in enhanced condylar growth [131,132].

As well as being a potent angiogenic peptide, the expression of VEGF is induced in chondrocytes under conditions of overloading and are therefore implicated in the onset of temporomandibular joint osteoarthritis [133]. Forsythe *et al.* [133] were able to show that VEGF induction in chondrocytes

under loading is linked to activation of hypoxia-inducible factor 1 (Hif-1). Pufe *et al.* [134] furthered this concept in an ex-vivo experiment on chondrocytes derived from bovine cultured cartilage discs. It was found that mechanical overloading of chondrocytes induced the release of Hif-1α, causing a subsequent production of VEGF. Under conditions of overloading, VEGF is capable of osteoclast recruitment, osteoclast differentiation, and osteoclastic bone resorption[135,136]. Very recently, Shikara *et al.* [137] overloaded the TMJs of rats using intra-oral sliding plates that repositioned the condyles upward and backward, to examine the roles of Hif-1 and VEGF in condylar cartilage degeneration in vivo. The authors reported an increase in Hif-1 activation in mature chondrocytes, paralleled by an increase in VEGF expression and tartrate resistant acid phosphatase (TRAP) positive cell numbers. In addition, it was confirmed that Hif-1α induces VEGF expression and that activated Hif-1 in overloaded chondrocytes can induce osteoclastogenesis via repression of osteoprotegrin expression. Finally, the authors reported that the degree of degeneration of the condylar cartilage was in proportion to the duration of overloading [137].

Xiong *et al.* [40] used seventy-eight, 120 day old female Sprague-Dawley rats to explore the relationship between neovascularisation, hypertrophic cartilage and the microstructural properties of cancellous bone in the adult rat's condyle in response to mechanical strain produced by mandibular advancement. Micro-CT tomography was used to carry out direct three dimensional morphometric analysis and the results correlated with the presence of markers of endochondral ossification determined histologically. The results showed that mechanical strain produced by mandibular advancement induced neovascularisation in the posterior condyle marked by an increased expression of VEGF. Bone morphometry showed new bone formation in the condyle characterised by thinner trabecular thickness, more trabecular number and increased trabecular space. They concluded that the mechanical strain produced by the mandibular advancement induces neovascularisation and osteogenesis leasing to adaptive growth of the condyle in adult rats.

Insulin type growth factors [64] and the expression of cell cycle genes such as cyclin D1, PCNA and Wnt5a [138] have been shown to increase with mandibular anterior repositioning in rats.

The above molecular changes in the mandibular condylar cartilage in rats have also been documented following bite opening [139] and lateral functional shift of the mandible [140-142].

Evidence from animal studies substantiate that the hypotheses that functional appliances exert their therapeutic effects through growth of the condylar cartilage, redirection of condylar growth, anterior relocation of the glenoid fossa and supplemental growth of the mandible.

The limitations of animal studies have been acknowledged. Results from animal studies cannot be directly related to humans, as human exhibit different growth rates, growth timing and masticatory systems compared to animals. Animals do not exhibit typical malocclusions and differ morphologically in suture orientation and therefore potential response to orthopaedic force. Experimental variables such as appliance design, duration of wear, experimental duration, sample size and control groups [143] may not simulate the same conditions in humans. Human studies are therefore required to truly determine the effect of functional appliance in humans.

3.5.2 Functional Appliance Studies in Humans

Given the scientific value of prospective randomised clinical trials (RCT), several were undertaken in the 1990's to determine the clinical significance of the effects of functional appliances. The RCTs are described below and tabulated in Appendix 1d.

Webster *et al.* [144] in Dunedin conducted their RCT on 42 male and female patients chosen for the study based on the presence of a Class II Division 1 malocclusion. The subjects wore either a Frankel functional appliance, a Harvold Activator or no appliance for 18 months and the average ages at the start of the study were 11.53, 11.70 and 11.70 respectively. Cephalometric comparisons indicated 0.44°, 0.75° and 0.66° changes in B-point with the Frankel, Activator and control respectively. The

authors concluded that although the mandibular length increased significantly in the treatment groups, when compared with the controls it was not significantly associated with treatment success and that most of the changes were due to an increase in the vertical dimension.

Tulloch *et al.* [145] at the University of North Carolina conducted a RCT to determine the benefit of early Class II treatment by assessing the clinically relevant and statistically significant changes in expected growth compared to an untreated matched sample. Based on the criteria of an overjet greater than 7mm, 166 patients with an average age of 9.9 years were included in the study. The subjects were divided randomly into a control group and two treatment groups receiving either Bionator or Headgear appliances, and were observed for 15 months. For the headgear, Bionator and control groups, the effect on the maxilla as measured by a change in A-point was 0.92mm, 0.11mm and 0.26mm respectively and the mandibular change as measured by a change in B-point was 0.15mm, 1.07mm and 0.43mm respectively. It was concluded that the headgear had a greater effect on the maxilla, the Bionator had a greater effect on the mandible and that the differences between the treatment and control groups were small.

The RCT conducted by Keeling *et al.* [91] at the University of Florida, included 249 patients of average age 9.6 years, having Class II molars including subdivisions. The patients were designated as controls or treated with either a Bionator or headgear and plate. The treatment was continued until Class I was achieved or at two years. The results revealed no maxillary changes between the three groups, however both the Bionator and the headgear with plate significantly affected anterior mandibular growth over the controls. It was therefore concluded that the Bionator and the headgear with plate did not influence maxillary growth but both enhanced mandibular growth.

Ghafari *et al.* [90] from the University of Pennsylvania conducted a RCT including 63 patients with a Class II molar relationship and an ANB angle greater than 4.5°. The subjects varied in age from 7 years and 4 months to 13 years and 4 months and were either treated with the Frankel appliance or

straight-pull headgear. There was no control group. Treatment time was determined by attainment of a Class I occlusion. They found that the headgear reduced SNA by 3.14° and SNB by 0.55°, whereas the Frankel appliance increased SNA by 0.15°and B-point by 1.44°. The authors concluded that the headgear has a distalising effect on the maxilla and the maxillary molars and the Frankel appliance affects the forward growth of the mandible and induced lower incisor proclination.

Finally, O'Brien *et al.* [146] from the University of Manchester conducted a multicentre RCT to assess the dental and skeletal effects of the twin block during early treatment. One hundred and seventy four patients were selected for the study satisfying the selection criteria of a Class I Division 1 malocclusion. The subjects, aged between 8 and 10 years, were divided into two groups, control or treatment with twin block, and the duration of the study was 15 months. The twin block altered A-point by 0.57mm and B-point by 3.52mm, whereas changes at these points in the control group were 1.45mm and 2.52mm respectively. The authors concluded that functional appliance treatment does not influence the Class II pattern to a clinically significant degree.

The overall outcomes of the RCT's were that functional appliances did not influence the Class II pattern to a clinically significant degree; that the difference between the treatment modalities were small; and that two phase treatment was not beneficial over one phase treatment. Such claims were scrutinised by Darendeliler in 2006 [147]. Darendeliler stated that RCT's are inappropriate for examining Class II treatment due to the variation in Class II morphology requiring the use of several treatment modalities, and that deprivation of treatment to control groups when otherwise indicated is considered unethical. Darendeliler highlighted that studies failed to select subjects based on skeletal pattern and retrognathic profile but rather on the degree of overjet, and the transverse and vertical dimensions were not considered. Darendeliler questioned the experience of the operator and stated that the study durations were excessive. In addition, the response to treatment was assessed using A-point and B-point which are known to change with growth, and the concept of individuality of treatment response was not considered. Freeman *et al.* add that the RCT's with the

exception of one, were conducted prior to the peak in mandibular growth implying that the maximum response to treatment would not have been attained [148,149].

Baccetti and co-workers have examined supplementary growth of the mandible across different stages of pubertal growth using the CVM method [150,151]. They claim that treatment during the peak pubertal growth, indicated by CS3 and CS4 on a lateral cephalogram, produces a clinically significant supplemental elongation of the mandible. When studying the effects of functional jaw orthopaedics in Class II subjects, Baccetti and co-workers use untreated Class II samples matched for skeletal maturity as the control group. This is based on the fact that Class I and Class II subjects grow differently during the pubertal peak [6].

Inconsistencies in the literature surrounding supplemental mandibular growth following functional jaw orthopaedics provided the impetus for Cozza *et al.* in 2006[152] to conduct a systematic review to investigate mandibular changes produced by functional appliances in Class II malocclusions in order to determine if the mandible grows more in Class II patients treated orthopaedically over untreated Class II subjects. Out of 704 articles reviewed, 22 articles qualified for review based on meeting the inclusion criteria. The 22 articles included four RCTs and the remainder were controlled clinical trials (CCT), two prospective and sixteen retrospective. This was considered feasible given the ethical issues of obtaining a true control sample required for RCTs. The outcome revealed that the amount of supplementary growth of the mandible in patients treated with functional jaw orthopaedics compared with Class II controls varied between studies with values being reported from 0.5-6.5mm. Review of the 22 studies revealed that the variability stemmed from lack of uniformity in treatment timing between studies. Put simply, the studies conducted early did not report any significant increase in supplemental mandibular growth [91,145,146,151,153-157] whereas the studies conducted during the pubertal peak did [148,149,151,153-155,158]. Importantly, only seven of the 22 studies, comprising nine samples, informed of the skeletal maturation of the patient. As reported by Cozza *et al.*, six of these

samples were treated prior to the peak pubertal growth showing no significant supplemental growth. The remaining three studies treated at CS3 or CS4, were able to evidence significant supplemental mandibular growth of 3.1mm, 4.3mm and 6.7mm. Randomised controlled trials are the source of the highest scientific evidence; however none of the RCTs found significant increases in mandibular length during functional appliance therapy. Upon closer examination of these studies, Cozza *et al.* highlight that all of the RCT's were conducted on very young subjects prior to the onset of the peak growth spurt and hence the reason for no significant mandibular lengthening. In summation, the systematic review shows that treatment with functional jaw orthopaedics prior to the pubertal growth peak shows no significant supplementary elongation of the mandible (1.5-2.2mm) in the short term, whereas treatment at the pubertal growth peak does (3.1mm-6.7mm). Therefore the timing of functional appliance treatment is related to treatment success.

In 2000, Baccetti *et al.* [150] conducted a retrospective cephalometric study to compare the short term treatment effects of the twin block before the pubertal growth spurt against treatment at the time of the pubertal growth spurt. The CVM method was used to determine the stage of growth. The peak growth was not included in the treatment period of the early treatment group, consisting of 21 subjects at CS1 and CS2. Conversely, the peak growth was included in the treatment period of the late treatment group consisting of 15 subjects at CS3 and CS4. The amount of supplementary elongation of the mandible in the late treatment group at the end of functional jaw orthopaedics was 4.75mm/year compared to 1.88mm/year in the early treatment group. The greater increase in the total mandibular length in the late treatment group was associated with significant increases in the ramus height and length of the mandibular body, which were not significant in the early treatment group. Mandibular growth modifications were observed in the late treatment group however cephalometric examination of the early treatment group was suggestive of only forward mandibular positioning. The outcome of this study showed that in the short term, the optimal time for functional jaw orthopaedics with the Twin Block is during the peak pubertal time.

It is therefore evident that in the short term, functional appliance treatment is effective during peak pubertal growth. A subsequent retrospective cephalometric longitudinal study by Faltin *et al.* [151] assessed the long term effects of Bionator treatment prior to, and during the pubertal growth spurt. Bionator therapy was initiated (T1) in 13 subjects prior to the pubertal growth spurt (CS1, CS2 – early treatment group) and in 10 subjects at the pubertal growth spurt (CS3, CS4 – late treatment group). Removal of the Bionator marked T2. T3 was taken at the completion of growth and included a period of fixed appliance treatment. The study found that in the long term (that is after the completion of pubertal growth) the amount of supplementary elongation of the mandible in subjects treated during the peak pubertal time is 5.1mm more than untreated controls and is associated with a backward direction of condylar growth and significant increases in ramus height. Conversely, subjects treated prior to cervical stage 3 showed only 1.9mm supplementary growth which is not statistically significant. This study concluded that in the long term, significant supplementary mandibular growth occurs in subjects treated during the peak pubertal time but not in subjects treated prior to this.

Recently a similar study by Malta *et al.*[159], examining 20 Class II subjects from T1 through to T3, not only found significant long term changes in mandibular length and morphology following Bionator therapy, but also showed a significant improvement in the soft tissue pogonion of the treated subjects of 2.6mm.

Pancherz and co-workers have studied the effect of the Herbst appliance treatment on TMJ growth in adolescent humans using magnetic resonance imaging. On MRI scans, tissues with high proton density appear bright and tissues with low proton density appear dark. The contrast in the image therefore reflects differences in proton density between the tissues. Newly formed cartilage consists of 80-90% water, and the hydrogen proton in the water is highly susceptible to the effects of magnetic fields. Consequently, new cartilage shows up bright on the MRI.

Ruf and Pancherz [23,24] examined the TMJs of 15 adolescent subjects, as determined by the hand-wrist method of skeletal maturation. The subjects on average were 13.5 years and were treated with the Herbst appliance for an average of seven months. MRI scans were taken prior to the start of Herbst treatment (T0), at the start of treatment with the appliance in place (T1), after 6-12 weeks of appliance treatment (T2) and following removal of the appliance (T3). The scans were analysed visually for possible signs of joint remodelling, and metrically to record changes in condylar position within the fossa. At T2, it was found that the posterior superior border of the condyle was bright on MRI scans in 96% of the subjects, indicative of condylar modelling at this area. The authors suggested that the bright areas on the MRI scans correspond to hyperplasia of the prechondroblastic and chondroblastic zones of the cartilage as seen histologically in animal studies [111,160]. The bright zone in the adolescent subjects disappeared after twelve weeks of Herbst wear and was thought to be due to enhancement of osteogenesis in the condyle in response to mandibular protrusion as seen in animal studies [9,19-22,111]. The glenoid fossa was seen to remodel in an anterior-inferior direction in 72% of the adolescent subjects. No statistically significant changes were found in the condyle-fossa relationship during Herbst treatment, hence discarding the possibility that the increase in mandibular prognathism is due to anterior mandibular posturing.

Pancherz and Fisher [161] investigated further the amount and direction of TMJ growth changes in Herbst treatment on a sample of 35 Class II Division 1 adolescent subjects. This retrospective cephalometric study assessed condylar growth and glenoid fossa displacement before treatment (T0), after 7.5 months of Herbst treatment (T3), 7.5 months post-treatment (T4) and three years post Herbst treatment (T5). Placement of the appliance marked T1, and during treatment marked T2. During Herbst treatment (T0-3) condylar growth was directed posteriorly and superiorly to a statistically significant degree and to a greater extent than the controls. In the post-treatment periods, condylar growth resumed to a more vertical orientation and the amount of growth was reduced. During the treatment period, the glenoid fossa was displaced in an anterior-inferior

direction. The displacement of the glenoid fossa in the control group was less and in the opposite direction to the experimental subjects. The changes at the glenoid fossa seen in adolescent human subjects are consistent with the TMJ remodelling in primates [111,160].

A posterior superior pattern of condylar remodelling was also noted by Paulsen in 1997 using orthopantomographic and trans-pharyngeal radiography [162].

From the MRI and radiographic studies described above, Pancherz concludes that in adolescent Herbst subjects, the growth of the condyle can be stimulated and the glenoid fossa displaced anteriorly. These TMJ adaptations will result in mandibular advancement, contributing to the skeletal component of Class II correction.

Given that the objective of Class II orthopaedic treatment is to achieve an improvement in facial balance, it is important to acknowledge how changes at the TMJ during Herbst appliance treatment translate clinically. In order to assess this, Pancherz *et al.* [163] studied 'effective TMJ growth' during Herbst treatment together with changes in chin projection and examination of mandibular rotation. 'Effective TMJ Growth' is defined as the sum of condylar modelling, glenoid fossa modelling and condyle-fossa relationship changes. A longitudinal cephalometric retrospective study was conducted on 98 subjects treated with the Herbst appliance for 7 months and compared with control subjects from the Bolton Standards. They found that chin position was a determined by 'effective TMJ growth' in combination with the direction of mandibular growth rotation. Chin position alterations during and after Herbst treatment mirror 'effective TMJ growth' provided no mandibular rotation occurs. Although highly variable amongst subjects, an anterior mandibular rotation increased chin projection whilst a posterior mandibular rotation was seen to decrease it.

Pancherz and Littmann [164] investigated the mandibular morphologic changes during Herbst treatment at different circumpubertal times in a retrospective cephalometric study. The results showed an increase in mandibular length (Co-Pog) and mandibular horizontal length (Gn-Me) in the

Herbst groups over the control groups. The increase in gonial angle, and reduction in the β angle was a result of the Herbst treatment. The posterior condylar growth and bone resorption at the posterior part of the lower border of the mandible was larger in the Herbst group than in the controls. The changes were more marked in the Herbst group treated during the pubertal peak. Pancherz explains that stimulated posterior-superior condylar growth results in lengthening of the mandible from condylion to pogonion and gonion to menton. The increase in the gonial angle and decrease in the β angle was explained by the change in condylar growth direction together with bone resorption at the posterior part of the lower mandibular border.

Pancherz and co-workers [165-167] conducted a series of EMG investigations to determine the activity of the temporalis and masseter muscles in subjects with normal occlusion, Class II Division 1 malocclusion and Class II Division 1 malocclusion treated with the Herbst appliance. Compared to individuals with Class I malocclusions [165], Class II division 1 subjects exhibit less EMG activity during both maximal biting force and chewing [166]. At the start of Herbst treatment, EMG activity from the temporalis and masseter muscles is markedly reduced and recovers to pre-treatment values by three months. The EMG activity increased after removal of the appliance and continued to do so at 1 and 7 years post-treatment and resembled the muscle activity of the untreated Class I subjects [167]. The initial decrease in muscle activity seen in the Herbst treated Class II Division 1 subjects, was suggested to be due to an altered sagittal jaw or dental relationship during the appliance period. The post-treatment increase in muscle activity most probably simulated normal age related changes [165]. Interestingly, Pancherz suggested that the change in gonial angle associated with Herbst treatment is likely to be due to altered muscle function as determined by the electromyographic studies [167].

As evidenced in human [23,24,81,148,149,151,153-155,158,164,168] and animal studies [14-16,18,19,114,160] an increase in mandibular length is credible in response to functional appliance treatment. The way in which this transpires is likely to be a combination of a change in condylar growth direction seen by opening of

the gonial angle, and increased condylar growth in a more posterior superior direction seen as increased bone deposition on the posterior aspect of the condylar head and the ramus. Such modifications are notable cephalometrically as an increase in total mandibular length, increase in ramus height, opening of the gonial angle and posterior rotation of the condylar line in relation to the mandibular line [150].

Proffit [41], on the other hand, views the action of functional appliances from a different perspective. He defines growth stimulation in two ways: as the attainment of a final size larger than would have occurred without treatment; and as the occurrence of more growth during a given period than would have been expected without treatment, or in other words, temporal stimulation of growth. Proffit supports the latter concept whereby the final size of the mandible will not be larger as a result of functional appliance treatment than it would be without treatment. He suggests that this occurs by an increase in growth increments during the first couple of months of functional appliance treatment followed by a slower than normal rate of mandibular growth.

Johnston [169] proposes a similar hypothesis to Proffit, explaining that functional appliance treatment is a 'mortgage on mandibular position'. He explains that during functional appliance treatment, the mandible is positioned anteriorly, positioning the condyles out of their fossas. The condyles then grow at a normal rate eventually restoring a normal condyle-fossa relationship. Johnston emphasises that the rate of condylar growth is not enhanced in a 'boom and bust' fashion during treatment, rather, what is seen as growth is 'probably' just bodily displacement of the mandible. If this is the case, functional appliances would have no long term impact on mandibular growth and would be the same as the results seen in conventional fixed appliance therapy. Finally, Johnston states on presumption, that the only long-term effect would be maxillary dento-skeletal retrusion.

Several limitations of human studies investigating the effects of Class II orthopaedic treatments have been highlighted in the literature over time. These include landmark identification on cephalograms

[116,170], the use of articulare, a non-anatomical point, to quantify mandibular length [6], lack of consideration of growth rotations [116], variable appliances used in different studies, inability to ethically acquire a control group [170], age and gender differences, consensus with respect to timing of treatment [81], adequate sample sizes and the inability to conduct implant studies [170]. Based on these potential limitations, the validity of the scientific literature pertaining to functional appliances has been questioned and thus some oppose the claims made regarding their mode of action and use in orthodontics [143]. In contrast, others believe that the abovementioned limitations have been acceptably overcome with the introduction of three dimensional imaging, the use of MRI, the use of the CVM method [81], access to records of untreated Class II subjects from archived growth studies [81] and the fact that these have inherently enabled more thorough investigations.

3.5.3 Functional Jaw Orthopaedics in Adolescent Humans

3.5.3.1 Patient Factors

Enhancement of mandibular length is best achieved during the peak of the pubertal growth spurt [81,114,148,149,151,153-155,158]. The peak pubertal growth spurt is best indicated by determination of the cervical vertebral maturation viewed on a lateral cephalogram [81]. Baccetti *et al.* document that the peak in mandibular growth occurs during CS3 and CS4 [81].

The amount of supplementary mandibular growth varies in subjects between and within studies suggesting patient variability also plays a role in orthopaedic treatment response. The classic study by Petrovic and Stutzmann [171] showed that the effectiveness of a functional appliance depended on the growth potential of the mandible at both tissue and cell levels. In this study, bone was taken from extraction sites of 95 boys between the ages of 10-12 years before and after the use of Class II or III elastics. The bone was studied for signs of bone resorption and bone deposition. The bone taken before the wear of the elastics establishes the *tissue level growth potential*, that is, the alveolar bone turnover rate and the subperiosteal ossification rate. The bone taken after elastic

wear established the *tissue level growth responsiveness*, that is, the magnitude of increase of alveolar bone turnover rate caused by ten days wearing the Class II or Class III elastics. These patients then wore the Frankel II appliance for 12 months and the response to this compared the bone response following elastic wear. It was found that the effects of the Frankel II paralleled the tissue level growth potential and responsiveness indicating heterogeneity of growing children.

Using a rat model, Rabie *et al.* [172] were able to endorse these findings. During functional protrusion, it was observed that an increase in cartilage synthesis depended on the rate of mesenchymal differentiation into chondrocytes. They were able to confirm that the number of replicating mesenchymal cells is genetically controlled and thus influences the rate of condylar and glenoid fossa growth during functional protrusion. These studies support a genetic basis for individual responsiveness to functional appliance therapy.

Franchi *et al.* [95] investigated the notion of good and bad responders to functional jaw orthopaedics on the basis of anatomical morphology of the mandible in 57 patients, 17 of which wore the twin block, 18 the stainless steel crown Herbst and 22 the acrylic splint Herbst. All patients were full unit Class II and started treatment at CS3. It was found that the gonial angle accounts for 80% of the variability of patient response to treatment, and therefore it was recommended to assess the gonial angle prior to orthopaedic treatment. An angle greater than 128° resulted in a response less than in an untreated control; an angle less than 128° showed a favourable response; and an angle less than 123° showed an excellent response. The remaining variability of 20% may be put down to hormonal factors, compliance and operator proficiency.

Rabie and co-workers [173-177] have directed their current research towards exploring gene therapy as a means of inducing condylar growth for the treatment of patients with craniofacial deformities. Preliminary studies aimed to determine whether genes could be transferred to the mandibular condyle in vivo. Sprague-Dawley rats were injected with either recombinant adeno-associated virus

mediated enhanced green fluorescence protein (rAAV-eGFP) or saline into both mandibular condyles and the spatial and temporal transgene expression was detected by in situ-hybridisation, reverse transcriptase polymerase chain reaction (RT-PCR) and real time polymerase chain reaction (PCR). The results showed that rAAV's were capable of infecting rat chondrocytes, the expression of which was detected at day 7 and peaked at day 21. This was the first study to report that rAAV-mediated genes could be transferred to the mandibular condyle in vivo. They concluded that this method of gene transfer was a promising approach for delivery of candidate genes to the mandibular condyle with the aim of regulating mandibular condylar growth in the future[173].

Vascular endothelial growth factor plays an instrumental role in angiogenesis, a crucial step in endochondral ossification at the mandibular condyle, and has therefore become of interest in the context of gene therapy [74]. Several delivery methods can be used to facilitate gene therapy. Rabie *et al.* [177] and Dai and Rabie [177,178] aimed to establish an effective in vivo gene delivery system to enhance mandibular condylar growth using local administration of recombinant adeno-associated virus-mediated vascular endothelial growth factor (rAAV-VEGF) in the condylar cartilage of rats. rAAV2 vectors were chosen for their high-infection efficiency in chondrocytes [176]. Results showed transgene expression in the mandibular condyles during the whole experiment period of 60 days, as detected with in situ hybridization, RT-PCR, immunostaining and Western blot. Osteogenetic and chondrogenetic markers were assessed by biochemical analysis and their expression significantly changed from day 30. A significant increase in cell proliferation was noted and morphological measurement indicated a significant increase in the size of mandibular condyle after day 30 [177,178].

More recently Rabie *et al.* [175] have studied the infection efficiencies of rAAV2 in vitro, and the transgene expression pattern mediated by rAAV2 in glenoid fossa, TMJ disc and condylar cartilage in vivo to determine whether rAAV2 can be used for future TMJ gene therapy. Thirty Sprague-Dawley rats were injected with either rAAV2-sec-Vastatin (experimental group) or rAAV2-eGFP (control group) into both sides of TMJ, sacrificed at defined time points over sixty days and prepared for RT-

PCR and immunostaining analysis. The results indicated that recombinant AAV2 could be considered as a promising vector for gene therapy in TMJ which can mediate therapeutic gene expression in glenoid fossa, articular disc and condylar cartilage in vivo.

The final patient factor is compliance. Fixed functional appliances such as the Herbst, bonded twin block and magnoglide, overcome this issue.

3.5.3.2 Treatment Factors

There is ongoing debate whether stepped-gradual advancement is more beneficial than full advancement, during functional appliance treatment. According to Rabie and co workers [172,179-183], stepped mandibular advancement provides better stimulation of condylar growth than full advancement and results in more mandibular protrusion clinically. Other studies show that there is minimal or no difference clinically between advancement protocols [181,184].

The effects of combined glucosamine sulphate and chondroitin sulphate supplements on the condylar cartilage during functional appliance therapy has recently been investigated [185,186]. These studies established that supplement therapy increased the volume of cartilage with and without functional appliance therapy and enhanced the normal biological response to functional appliance therapy in the rat model.

Finally, vibration has evolved as a therapeutic means in several areas of medicine and dentistry. The effect of vibration along with functional appliance therapy has not yet been investigated and reported in the literature to date.

3.5.3.3 Stability of Orthopaedic Class II correction

Long-term data derived from studies of Pancherz and co-workers show that following Herbst treatment, glenoid fossa displacement reverts back to a posterior direction and condylar growth resumes in a more vertical direction [161,187]. Despite this, the stability of the Class II correction is

conferred by adequate interdigitation of the maxillary and mandibular teeth, as hypothesised by Petrovic's Cybernetic Model [115] and Solow's Dentoalveolar Compensatory Mechanism [52], and observed during clinical studies by Pancherz [163,188-190]. This is supported by Baccetti and co-workers who states that functional jaw orthopaedics performed at the correct timing allows transition immediately into full fixed appliances, enhancing Class I dental interdigitation. Further, the minimal amount of growth in Class II subjects after puberty, shown to match that of Class I subjects, assists in the stability of the orthopaedic treatment of the Class II malocclusion performed at puberty [6].

4 Bone

4.1 Definition, Function and Categories

Bone is defined as a specialised connective tissue that serves as both a tissue and organ system within higher vertebrates [191].

The functions of bone are structural support of the body, protection of important organs and structures, locomotion, mineral storage and homeostasis, acid-base balance, reservoir for growth factors and cytokines, and haematopoiesis within the marrow spaces [192].

Bones have been classified as long (for example clavicles, tibiae, femurs, radii, humeri and ulnae), short (for example patellae, carpal and tarsal bones), flat (for example sternum, ribs, skull, scapulae and mandible) and irregular (for example vertebrae, sacrum and hyoid) [192].

4.2 Cellular Composition of Bone

Four distinctly different cell types can be found within bone namely osteoblasts, osteocytes, bone lining cells and osteoclasts [191]. Self renewing, pluripotent mesenchymal stem cells derived from the bone marrow give rise to osteoprogenitor cells which in turn generate osteoblasts, osteocytes and

bone lining cells [192]. In contrast, osteoclasts are derived from mononuclear monocyte-macrophage precursor cells thought to originate from the bone marrow [192].

4.2.1 Osteoblasts

Functionally, osteoblasts synthesise new bone matrix on bone-forming surfaces [192] and regulate its mineralisation [193]. Morphologically, active mature osteoblasts are large, plump cuboidal cells that exhibit abundant and well developed synthetic organelles characterised by a large nuclei, enlarged Golgi structures and extensive endoplasmic reticulum, for matrix production [192,194]. Both collagen and non-collagen matrix products are deposited toward the bone formation surface [192]. In addition to protein synthesis, osteoblasts also secrete cytokines, regulators of cell metabolism, as well as mediators of bone remodelling such as growth factors and bone morphogenetic proteins [194]. Along with their precursors, osteoblasts form a tight layer of cells at the bone surface and rely on extensive cell-matrix and cell-cell contacts via trans-membrane proteins and receptors that allow maintenance of cellular function and reaction to metabolic and mechanical stimuli [193].

Following bone formation, 50-70% of osteoblasts undergo apoptosis with the remainder becoming bone lining cells or osteocytes [192].

4.2.2 Bone Lining Cells

Upon completion of bone growth, some osteoblasts maintain their location along the surface of the bone where they flatten and reduce their functional capacity [194]. Such quiescent osteoblasts are termed bone lining cells [191,193,194]. Being less metabolically active, these cells contain less organelles and cytoplasm, however maintain their communications with other bone cells via cellular intercellular junctions [194]. The function of these cells is still speculative, however they may regulate crystal growth in bone, act as a barrier between extracellular fluid and bone, be precursors for osteoblasts, and in the presence of parathyroid hormone may secrete enzymes that remove osteoid in preparation for bone resorption [191].

4.2.3 Osteocytes

Osteocytes are the most abundant cell type, constituting up to 90% of the bone cells in the adult skeleton [191]. In the event that osteoblasts become entrapped in their own calcified matrix, the cells undergo a functional and phenotypic change after which they are called osteocytes. Osteocytes are housed in osteocytic lacunae [194] and over time reduce in size, contain less synthetic organelles and have an increased nucleus to cytoplasmic ratio [191]. The osteocytes maintain an extensive network of communication with other osteocytes and bone lining cells via cytoplasmic extensions that occupy small channels in the bone called canaliculi. This osteocyte 'syncytium' is referred to as the lacuno-canalicular system [195] and is thought to organise the cellular events leading to bone resorption and formation [191,193] in response to metabolic and mechanical demands in order to maintain bone vitality and integrity [194].

4.2.4 Osteoclasts

Osteoclasts are multinucleated giant cells responsible for the resorption of fully mineralised bone in both normal and pathological conditions at the sites of Howship's lacunae [191,193]. They contain tartrate-resistant acid phosphatase in the cytoplasmic vesicles and vacuoles differentiating them from other multinucleated giant cells [194]. Tartrate resistant acid phosphatise stain used histologically can confirm the presence or absence of osteoclastic activity.

The osteoclast features a unique area on its membrane called the 'clear zone', an area devoid of cell organelles and rich in fibrilar contractile proteins. The clear zone is able to attach to the bone and create a tight seal with the calcified matrix, ideal for an acidic microenvironment. The enzymes that break down bone are synthesised in rough endoplasmic reticulum of the osteoclast, transported to the Golgi apparatus and move to the ruffled border on the cell membrane, where they released via exocytosis into the sealed area [194]. Initially, at the sealed area, the inorganic components are degraded by hydrochloric acid, followed by organic degradation by cathepsin K, a lysosomal

protease [191]. The ruffled border also features a proton pump that pumps hydrogen ions into the sealed zone for bone degradation [194] and further activates the secretion of enzymes [193]. Following breakdown of the bone, the inorganic and organic bone remnants are endocytosed at the ruffled border, transcytosed to the opposite side of the cell where they are released from the cell [194].

4.2.5 Osteoblast – Osteoclast Interactions During Bone Remodelling

Osteoblast – osteoclast interactions during bone remodelling occur via RANK/RANKL/OPG interactions. RANKL, receptor activator of nuclear factor kappa ligand, is a tumour necrosis factor related ligand that is expressed on the osteoblast and exerts its effect by binding to the receptor activator of nuclear kappa (RANK) receptor on the osteoclast lineage cells. This binding leads to rapid differentiation of hematopoietic osteoclast precursors to mature osteoclasts, thereby favoring osteoclastogenesis (Yasuda et al 1999). Osteoprotegrin (OPG) is a decoy receptor for RANKL, produced by osteoblastic cells, which compete with RANK for RANKL binding. The biologic effects of OPG on osteoclasts include inhibition of terminal stages of osteoclast differentiation, suppression of activation of matrix osteoclasts, and induction of osteoclast apoptosis - thereby working against osteoclastogenesis (Yasuda et al 1998b, 1999). It can therefore be concluded that osteoblasts somewhat control osteoclast expression during bone remodelling.

4.3 Extracellular Composition of Bone

The extracellular matrix of bone consists of both organic and inorganic components, collectively accounting for 90% of the entire bone volume. Sixty five percent of the extracellular matrix is inorganic and the remaining thirty five percent is organic.

4.3.1 Organic Bone Matrix

4.3.1.1 Collagen

Collagen is synthesised and secreted by the osteoblasts and is the most abundant protein of the organic matrix. Type I collagen predominates, making up 90% of the total collagen content, the

remaining 10% being collagen types V, VI, VIII and XII. Type I collagen molecules are made up of a triple helix of polypeptide chains and form collagen fibrils in the extracellular environment. Morphological arrangement and cross linking of the fibrils create a stable porous structure, providing bone with its ultimate tensile strength [191,196].

4.3.1.2 Proteoglycans

Originally, the role of proteoglycans was thought to be solely structural in that they contribute to the compressive strength of bone [193]. More recently, studies on transgenic mice have confirmed the role of proteoglycans (such as perlecan and biglycan) in defining spacial organisation of the extracellular matrix and have suggested that they also facilitate cellular signalling and interactions with growth factors during development [197].

4.3.1.3 Osteocalcin

Osteocalcin is synthesised and secreted by osteoblasts [192] and is unique to bone [193]. It may have important signalling functions, act as a marker for bone turnover and regulate hydroxyapatite crystal formation [192,193,198].

4.3.1.4 Osteonectin

Osteonectin is the most abundant non-collagenous organic component of bone [198]. It bonds calcium and therefore may have a role in the mineralisation process. It also affects osteoblast growth and proliferation [192,198].

4.3.1.5 Osteopontin

Osteopontin is a phosphoprotein, that is, an acid protein that is phosphorylated. It contains a tripeptide sequence also found in proteins with cell binding properties via receptors called integrins. Osteopontin therefore may bind the osteoclast to the bone to facilitate bone resorption. This is consistent with the fact that osteopontin synthesis is stimulated by calcitrol, which is known to stimulate bone resorption [198]. It may also aid in the mineralisation process [192].

4.3.2 Inorganic Bone Matrix

The porous organic matrix is permeated by inorganic components that make up approximately 65% of the bone [194]. The inorganic matrix of bone is generically referred to as hydroxyapatite, [$Ca_{10}(PO_4)_6(OH)_2$], and is a plate-like crystal 20-80nm in length and 2-5nm in thickness. This crystal is amenable to apposition and resorption due to its small size and imperfect structure when compared to other apatites [193].

The functions of the inorganic matrix are to provide the bone with tensile strength and provide the principle site for ion storage [191].

4.3.2.1 Mineralisation

The organic matrix begins to mineralise 10-15 days following its synthesis. Once initiated, 70% of the total mineral content is rapidly laid down with the remaining 30% taking several months to deposit. The exact process is unclear however is believed to involve small, round, extracellular, bilaminar organelles that bud from hypertrophic chondrocytes or osteoblasts [193]. These organelles disintegrate and their contents (alkaline phosphatase, pyrophosphates, calcium adenosinetriphosphatase, metalloproteinases, proteoglycans, and anionic phospholipids) are exposed to the matrix providing a suitable micro-environment for initial mineralisation [194]. Collagen fibrils, fibronectin, osteocalcin and osteonectin organise the bone mineral crystal. Other glycoproteins, such as matrix-gla, ensure over-mineralisation does not occur [193].

4.4 Gross Bone Structure

Bones exists in two morphological forms- cortical bone and cancellous bone. They are histologically identical [194].

4.4.1 Cortical Bone

Cortical bone surrounds the marrow cavity and the trabecular bone. It accounts for 80% of the skeletal mass [191,192] and has a high modulus of elasticity.

4.4.2 Cancellous Bone

The cancellous, or trabecular bone occupies the central medullary cavity and is interspersed throughout the bone marrow [194,199]. Due to its porous nature, cancellous bone has a low modulus of elasticity.

4.5 Microscopic Bone Structure

Microscopically, bone is made up of two distinct phenotypes - woven bone and lamellar bone.

4.5.1 Woven Bone

Woven, or primary bone, is characteristic of embryonic and foetal development, and is also found in the healthy adult skeleton at ligament and tendon insertions [193], cranial sutures, ear ossicles, and epiphyseal plates [191]. Woven bone presents during the initial stages of fracture healing and under other pathological conditions such as osteogenic tumour and metastasis formation [191,193].

The collagen fibre orientation of woven bone is irregular and disorganised and the osteocytes are randomly scattered throughout the matrix [191,193]. Woven bone has a high rate of metabolic activity [191].

4.5.2 Lamellar Bone

Lamellar or secondary bone, replaces woven bone during development or bone repair [191]. Both cortical and cancellous bone are histologically identical and consist of microscopic layers or lamellae [194]. The three types of lamellae are[194,199]:

1. Circumferential lamellae enclose the entire bone and are located just below the periosteum.
2. Concentric lamellae form the bulk of compact bone and form the basic metabolic unit of both cortical and cancellous bone called the osteon or Haversian system. Osteons run parallel to the long axis of the bone. In the centre of the osteon there is a canal called the Haversian canal that is lined by a single layer of bone cells and houses a single capillary. The

capillaries of the Haversian canals communicate by Volkmann's canals that run perpendicular to the long axis of the bone.

3. Interstitial lamellae which are remnant osteons lie between intact osteons to fill the gaps between the concentric lamellae.

4.5.3 Periosteum

The outer layer of cortical bone is covered by the periosteum, a double layered connective tissue membrane [194,199]. The outer layer (or fibrous layer), consists of dense irregular connective tissue. The inner layer (or osteogenic layer) abuts the bone surface and houses osteoblasts and osteoclasts. The periosteum is supplied by nerves, blood vessels and lymphatic vessels that enter the bone via foramen and is firmly attached to the bone via Sharpey's fibres that become particularly dense at insertion points for tendons and ligaments [192,199].

4.5.4 Endosteum

The internal surfaces of the compact bone, surfaces of the cancellous bone and the Haversian and Volkmann canals are covered by the endosteum [199]. This is a delicate membranous connective tissue [194] containing osteoblasts, osteoclasts and blood vessels [192].

4.6 Osteogenesis

Osteogenesis refers to the formation of bone which involves osteoid production by osteoblasts followed by hydroxyapetite deposition [191]. There are two modes of ossification namely endochondral ossification and intramembranous ossification [194].

4.6.1 Endochondral Ossification

Endochondral ossification takes place when cartilage is replaced by bone and occurs at the extremities of long bones, vertebrae, ribs and mandibular condyle. Cartilage cells differentiate from condensations of mesenchymal cells and proliferate rapidly by either interstitial or appositional growth. In general, zones of cartilage cells stratify into layers of proliferative, hypertrophic and

mature phenotypes as well as a zone of initial mineralisation. The mature chondrocytes release type X collagen and non-collagenous proteins and at the same time proteoglycans begin to break down creating an environment fit for mineralisation [194].

4.6.2 Intramembranous Ossification

Intramembranous ossification is bone formation from an organic matrix membrane. Following an increase in vasculature at the site of bone formation, mesenchymal cells proliferate, condense and differentiate into osteoblasts that secrete the bone matrix. During differentiation, the mesenchymal cells begin to display alkaline phosphatase activity and mineralisation ensues [194].

4.7 Physical Properties of Bone

Bone is able to respond to its external environment including gravity, impact, and muscle contraction and possesses the physical properties of anisotrophy and viscoelasticity to facilitate this and carry out the functions of mechanical support and locomotion. After mechanical loading, a cascade of cellular events translates external signals into chemical messages that can instigate bone turnover and remodelling.

4.7.1 Stress

Stress is defined as force per unit area, and is equal in magnitude but opposite in direction to the applied load.

Tensile stress is two forces acting along the same line in opposite directions; compressive stress is two forces acting along the same line in the same direction; and shear stress is two forces acting parallel to each other but not along the same line.

4.7.2 Strain

Following the application of a mechanical stimulus, strain is produced in the bone. Mechanical strain (ε or microstrain με- 10^{-6}) is a measure to quantify mechanical deformation in bone and is the change in length over the original length (ε= ΔL/L) [200].

4.7.3 Anisotrophy

Bone strength and stiffness varies with the direction of trabecular alignment, in response to the specific type of load applied. This phenomenon is called anisotrophy and allows an increase in strength without an increase in mass, thereby favouring tissue economy [201] The strength and rigidity of bone are therefore greatest in the direction of normal loading [191].

4.7.4 Viscoelasticity

Viscoelasticy is the phenomenon that allows bone to demonstrate different properties according to the rate of force application. At lower rates of loading, bone demonstrates a lower modulus of elasticity and behaves like a viscous material; at higher rates of loading, bone behaves as a brittle material [191].

4.8 Bone Modelling and Remodelling

4.8.1 Bone Modelling

Modelling is the gradual process by which bones change their overall shape in response to physiological or mechanical factors. During this process, the osteoblasts and osteoclasts act independently in response to the stimulating factors [192,193].

4.8.2 Bone Remodelling

Bone remodelling is the process whereby bone is renewed to maintain bone strength and mineral homeostasis throughout the whole life span. This process involves the coupling of osteoblasts and osteoclasts to perform resorption of old bone and synthesis of new bone. Bone is completely turned

over through the resorptive process, followed by matrix deposition and mineralisation in order to prevent the accumulation of micro damage. Sites of bone remodelling occur randomly [192,193].

4.9 Structural Adaption of Bone

Associations between bone morphology and mechanical load stimuli were first made by Galileo [202], Wyman [203], Roux [204] and Wolff [25] all of whom supported the Trajectorial Theory of bone structure. This theory was based on the observation that bony trabeculae are arranged in particular morphological patterns dictated by lines of stress induced by function in order to optimise resistance to loading. This concept of 'form follows function' was first published by Julius Wolff in 1892 [25] in the book titled *"Das Gesetz der Transformation der Knochen" ("The Law of Bone Transformation")* and is currently widely referred to as Wolff's Law [25].

Following the publication of Wolff's Law, other research attempted to further explain the relationship between bone form and function. Koch in 1917 [205] analysed mathematically static stress trajectories in a human femur analogue following application of loads similar to body weight. His conclusions were consistent with Wolff's law in that the trabeculae arrangement of his model was determined by maximum and minimum stresses in either a compressive or tensile systems. Carey in 1929 [206] disqualified Kock's findings thereby opposing Wolff's Law based on the belief that dynamic stresses associated with muscle activity rather than static stresses were essential in skeletal adaption and morphology. Frost in 1964 [207] concurred with Carey, however believed the dynamic factors of stress originated from changes in the bone marrow during loading. Frost likened bone adaption to the external environment to that of a thermostat and hence proposed his 'mechanostat' theory [208] which proposes that bones adapt their strength to keep the strain caused by physiological loads close to a set point.The mechanostat was considered to be 'off' (anabolically inactive) under normal strain circumstances and 'on' (anabolically active) when mechanical input produced strains above the normal strain thresholds. This is an effective analogy, however by only taking into

consideration the strain magnitude, the mechanostat theory omits the other parameters of the mechanical milieu, thereby over simplying the role of strain in bone remodelling [209].

Enlow in 1968 [210] reviewed the theories of the time and concluded that available evidence could not validate Wolff's Law. Enlow concluded that mechanical stimuli alone could not account for bone growth and remodelling and that several other factors were involved.

Lanyon in 1974 used in vivo rosette strain gauges not previously available, on the lateral calcaneus of eight sheep which allowed recordings of bone deformation during various physical activities. The sites were examined radiographically and it was concluded that at that particular sites of bone, the Trajectorial Theory of bone structure, and hence Wolff's Law could be supported experimentally [211].

4.9.1 The Optimal Strain Environment

Originally, Wolff's Law was interpreted such that the ultimate goal of bone adaption to the external environment was to minimise the strain in the bone as far as possible through bone remodelling. Contrary to this static material based explanation, it is currently believed that the ultimate goal of bone adaption is to strive toward a particular strain environment at each particular site in each particular bone [193].

Each region of each bone is genetically programmed to perceive a particular amount and pattern of dynamic strain to be its normal. Different bones serve different functions resulting in different distributions of strain across different bones [28]. Therefore, it is feasible that each area on each bone has its own 'optimal strain environment'[27]. A deviation from this optimal strain environment in response to a change in function, results in bone remodelling to suit the demand. Resorption is driven by systemically derived factors that control metabolic output for the optimal conservation of energy. At the other end of the dynamic equilibrium, apposition is driven by local mechanically derived stimuli in the form of external loading. Complete disuse results in depletion of bone to a genetically determined baseline [27,212,213].

4.9.2 The Cellular Basis of Structural Bone Adaption

Maintenance of the optimal strain environment requires cells that can respond to the demands of the mechanical environment [213]. These cells enable the conversion of a physical force into a biochemical, cellular response. This process is called mechanotransduction [201].

Osteocytes are believed to be the predominant mechanosensitive cells in bone, as evidenced by many studies reviewed by Burger and Klein-Nulend in 1999 [195], and are therefore considered the determinants of bone modelling and remodelling and thus the optimal strain environment. The lacuno-canalicular system [195], is comprised of copious osteocytes in osteocytic lacunae that communicate with osteoblasts and bone lining cells [214] via cell processes and gap junctions [215,216] that penetrate through the bone's canaliculi. This morphological arrangement permits mechanosensation and mechanotransduction of mechanical signals in bone [216-218].

The maximum deformations in bone are relatively small at <0.3%, however strain in the order of 1-3% are needed to induce a cellular response and therefore bone remodelling [219]. This can be explained by mechanical activation of osteocytes by flow of interstitial fluid through the lacuno-canalicular, first proposed by Cowin *et al.* [220]. Bone deforms following the application of a load, producing strain concentrations at the osteocytic lacunae as interstitial fluid is expressed out through thin layers of non-mineralised matrix surrounding the cell bodies and cell processes [195]. The combination of the canalicular diameter and the osteocyte diameter produces an annular porosity that is able to generate fluid flow at the osteocyte membrane in the form of fluid sheer stresses [221] and electric potentials called streaming potentials [222]. Fluid sheer stresses primarily influence the cell wall processes of the mechanosensitive osteocytes via integrins and induce reorganisation of the cytoskeleton resulting in a change in the cells metabolic activity [223,224]. Electric potentials play only a very minor role in this process [225].

Burger and Klein-Nulend [195] explain the hypothesis on how the lacuno-canalicular network and bone remodelling relate. Normal physical activity induces fluid sheer stresses across the osteocyte membranes that maintain osteocyte homeostasis and provides adequate mechanical stimulation to induce basal fluid sheer stress. Increases in physical activity results in abnormally high fluid sheer stresses and recruitment of osteoblasts by the osteocytes. Bone modelling follows to restore the normal level of loading and the 'normal' state of the osteocyte. Decreases in physical activity results in a decrease in sheer fluid stress and perturbance of cell homeostasis resulting in osteocyte apoptosis and recruitment of osteoclasts. Bronckers *et al.* [226] in 1996 found a strong positive correlation between the presence of osteocytes and osteoclasts in highly resorptive areas. Osteoclastic activity results in bone resorption and, once again, restoration of the bone to its 'normal' level of loading.

This hypothesis relates to attainment of the optimal strain environment whereby bone is remodelled until the strain engendered by loading is at the 'normal' strain value for that particular area on that particular bone. This is the mechanism by which bone responds to the demands of its mechanical environment [213].

5 The Evolution of High-Frequency, Low-Magnitude Mechanical Stimulation as a Therapeutic Means

It is undisputed that external mechanical signals in general, are vital in maintaining skeletal structure. Given that mechanical stimuli are variable in character, further consideration of the specific parameters of the mechanical milieu and their individual involvement in bone adaption is crucial. Mechanical stimuli may be static or dynamic; axial or torsional; and variable in duration, magnitude and frequency. Wolff's Law fails to identify the specific parameters of the osteogenic

mechanical stimulus and is therefore limited in being able to fully explain functional bone adaption [227]. Research has investigated the separate and distinct roles of the different derivatives of the mechanical environment to determine which of these are relevant to osteoregulation and which are simply superfluous to loading [227]. Osteoporosis, the disease characterised by increased porosity of the skeleton resulting from reduced bone mass [228], formed the impetus for most of these studies, through which high-frequency, low-magnitude mechanical stimuli have emerged as a potential therapeutic entity.

5.1 Mechanical Loading

5.1.1 Observational Studies

Early studies make the overall link between weight bearing activity and bone mineral density (grams per square centimetre) [229,230] and were qualitative evidence of Wolff's Law. Human exercise studies show that high impact physical activity such as tennis, squash, gymnastics and softball have a higher osteogenic potential than low impact activity such as swimming and rowing [231,232]. Studies investigating exercises executed unilaterally such as tennis, show greater bone mass in the dominant playing arm where the load is applied [233,234].

Conversely, disuse in the form of immobilisation [235-240] or anti-gravity during space travel [241-244] induces catabolic effects.

Whilst the evidence from these studies supports the form-follows function concept of Wolff's Law, subsequent studies strived to define the specific parameters of the mechanical stimuli responsible for bone remodelling.

5.1.2 Experimental Studies

Hert and co-workers [245,246] carried out a series of experiments testing the reaction of bone to mechanical stimuli using pins inserted into the diaphysis of the tibiae of mature and immature

rabbits. Their most significant finding was that dynamic but not static loads were osteogenic, irrespective of the age of the animal and the manner in which the load was applied (i.e. compressive or tensile). The studies were carried out prior to the introduction of strain gauges, limiting the studies in two ways; i) the magnitude of the osteogenic loads during normal locomotion had not yet been established so the magnitude of experimental loading used in these studies was estimated based on the body weight of the animal and ii) the strains engendered in the bone by the load could not be measured.

To establish the epigenetic involvement of individual components of the physical milieu, more specific information of the skeleton's loading history was required. The discovery of the strain gauge was instrumental in the progression of the knowledge on bone remodelling in response to mechanical loading, as it enabled quantification of the mechanical environment. The use of strain gauges in animal experiments enabled specific correlations to be made between changes in the mechanical milieu and the resultant increases or decreases in skeletal mass [247]. The uniaxial, single element strain gauge was described by Lanyon and Smith in 1970 [248]. This device was only able to measure surface strains in the direction of its alignment over the small area on which it adheres. Due to such limitations, the rosette strain gauges became the device of choice. They were comprised of three stacked elements arranged at 45 degrees bonded to the bone surface as one unit. Such a design allowed the simultaneous measurement of surface strains in three directions and could accurately measure the magnitude, direction and distribution of the principle strain and the maximum sheer strain [249] during normal locomotion and in response to experimentally applied loads.

Strain gauges were used early on to demonstrate the sensitivity of bones to adaptive remodelling to minor alterations in the mechanical environment. Goodship and co-workers [250] performed unilateral ostectomy of the ulna diaphysis in young pigs. The principle compressive strain or over-strain on the

remaining radial shaft was two to two and a half times that of the pre-surgical values and was followed by considerable rapid bone remodelling, thereby doubling the cross-sectional area of the bone. After three months, the principle compressive strain in the radius on the operated side was not significantly different to the contra lateral radius and approached normal strain values.

To eliminate the factor of growth Lanyon *et al.* [251] conducted a similar study on adult sheep. Interestingly, the over-strain on the cranial surface of the radius was 20% - more than twice the amount at the caudal surface, however more bone was deposited over the caudal surface over one year. Towards the end of the experiment, the absolute levels of functional strain at the bone forming surfaces were less than normal. It was therefore concluded that adaptive remodelling is influenced by the distribution of strain, rather than the value of absolute peak strain.

These experiments however, still did not disclose the specific nature of the mechanically induced osteogenic stimulus. Specific mechanical parameters could not be determined due to the presence of loads applied during normal function of the animal. For this reason, the inability to control the strain environment prevented the identification of the precise osteogenic signal.

5.2 Studies on the Mechanical Milieu

The introduction of the avian ulna model allowed a unique means to study the mechanical milieu, without the confounding loads of normal ambulation. This model allowed the investigator to control and monitor the strain environment of any specific bone, thereby allowing investigation of the derivatives of the mechanical environment in order to elucidate which ones are osteogenic and which ones are superfluous to the applied loads. Functional isolation of the ulna diaphysis is achieved by osteotomy at the epiphyseal-metaphyseal junction and covering the ends of the shaft with stainless steel caps [227]. The desired load is applied to the bone using a modified servo-hydraulic materials testing machine connected to the bone transcutaneously via Steinmann pins that penetrate the stainless steel caps at the ends of the bone shafts. The mobility of the animal and

therefore the animal's quality of life is not perturbed, and the contra-lateral wing easily serves as a control [252].

5.2.1 Parameters of the Mechanical Milieu

Using the Avian Ulna Model, derivatives of the mechanical environment were able to be investigated. The derivatives of the mechanical environment of interest here include strain duration, strain magnitude, strain frequency and strain history. The character of the load is also of importance.

5.2.1.1 Character of the Load

5.2.1.1.1 Static or Dynamic Load

Lanyon and Rubin in 1984 [253] evaluated and compared the osteoregulatory potential of a dynamic (intermittent) load regime with a static (continuous) load regime in the avian ulna model using three male turkeys over 8 weeks. Bone pins were placed at either end of the ulna shaft and joined externally by helical springs that were loaded continuously to create static loading (528N), or intermittently by an Instron machine (modification of a servo-hydraulic materials test machine able to apply load in a controlled manner [213]) to create dynamic loading (525N) at a frequency of 1Hz as a ramped square wave at a strain rate of $0.01s^{-1}$ during the ramps. The strain engendered in the statically loaded bone was equal to the peak strain encountered during dynamic loading (2000με). These were compared to one control of disuse alone. Results showed a 40% increase in bone area in the dynamically loaded bone. Cortical thinning and intracortical porosis was observed in both statically loaded bone and disuse bone. This is consistent with the natural environment whereby absolute strain fails to induce a cellular response within bone when there is no mechanical skeletal advantage. Static loads of the same magnitude as peak dynamic loads applied for short daily periods fail to induce favourable bone remodelling, whereas dynamic loads are osteogenic. This is consistent with the findings of Hert and Liskova [245].

5.2.1.1.2 Axial or Torsional Load

The use of the avian ulna model showed that intracortical bone response was dependant on the manner in which bone was loaded [254]. Axial loading promoted cell activity inducing an increase in intra-cortical turnover seen as intracortical porosis, increase in the area lost and increase in mean pore size similar to that seen in disuse. On the contrary, torsional loading inhibited bone resorption indicated by, no intracortical porosis, no area loss and no change in the size of the pores. This demonstrates that cells are able to discern between different loading environments and that both axial and torsional loading influence bone mass positively, but in different ways. This furthered the idea that specific parameters of the mechanical environment have specific roles in defining bone architecture [254].

5.2.1.2 Strain Duration

Rubin and Lanyon [219] demonstrated that a considerable osteogenic response can occur in response to few cycles of loading lasting a short period of time. The ulna of roosters were either not loaded or loaded daily with 4, 36, 360 or 1800 consecutive load cycles at 0.5Hz for an experimental duration of six weeks. The unloaded ulnae showed no change for two weeks followed by a gradual decline to 88±2% of normal bone mineral content. Four 0.5Hz loading cycles per day (taking only 8 seconds) were enough to maintain status quo and prevent disuse osteoporosis. Thirty six 0.5Hz daily loading cycles (taking only 72 seconds) induced rapid periosteal and endosteal bone apposition over the first two to three weeks, peaking at 28 days. The bone was stable at 6 weeks with a bone mineral content 133±11% above normal. Interestingly, both the 360 and 1800 cycle loading regimes did not induce any additional changes in bone character or size than the 36 cycle regime.

This study demonstrated the extreme sensitivity of bone remodelling to a small number of strain cycles, however did not indicate which aspect of the strain regimen engendered the response [227].

5.2.1.3 Strain Magnitude

Rubin and Lanyon in 1985 [28] designed an experiment using the avian ulna model to determine the effect of strain magnitude on regulation of bone mass. Thirty turkey ulnae were investigated over 8 weeks. The number of loading cycles (100), frequency (1Hz), duration of loading (100s) and the rate of strain (10000 με/s) were kept constant throughout the experiment. The controlled variable, namely the peak strain magnitude was set at 500, 1000, 1500, 2000, 3000 and 4000 microstrains. To avoid confounding variables, the bones were deprived of natural loading by external fixation. Following sacrifice, the experimental ulnae were compared with their contra-lateral counterparts. Strains less than 1000με resulted in bone loss whereas strains above 1000με were osteogenic on the periosteal and endosteal surface only. Bone was maintained at 1000με. This experiment demonstrates a positive dose-response relationship between peak strain magnitude and change in bone mass. Interestingly, the sites of new bone formation were not associated with those areas of the bone exposed to the highest strains. This would indicate that bone tissue does not adapt to peak strain *per se*, but rather to the distribution of the strain (i.e. the spacial pattern of strain in response to an applied load.)

5.2.1.4 Strain Frequency

Synthesis of the data from the studies described above begins to demonstrate the role of frequency in maintaining bone mass. Strain frequency refers to the number of loading cycles that occur within one second. Rubin and Lanyon's study demonstrating the effect of strain duration on bone [219] showed that a mechanical stimulus with a frequency of 0.5Hz over 4 cycles and 8 seconds engendering a strain of 2000με maintains bone mass. This strain magnitude is comparable to the peak strains generated during vigorous activity over several animal species [27,255-258]. Rubin and Lanyon's study on strain magnitude [28] showed that bone mass could also be maintained with a frequency of 1Hz over 100 load cycles and 100 seconds engendering a peak strain of 1000με.

Another study by McLeod and Rubin [259] investigated the effect of varying the frequency of the applied load between 1Hz and 60Hz for a constant of 10minutes per day using the avian ulna model. The strains required to maintain bone mass were recorded. At a frequency of 1Hz (600 load cycles), strain greater than 700με were required to maintain bone mass; at 30Hz (18000 load cycles), a strain of 400με was required to maintain bone mass; at 60Hz (36000 load cycles), a strain of only 270με was required to maintain bone mass.

The above experiments explained the components of the mechanical environment important in determining bone mass. In particular, they illustrated that bone is influenced more by strain magnitude than cycle number and that the temporal characteristic of the strain signal, that is the frequency, is extremely important. An examination of the role of these aspects of the mechanical environment during normal functional conditions furthers the explanation of the goals of bone adaption in vivo.

5.2.1.5 Strain History

Several key studies were able to implicate the importance of loading frequency in bone adaptation in the natural state, from which the authors proposed the use of high-frequency stimulation to bone as a potential therapeutic means. These studies are discussed below.

5.2.1.5.1 Dynamic Strain Similarity

Locomotion represents the principle source of functional stimuli within the appendicular skeleton and therefore may reflect the ultimate product of the adaptive process. Rubin and Lanyon in 1982 [256] used rosette gauges attached to the radius of tibia of horses and dogs and measured the strain in bone over the entire ranges of gait and speed while the animals ran on a treadmill. Peak strain magnitudes ranged between 2000-3000με which were consistent with peak strains found in buffalo, elephants, turkey, pig and sheep [256-258]. Hylander and Cropmton [260] found this to be the case in the mandible of *Macaca fascicularis* during mastication. Hence, there is uniformity in peak bone strains

during vigorous activity across species, regardless of size and mode of locomotion of the animal, and a 350 times difference in mass across the range of species. In addition there is a similar safety margin to mechanical failure in the load bearing bones of different species. This was found to be 2-3 times greater than the peak strain encountered during physical activity [27,255,256]. This has been coined 'dynamic strain similarity' and shows that the safety factors of bone are maintained not by allometrically scaling bone dimensions but rather by allometrically scaling the magnitude of peak forces applied to them during vigorous locomotion [255]. This concept also advocates the concept of bone working towards achieving a favourable strain environment, rather than reducing it as far as possible as Wolff's Law implies [255].

Recognition of the concept of dynamic strain similarity formed the foundation of Fritton *et al.* study on strain history.

5.2.1.5.2 Strain History: The Importance of Strain Magnitude and Frequency

Despite extensive experimental proof of the specific mechanical parameters relevant to defining bone morphology, the specific parameters of the mechanical milieu defining bone morphology in the natural state were still unclear. Fritton *et al.* in 2000 [29] addressed this matter by investigating the strain history in bones of animals of different species. Strain history is defined as the value of all strain components as a function of time for a specified time period at that place characterised by its significant features such as frequency or peak magnitude [29]. It was hypothesised that if a broad spectrum of bone strain is considered, some portions of the strain history must be similar and spatially uniform, that is, similar at different locations, for different bones of different species. This hypothesis evolved from the concept of dynamic strain similarity whereby, peak strains engendered during vigorous activities are of similar magnitudes across different species, but are not spatially uniform across a bone section. For example, during the course of a day, the turkey ulna show relatively few peak strain events [261], yet this bone is normal and capable of supporting the animal

during brief periods of peak usage. The tibiae in the turkey and the bones of more active animals such as the dog are subject to greater functional demands but once again, it is known that all bones have similar peak strain values. This suggests that i) events other than peak strain magnitudes are involved in bone adaption and make a significant contribution to the strain history and ii) each bone in each animal has a different threshold at which modelling must begin. This is contrary to common belief that maximum strain during vigorous activity has the greatest influence on bone adaption.

In vivo rosette strain gauges were placed on the tibia of one adult male dog, one adult male turkey, one adult female sheep and the ulna of three adult male turkeys and the strain signals collected over 12-24 hours. Computer software was designed to quantify the number of daily occurrences of the strain and to estimate the average spectral characteristics of the bone strain signals.

Results showed that peak strains encountered during vigorous activities occur relatively only a few times per day (once in the order of 1000με), while the very small strains occur many times a day (hundreds of times in the order of 100με and thousands of times in the order of 10με). The peak strains encountered during more vigorous activity such as walking occurred at a low frequency (for example 1000με at 0.6Hz in the turkey tibia), whereas the peak strains engendered when standing were in the order of 10με and up to 40Hz. This is in accordance with the findings of Rubin and Lanyon [256] who showed that the spectral distribution of the low frequency strain energy (1-10Hz) changes substantially as a function of speed and gait but the higher frequency strains (20-30Hz) remain in a narrow frequency band which is independent of species, animal size, gait or speed of travel. Based on these findings, the authors concluded that the constant occurrence of strain events in bone spanning a wide but consistent range of frequency and amplitude is important in the organisation of bone tissue [29]. Other findings from this experiment are found in Appendix 1e.

5.2.1.5.3 Disproving the Daily Stress Stimulus Theory

This concept of a continual barrage of activity required to maintain skeletal mass is contrary to the original theories of bone adaption. Initially, it was thought that homeostasis is maintained over some range of routine daily stress / strain stimuli and deviations away from certain set-points initiate bone remodelling [208]. The daily stress strain stimulus theory reflected these ideas suggesting that the mechanical stimulus arises from a synthesis of peak magnitudes from each loading event during the day and that the critical aspects of loading are stress/strain magnitude and number of loading cycles. The daily stress strain stimulus theory was expressed as a mathematical formula [26] and was commonly used in computational models of bone adaption without having been tested in vivo. Based on the evidence that increasing frequency of loading events reduces the magnitude of the strain required to maintain mass [259], and that a continual barrage of small events are critical in the design of the skeleton [29], Qin *et al.* [26] set out to disprove the 'daily stress strain stimulus theory'. Qin *et al*. [26] proposed that the number of loading cycles and stress/strain magnitude are insufficient in defining the bone maintenance signal and that the limitation should become apparent as the number of daily load cycles is dramatically increased. The avian ulna model in turkeys was used and changes in morphology investigated following eight weeks of disuse, compared with eight weeks of disuse and loading at 30Hz over 60 minutes per day (corresponding to 108000 loading cycles), enough to engender peak strains of 100με. The loading regime was designed to maintain bone mass and was prescribed based on findings from previous studies. As expected, the disuse group showed a decrease in the cross sectional area of each sector of bone. In the loaded group, there was a significant inhibition of bone loss and approximately 100,000 load cycles, engendering a minimum threshold of 70με, were required for bone maintenance. When these values were put into the daily stress stimulus theory formula, using the recommended value for the constant 'm' (a value of 4 in humans), it predicted that a strain greater than 300με would be necessary to maintain bone mass. Hence, when an increased number of loading cycles was incorporated into the daily stress strain

formula, it became apparent that the formula does not fit the wider range of loading cycle numbers. They concluded that for the daily stress strain stimulus theory to be true, either the constant 'm' must be a nonlinear function of the number of cycles, or be dependent on frequency, strain rates or duration associated with the loading regime.

A subsequent study by Adams *et al.* [261] applied different loading regimens to the adult turkey ulna known from previous data to maintain bone mass or cause bone formation. When the data from this experiment was incorporated into the daily stress stimulus formula, the theory failed to predict cortical bone adaption. Some maintenance regimes were associated with a higher daily stimulus than some appositional surface modelling regimens. They concluded that the daily stress stimulus theory did not consistently discriminate appositional surface modelling regimens from maintenance regimens.

Qin *et al.* [26] showed that the sensitivity of bone to mechanical loading increases dramatically with an increase in frequency, and therefore, smaller strains are required to maintain bone mass. Contrary to the normal interpretation of Wolff's Law, minimising strain is not the prime goal of bone adaption. Rather the goal of bone adaption is to alter the skeletal morphology in response to environmental influence to generate a certain type of strain [247]. Given that loads of higher frequency can reduce the strain in bone and still maintain skeletal mass, Qin proposed the idea that extremely low strain magnitudes, induced at a high-frequency, for a sufficient period of time may be used therapeutically to promote osteogenesis in bone.

5.2.1.5.4 The Role of Muscles in Bone Morphology

A constant barrage of small loading events, engendering many small strains in the bone, define bone mass [29]. Based on this, it is reasonable to implicate the role of muscles in bone morphology characterisation [30]. Compared to impact loads, muscle contraction imposes much smaller strains on the skeleton and therefore might dominate the strain history of bone. This has been demonstrated

by looking at the reduction of bone mass with age and the possible correlation with muscle changes occurring with age.

Huang *et al*. [262] recorded the acoustic vibrations, reflective of the firing rates of motor neurons, in forty human subjects spanning from 20-83 years of age. The recordings were categorised as 1-50Hz, 1-25Hz and 25-50Hz. It was observed that the high-frequency band (25-50Hz) decreased significantly with age, at a rate of 1.2% per year, resulting in a reduction in the mechanical stimuli important in bone maintenance. Hence, with a degeneration of the high-frequency strain inputs from the muscle, a decrease in bone mass with age may still be seen, despite physical activity and/or pharmacological intervention. Given that bone is more sensitive to higher frequencies, generating high-frequency mechanical stimuli through mechanical vibration may be the best therapeutic means in combating bone loss associated with ageing [26].

6 High-frequency, Low-magnitude Mechanical Stimuli for Therapeutic Use

High-frequency, low-magnitude stimulation, more simply referred to as vibration, is defined as a mechanical stimulus characterised by an oscillatory motion. The biomechanical variables that determine the intensity of the vibratory stimulus are the frequency (the rate at which the load is applied, measured in Hertz- Hz) and the amplitude (the extent of the oscillatory motion, measured in millimetres - mm) [39,263]. The vibration also has a magnitude expressed as a function of the earth's gravitational field ($9.8 m.s^{-2}$ =1g), measured in grams (g) [39].

Given that the weight supporting skeleton facilitates transmission of mechanical energy into bone tissue, a dynamic strain on the skeleton can be induced by modulating the g-force [31]. By altering the gravitational force, the resultant strains would be transferred to the skeleton along a normal

trajectory, hence concentrating the stimulus in high weight bearing areas over the low weight bearing areas [31].

6.1 Whole Body Vibration

6.1.1 Development of the Whole Body Vibration Device

Fritton *et al.* [31] developed a small low cost device for performing controlled whole body vibration of the human skeleton to assist in studies of vertical acceleration in a clinical setting. Fritton *et al.* [31] aimed to design and construct a portable device to deliver peak floor accelerations of up to 0.15g at frequencies of approximately 30Hz in the 40 to 80 kilogram (Kg) adult that adhered with ISO standards. The device consisted of five basic components: the base; a support plate on which the subject stands; twelve stainless steel compression springs between the base and the support plate; an electronic linear actuator that provides the force input into the platform consisting of the magnetic core and coil and the electronics required to drive the actuator. The vibration platform was tested on one turkey and one human and proved successful in delivering mechanical vibration in the vicinity of 30Hz at 0.15g with variable transmissibility at different sites of the body.

Currently, vibration platforms are manufactured and advertised by many companies as an effective means to strengthen muscles, improve bone mass and promote reduction in fat.

6.1.2 Transmissibility of Whole Body Vibration to the Skeleton

Rubin *et al.* in 2003 [32] tested the degree to which high-frequency, low-magnitude vibratory stimuli are transmitted to the proximal femur and lumbar vertebrae of the standing human using whole body vibration. Six healthy subjects took part in the investigation. Transcutaneous pins were placed by an orthopaedic surgeon under local anaesthesia and sterile conditions into the spinous process of the fourth lumbar vertebra and the greater trochanter of the femur. The pins were oriented parallel to the floor and perpendicular to the spinal column. Accelerometers attached to the pins recorded

the data. The whole-body vibration device developed by Fritton *et al*. [31] was used and vibration at 2Hz intervals was recorded between 15Hz and 35Hz. The subjects were asked to stand in three different postures: erect with knees extended and locked; relaxed with knees straight; and knees flexed at 20 degrees. Subjects were asked to report any discomfort if and when it occurred. One subject was excluded from the experiment and the trochanter pin placement was not considered in another subject. Results showed that with the subject standing erect at frequencies below 20Hz, the transmissibility at the hip exceeded 100% suggesting resonance of the stimulus. However in the same stance above 25Hz, the transmissibility reduced to 80% in the hip and spine. A relaxed stance reduced this to 60%, and when the knees were bent the transmissibility was further reduced to 30%.

It is therefore evident that vibrations from high-frequency, low-magnitude whole body vibration are effectively transmitted to the hip and spine. The degree of attenuation of the stimulus depends on the stance of the individual in terms of the amount of bending at the knees [32].

6.2 Whole Body Vibration and Bone

The experimental application of whole body vibration on the skeleton has been studied in animals and humans. Results suggest that whole body vibration may be effective therapy when bone maintenance or anabolism is required in cases such as mobility impaired patients, decreased bone density and surgical healing.

6.2.1 Disuse

Skeletal unloading in the absence of vibration, has shown the pattern and molecular processes associated with disuse. These following studies provide baseline information when considering the effects of vibration on the skeleton with many of the vibration studies testing the effects of high-frequency mechanical stimulation in disuse situations.

Weinreb *et al.* [239] investigated short term recovery of osteopenia in cancellous and cortical bone induced by skeletal unloading in young rats. The control group experienced normal loading and was compared against the group unloaded by sciatic neurectomy and the group unloaded for 9 days by fixation, followed by reloading for 1-3 weeks. The bone parameters were investigated with bone histomorphometry. The results showed that: greater loss of bone mass occurred with unloading by fixation; bone loss is more rapid than bone recovery; and cancellous bone recuperates faster than the cortical bone.

Sakata *et al.* [240] aimed to clarify how skeletal unloading induces resistance to the effects of IGF administration in vivo and in vitro with respect to bone formation. Male growth hormone deficient dwarf rats were used to investigate: i) in vivo response of bone to IGF-I during skeletal unloading; ii) the response of progenitor cells from unloaded bone to IGF-I in vitro; iii) the role of integrins in mediating progenitor cell response to IGF-I. The results showed that skeletal unloading induces resistance to IGF-I by inhibiting the activation of the IGF-I signalling pathways at least in part by down regulation of the integrin signalling pathway resulting in decreased proliferation of the osteoblast and their precursors.

6.2.2 Anabolism

Rubin *et al.* [39] aimed to determine whether low-magnitude, high-frequency mechanical signals can restore anabolic bone cell activity inhibited by disuse. Adult female Sprague-Dawley rats divided into 6 groups: baseline controls (n=15), age matched controls (n=30), mechanical stimulation for 10 minutes per day at 90Hz and 0.25g (n=21), disuse via hind leg suspension (n=11), disuse interrupted by 10 minutes per day of normal weight bearing (n=7) and disuse interrupted by 10 mins per day mechanical stimulation at 90Hz and 0.25g (n=19). The duration of the experiment was 28 days, after which bone forming rates (BFR) were examined. Mechanical stimulation increased BFR by 97% compared to baseline controls; disuse via hind leg suspension reduced BFR by 92%; disuse

interrupted by normal weight bearing reduced BFR by 61%; disuse interrupted by mechanical stimulation had BFR the same as the age matched controls. The conclusions reached were that low level, high-frequency vibration prevents bone loss and may be therapeutically beneficial for treating bone loss associated with space travel, bed rest and paralysis.

Garman *et al.* [37] investigated whether low-level oscillatory displacements using whole body vibration in the absence of weight bearing, are anabolic to the skeletal tissue. Adult female mice were vibrated for 10 minutes per day for 3 weeks with 45Hz sinusoidal accelerations of 0.3g or 0.6g intensity and compared to controls. There was an Increase in bone forming rates in vibrated tibias compared with the controls (0.3g 88% greater; 0.6g 66% greater) and an increase in percentage of mineralising surfaces in the vibrated tibias compared with the controls (0.3g 64% greater; 0.6g 22% greater). It was concluded that low magnitude, high-frequency vibration can influence bone morphology and formation in the absence of wt bearing, and may be useful to remedy disuse osteoporosis.

Ozcivici *et al.* [38] aimed to test the hypothesis that high-frequency oscillations in non-wt bearing bones can be sensed by the trabecular bone to produce a structure that is more efficient in sustaining applied loads. Vibration simulating by way of whole body vibration was delivered to the left tibia of anaesthetised adult female mice (n=18) at 45Hz and 0.6g for 20 mins per day 5 days per week for a duration of 3 weeks. No vibration to the right tibia was applied and therefore served as the control. At all other times the limbs were unloaded. Micro-CT and finite element were used for the analysis. The results showed the stimulus was sensed primarily by trabecular bone. Compared to the non-weight bearing control, the vibrated tibia showed a 38% increase in trabecular bone stiffness. The authors concluded that compared to the normal age matched controls, oscillations were attenuated but did not fully prevent the decline in trabecular properties associated with the removal of weight bearing. Bone cells can sense high-frequency oscillations and can orchestrate a

structural response that produces stiffer trabecular bone that may be less prone to fracture in a clinical setting.

The mandibular condyle is not classified as a weight bearing bone. Sriram *et al.* [34] investigated the effects of low-magnitude, high-frequency stimuli on the mandibular condylar bone and found that vibration is anabolic at this site consistent with the findings of Garman *et al.* [37] and Ozcivici *et al.* [38]. Forty adult female C3H mice were divided into three groups; base line control, age matched control and an experimental group exposed to whole body vibration (30Hz and 0.3g) for 20 mins per day, 5 days per week for an experimental duration of four weeks. The samples were analysed using micro computed tomography. Significant changes in bone morphometric parameters seen in the experimental group indicated an anabolic response in the mandibular condylar bone. From this, Sriram hypothesised that mechanical vibration may have potential for use in orthopaedic application related to the adaptive growth of the mandibular condyle.

Several investigations have focused on determining the effect of high-frequency, low-magnitude vibration applied simultaneously with normal ambulation. The rationale behind such investigations was based on the shift away from the idea that peak strains resulting from vigorous activity were the primary determinants of bone morphology [255], for example, mastication in the mandible of the macaque [260]. The new concept suggested that extremely small strains engendered by less vigorous but more frequent activities, such as maintaining posture, are strong determinants of bone morphology [29,262]. Rubin *et al.* [264,265] hypothesised that high-frequency, low-magnitude, mechanical signals that continually barrage the skeleton during longer term activities such as standing, regulate skeletal architecture. Nine adult female sheep were vibrated using whole body vibration for 20 minutes per day 5 days per week at 0.3g and 30Hz for 1 year and compared with nine control animals. The mechanical stimuli engendered 5με in the tibiae, one thousandth of the strain magnitude necessary to cause yield failure. Morphometric bone parameters were determined

following peripheral quantitative computed tomography and were indicative of cancellous bone formation de novo. The bone forming rate increased 2.1 times in the experimental group. It was concluded that low-level, high-frequency mechanical signals: produce strain levels three orders of magnitude below strains that can damage bone [255]; stimulate formation of lamellar bone; improve cancellous bone quality and quantity; and may have the potential to treat osteoporosis. The notion that subtle mechanical activities arising from normal activities may determine bone morphology was supported by this study.

Rubin *et al.* using a similar experimental design found equivocal results and concluded that significant increases in stiffness and strength were observed in the longitudinal direction indicating that the change occurs in the plane of weight bearing and that vibration improves both the quality and quantity of bone and may serve to remedy osteoporosis [266].

In 2006, Xie *et al.* [35] aimed to determine if short durations of high-frequency, low-magnitude mechanical stimuli can influence trabecular and cortical formative and resorptive activity in the growing skeleton. In addition, they aimed to determine if the newly formed bone is of high quality and, if the insertions of rest periods during the loading phase enhance the efficiency of the mechanical regimen. The experiment was carried out over a *three week* period but after not yielding significant results was repeated by the same investigator two years later over a *six week* period and the effect of the vibration on muscle was also investigated[36]. Eight week old female BALB/cByJ mice were divided into four groups: 8 baseline controls; 10 age matched controls; 10 whole body vibration only (45Hz 0.3g 15 mins day); and 10 whole body vibration with a 10 second rest period after 1s vibration. When compared to the age matched controls the whole body vibration group showed that the bone mineralising surfaces of the trabeculae were 75% greater, the tibial metaphysis had 14% more bone volume, no change in osteoclastic activity and the periosteal bone area, bone marrow and cortical bone area were all significantly greater. The muscles had gains of up

to 29%. They concluded that six weeks of vibration showed anabolic effects (unlike three weeks duration) and postulated that exercise during childhood and adolescence or an early vibration regimen could prevent osteoporosis and sarcopoenia later in life.

6.2.3 Pathological States and Bone Healing

Pathological conditions affecting bone density have been potential targets for high-frequency, low-magnitude vibration therapy. The role of vibration in bone healing has also been investigated.

6.2.3.1 Children with Disabling Conditions

Ward *et al.* [267] aimed to determine whether high-frequency, low-magnitude vibration could increase tibial and spinal volumetric trabecular bone mineral density (BMD) in children with disabling conditions using a prospective double blind randomised placebo controlled pilot trial. Twenty pre and post pubertal disabled but ambulant children (14M; 6 F) of mean age 9.1 ± 4.3 years were recruited for the experiment. Ten subjects were exposed to 90Hz 0.3g vibration, ten minutes per day, five days per week for six months; 10 subjects served as placebos. 3D quantitative computed tomography was used to examine tibial and spinal bones. Compliance was poor such that mean vibration time was 4.4 mins per day. Despite this, the trabecular bone in the tibia increased by 6.3% in the vibration group and decreased by 11% in the placebo group resulting in a net benefit of 15.72%. The net benefit in the spine was 6.72%. It was concluded that Vibration is anabolic to trabecular bone in children. This is a potential non pharmacological treatment for bone fragility in children with disabling conditions.

6.2.3.2 Young Women with Low Bone Mineral Density

Gilsanz *et al.* [268] investigated the ability of low-level, high-frequency mechanical signals to enhance bone and muscle mass in young women with low bone mineral density, based on the hypothesis that the incidence of osteoporosis may be reduced by increasing bone mass in the young. Forty-eight females aged 15-20 years with low BMD and a history of at least one skeletal fracture, were

included in the study. Twenty four subjects received vibration at 30Hz 0.3g for 10 minutes a day over one year. The remainder served as controls. Using quantitative CT, it was found and concluded that high-frequency, low-magnitude vibration increased bone and muscle mass in the weight bearing skeleton of young adult females with low BMD. This intervention may reduce the risk of osteoporosis later in life if the achieved results can be maintained.

6.2.3.3 Postmenopausal Osteoporosis

Using ovariectomised rats, both Flieger *et al.* [269] and Oxlund *et al.* [270] investigated the effect of whole body high-frequency, low-magnitude vibration on bone mineral density in simulated postmenopausal conditions. The vibration parameters ranged from 17-50Hz and 0.5-3g. In both studies, bone mineral density decreased in the ovariectomised rats without vibration over the 90 day experiment, whereas bone density was either maintained or increased in vibrated animals. These studies concluded that there is a possible beneficial effect of passive physical loading on the preservation of bone in ovariectomised rats.

Rubin *et al.* [271] conducted a human study to determine whether high-frequency, low- magnitude vibration could inhibit bone loss in postmenopausal women by way of a one year prospective randomised double blind and placebo controlled clinical trial. Seventy women, 3-8 years post menopause were involved in the study. Thirty-five served as placebo controls and 35 as experimental subject receiving two 10 minute treatments per day of low-magnitude (0.2g) high-frequency (30Hz) whole body vibration. Bone mineral density was measured at hip, spine and distal radius at t=0, 6 and 12 months. Fifty six women completed the experiment. The results formed the conclusion that brief periods of low-magnitude, high-frequency vibration during quiet standing can effectively inhibit bone loss, that is, prevent a decline in bone mineral density, in the spine and femur with efficacy increasing significantly with greater compliance particularly in the subjects with low body mass.

Verschueren *et al.* [272] also conducted an investigation to assess the musculoskeletal effects of high-frequency loading, by means of whole body vibration in post menopausal woman. Using a randomised controlled study, seventy post-menopausal women were randomly assigned to three groups, one receiving whole body vibration between 35-40Hz and 2-5g whilst doing dynamic knee extensor exercises to load bone and induce muscle contractions; one carrying out resistance training and the other serving as a control without training. The results showed that vibration significantly improved BMD in the hip and improved isometric and dynamic muscle strength. No changes in hip density were observed in the resistance training and control groups. It was concluded that vibration may be an effective way to modify well recognised risk factors for falls and fractures in post menopausal women by modifying muscle strength, balance and bone mineral density in the hip, and suggested that further human studies were required.

6.2.3.4 Bone Healing

Two recent studies investigated the effect of high-frequency, low-magnitude vibration on bone healing following surgery and bone fractures.

Omar *et al.* [33] investigated the effect of low-magnitude, high-frequency vibration on healing surgical defects on cranial bones using 40 C3H mice. The experimental animals underwent surgery followed by vibration at 30Hz for 20 mins per day, five days per week for 28 days and were compared with a control group who underwent surgery without subsequent vibration. The animals were sacrificed at 0, 14 and 28 days. Micro-CT was used. Significant healing over time of the surgical defects was observed in both groups, however the healing was significantly more pronounced in the vibration group. It was concluded that low-magnitude, high-frequency vibration in healing bone lesions in the non-weight bearing bone may significantly increase its healing capacity.

Goodship *et al.* [273] aimed to determine if low-magnitude, high-frequency mechanical signals influence fracture healing in bone of sheep. Following 3mm osteotomies in sheep tibia, the animals

were vibrated at 30Hz for 17 min per day for 10 weeks. At 10-weeks, the callus in the experimental group was 3.6-fold stiffer, 2.5-fold stronger, and 29% larger than controls, all of which were statistically significant. The bone mineral content was 52% greater in the experimental group, with a 2.6-fold increase in bone mineral content in the region of the periosteum. It was concluded that mechanical factors play a critical role in the enhancement of fracture healing and that low-magnitude, high-frequency vibration can enhance bone healing in sheep.

6.3 Vibration and Cartilage

Evidence of the positive effects of vibration on bone has provoked research into the effect of vibration on cartilage [274]. This is in anticipation of formulating a therapeutic regime for the treatment of osteoarthritis, a disease typified by deterioration of articular cartilage over time, associated with joint pain, deformation and functional inhibition [274]. In vitro investigations on the effects of vibration on cultured chondrocytes have dominated the research and results indicate that vibration may be useful in maintaining or preventing a decline in chondrocyte function with advancing age. No in vivo investigations have been conducted to date on the role of vibration on cartilage in the prevention of osteoarthritis [274] and only one experiment has been conducted examining the effect of vibration on healthy cartilage at the site of the mandibular condyle in rats [34]. Hence, neither long term effects of vibration on cartilage have been ascertained, nor safe in vivo vibration regimens been devised [274].

6.3.1 In Vitro Studies

Liu *et al.* [275] aimed to determine the effects of mechanical vibration on DNA and proteoglycan synthesis using cultured rabbit articular chondrocytes in vitro. A sinusoidal waveform on a vibration platform was used at 1.4g acceleration and 200, 300, 400, 800 or 1600 Hz. The results showed that the activity of articular cartilage cells under vibration is a function of frequency. Above 400HZ and below 200Hz DNA synthesis is down regulated whereas at 300Hz it is up-regulated. At a vibratory stimulus of 300Hz and 1.4g for eight hours per day, DNA synthesis and proteoglycan synthesis

reached a maximum. Peak DNA synthesis occurred at 3 days and peak proteoglycan synthesis at 15 days. It was concluded that vibration at different frequencies can enhance or depress ^{3}H-thymidine and H_2 ^{35}SO incorporation into DNA and proteoglycans respectively. Vibration may be able to facilitate metabolism of articular cartilage particularly during the regeneration process.

Yamazaki *et al.* [276] investigated the relationship between vibratory loading and extracellular matrix expression in cultured annulus fibrosis cells isolated from normal intervertebral discs of rabbits. Following isolation, these cells were vibrated in vitro at 0.1g and 6Hz for 2, 4, 6 and 8 hours. Gene expression of aggrecan, collagen III and matrix metallo-proteinase (MMP)-3 was assessed by RT-PCR. Results showed that there was suppression in gene expression of aggrecan, collagen type III and MMP-3 in vibrated annulus cells of the rabbit. Suppression of the aggrecan gene may lead to a decrease in proteoglycan synthesis. It was concluded that vibration may play an important role in extracellular matrix metabolism of intervertebral disc cells especially in the gene expression pathway of proteoglycans. Vibration may increase the production of matrix-degrading proteolytic enzymes which may explain the pathomechanism of disc degeneration.

Takeuchi *et al.* [277] aimed to investigate the effects of 100Hz vibration (Vib) and hyaluraonic acid (HA) on 3-dimensional cultured chondrocytes in vitro. Cultured chondrocytes from joints of six month old pigs were divided into four groups: 1) HA^- Vib^- 2) HA^- Vib^+ 3) HA^+ Vib^- 4) HA^+ Vib^+. At 3, 7, 10 and 14 days, measurements for the production of chondroitin 6 sulfate and chondroitin 4 sulfate were recorded as an indicator for proteoglycan synthesis. Data analysis included histology, immunohistochemistry and electron microscopy. The HA^+ Vib^+ group had the most abundant increase in the chondroitin 6 sulfate and chondroitin 4 sulfate whereas the HA^- Vib^- group had the least increase. The chondrocytes in the HA^+ Vib^+ group formed the thickest stratified structures on the collagen, showed the strongest chromatic features under electron microscopy and exhibited long and slender prominences on their surface with associated extracellular substance under

electron microscopy. It was concluded that vibration and hyaluronic acid activates the production of proteoglycan in 3-dimensional cultured chondrocytes. This suggests that mechanoreceptors on the surface of the chondrocytes exist and respond to vibration in a positive way by activating the intracellular pathways.

6.3.2 In Vivo Study

Sriram *et al.* [34] examined the effects of high-frequency, low-magnitude vibration on the mandibular condylar cartilage and its endochondral bone in 40, 12-week old C3H mice. The controls received no vibration whereas the experimental animals were exposed to 30Hz 0.3g vibration for 20 minutes per day, five days per week, for an experimental period of 28 days. Micro-CT was used to analyse the specimens. A reduction in condylar cartilage volume in the experimental group was seen with the concomitant increase in trabecular bone. It was concluded that the decrease in mandibular condylar cartilage volume could be explained by the process of endochondral bone replacing the hypertrophic cartilage more rapidly than the cartilage could be produced. From this, the authors hypothesised that mechanical vibration may have potential for use in orthopaedic application related to the adaptive growth of the mandibular condyle.

6.4 Vibration in Dentistry and Orthodontics

Low-magnitude, high-frequency vibration has been applied experimentally in the field of orthodontics with the main focus being on increasing the rate of orthodontic tooth movement. It has been hypothesised that vibration may be useful in reducing pain associated with dental injections.

6.4.1 Vibration and the Rate of Orthodontic Tooth Movement

Darendeliler *et al.* [278] sought to determine if high-frequency, low-magnitude vibration induced by magnets in pulsed electromagnetic fields (PEMF) affects the rate of orthodontic tooth movement. Previous studies showing that orthodontic tooth movement can be enhanced by static and pulsed electromagnetic fields alone [279,280] formed the foundations of this study. Forty Wistar rats were used

in the experiment to test: the effect of vibration alone; vibration compared with vibration and coil spring; PEMF alone compared with PEMF and coil spring; and vibration and coil spring compared with PEMF and coil spring. The results showed that: coil spring with sham or active magnets moved the teeth more than the magnets with or without vibration; coil spring moved the teeth more than coil-magnet combination under PEMF; the magnets moved the teeth more than the sham magnets under PEMF; no significant difference in tooth movement between coil spring and magnet combinations without PEMF; and there was no difference between magnets and sham magnets without PEMF. It was concluded that orthodontic tooth movement with coil and magnets may be enhanced by vibration induced by PEMFs.

Nishimura *et al.* [281] investigated the effects of stimulation by resonance vibration on the speed of tooth movement and root resorption during experimental tooth movement in rats and to elucidate the cellular and molecular mechanisms underlying the acceleration of tooth movement. Twelve male Wistar rats were used for the experiment of 21 days. Six rats served as controls, whereby a buccal force was placed on the molar. Six rats served as experimentals whereby a buccal force was placed on the molar and with a vibratory stimulus of 60Hz and 1g for 8 minutes duration on days 0, 7 and 14. Immunohistochemical analysis for RANKL expression and number of osteoclasts using TRAP stain was performed and root resorption was measured using haematoxylin and eosin. The results showed that tooth movement in the experimental group was significantly greater than the control group, as seen by enhanced RANKL expression at fibroblasts and osteoclasts in the periodontal ligament of the experimental group. No significant difference in root resorption between the two groups was observed. It was concluded that vibration might increase the rate of orthodontic tooth movement via enhanced expression of RANKL in the PDL without additional damage to the tissues, such as root resorption.

6.4.2 Vibration and Pain Control

The gate control theory of pain proposed by Melzack and Wall 1965 [282] suggests pain can be reduced by simultaneous activation of nerve fibres that conduct non-noxious stimuli (such as those that respond to vibration), that close the neural gate to nociception resulting in a decrease in perception of pain. It is possible that vibration may stimulate mechanoreceptors such as Pacinian corpuscles, primary endings of nerve fibres, Meissner's corpuscles in skin, receptors in bone and other tissues to accomplish this effect.

Nanitsos *et al.* [283] investigated the perception of pain during oral local anaesthetic administration in order to determine if vibration reduces the perception of such pain. Block and infiltrations injections were performed on the same patients, first without vibration and secondly with vibration. The visual analogue scale and McGill pain descriptors were used to assess the pain.

Vibration was administered using the HoMedics Atom massager (HoMedics, Pty *Australia*). The vibration parameters were not stated. The results showed injections given with vibration had a lower pain rating and less pain descriptors were chosen. It was concluded that vibration can be used to decrease the pain during dental local anaesthesia.

7 X-Ray Microtomography

X-ray microtomography is a relatively new imaging method that has the spatial resolution to visualise and quantify the morphology of small structures at high resolution. This imaging modality was conceived and built by Elliott and Dover in the early 1980's [284] however the technology was advanced by Feldkamp following the advent of the cone beam reconstruction algorithm [285]. Feldkamp used a micro focus x-ray tube as a source, an image intensifier as a two dimensional (2D) detector and a cone beam reconstruction to create a three dimensional (3D) object with a typical resolution of 50µm. The advantage of 3D imaging over 2D imaging is the capability of structural and

volumetric analysis. In addition, investigations can be done without perturbing the sample, as occurs during histological preparation.

Tomography produces a 2D map of x-ray absorption in two dimensional slices of the subject by taking a series of x-ray projections through the slice at various angles around the axis perpendicular to the slice. Digital computing allows the series of projections or two-dimensional absorption maps to be combined into three dimensional maps [285-287].

The 2D unit of resolution is a pixel, the smallest unit of colour or greyscale value within an image, the number of pixels per surface area gives the resolution of the image. The 3D unit of resolution is the voxel – a three dimensional representation of the smallest unit of colour value or grey scale value within a three dimensional image. Therefore, a voxel represents a volume and its dimensions have an x, y and z axis.

The Skyscan 1172 x-ray microtomograph (Skyscan *Aatselaar, Belgium*) is a compact desktop fifth generation system for microscopy and micro-CT. The components include a cone beam x-ray source with spatial resolution of 2-5 micrometers. The sample is positioned on a rotating platform programmed to revolve over 180 or 360 degrees. The distance between the object and x-ray source determines the magnification. The x-ray detector consists of a high resolution charged couple device with resolution of 1024x10x24 pixels. The images received are sorted as 16 bit Tagged Image File Format (TIFF) pictures with a resolution of 1024x1024 pixels.

After image acquisition is completed software for axial slice by slice reconstruction uses Feldkamp cone beam algorithm using Skyscan's volumetric reconstruction software [285]. The resultant axial 2D images are generated as 1024x1024 pixel bitemap (BMP) images having an 8 bit grey scale dynamic range (indexed grey levels ranging from 0, black, to 255, white).

The software package VGSM version 2.0 (Volume Graphics, GmbH, Heidelberg, Germany) is used to collate the axial two dimensional slices to generate three dimensional reconstruction of the images. Regions of interest can be isolated using interactive thresholding and the volume subsequently

measured in voxels by the software. The software package CT Analyser (Version 1.10.1.0 Skyscan) is used to collate all the axial slices to form a three dimensional reconstruction of the scanned image and facilitate bone morphometric analysis in three dimensions.

7.1 Cartilage Imaging

In vitro imaging of cartilage traditionally has been done using histology. Cationic, positively charged dyes such as Safranin O and alcian blue interact with the negatively charged groups on the proteoglycan in the cartilage matrix through electrostatic attraction. Although reliable and detailed, this method requires biopsy and which is an invasive procedure.

In vivo cartilage imaging has been limited to arthrography that uses x-rays in the presence of contrast medium to show the morphology of the cartilage. This method is limited in that it can only indicate surface irregularity and thinning. Arthroscopy, a more invasive method can investigate the surface of the cartilage in joints in vivo.

Traditionally, computed tomography and micro computed tomography have focused on bone analysis of trabecular architecture and quality [287,288]. The inherent intensity of cartilage in micro-CT imaging is weak and thus staining methods have been devised and employed to enhance the contrast of the cartilage on micro-CT scans to facilitate qualitative and quantitative analysis. Preceding this advancement was the use of dyes for cartilage visualisation using MRI. The dyes were selected to interact with the proteoglycans in the cartilage. Proteoglycans are composed of glycosaminoglycans which contain negatively charged groups. Kusaka in 1992 [289] used MRI to show that the uptake of manganese (Mn^{2+}) or gadolinium (as gadopentetate- Gd-$DTPA^{2-}$) in cartilage is associated with the proteoglycan distribution. Manganese and gadolinium are paramagnetic and thus alter the appearance of the cartilage on the MRI. Bashir [290] used this staining technique with MRI to show that Gd-$DTPA^{2-}$ is taken up in cartilage in inverse concentration to the proteoglycan

concentration. Further, Laurent [291] showed that Gd-DTPA^{2-} and MRI could measure proteoglycan depletion induced by papain in the rabbit knee.

Sriram *et al.* successfully stained the cartilage of the mandibular condyle of rats using osmium tetroxide for improved cartilage imaging and segmentation using micro-CT.

Gadolinium (Gd) is a lanthanide element with a high atomic number and is therefore utilised as an effective contrast medium in imaging due to its absorption of highly energetic photons. Due to its toxicity in mammals, gadolinium has been combined with other agents to make it usable in the in vivo environment. Animal studies [292,293] established that the chelation of Gadolinium with DTPA at certain concentrations was safe. The safety of Gd-DTPA^{2-} is well established at doses up to 0.3mmol Gd/Kg in man [294].

Based on the success of Gd- DTPA^{2-} with MRI, Cockman *et al.* investigated the efficiency of 200mM of Gd^{3+} and 200mM Gd- DTPA^{2-} as a contrast media for bovine nasal cartilage disks in micro-CT analysis. Results showed that there was a 2.8 fold increase in intensity on the micro-CT images with 200mM Gd^{3+} and a 1.4 fold increase with the 200mM Gd- DTPA^{2-}. It was concluded that gadolinium used as a stain improves the visualisation of cartilage on micro-CT scans.

7.2 X-Ray Microtomography of Bone

Bone histomorphometry was developed in the 1950's to explore the various metabolic bone diseases. The microscopic technique was done on two dimensional sections and trabecular structures were measured by point and line counting using microscopic eyepieces, and image analyser systems. Several mathematical formulations have been proposed to extrapolate the two dimensional measurements into three dimensional information [295].

More recently, micro-computed tomography has been utilised to image and quantify trabecular bone. This type of bone morphometry is a non-destructive and precise procedure that allows for

determining three dimensional stereological bone indices. Micro-CT scans of resolution less than 10µm are adequate to obtain bone morphometric data [295,296]. Bone morphometry is descriptive of trabecular micro architecture relating to trabecular quality and complexity. It has been used extensively for research investigating the biomechanical properties of bone, the pathophysiology of osteoporosis, the efficiency and effectiveness of pharmaceutical intervention, bone healing and arthritis [297]. It has been used extensively to study the effects of vibration on bone. With respect to the trabecular bone of the mandibular condyle, bone morphometry has been used to study the effects of functional appliances [40] and the effects of mechanical vibration [34] independently.

The morphometric parameters are summarised in Appendix 1f. The bone morphometric parameters are most useful when assimilated, rather than considered individually[296]. For example, in the case of bone deterioration, it is feasible to expect that as the trabecular number and trabecular thickness decrease, there will be an increase in trabecular separation and a shift to a more rod like trabecular structure seen by an increase in structure model index [296]. In contrast, an anabolic response to loading would show an increase in trabecular number and trabecular thickness with a corresponding decrease in trabecular separation, a shift to better trabecular connectivity (seen by a decrease in trabecular pattern factor) and plate-like trabeculae (seen by a decrease in structure model index) [296].

8 Conclusion

From the literature it is evident that both functional protrusion and low-magnitude, high-frequency vibration in isolation enhance condylar cartilage and condylar bone changes during the process of endochondral ossification. It is therefore of interest to investigate the effect of these two variables when used simultaneously.

The effect of mechanical vibration on the rat mandibular condyle during functional protrusion has not yet been investigated.

9 References

1. Bishara SE. Textbook of Orthodontics. In: Bishara SE, editor. Philadelphia: Saunders; 2001: p. 592.
2. Angle E. Classification of malocclusion. Dental Cosmos 1899;41:248-264

3. Angle EH. Treatment of malocclusion of the teeth. 7th edition. Philadelphia: SS White; 1907.
4. Baccetti T, Franchi L, McNamara JA, Jr., Tollaro I. Early dentofacial features of Class II malocclusion: a longitudinal study from the deciduous through the mixed dentition. American Journal of Orthodontics & Dentofacial Orthopedics 1997;111:502-509.
5. Bishara SE, Hoppens, B.J., Jakobsen, J.R., Kohout, F.J. . Changes in the molar relationship between the deciduous and permanent dentitions; a longitudinal study. Am J Orthod 1988;93:19-28.
6. Stahl F, Baccetti T, Franchi L, McNamara JA, Jr., Stahl F, Baccetti T et al. Longitudinal growth changes in untreated subjects with Class II Division 1 malocclusion. American Journal of Orthodontics & Dentofacial Orthopedics 2008;134:125-137.
7. Kerr W, Hirst D. Craniofacial characteristics of subjects with normal and postnormal occlusions- a longitudinal study. Am J Orthod Dentofacial Orthop. 1987;92:207-212.
8. Ngan P, Byczek E, Scheik J. Longitudinal evaluation of growth changes in class II division 1 malocclusion. Semin Orthod. 1997;3:222-231.
9. Woodside DG, Metaxas, A., Altuna, G. The influence of functional appliance therapy on glenoid fossa remodelling. Am J Orthod Dentofacial Orthop 1987;92:181-198.
10. Rabie AB, She, T.T., Hagg, U. Functional appliance therapy accelerates and enhances condylar growth. Am J Orthod Dentofacial Orthop. 2003;123:40-48.
11. Shen G, Darendeliler, M. The Adaptive remodelling of condylar cartilage – A transition from Chrondrogenesis to Osteogenesis. Journal of Dental Research 2005;84.
12. Hinton RJ, Carlson, D.S. Regulation of growth in mandibular condylar cartilage. Seminars in Orthodontics 2005;11:209-218.
13. Breitner C. Bone changes resulting from experimental orthodontic treatment. Am J Orthod 1940;26:521-547.
14. Breitner C. Further investigations of bone changes resulting from experimental orthodontic treatment. Am J Orthod 1941;27:605-632.
15. Adams C, Meikle M, Norwick K, Turpin D. Dentofacial remodelling produced by intermaxillary forces in the *Macaca mulatta*. Archives of Oral Biology 1972;17:1519-1534.
16. Baume L, Derichsweiler H. Is the condylar growth centre responsive to orthodontic therapy? Oral Surgery Oral Medicine and Oral Pathology 1961;14:347-362.
17. Hiniker J, Ramfjord S. Anterior displacement of the mandible in adult rhesus monkeys. J Prosthet Dent. 1966 16:503-512.
18. Meikle M. The effect of a class II intermaxillary force on the dentofacial complex in the adult *Macaca mulatta* monkey. Am J Orthod 1970;58:323-340.
19. Stockli PW, Willert, H.G. TMJ reaction to anterior displacement of mandible. Am J Orthod 1971;60:142-154.
20. Voudouris JC, Woodside, D.G., Altuna, G., Angelopoulos, G., Bourque, P.J., Lacouture, C.Y., Kuftinec, M.M. Condyle-fossa modifications and muscle interactions during Herbst treatment, Part 2. Results and conclusions. Am J Orthod Dentofacial Orthop. 2003;124:13-29.
21. Shen G, Zhao, Z., Kaluarachchi, K., Rabie, B.A. Expression of type X collagen and capillary endothelium in condylar cartilage during osteogenic transition--a comparison between adaptive remodelling and natural growth. Eur J Orthod 2006;28:210-216.
22. McNamara JA, Carlson D.S. Quantitative analysis of temporomandibular joint adaptations to protrusive function. Am J Orthod 1979;79.

23. Ruf S, Pancherz, H. Temporomandibular joint growth adaptation in Herbst treatment. A prospective magnetic resonance imaging and cephalometric roentgenographic study. Eur J Orthod 1998;20:375-388.
24. Ruf S, Pancherz, H. Temporomandibular joint remodelling in adolescence and young adults during Herbst treatment: a retrospective longitudinal magnetic resonance imaging and cephalometric radiographic investigation. Am J Orthod Dentofacial Orthop. 1999;115:607-618.
25. Wolff J. Das Gesetz der Transformation der Knochen 1892.
26. Qin YX, Rubin CT, McLeod KJ. Nonlinear dependence of loading intensity and cycle number in the maintenance of bone mass and morphology. Journal of Orthopaedic Research 1998;16:482-489.
27. Rubin CT. Skeletal strain and the functional significance of bone architecture. Calcified Tissue International 1984;36 Suppl 1:S11-18.
28. Rubin CT, Lanyon LE. Regulation of bone mass by mechanical strain magnitude. Calcified Tissue International 1985;37:411-417.
29. Fritton SP, McLeod KJ, Rubin CT. Quantifying the strain history of bone: spatial uniformity and self-similarity of low-magnitude strains. Journal of Biomechanics 2000;33:317-325.
30. Rubin C, Sommerfeldt D, Judex S, Qin Y. Inhibition of osteopenia by low magnitude, high frequency mechanical stimuli. DDT 2001;6:848-858.
31. Fritton JC, Rubin CT, Qin YX, McLeod KJ. Whole-body vibration in the skeleton: development of a resonance-based testing device. Annals of Biomedical Engineering 1997;25:831-839.
32. Rubin C, Pope M, Fritton JC, Magnusson M, Hansson T, McLeod K et al. Transmissibility of 15-hertz to 35-hertz vibrations to the human hip and lumbar spine: determining the physiologic feasibility of delivering low-level anabolic mechanical stimuli to skeletal regions at greatest risk of fracture because of osteoporosis. Spine 2003;28:2621-2627.
33. Omar H, Shen G, Jones AS, Zoellner H, Petocz P, Darendeliler MA. Effect of low magnitude and high frequency mechanical stimuli on defects healing in cranial bones. Journal of Oral & Maxillofacial Surgery 2008;66:1104-1111.
34. Sriram D, Jones, A., Alatli-Burt, I., Petocz, P., Darendeliler, M.A. The effects of low magnitude, high frequency mechanical stimuli on adaptive remodeling of condylar cartilage and bony tissue. A Micro-CT study. Journal of Dental Research 2009.
35. Xie L, Jacobson JM, Choi ES, Busa B, Donahue LR, Miller LM et al. Low-level mechanical vibrations can influence bone resorption and bone formation in the growing skeleton. Bone 2006;39:1059-1066.
36. Xie L, Rubin C, Judex S, Xie L, Rubin C, Judex S. Enhancement of the adolescent murine musculoskeletal system using low-level mechanical vibrations. Journal of Applied Physiology 2008;104:1056-1062.
37. Garman R, Gaudette G, Donahue LR, Rubin C, Judex S, Garman R et al. Low-level accelerations applied in the absence of weight bearing can enhance trabecular bone formation. Journal of Orthopaedic Research 2007;25:732-740.
38. Ozcivici E, Garman R, Judex S, Ozcivici E, Garman R, Judex S. High-frequency oscillatory motions enhance the simulated mechanical properties of non-weight bearing trabecular bone. Journal of Biomechanics 2007;40:3404-3411.
39. Rubin C, Xu G, Judex S. The anabolic activity of bone tissue, suppressed by disuse, is normalized by brief exposure to extremely low-magnitude mechanical stimuli. FASEB Journal 2001;15:2225-2229.
40. Xiong H, Rabie A, Hagg U. Neovascularisation and mandibular condylar bone remodelling in adult rats under mechanical strain. Frontiers in Bioscience 20005;10:74-82.
41. Proffit WR, Fields, H.W., editors. Contemporary orthodontics. 4th ed. : St Louis: Mosby; 2007.
42. Nanci A. Ten Carte's Oral Histology. Development, Structure and Function. In: Rudolph P, editor. Philadelphia: Mosby; 2003.

43. Lee S, Kim Y, Yang K, Kim E, Chi J. Prenatal development of the human mandible. Anatomical Record 2001:314-325.
44. Bjork A. Variations in the growth pattern of the human mandible: Radiographic longitudinal study by the implant method. J Dent Res 1963;42:400-411.
45. Enlow DH, Hans, M.G. Essentials of facial growth. Philadelphia W.B Saunders; 1996.
46. Broadbend B. The face of the normal child. Angle Orthod. 1937;7:183-208.
47. Brodie A. On the growth pattern of the human head from the thid month to the eighth year of life. Am J Anat 1941;68:209-262.
48. Bjork A. The use of metallic implants in the study of facial growth in children: method and appliacation. Am J Phys Anthropol 1968;29.
49. Bjork A, Skieller, V. Normal and abnormal growth of the mandible, a synthesis of longitudinal cephalometric implant studies over a period of 25 years. Eur J Orthod 1983;5:1-46.
50. Bjork A. Prediction of mandibular growth rotation. Am J Orthod 1969;55:585-599.
51. Enlow. Functional growth boundaries in the human and mammalian face. Birth Defects 1975;11:217-230.
52. Solow B. 1980.
53. Suda N, Yamazaki K, Kuroda T, Senior P, Beck F. Parathyroid related protein regulates proliferation of condylar hypertrophic chondrocytes. J Bone Miner Res 1999;14:1838-1847.
54. Meikle C. Craniofacial development, growth and evolution. Norfolk: Bateson; 2002.
55. Enlow D. The condyle and facial growth. In: Sarnat B, Laskin D, editors. The temporomandibular joint: a biological basis for clinical practice. Philadelphia: Saunders; 1992: p. 48-59.
56. Scott JH. The growth of the human face. Proc R Soc Med 1954;47:91-100.
57. Rabie AB, Hagg, U. Factors regulating mandibular condylar growth. Am J Orthod Dentofacial Orthop 2002;122:401-409.
58. Lefebvre V, Bheringer R, Crombrugghe Bd. L-Sox5, Sox-6 and Sox 9 control essential steps of the chondrocyte differentiation pathway. Osteoarthritis & Cartilage. 2001;Spplement A:S69-S75.
59. Lefebvre V, deCrombrugghe B. Towards understanding SOX9 in chondrocyte differentiation. Matrix Biol 1998:529-540.
60. deCrombrugghr B, Lefebre V, Behringer R, Bi W, Murakami S, Huang W. Transcriptional mechanisms of chondrocyte differentiation. Matrix Biol 2000;19:389-394.
61. Ng L, Wheatley S, Muscat G, Conway-Campbell J, Bowles J, Wright E. SOX9 binds DNA, activates transcription and coexpresses with type II collagen during chondrogenesis in the mouse. Dev Biol 1997:108-121.
62. Tsuda M, Takahashi S, Asahara H. Transcriptional c-activators CREB-binding protein and p300 regulate chondrocyte specific gene expression via association with Sox9. J Biol Chem 2003;278:27224-27229.
63. Hiraki Y, Shukunami C, Iyami K, Mizuta H. Differentiation of chondrogenic precursor cells during regeneration of articular cartilage. Osteoarthr Cart 2001;9(Suppl A):S102-S108.
64. Hajjar D, Santos, M.F., Kimura, E.T. Propulsive appliance stimulates the synthesis of insulin-like growth factors I and II in the mandibular condylar cartilage of young rats. Archives of Oral Biology 2003;48:635-642.
65. Reinecke M, Schmid A, Heyberger-Meyer B, Hunzinker E, Zapf J. Effect of GH and IGF-I on the expression of IGF-I mRNA and peptide in rat tibial growth plate and articular chondrocytes in vivo Endocrinology 2000;141:2847-2853.
66. Itoh K, Suzuki S, Kuroda T. Effects of local administration of insulin-like growth factor I on mandibular condylar growth in rats. J Med Dent Sci 2003;50:79-85.
67. Wildemann B, Scmidmaier G, Ordel S, Stange R, Haas N, Raschke M. Cell proliferation and differentiation during fracture healing are influenced by locally applied IGF-I and TGF-beta-1: Comparision of two proliferation markers, PCNA and BrdU. Journal of Biomed Mter Res B Appl Biomater 2003;65:150-156.

68. Tuli R, Tuli S, Nandi S, Huang X, Manner P, Hozak W. Transforming growth factor-beta-mediated chondrogenesis of human mesenchymal progenitor cells involves N-cadherin and mitogen-activated protein kinase and Wnt signalling crosstalk. J Biol Chem 2003;278:41227-41236.
69. Shen G, Rabie, B., Hagg, U. Neovascularisation in the TMJ in response to mandibular protrusion. Clin J Dent Res 2003;6:28-38.
70. Alvarez J, Sohn P, Zeng X, doetschman T, Robbins D, Serra R. TGFbeta2 mediates the effects of hedgehog on hypertrophic differentiation and PTHrP expression. Development 2002;129:1913-1924.
71. Rabie AB, Tang, G.H., Xiong, H., Hagg, U. PTHrp regulates chondrocyte matuation in condylar cartilage. J Dent Res 2003;82:627-631.
72. Rabie AB, Tang GH, Hagg U, Rabie ABM, Tang GH, Hagg U. Cbfa1 couples chondrocytes maturation and endochondral ossification in rat mandibular condylar cartilage. Archives of Oral Biology 2004;49:109-118.
73. Karsenty G, Ducy P, Starbuck M, Priemel M, Shen J, Geoffroy V. Cbfa1 as a regulator of osteoblast differentiation and function. Bone 1999:107-108.
74. Dai J, Rabie A. VEGF: an essential mediator of both angiogenesis and endochondral ossification. J Dent Res 2007;86:937-950.
75. Shen G, Rabie, A.B., Zhao, Z.H., Kaluarachchi, K. Forward deviation of the mandibular condyle enhances endochondral ossification of condylar cartilage indicated by increased expression of type X collagen. Arch Oral Biol. . 2006;51:315-324.
76. Shen G, Hagg U, Rabie A, Kaluarachchi K. Identification of temporal pattern of mandibular condylar growth: a molecular and biochemical experiment. Orthod Craniofacial Res 2005;8:114-122.
77. McNamara JA, Jr. . Components of Class II malocclusion in children 8-10yrs of age. Angle Orthod. 1981;51:177-202.
78. Baccetti T, Antonini A, Franchi L, Tonti M, Tollaro I. Glenoid fossa position in different facial types: a cephalometric study. British Journal of Orthodontics 1997;24:55-59.
79. Moore AW. Orthodontic treatment factors in Class II malocclusion. Am J Orthod 1959;45:323-352.
80. Buschang P. Mathematical models of longitudinal mandibular growth for children with normal and untreated class II division 1. Eur J Orthod 1988;10:227-234.
81. Baccetti T, Franchi, L., McNamara, J.A. The cervical vertebral maturation (CVM) method for the assessment of optimal treatment timining in dentofacial orthopedics. Semin Orthod. 2005;11:119-129.
82. Vasquez MJ, Baccetti T, Franchi L, McNamara JA, Jr., Vasquez MJ, Baccetti T et al. Dentofacial features of Class II malocclusion associated with maxillary skeletal protrusion: a longitudinal study at the circumpubertal growth period. American Journal of Orthodontics & Dentofacial Orthopedics 2009;135:568.e561-567; discussion 568-569.
83. Bishara SE, Jacobsen, J.R., Vorhies, B. Changes in dentofacial structures in untreatee Class II Division I and normal subjects; a longitudinal study. Angle Orthod. 1997;67:55-66.
84. Bishara S. Mandibular changes in persons with untreated and treated class II division 1 malocclusion. American Journal of Orthodontics & Dentofacial Orthopedics 1998;113:661-673.
85. Baccetti T, Stahl F, McNamara JA, Jr., Baccetti T, Stahl F, McNamara JA, Jr. Dentofacial growth changes in subjects with untreated Class II malocclusion from late puberty through young adulthood. American Journal of Orthodontics & Dentofacial Orthopedics 2009;135:148-154.
86. Buschang P, Santos-Pinto A. Condylar growth and glenoid fossa displacement during childhood and adolescence. Am J Orthod Dentofacial Orthop. 1998;113:437-442.
87. Bjork A. Cranial base development. Am J Orthod 1955;41:198-225.
88. Baumrind S, Korn, E.L., Isaacson, R.J., West E.E., Molthen, R. Quantitative changes of the orthodontic and orthopedic effects of maxillary traction. Am J Orthod 1978;84:384-369.
89. Baumrind S, Korn, E.L. Patterns of change in mandibular and facial shape associated with the use of forces to retract the maxilla. Am J Orthod 1981;80:31-47.

90. Ghafari J, Schofer, F.S., Hunt-Jacobsson, U. Headgear versus functional regulator in the ealy treatment of Class II, Division I malocclusion: a randomized clinical study Am J Orthod Dentofacial Orthop 1998;113:51-61.
91. Keeling SD, Wheeler, T.T., King, G.J. Anteroposterior skeletal and dental changes after early Class II treatment with bionators and headgear. Am J Orthod Dentofacial Orthop 1998;113.
92. Haralabakis N, Halazonetis D, Sifakakis I. Activator versus cervical headgear: superimpositional cephalometric comparison. Am J Orthod and Dentofacial Orthop 2004;123:296-305.
93. Phan K, Bendeus M, Hagg U, Hansen K, Rabie A. Comparison of Headgear Activator and Herbst Appliance-effects and post treatment changes. European Journal of Orthod 2006;28.
94. Baccetti T, Franchi L, Stahl F, Baccetti T, Franchi L, Stahl F. Comparison of 2 comprehensive Class II treatment protocols including the bonded Herbst and headgear appliances: a double-blind study of consecutively treated patients at puberty. American Journal of Orthodontics & Dentofacial Orthopedics 2009;135:698.e691-610; discussion 698-699.
95. Franchi L, Baccetti T, Franchi L, Baccetti T. Prediction of individual mandibular changes induced by functional jaw orthopedics followed by fixed appliances in Class II patients. Angle Orthodontist 2006;76:950-954.
96. Bishara SE, Ziaja, R. . Functional appliances: A review. Am J Orthod Dentofacial Orthop 1989;95:250-258.
97. Teuscher U. A growth-related concept for skeletal class II treatment. Am J Orthod 1978;28:258-275.
98. Balters W. Dtsch Zahnaerztl 1960;15:241.
99. Frankel R. The treatment of class II division 1 malocclusion with functional correctors. Am J Orthod 1969;55:265-275.
100. Clark W. The twin block traction technique. Eur J Orthod 1982;4:129-138.
101. Darendeliler MA, Darendeliler A, Mandurino M. Clinical application of magnets in orthodontics and biological implications: a review. European Journal of Orthodontics 1997;19:431-442.
102. Darendeliler MA, Joho JP. Magnetic activator device II (MAD II) for correction of Class II, division 1 malocclusions. American Journal of Orthodontics & Dentofacial Orthopedics 1993;103:223-239.
103. Pancherz H. Treatment of class II malocclusion by jumping the bite with th Herbst appliance. Am J Orthod 1979;76:423-442.
104. Pancherz H. The mechanism of class II correction in Herbst appliance treatmenr. A cephalometric investigation. Am J Orthod 1982;82:104-113.
105. Cozza P, Baccetti T, Franchi L, De Toffol L, McNamara JAJ. Mandibular changes produced by functional appliances in Class II malocclusion: a systematic review. Am J Orthod Dentofacial Orthop 2006;129:599.e591-512.
106. Creekmore TD, Radney LJ. Frankel appliance therapy: orthopedic or orthodontic? American Journal of Orthodontics 1983;83:89-108.
107. Bishara SE, Ziaja, R.R. Functional appliances : A review. Am J Orthod and Dentofac Orthop 1989;95:250-258.
108. Charlier JP, Petrovic, A., Herrmann–Stutzmann, J. Effects of mandibular hyperpropulsion on the pre chondroblastic zone of young rat condyle. Am J Orthod 1969:71-74.
109. Petrovic AG, Stutzman, J.J., Oudet, C.L. Control processes in the postnatal growth of the condylar cartilage of the mandible In: McNamara JAJ, editor. Determinants of mandibular form and growth Ann Arbor ; Center for Human Growth and Development: University of Michigan; 1975. p. 101-154.
110. Elgoyhen JC, Moyers, R.E., McNamara, J.A. Jr., Riolo, M.L. Craniofacial adaptation to protrusive function in young rhesus monkeys. Am J Orthod 1972;62:469-480.
111. Peterson J, McNamara J. Temporomandibular joint adaptions associated with Herbst appliance treatment in juvenille rhesus monkeys. Sem Orthod 2003;9:12-25.

112. Hinton R, McNamara JJ. Temporal bone adaptations in response to protrusive function in juvenile and young adult rhesus monkeys (*Macaca mulatta)*. Eur J Orthod 1984;6:155-174.
113. Voudouris JC, Kuftinec, M.M. Improved clinical use of Twin-block and Herbst as a result of radiating viscoelastic tissue forces on the condyle and fossa in treatment and long-term retention: growth relativity. Am J Orthod Dentofacial Orthop. 2000;117:247-266.
114. McNamara JAJ, Bryan, F.A. Long-term mandibular adaptations to protrusive function: An experimental study in Macaca Mulatta. Am J Orthod Dentofac Orthop 1987;92:98-108.
115. Petrovic A. Experimental and cybernetic approaches to the mechanism of action of functional appliances on mandibular growth. In: McNamara J, Ribbens K, editors. Craniofacial Growth Series. Ann Arbor; Centre for Human Growth and Development: University of Michigan; 1984.
116. Meikle MC. Remodeling the dentofacial skeleton: the biological basis of orthodontics and dentofacial orthopedics. Journal of Dental Research 2007;86:12-24.
117. Bjork A, Skieller V. Facial development and tooth eruption. An implant study at the age of puberty. Am J Orthod 1972;62:339-383.
118. McNamara JAJ. Neuromuscular and skeletal adaptions to altered function in the orofacial region. Am J Orthod 1973;64:578-606.
119. Stutzmann J, Petrovic A. Role of the lateral pterygoid muscle and meniscotemporomandibular frenum in spontaneous growth of the mandible and in growth stimulated by the postural hyperpropulsor. Am J Orthod and Dentofacial Orthop 1990;97:381-392.
120. Hiyama S, Ono PT, Ishiwata Y, Kuroda T, McNamara JA, Jr. Neuromuscular and skeletal adaptations following mandibular forward positioning induced by the Herbst appliance. Angle Orthodontist 2000;70:442-453.
121. Easton J, Carlson D. Adaptation of the lateral pterygoid and superficial masseter muscles to mandibular protrusion in the rat.
. Am J Orthod Dentofacial Orthop. 1990;97:149-158.
122. Whetten L, Johnston L. The control of condylar growth: an experimental evaluation of the role of the lateral pterygoid muscle. Am J Orthod 1985;88:181-190.
123. Sessle B, Woodside D, Bourque P, Gurza S, Powell G, Voudouris J et al. Effect of functional appliances on jaw muscle activity. Am J Orthod and Dentofacial Orthop 1990;98:222-230.
124. Luder H. Post natal development, ageing and degeneration of the TMJ in humans monkeys and rats. In: J M, editor. Craniofacial growth series. Michigan Ann Arbor Centre for Human Growth and development; University of Michigan 1993.
125. Rabie AB, Wong, L., Tsai, M. Replicating mesenchymal cells in the condyle and the glenoid fossa during mandibular forward positioning. Am J Orthod Dentofacial Orthop. 2003;123:49-57.
126. Rabie AB, She TT, Harley VR, Rabie ABM. Forward mandibular positioning up-regulates SOX9 and type II collagen expression in the glenoid fossa. Journal of Dental Research 2003;82:725-730.
127. Tang GH, Rabie AB, Hagg U, Rabie ABM. Indian hedgehog: a mechanotransduction mediator in condylar cartilage. Journal of Dental Research 2004;83:434-438.
128. Marques MR, Hajjar D, Franchini KG, Moriscot AS, Santos MF, Marques MR et al. Mandibular appliance modulates condylar growth through integrins. Journal of Dental Research 2008;87:153-158.
129. Nishida T. CTGF/Hcs24, a hypertrophic chondrocyte specific gene product, stimulate proliferation, differentiation but not hypertrophy of cultured articular chondrocytes. Journal of Cellular Physiology 2002;192:55-63.
130. Tang GH, Rabie AB, Rabie ABM. Runx2 regulates endochondral ossification in condyle during mandibular advancement. Journal of Dental Research 2005;84:166-171.
131. Rabie AB, Leung, F.Y., Chayanupatkul, A., Hagg, U. The correlation between neovascularization and bone formation in the condyle during forward mandibular positioning. Angle Orthod. 2002;72:431-438.

132. Rabie AB, Shum L, Chayanupatkul A, Rabie ABM, Shum L, Chayanupatkul A. VEGF and bone formation in the glenoid fossa during forward mandibular positioning. American Journal of Orthodontics & Dentofacial Orthopedics 2002;122:202-209.
133. Forsythe J, Jiang B, Iyer N, Agani F, Leung S, Koos R et al. Activation of vascular endothelial growth factor gene transcription by hypoxia-inducible factor 1. Mol. Cel. Biol 1996;16:4604-4613.
134. Pufe T, Lemke A, Kurz B, Petersen W, Tillmann B, Grodzinsky A et al. Mechanical overload induces VEGF in cartilage discs via hypoxia-inducible factor. Am J Pathol 2004;164:185-192.
135. Niida S, Kaku H, Amano H, Yoshida H, Kataoka H, Nishikawa S et al. VEGF can substitue for macrophase CSF in the support of osteoclastic bone resorption. J Exp Med 1999;190:293-298.
136. Engsig M, Chen T, Vu T, Pedersen A, Thirkidsen B, Lund L et al. MMP9 and VEGF are essential for osteoclast recruitment into developing long bones. J Cell Biol 2000;151:879-889.
137. Shirakura M, Tanimoto K, Eguchi H, Miyauchi M, Nakamura H, Hiyama K et al. Activation of the hypoxia-inducible factor 1 in overloaded temporomandibular joint and induction of osteoclastogenesis. Biochem Biophys Res Com 2010;393:800-805.
138. Al-kalaly A, Wu C, Wong R, Rabie A. The assessment of cell cycle genes in the rat mandibular condyle. Archives of Oral Biology 2009;54:470-478.
139. Chu FT, Tang GH, Hu Z, Qian YF, Shen G, Chu FT et al. Mandibular functional positioning only in vertical dimension contributes to condylar adaptation evidenced by concomitant expressions of L-Sox5 and type II collagen. Archives of Oral Biology 2008;53:567-574.
140. Fuentes MA, Opperman LA, Buschang P, Bellinger LL, Carlson DS, Hinton RJ et al. Lateral functional shift of the mandible: Part I. Effects on condylar cartilage thickness and proliferation. American Journal of Orthodontics & Dentofacial Orthopedics 2003;123:153-159.
141. Fuentes MA, Opperman LA, Buschang P, Bellinger LL, Carlson DS, Hinton RJ et al. Lateral functional shift of the mandible: Part II. Effects on gene expression in condylar cartilage. American Journal of Orthodontics & Dentofacial Orthopedics 2003;123:160-166.
142. Nakano H, Watahiki, J., Kubota, M., Maki, K., Shibasaki, Y., Hatcher, D., Miller, A.J. Micro X-ray computed tomography analysis for the evaluation of asymmetrical condylar growth in the rat. Orthod Craniofac Res 2003;6:168- 172.
143. Dermaut LR, Aelbers, C.M. Orthopedics in orthodontics: Fiction or reality. A review of the literature--Part II. Am J Orthod Dentofacial Orthop 1996;110:667-671.
144. Webster T, Harkness, M., Herbison, P. Associations between changes in selevted facial dimensions and the outcome of orthodontic treatment. Am J Orthod Dentofacial Orthop 1996;110:46-53.
145. Tulloch JF, Phillips, C., Koch, G., Proffit, W.R. The effect of early intervention on skeletal pattern in Class II malocclusion: a randomized clinical trial. Am J Orthod Dentofacial Orthop. 1997;111:391-400.
146. O'Brien K, Wright J, Conboy F, Chadwick S, Connolly I, Cook P et al. Effectiveness of early treatment with the Twin-block appliance: a multi-center, randomized, controlled trial. Part 1: dental and skeletal effects Am J Orthod Dentofacial Orthop 2003;124:234-243.
147. Darendeliler MA. Validity of Randomized Clinical Trials in Evaluating the Outcome of Class II treatment. Seminars in Orthodontics 2006;12:67-79.
148. Freeman DC, McNamara JA, Jr., Baccetti T, Franchi L, Frankel C, Freeman DC et al. Long-term treatment effects of the FR-2 appliance of Frankel. American Journal of Orthodontics & Dentofacial Orthopedics 2009;135:570.e571-576; discussion 570-571.
149. Lund D, Sandler P. The effects of twin blocks: a prospective controlled study. Am J Orthod Dentofacial Orthop. 1998;113:104.
150. Baccetti T, Franchi L, Toth LR, McNamara JA, Jr. Treatment timing for Twin-block therapy. American Journal of Orthodontics & Dentofacial Orthopedics 2000;118:159-170.
151. Faltin KJ, Faltin RM, Baccetti T, Franchi L, Ghiozzi B, McNamara JA, Jr. et al. Long-term effectiveness and treatment timing for Bionator therapy. Angle Orthodontist 2003;73:221-230.

152. Cozza P, Baccetti T, Franchi L, De Toffol L, McNamara JA, Jr., Cozza P et al. Mandibular changes produced by functional appliances in Class II malocclusion: a systematic review. American Journal of Orthodontics & Dentofacial Orthopedics 2006;129:599.e591-512; discussion e591-596.
153. McNamara JAJ, Bookstein, F.L., Shaughnessy, T.G. Skeletal and dental changes following functional regulator therapy on class II patients. Am J Orthod 1985;88:91-110.
154. Baccetti T FL, Toth LR, McNamara JA Jr. Treatment timing for Twin-block therapy. Am J Orthod Dentofacial Orthop. 2000;118:159-170.
155. Baccetti T, L F. Maximising esthetic and functional changes in class II treatment by means of appropriate treatment timing. In: McNamara JAJ, Kelly K, editors. New Frontiers in Facial Michigan: Ann Arbor MI Center for Human Growth and Development University of Michigan; 2001: p. 237-251.
156. Janson G, Toruno J, Martins D. Class II treatment effects of the Frankel appliance. Eur J Orthod. 2003;25:301-309.
157. DeAlmeida M, Henriques J, Ursi W. Comparative study of the Frankel and Bionator appliance in the treatment of class II malocclusion. Am J Orthod Dentofacial Orthop. 2002;121:458-466.
158. Franchi L, Baccetti T, McNamara JA, Jr. Treatment and posttreatment effects of acrylic splint Herbst appliance therapy. American Journal of Orthodontics & Dentofacial Orthopedics 1999;115:429-438.
159. Malta L, Baccetti T, Franchi L, Faltin K, McNamara J. Long-term Dentoskeletal Effects and facial Profile Changes Induced by Bionator Therapy. Angle Orthod 2010;80:10-17.
160. McNamara J, Peterson J, Pancherz H. Histological changes associated with the Herbst appliance in adult rhesus monkeys (*Macaca mulatta)*. Sem Orthod 2003;9:26-40.
161. Pancherz H, Fisher S. Amount and direction of temporomandibular joint growth changes in Herbst treatment: a cephalometric long term investigation. Angle Orthod. 2003;73:493-501.
162. Paulsen H. Morphological changes of the TMJ condyles of 100 patients treated with the Herbst appliance in the period of puberty to adulthood: A long-term radiographic study. Eur J Orthod 1997;19:657-668.
163. Pancherz H, Ruf S, Kholhas P. "Effective condylar growth" and chin position changes in Herbst treatment: a cephalometric roentgenographic long term study. Am J Orthod Dentofacial Orthop. 1998;114:437-446.
164. Pancherz H, Littmann C. Somatic maturity and manibular morphological changes during Herbst treatment. Inf Orthod Keiferorthop 1988;20:455-470.
165. Pancherz H. Temporal and masseter activity in children and adults with normal occlusion. An electromyographic investigation. Acta Odontol Scand. 1980;38:343.
166. Pancherz H. Activity of the temporal and masseter muscles in class II division 1 malocclusions. An electromyographic investigation. Am J Orthod 1980;77:679.
167. Pancherz H, AnehusPancherz M. Muscle activity in class II division 1 malocclusion treated by bite jumping with the Herbst appliance. Am J Orthod 1980;78:321-329.
168. Franchi L, Baccetti, T., McNamara, J.A. Jr. Treatment and posttreatment effects of acrylic splint Herbst appliance therapy. Am J Orthod Dentofacial Orthop. 1999;115:429-438.
169. Johnston LE. Functional appliances; a mortgage on mandibular position. Aust Orthod J 1996;14:154-157.
170. Aelbers CM, Dermaut LR. Orthopedics in orthodontics: Part I, Fiction or reality--a review of the literature. American Journal of Orthodontics & Dentofacial Orthopedics 1996;110:513-519.
171. Petrovic AG, Stutzman, J.J. The concept of mandibular tissue level responsiveness to a functional appliance. In: Graber, editor. Orthodontics State of the Art, Essence of the science. St Louis: Mosby Co; 1986: p. 59-74.
172. Rabie AB, Wong L, Hagg U, Rabie ABM, Wong L, Hagg U. Correlation of replicating cells and osteogenesis in the glenoid fossa during stepwise advancement. American Journal of Orthodontics & Dentofacial Orthopedics 2003;123:521-526.
173. Dai J, Rabie A. Direct AAV-mediated gene delivery to the temporomandibular joint.

. Front Biosci 2007;12:12-20.
174. Dai J, Rabie A. Gene Therapy to Enhance Condylar Growth Using rAAV-VEGF. Angle Orthod 2008;78:89-94.
175. Li Q, Dai J, Rabie A. Recombinant adeno-associated virus serotype 2 (rAAV2)-An efficient vector for gene delivery in condylar cartilage, glenoid fossa and TMJ disc in an experimental study in vivo Arch Oral Biol 2009;10:943-950.
176. Li Q, Rabie A. A new approach to control condylar growth by regulating angiogenesis. Archs Oral Biol 2007;52:1009-10017.
177. Rabie A, Dai J, Xu R. Recombinant AAV-mediated VEGF gene therapy induces condylar growth. Gene Therapy 2007;14:972-980.
178. Dai J, Rabie A. Gene therapy to enahnce condylar growth using rAAV-VEGF. Angle Orthodontist 2008;78:89-94.
179. Rabie AB, Tsai MJ, Hagg U, Du X, Chou BW, Rabie ABM et al. The correlation of replicating cells and osteogenesis in the condyle during stepwise advancement. Angle Orthodontist 2003;73:457-465.
180. Leung FY, Rabie AB, Hagg U, Leung FYC, Rabie ABM. Neovascularization and bone formation in the condyle during stepwise mandibular advancement. European Journal of Orthodontics 2004;26:137-141.
181. Wey M, Bandeus M, Peng L, Hagg U, Rabie A, Robinson W. Stepwise advancement versus maximum jumping with headgrea activator. European Journal of Orthodontics 2007;29:283-293.
182. Hagg U, Rabie A, Bendeus M, Wong R, Wey M, Du X et al. Condylar growth and mandibular positioning with stepwise versus maximum advancement. Am J Orthod Dentofacial Orthop. 2008;134:252-236.
183. Du X, Hagg U, Rabie A. Effects of headgear Herbst and mandibular step-by-step advancement versus conventional Herbst appliance and maximal jumping of the mandible. European Journal of Orthodontics 2002;24:167-174.
184. Banks P, Wright J, O'Brien K, Banks P, Wright J, O'Brien K. Incremental versus maximum bite advancement during twin-block therapy: a randomized controlled clinical trial. American Journal of Orthodontics & Dentofacial Orthopedics 2004;126:583-588.
185. Tan A. The effects of combined glucosamine sulfate and chondroitin sulfate supplements on condylar cartilage during functional appliance therapy. A micro CT Study. Orthodontics. Sydney: University of Sydney; 2008.
186. Barley G. The effects of combined glucosamine sulfte and chondroitin sulfate supplements on condylar cartilage remodelling during functional appliance therapy. A micro-CT study. Orthodontics. Sydney: University of Sydney 2008.
187. Pancherz H, Littmann C. Mandibular morphology and position in Herbst treatment. A cpehalometric analysis of changes to the end of growth. Inf Orthod Keiferorthop 1989;21.
188. Pancherz H. The effect of continuous bite jumping on the dentofacial complex: a follow up study after Herbst appliance treatment of class II malocclusions. Eur J Orthod. 1981;3:49-60.
189. Pancherz H. The nature of class II relapse after Herbst appliance treatment: a cephalometric long-term investigation. Am J Orthod Dentofacial Orthop. 1991;100:220-233.
190. Pancherz H, Hansen K. Occlusal changes during and after Herbst treatment: A cephalometric investigation. Eur J Orthod. 1986;8:215-228.
191. Downey P, Siegel M. Bone biology and the clinical implications for osteoporosis. Physical Therapy 2006;86:77-91.
192. Clarke B. Normal Bone Anatomy and Physiology. Clinical Journal of th American Society of Nephrology 2008;3:S131-S139.
193. Sommerfeldt DW, Rubin CT. Biology of bone and how it orchestrates the form and function of the skeleton. European Spine Journal 2001;10 Suppl 2:S86-95.

194. Nanci A. TenCate's Oral Histology; Development, Structure and Function. In: Rudolph P, editor. St Louis: Mosby; 2003.
195. Burger EH, Klein-Nulend J. Mechanotransduction in bone--role of the lacuno-canalicular network. FASEB Journal 1999;13 Suppl:S101-112.
196. Alberts B, Johnson A, Lewis J, Raff M, Roberts K, walter P. Molecular Biology of the Cell. In: Gibbs S, editor. New York: Garland Science; 2002.
197. Aszodi A, Bateman J, Gustafsson E, Boot-Hanford R, Fassler R. Mamalian skeletogenesis and extracellular matrix: what can we learn from knockout mice? Cell Struc Funct 2000;25:73-84.
198. Sandberg M. Matrix Cartilage and Bone Development: Current Views on the Function and Regulation of Major Organic Components. Ann Med 1991;23:207-217.
199. Marieb EN. Human Anatomy and Physiology. Redwood City: The Benjamin/Cummings Publishing Company, Inc
1995.
200. Judex S, Gupta S, Rubin C. Regulation of mechanical signals in bone. Orthodontics & Craniofacial Research 2009;12:94-104.
201. Robling A, Castilli A, Turner C. Biomechanical and molecular regulation of bone remodeling. Annual Review of Biomedical Engineering 2006;8:455-498.
202. Galileo G. Discorsi e dimonstrazioni matematiche, intorno a due nuove scienze attentanti alla meccanica ed a muovementi localli 1638.
203. Wyman J. On the cancellated structure of some of the bones of the human body. J. Nat. History 1857;6:125-140.
204. Roux W. Beitrage zur Morphologie der funktionellen Anpassung. 3. Beschreibung und Erlauterung einer knochernen Kniegelenksankylose. Archiv fur Anatomie, Physiologie und wissenschaftliche Medizin 1885:120-158.
205. Koch J. The laws of bone architecture. American Journal of Anatomy 1917;21:177.
206. Carey EJ. Studies in the dynamics of histogenesis. Radiology 1929;13:127.
207. Frost HM. The Laws of Bone Structure. Springfield Illinois: Charles C Thomas; 1964.
208. Frost HM. Bone 'mass' and the 'mechanostat'. Anatomical Record 1987;219:1-9.
209. Ehrlich PJ, Noble BS, Jessop HL, Stevens HY, Mosley JR, Lanyon LE. The effect of in vivo mechanical loading on estrogen receptor alpha expression in rat ulnar osteocytes. Journal of Bone & Mineral Research 2002;17:1646-1655.
210. Enlow DH. Wollf's Law and the factor of architectonic circumstance. Am J Orthod 1968;54:803-822.
211. Lanyon LE. Experimental support for the trajectorial theory of bone structure. Journal of Bone & Joint Surgery - British Volume 1974;56:160-166.
212. Ehrlich PJ, Lanyon LE. Mechanical strain and bone cell function: A review. Osteoporosis International 2002;13:688-700.
213. Rubin CT, Lanyon LE. Kappa Delta Award paper. Osteoregulatory nature of mechanical stimuli: function as a determinant for adaptive remodeling in bone. Journal of Orthopaedic Research 1987;5:300-310.
214. Rubin J, Murphy T, Nanes MS, Fan X. Mechanical strain inhibits expression of osteoclast differentiation factor by murine stromal cells. American Journal of Physiology - Cell Physiology 2000;278:C1126-1132.
215. Yellowley CE, Li Z, Zhou Z, Jacobs CR, Donahue HJ. Functional gap junctions between osteocytic and osteoblastic cells. Journal of Bone & Mineral Research 2000;15:209-217.
216. Doty SB. Morphological evidence of gap junctions between bone cells. Calcified Tissue International 1981;33:509-512.
217. Cowin SC. Bone poroelasticity. Journal of Biomechanics 1999;32:217-238.
218. Donahue HJ. Gap junctional intercellular communication in bone: a cellular basis for the mechanostat set point. Calcified Tissue International 1998;62:85-88.

219. Rubin CT, Lanyon LE. Regulation of bone formation by applied dynamic loads. Journal of Bone & Joint Surgery - American Volume 1984;66:397-402.
220. Cowin SC, Moss-Salentijn L, Moss ML. Candidates for the mechanosensory system in bone. Journal of Biomechanical Engineering 1991;113:191-197.
221. Weinbaum S, Cowin S, Zeng Y. A model for the excitation of osteocytes by mechanical loading-induced bone fluid sheer stresses. Journal of Biomechanics 1994;27:339-360.
222. Pienkowski D, Pollack SR. The origin of stress-generated potentials in fluid-saturated bone. Journal of Orthopaedic Research 1983;1:30-41.
223. Reich KM, Gay CV, Frangos JA. Fluid shear stress as a mediator of osteoblast cyclic adenosine monophosphate production. Journal of Cellular Physiology 1990;143:100-104.
224. Pavalko FM, Chen NX, Turner CH, Burr DB, Atkinson S, Hsieh YF et al. Fluid shear-induced mechanical signaling in MC3T3-E1 osteoblasts requires cytoskeleton-integrin interactions. American Journal of Physiology 1998;275:C1591-1601.
225. Hung CT, Allen FD, Pollack SR, Brighton CT. What is the role of the convective current density in the real-time calcium response of cultured bone cells to fluid flow? Journal of Biomechanics 1996;29:1403-1409.
226. Bronckers AL, Goei W, Luo G, Karsenty G, D'Souza RN, Lyaruu DM et al. DNA fragmentation during bone formation in neonatal rodents assessed by transferase-mediated end labeling. Journal of Bone & Mineral Research 1996;11:1281-1291.
227. Rubin C, Lanyon L. Osteoregulatory nature of mechanical stimuli: Function as a determinant for adaptive remodelling in bone. Journal of Orthopaedic Research 1987;5:300-310.
228. Kumar V, Abbas A, Fausto N, Mitchell R. Robbins Basic Pathology. Philadelphia: Saunders Elsevier; 2007.
229. Tervo T, Nordstrom P, Neovius M, Nordstrom A, Tervo T, Nordstrom P et al. Constant adaptation of bone to current physical activity level in men: a 12-year longitudinal study. Journal of Clinical Endocrinology & Metabolism 2008;93:4873-4879.
230. Dook JE, James C, Henderson NK, Price RI. Exercise and bone mineral density in mature female athletes. Medicine & Science in Sports & Exercise 1997;29:291-296.
231. Mudd LM, Fornetti W, Pivarnik JM, Mudd LM, Fornetti W, Pivarnik JM. Bone mineral density in collegiate female athletes: comparisons among sports. Journal of Athletic Training 2007;42:403-408.
232. Suominen H. Bone mineral density and long term exercise. An overview of cross-sectional athlete studies. Sports Medicine 1993;16:316-330.
233. Pirnay F, Bodeux M, Crielaard JM, Franchimont P. Bone mineral content and physical activity. International Journal of Sports Medicine 1987;8:331-335.
234. Huddleston AL, Rockwell D, Kulund DN, Harrison RB. Bone mass in lifetime tennis athletes. JAMA 1980;244:1107-1109.
235. Skerry TM, Lanyon LE. Interruption of disuse by short duration walking exercise does not prevent bone loss in the sheep calcaneus. Bone 1995;16:269-274.
236. Skerry TM, Lanyon LE. Immobilisation induced bone loss in the sheep is not modulated by calcitonin treatment. Bone 1993;14:511-516.
237. O'Doherty DM, Butler SP, Goodship AE. Stress protection due to external fixation. Journal of Biomechanics 1995;28:575-586.
238. Adolphson P, Jonsson U, Dalen N, Ehrnberg A. Stress protection by external fixation of the rabbit tibia. Acta Orthopaedica Scandinavica 1990;61:324-326.
239. Weinreb M, Patael H, Preisler O, Ben-Shemen S. Short-term healing kinetics of cortical and cancellous bone osteopenia induced by unloading during the reloading period in young rats. Virchows Archiv 1997;431:449-452.
240. Sakata T, Wang Y, Halloran BP, Elalieh HZ, Cao J, Bikle DD et al. Skeletal unloading induces resistance to insulin-like growth factor-I (IGF-I) by inhibiting activation of the IGF-I signaling pathways. Journal of Bone & Mineral Research 2004;19:436-446.

241. Money KE. Biological effects of space travel. Canadian Aeronautics & Space Journal 1981;27:195-201.
242. Keller TS, Strauss AM, Szpalski M. Prevention of bone loss and muscle atrophy during manned space flight. Microgravity Quarterly 1992;2:89-102.
243. Johnson PC, Jr. Space medicine. American Scientist 1984;72:495-497.
244. Hawkey A, Hawkey A. The physical price of a ticket into space. Journal of the British Interplanetary Society 2003;56:152-159.
245. Hert J, Liskova M, Landa J. Reaction of bone to mechanical stimuli. 1. Continuous and intermittent loading of tibia in rabbit. Folia Morphologica 1971;19:290-300.
246. Liskova M, Hert J. Reaction of bone to mechanical stimuli. 2. Periosteal and endosteal reaction of tibial diaphysis in rabbit to intermittent loading. Folia Morphologica 1971;19:301-317.
247. Rubin CT, McLeod KJ, Bain SD. Functional strains and cortical bone adaptation: epigenetic assurance of skeletal integrity. Journal of Biomechanics 1990;23 Suppl 1:43-54.
248. Lanyon LE, Smith RN. Bone strain in the tibia during normal quadrupedal locomotion. Acta Orthopaedica Scandinavica 1970;41:238-248.
249. Lanyon LE. The measurement of bone strain "in vivo". Acta Orthopaedica Belgica 1976;42 Suppl 1:98-108.
250. Goodship AE, Lanyon LE, McFie H. Functional adaptation of bone to increased stress. An experimental study. Journal of Bone & Joint Surgery - American Volume 1979;61:539-546.
251. Lanyon LE, Goodship AE, Pye CJ, MacFie JH. Mechanically adaptive bone remodelling. Journal of Biomechanics 1982;15:141-154.
252. Ehrlich PJ, Lanyon LE, Lanyon LE. Mechanical strain and bone cell function: a review. Osteoporosis International 2002;13:688-700.
253. Lanyon LE, Rubin CT. Static vs dynamic loads as an influence on bone remodelling. Journal of Biomechanics 1984;17:897-905.
254. Rubin C, Gross T, Qin YX, Fritton S, Guilak F, McLeod K. Differentiation of the bone-tissue remodeling response to axial and torsional loading in the turkey ulna. Journal of Bone & Joint Surgery - American Volume 1996;78:1523-1533.
255. Rubin CT, Lanyon LE. Dynamic strain similarity in vertebrates; an alternative to allometric limb bone scaling. Journal of Theoretical Biology 1984;107:321-327.
256. Rubin CT, Lanyon LE. Limb mechanics as a function of speed and gait: a study of functional strains in the radius and tibia of horse and dog. Journal of Experimental Biology 1982;101:187-211.
257. Carter D, Caler W, Spengler D, Frankel V. Fatigue behaviour of adult cortical bone: the influence of mean strain and strain range. Acta Odontol Scand. 1981;52:481-490.
258. Alexander RM, Maloiy G, Hunter B, Jayes A, Nturibi J. Mechanical stresses in fast locomotion in buffalo and elephant. J Zool (Lond) 1979;189:135-144.
259. McLeod K, Rubin C. Sensitivity of the bone remodeling response to the frequency of aplied strain. Trans Orthop Res Soc 1992;17:533.
260. Hylander W, Crompton A. Jaw movements and patterns of mandibular bone strain during mastication in the monkey *Macaca fascicularis*. Archs Oral Biol 1986;31:841-848.
261. Adams DJ, Spirt AA, Brown TD, Fritton SP, Rubin CT, Brand RA. Testing the daily stress stimulus theory of bone adaptation with natural and experimentally controlled strain histories. Journal of Biomechanics 1997;30:671-678.
262. Huang RP, Rubin CT, McLeod KJ. Changes in postural muscle dynamics as a function of age. Journals of Gerontology Series A-Biological Sciences & Medical Sciences 1999;54:B352-357.
263. Carindale M, Wakeling J. Whole body vibration exercise: are vibrations good for you? Br J Sports Med 2005;39:585-589.
264. Rubin C, Turner AS, Bain S, Mallinckrodt C, McLeod K. Anabolism. Low mechanical signals strengthen long bones. Nature 2001;412:603-604.

265. Rubin C, Turner AS, Mallinckrodt C, Jerome C, McLeod K, Bain S. Mechanical strain, induced noninvasively in the high-frequency domain, is anabolic to cancellous bone, but not cortical bone. Bone 2002;30:445-452.
266. Rubin C, Turner AS, Muller R, Mittra E, McLeod K, Lin W et al. Quantity and quality of trabecular bone in the femur are enhanced by a strongly anabolic, noninvasive mechanical intervention. Journal of Bone & Mineral Research 2002;17:349-357.
267. Ward K, Alsop C, Caulton J, Rubin C, Adams J, Mughal Z et al. Low magnitude mechanical loading is osteogenic in children with disabling conditions. Journal of Bone & Mineral Research 2004;19:360-369.
268. Gilsanz V, Wren TA, Sanchez M, Dorey F, Judex S, Rubin C et al. Low-level, high-frequency mechanical signals enhance musculoskeletal development of young women with low BMD. Journal of Bone & Mineral Research 2006;21:1464-1474.
269. Flieger J, Karachalios T, Khaldi L, Raptou P, Lyritis G. Mechanical stimulation in the form of vibration prevents postmenopausal bone loss in ovariectomized rats. Calcified Tissue International 1998;63:510-514.
270. Oxlund BS, Ortoft G, Andreassen TT, Oxlund H. Low-intensity, high-frequency vibration appears to prevent the decrease in strength of the femur and tibia associated with ovariectomy of adult rats. Bone 2003;32:69-77.
271. Rubin C, Recker R, Cullen D, Ryaby J, McCabe J, McLeod K et al. Prevention of postmenopausal bone loss by a low-magnitude, high-frequency mechanical stimuli: a clinical trial assessing compliance, efficacy, and safety. Journal of Bone & Mineral Research 2004;19:343-351.
272. Verschueren SM, Roelants M, Delecluse C, Swinnen S, Vanderschueren D, Boonen S et al. Effect of 6-month whole body vibration training on hip density, muscle strength, and postural control in postmenopausal women: a randomized controlled pilot study. Journal of Bone & Mineral Research 2004;19:352-359.
273. Goodship AE, Lawes TJ, Rubin CT, Goodship AE, Lawes TJ, Rubin CT. Low-magnitude high-frequency mechanical signals accelerate and augment endochondral bone repair: preliminary evidence of efficacy. Journal of Orthopaedic Research 2009;27:922-930.
274. Prisby R, Lafage-Proust M, Malaval L, Belli A, Vico L. Effects of whole body vibration on the skeleton and other organ systems in man and animal models: What we know and what we need to know. Ageing Research Reviews 2008;7:319-329.
275. Liu J, Sekiya I, Asai K, Tada T, Kato T, Matsui N. Biosynthetic response of cultured articular chondrocytes to mechanical vibration. Research in Experimental Medicine 2001;200:183-193.
276. Yamazaki S, Banes AJ, Weinhold PS, Tsuzaki M, Kawakami M, Minchew JT et al. Vibratory loading decreases extracellular matrix and matrix metalloproteinase gene expression in rabbit annulus cells. Spine Journal: Official Journal of the North American Spine Society 2002;2:415-420.
277. Takeuchi R, Saito T, Ishikawa H, Takigami H, Dezawa M, Ide C et al. Effects of vibration and hyaluronic acid on activation of three-dimensional cultured chondrocytes. Arthritis & Rheumatism 2006;54:1897-1905.
278. Darendeliler MA, Zea A, Shen G, Zoellner H, Darendeliler MA. Effects of pulsed electromagnetic field vibration on tooth movement induced by magnetic and mechanical forces: a preliminary study. Australian Dental Journal 2007;52:282-287.
279. Stark TM, Sinclair PM. Effect of pulsed electromagnetic fields on orthodontic tooth movement. American Journal of Orthodontics & Dentofacial Orthopedics 1987;91:91-104.
280. Darendeliler MA, Sinclair PM, Kusy RP. The effects of samarium-cobalt magnets and pulsed electromagnetic fields on tooth movement. American Journal of Orthodontics & Dentofacial Orthopedics 1995;107:578-588.
281. Nishimura M, Chiba M, Ohashi T, Sato M, Shimizu Y, Igarashi K et al. Periodontal tissue activation by vibration: intermittent stimulation by resonance vibration accelerates experimental

tooth movement in rats. American Journal of Orthodontics & Dentofacial Orthopedics 2008;133:572-583.
282. Melzack R, Wall P. Pain mechanisms: a new theory. Science 1965;150:971-979.
283. Nanitsos E, Vartuli R, Forte A, Dennison PJ, Peck CC. The effect of vibration on pain during local anaesthesia injections. Australian Dental Journal 2009;54:94-100.
284. Elliott J, Dover S. X-ray microtomography. J Microscopy 1982;126:211-213.
285. Feldkamp LA, Davis, LC, Kress, J.W. Practical cone-beam algorithm. J. Opt.Soc Am A 1984:612-619.
286. Davis G, Wong S. X-Ray microtomography of bones and teeth. Physiological Measurement 1996;17:121-146.
287. Feldkamp LA, Goldstein, S.A., Parfitt, A.M., Jesion, G., Kleerekoper, M. The direct examination of three-dimensional bone architecture in vitro by computed tomograrphy J Bone Miner Res 1994;4:3-11.
288. Cockman MD, Blanton, C.A., Chmielewski, P.A., Dong, L., Dufresne, T.E., Hookfin, E.B., Karb, M.J., Liu, S., Wehmeyer, K.R. Quantitative imaging of protegoglycan in cartilage using a gadolinium probe and microCT. Osteoarthritis & Cartilage. 2006;14:210-214.
289. Kusaka Y, Grunder, W., Rumpel, H., Dannhauer, K.H., Gersonde, K. MR microimaging of articular cartilage and contrast enhancement by manganese ions. Magn Reson Med 1992;24:137-148.
290. Bashir A, Gray, M.L., Burstein, D. Gd-DTPA^{2-} as a measure of Cartilage degradation. Magn Reson Med 1996;36:665-673.
291. Laurent D, Wasvary, J,. O'Byrne, E., Rudin, M. *In vivo* qualitative assessments of articular cartilage in the rabbit knee with high-resolution MRI at 3 T. Magn Reson Med 2003;50:541-549.
292. Schmitz SA, Wagner, S., Schuhmann-Giampieri, G., Wolf, K.J. Evaluation of gadobutrol in a rabbit model as a new lanthanide contrast agent for computed tomography. Investigative Radiology 1995;30:644-649.
293. Weinmann H, Brasch, R., Press, W.R., Webey, G. Characteristics of gadolinium-DTPA complex: A potential NMR contrast agent. AJR 1984;142:619-624.
294. Haustein J, Laniado, M., Niendorf, H. Triple-dose versus standard-dose gadopentetate dimeglumine: A randomized study in 199 patients. Radiology 1993;186:855-860.
295. Chappard D, Retailleau-Gaborit N, Legrand E, Basle MF, Audran M. Comparison Insight Bone Measurements by Histomorphometry and micro-CT. Journal of Bone and Mineral Res 2005;20:1177-1184.
296. Ito M. Assessment of bone quality using micro-computed tomography (micro-CT) and synchrotron micro CT. Journal of Bone and Mineral Res 2005;23(suppl):114-121.
297. Jiang Y, Zhao J, Liao E, Dai R, Wu X, Genant H. Application of micro-CT assessment of 3D bone microstructure in preclinical and clinical studies. Journal of Bone and Mineral Res 2005;23(Suppl):122-131.

10 Manuscript

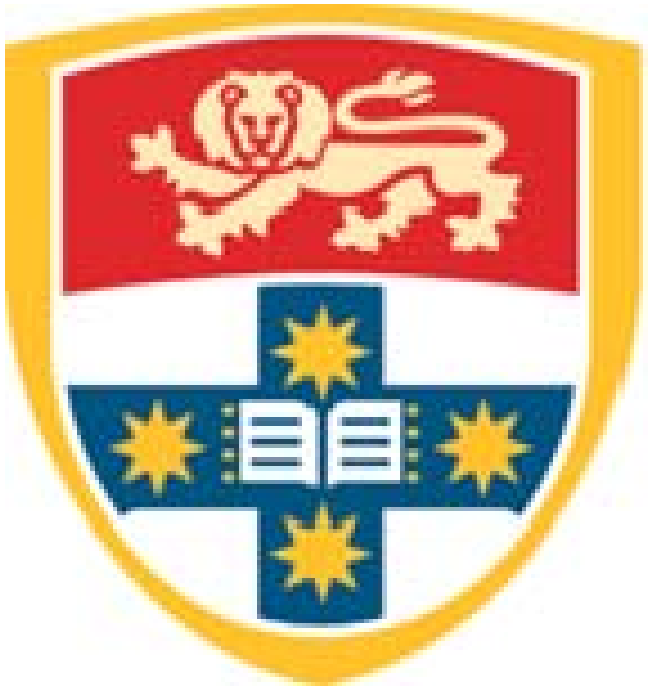

The effect of high-frequency, low-magnitude mechanical stimuli on the rat condyle during mandibular protrusion.

A Micro-CT Study

A condensed version of this manuscript will be submitted for publication

11 Abstract

Functional appliances in orthodontics can improve the dentofacial relationship of growing patients with mandibular retrognathia associated with Class II skeletal patterns partly through functional adaption of the mandibular condylar cartilage and bone. High-frequency, low-magnitude mechanical stimuli (vibration) have been shown to induce positive responses in bone integrity in condylar trabecular bone. This study aimed to investigate the effect of these stimuli on mandibular condylar cartilage and its endochondral bone during functional appliance treatment.

One hundred and thirty, five-week old Sprague-Dawley rats were divided into five groups: baseline controls, age-matched untreated animals representing normal growth, animals exposed to vibration alone, animals fitted with functional appliances alone, and those receiving functional appliance together with vibration. The baseline controls were sacrificed at day 0 and the animals in the other groups were sacrificed at time points 7, 21 and 30 days. The animals receiving the functional appliance treatment wore a mandibular protrusion appliance consisting of paediatric strip crowns placed on their upper and lower incisors. The vibration groups received 30Hz, 0.3g whole body vibration for 20 minutes per day, 5 days per week for up to 30 days. Following specimen preparation, the right condyles were stained with Gadolinium Chloride and imaged using X-ray microtomography for subsequent measurement of the mandibular condylar cartilage volume and bone morphometric parameters.

X-ray microtomographic images of the condyles revealed that the functional appliances in this study, with or without vibration caused a loss of integrity of the mandibular condylar cartilage, and bone resorption at the anterior aspect of the condyle, while the cartilage and bone remained intact at the posterior aspect, showing signs of endochondral ossification. The volume of cartilage significantly decreased ($p<0.01$) due to the cartilage breakdown. The bone quality and complexity in the condyle of the functional appliance only group significantly decreased, whereas the bone quality in the

condyle of the functional appliance group with vibration remained statistically undifferentiated from the untreated animals. It was concluded that functional loading with anterior mandibular positioning can cause adverse effects at the anterior aspect of the condyle that are significantly reduced in the presence of high-frequency, low-magnitude mechanical stimuli. Despite the loss of integrity at the anterior aspect of the condyle, endochondral ossification is likely to proceed at the posterior aspect of the condyle in response to the mechanical strain, accounting for the modification in gross condylar morphology favourable to Class II correction.

Key words: condylar cartilage, trabecular bone, functional appliance, high-frequency, low-magnitude mechanical stimuli, X-ray microtomography (micro-CT), gadolinium

12 Introduction

The aims of mandibular growth modification are to correct the Class II dental and skeletal malocclusion and to achieve an improvement in balance of the facial profile. The action of functional appliances is believed to be multifactorial, exerting effects in the mandible, maxilla and dentoalveolus [1]. The effect of functional appliances on the temporomandibular joint (TMJ) has been widely reported in the literature, however remains controversial.

The adaptive nature of the mandibular condylar cartilage is suggestive of its possible participation in achieving positive results in response to functional appliance treatment [2,3]. The mandibular condylar cartilage is a unique type of articular cartilage, able to respond and adapt to the external environment throughout life [3,4]. It is a secondary cartilage and is characterised by its unique histomorphology that typifies its function of chondrogenesis and endochondral ossification during normal growth and adaption.

Condylar and glenoid fossa adaption to mandibular protrusion has been reported in the literature since the early 1940's based on histological studies conducted on monkeys [5,6]. Subsequent to this, consistently similar findings have been reported [7-12]. These studies observed that, in response to mandibular protrusion, growth of the condyle is redirected posteriorly, with the glenoid fossa relocating anteriorly, thereby contributing to the Class II correction. Histological studies on rats [13] and monkeys [5,6,11,12,14-16] show that there is an initial increase in condylar cartilage thickness, followed by thinning to baseline levels as endochondral ossification ensues . A similar temporal change in cartilage thickness has been observed in human studies investigating the effects of the Herbst appliance on the TMJ using magnetic resonance imaging [17,18].

The use of high-frequency, low-magnitude mechanical stimuli for therapeutic purposes has evolved from a long history of studies investigating the relationship between bone and the external environment. The original concept of 'form follows function' was introduced by Wolff [19] however did

not explain the specific parameters of the osteogenic stimulus responsible for functional bone adaption. Extensive subsequent experimental investigations [20-22] found that the frequency of the applied load is important in functional bone adaption, such that, as the frequency of the applied load increased, the strain required to maintain bone was dramatically reduced. Fritton *et al.* [23] and Rubin *et al.* [24] have shown that loading frequency is also of prime importance in defining bone morphology in the natural state. Fritton *et al*. [23] showed that very small strains occur many times a day (hundreds of times in the order of 100με and thousands of times in the order of 10με), whereas peak strains occur only a few times per day. The continual barrage of high-frequency stimuli in the range of 20Hz to 40Hz that engender small but continual strains in bone are therefore considered important in the organisation of bone tissue. It was therefore concluded from these studies that extremely high frequencies, engendering extremely small strain magnitudes for a sufficient period of time may be used therapeutically to maintain bone or promote osteogenesis [20,23,24]. A whole body vibration device has been developed capable of delivering high-frequency, low-magnitude stimuli to bone [25] and has proven effective in transmitting the vibratory stimuli to the skeleton in humans [26] and small experimental animals [27-33].

Recent studies have reported an increase in bone formation in the condyles of adult mice in response to whole body vibration[28] and in the condyles of Sprague-Dawley rats in response to mechanical strain produced by mandibular advancement [34]. No study, however had investigated the concomitant use of functional appliances and vibration on the mandibular condylar cartilage and bone.

13 Aims and Objectives

The aim of this study was to investigate the possibility that high-frequency, low-magnitude mechanical stimuli could enhance the effect of functional appliance therapy through positively

influencing mandibular condylar cartilage and bone remodelling in the mandibular condyle during functional protrusion in growing rats using X-ray microtomography (micro-CT).

The objectives were:

1) To compare the quantitative changes in the mandibular condylar cartilage volume during functional protrusion with and without vibration;

2) To compare the quantitative changes in the mandibular condylar bone during functional protrusion with and without vibration;

3) To describe and compare the qualitative two and three dimensional morphological changes occurring in the rat mandibular condyle and glenoid fossa during functional protrusion, with and without vibration.

14 Materials and Methods

14.1 Animal Grouping and Housing

One hundred and thirty, four week old female Sprague-Dawley rats were used for this investigation (Ethics Approval: UNSW Animal Ethics; Application ID: 4049566/2; Approval #: 09/65A). Previous studies investigating the effects of functional appliances on the mandibular condyle have utilised this species [2,13,35-48].

The animals were received at 4 weeks of age and randomly divided into four experimental groups of thirty, and one baseline control group of ten.

Baseline controls (n=10);

Group 1 - normal growth (age matched controls) (n=30) receiving no functional appliance and no vibration

Group 2 - functional appliance group (n=30) receiving functional appliance only

Group 3 - vibration group (n=30) receiving vibration only

Group 4 - functional appliance with vibration group (n=30) receiving both functional appliance and vibration.

The animals were housed in approved housing and environment with 12 hour day-night cycle with water and food available 24 hours per day. The diet consisted of Purina Supercoat Puppy kibble (Purina, Nestle Australia Ltd, Sydney, Australia) containing 29% protein and 14% fat, and Nutrigel a highly palatable oral supplement used in veterinarian medicine to provide full or partial nutritional support for mammals. The control animals were housed four per box and the experimental animals two per box.

Following one week of acclimatisation, functional appliance treatment and vibration were started in the designated groups at 5 weeks of age in order to coincide with peak growth reported to start in the rat model at 31.5 days (4 weeks 3.5 days) and end by 135 days (19 weeks 2 days) [49].

14.2 Functional Appliance Placement

In preparation for the appliance placement, the animals were anaesthetised with isofluorane inhalation (2%) and oxygen (2%). Whilst under anaesthesia the animals were weighed and administered with 0.01mg/kg Buprenophine analgesia.

To ensure adequate and continuous protrusion of the mandible throughout the experiment, paediatric strip crown forms (3M™ ESPE™ Strip Crown Form *USA*) were placed on the upper and lower incisor teeth of the rats. (Figure 1) The lower incisor teeth were dried with cotton pellets, primed with self etching primer (3M™ Unitek, *Monrovia, California, USA*) and the composite resin (3M™ ESPE™ Z100 restorative capsule; 3M™ ESPE™ dispenser for capsule) filled paediatric strip crown positioned back to front with the inclined plane sloping upwards anteriorly. The composite

resin was set before repeating the bonding procedure for the upper crown placement. The upper crown was positioned back to front with the inclined plane sloping downwards posteriorly. Any rough areas were smoothed and excess composite resin removed**.**

14.3 Vibration

High-frequency, low-magnitude mechanical stimulation was administered to the rats via whole body vibration platforms (Juvent®™ *Inc, New Jersey, USA)* that generated vertical ground based vibration. The cages containing the rats were placed on the platforms one at a time (Appendix 2a), with the vibratory stimulus preset at a frequency of 30Hz and magnitude of 0.3g, where $g=9.8m.s^{-1}$ producing peak strains of approximately 5με [50]. The stimulus was applied for 20 minutes per day, five days per week for 30 days based on previous studies [27,28,50-56].

14.4 Animal Monitoring

The weight of each animal was taken and recorded upon arrival at the animal housing facility, at the start of the experimental period and at the time of sacrifice. Scientific scales with a dynamic weighing application were used (OHAUS™ Explorer® Proanalytical Precision Balance, *Victoria Australia*) (Appendix 2b). Dynamic weighing allows weight determination of unstable objects such as moving animals, by calculating the mean value of a certain number of weights recorded over a given time. The monitoring protocol deemed additional weighing necessary if weight loss was suspected as indicated by palpation of the animal, lack of food consumption or alteration in behaviour.

Intra-operative observations of vital signs including respiration, pulse, eye discharge, and body reflexes were carried out and recorded at ten minute intervals. Maintenance of body temperature was aided by the use of heat pads and immediate post-operative recovery took place under a heat lamp.

Post surgical monitoring and recording of each animal took place daily for the week following appliance placement and then twice weekly for the remainder of the experimental period. Observations were made for changes in the coat of the animal, alterations in behaviour and mobility, decreases in dietary intake, integrity of the appliances and adequacy of mandibular protrusion. The animals receiving vibration were monitored while on the vibration platforms. All animals were checked twice daily during feeding times throughout the experiment.

14.5 Study Design

The baseline control animals were sacrificed at the start of the experimental period. The age matched control group, functional appliance only group, vibration only group and functional appliance with vibration group were sacrificed in sub-groups of ten at days 7, 21 and 30. (Figure 2) Carbon dioxide inhalation was used for euthanasia.

14.6 Specimen Preparation

Post-mortem photographic and radiographic records (32kV for 22 seconds) of each rat were collected as a record of the functional appliance integrity and jaw position. (Appendix 2c)

Subsequently, the heads were decapitated, degloved and hemi-sectioned in the median plane. The right side of the skulls were used for this study and were further void of superfluous tissue before being fixed and stored in 10% buffered formalin. (Appendix 2d)

Each sample was stained with 0.2M gadolinium chloride ($GdCl_3$) for a period of six days in a refrigerator at 4^oC following a previously devised staining protocol [57,58] based on the research of Cockman *et al*. [59]. Gadolinium (Gd) is a lanthanide element with a high atomic number and at the concentration of 0.2M has been shown to effectively stain cartilage for micro-CT scanning [59]. It is positively charged and is attracted to the negatively charged groups of the glycosaminoglycans that make up proteoglycans in cartilage. Through such binding it can be utilised as an effective contrast

medium in cartilage imaging using magnetic resonance imaging (MRI) or micro-CT, due to its absorption of highly energetic photons [59]. The gadolinium stain therefore aids the segmentation procedure for condylar cartilage morphologic and volumetric analysis using micro-CT.

After the six days, the samples were removed from the stain, rinsed three times in Milli-Q Ultra Pure water (Millipore, *USA*), dried with Kimwipe tissues (Kimberly-Clarke Pty Ltd *Australia*) and sealed in Para film Sealing Film (Brand, USA). The waste stain and run-off were discarded following laboratory protocols.

14.7 Specimen Imaging

The Skyscan 1172 (Skyscan™, *Aartselaar, Belgium*) high-resolution, in-vitro, desk top X-ray microtomograph was used to acquire scans of each sample. The specimen was mounted onto a purpose made radiolucent positioning jig and secured with parafilm. To ensure consistency in sample positioning, the mandibular plane of the rat mandible was aligned with the straight edge of the jig and the condylar position aligned with a predetermined marking on the jig. (Appendix 2e)

Prior to starting each scan, preliminary viewing of the specimen at rotation steps of 45, 90, 135, 180, 270 and 360 degrees ensured the region of interest was included in the field of view throughout the entire scan.

Three-dimensional microstructural information was captured as the sample was rotated over a total range of 360 degrees, taking digital recordings of X-ray absorption radiographs at angular increments of 0.39 degrees, creating 923 projections, each 2048x1024 pixels (medium camera pixel size). The exposure was set at 60kV and 160mA. A resolution of 6.8µm was predetermined to be adequate to analyse the morphology of the condyle and volume of the mandibular condylar cartilage [57,58] and was therefore used in this study. Micro-CT scans of resolution less than 10µm are reported in the literature to be adequate to obtain bone morphometric data from trabecular bone [60-62].

Upon completion of the scan, the specimen was returned to the 10% buffered formalin for storage.

Three dimensional (3D) data sets were created for each sample from the set of acquired angular two dimensional (2D) projections using Skyscan's volumetric reconstruction software, 'NRecon' (Skyscan™, *Aartselaar, Belgium*) and saved in bitemap data format with the software generating a series of approximately 1000, 8 bit axial slices each of 2048x2048 pixels with a Z dimensional spacing equal to the within slice pixel spacing i.e. isotrophic sampling. This program uses a modified Feldkemp algorithm with automatic adaption to the scan geometry in each micro-CT scanner. The reconstruction involved interactive thresholding including beam hardening correction, ring artefact correction, minimal smoothing, alignment optimisation and contrast adjustment.

The three dimensional data was subsequently rendered as 3D visualisations using the VG Studio Max Version 2.0 software (Volume Graphics GmbH, *Heidelberg, Germany*) from which condylar cartilage volume was analysed. 'CT analyser' software Version 1.10.1.0 (Skyscan™, *Aartselaar, Belgium*) was used to analyse the trabecular bone of the mandibular condyle.

14.8 Sample analysis

14.8.1 Qualitative Analysis of the Condyle

Qualitative analysis was achieved by visualisation and observation of each sample within their sub-groups. Descriptions of condylar morphology, mandibular condylar cartilage integrity and thickness, and bone integrity of the condyle and glenoid fossa were noted. Comparisons of these features were made between time points and groups.

14.8.2 Quantitative Analysis of Mandibular Condylar Cartilage

The initial 3D visualisation of the rat condyles on VG Studio Max (Version 2.0 software; Volume Graphics GmbH, Heidelberg, Germany) was used to determine the area of the condylar cartilage, as defined by anatomical landmarks on the condylar head. The perimeter of the cartilage was

demarcated by the prominent bony ridges on the medial and lateral surfaces of the condyle that were joined by lines of best fit across the less defined anterior and posterior anatomical contours.

The gadolinium chloride stain further enhanced isolation and reconstruction of the intact condylar cartilage to show its spatial configuration and volume. During the segmentation process, slices in the x-z imaging plane were interactively partitioned using the 2D static region growing tool to select grey scale values corresponding to the cartilage. The tolerance yielding the best results was subsequently applied in three dimensions. Voids remaining in the continuity of the cartilage after region growing were eliminated using the opening and closing feature and an interactive drawing tool. Conversely, the areas designated by region-growing beyond the anatomical landmarks circumscribing the cartilage perimeter were eliminated using an interactive editing tool. The accuracy of the segmentation process was enhanced by the use of the Gaussian filter, used to smooth the image by removing noise. Only intact cartilage was measured. This was visualised as a continuous band of cartilage over intact bone.

The region of cartilage, also called the region of interest, was subsequently visualised as a separate 3D rendering. The colouring tool was utilised to pigment the region of interest. Superimposition of the pigmented region of interest over the entire 3D image of the condylar head confirmed adequate cartilage segmentation in 3D. Refinements were made as necessary to maximise the accuracy of the segmentation process. (Figure 3) A volumetric measurement of the region of interest could then be calculated by the software.

14.8.3 Quantitative Bone Analysis: Bone Morphometry

Skyscan's CT Analyser software (Version 1.10.1.0) was used to analyse the trabecular bone representative of the entire mandibular condyle and generate quantitative morphometric data from the reconstructed micro-CT scans. A three dimensional volume of interest measuring 0.084mm^3 was segmented from the condylar bone. This was constructed by measuring an area of 0.45mm^2 in the x-

y imaging plane on the anatomical mid-coronal slice of the condyle. The region of interest was expanded through 30 slices in both directions in the x-z imaging plane. The volume of interest was localised immediately beneath the condylar cartilage in intact bone with the middle slice co-incident with the anatomical mid-coronal plane of the condyle. (Figure 4)

The morphometric parameters were recorded using the Bone ASBMR nomenclature devised by Parfitt *et al.* [63]. (Table 1) Bone morphometry is descriptive of trabecular micro architecture that relates to trabecular quality, complexity and biomechanical properties [60,63]. Bone morphometry is useful for studying bone changes under different loading circumstances over time and is therefore appropriate for examining the effects of functional appliances and vibration on condylar bone in this study. Trabecular number (Tb.N) represents the number of traversals across the trabecular structure made per unit length through the region of interest. Trabecular thickness (Tb.Th) represents the 3D thickness of the trabecular structure. Trabecular separation is the thickness of the spaces between trabecular structures, as defined by binarisation within the volume of interest. Parameters indicating connectivity and structure of the bone are trabecular bone pattern factor (Tb.Pf) and structure model index (SMI). A decrease in Tb.Pf [64], indicates a well connected spongy lattice of greater connectivity. Negative values are symbolic of enclosed cavities and concave spaces. The structure model index indicates the relative prevalence of rods and plates in trabecular bone. A well structured bone consists predominantly of plates, empirically measuring values close to 0. A more rod-like trabecular bone approaches empirical values close to 3 and indicates poorly structured bone. The complexity of the bone is represented by the bone surface (BS - surface area of the bone within the region of interest), bone surface to bone volume ratio (BS/BV) and the bone surface density (BS/TV). Bone morphometric parameters are most useful when assimilated, rather than considered individually[60]. For example, in the case of bone deterioration, it is feasible to expect that as the trabecular number and trabecular thickness decrease, there will be an increase in trabecular separation and a shift to a more rod like trabecular structure seen by an increase in structure model

index [60]. In contrast, an anabolic response to loading would show an increase in trabecular number and trabecular thickness with a corresponding decrease in trabecular separation, a shift to better trabecular connectivity (seen by a decrease in trabecular pattern factor) and plate-like trabeculae (seen by a decrease in structure model index) [60]. Other parameters measured include tissue volume (TV – the total volume of interest selected); bone volume (BV the total volume of binarised objects within the region of interest); percent bone volume (BV/TV the portion of the bone volume occupying the total volume of interest) and tissue surface (TS the surface area of the volume of interest).

14.9 Statistical Analysis

The data for mandibular condylar cartilage volume and bone morphometric variables were collected by a single operator and processed using PASW Version 18 statistical software (SPSS Inc., IBM, Chicago, Illinois, USA). Univariate ANOVA was used to assess the significance on the cartilage volume and multiple bone morphometric parameters of group *(P<0.05)*, day of sacrifice *(p<0.05)* and group-by-day interaction *(P<0.01.)* Post hoc comparisons were carried out to determine any significant change between time points within each group *(p<0.01)* and any significant difference between groups at any given time point *(P<0.01)*. A multivariate ANOVA, using Wilks' Lambda, for the bone parameters was used to investigate whether group *(p<0.01)*, day *(p<0.01)* and group-by-day *(p<0.01)* showed significant effects on the collective bone measurements. The results were depicted graphically using line graphs and box plots. (Appendix 2f)

Error of Measurement

The error of measurement was tested by repeating measurements for the condylar cartilage volume and each bone morphometric variable, twice over 13 samples. The standard error of measurement, and coefficient of variation for the variables of interest in this study were respectively 0.021mm^3 and 11.09% for condylar cartilage volume; 0.36mm^2 and 13.27% for bone surface; 12.06mm^{-1} and

12.04% for bone surface to volume ratio; 4.15mm^{-1} and 13.26% for bone surface to tissue volume; 1.21mm^{-1} and 16.0% for trabecular number; 0.04mm and 44.75% for trabecular separation and 0.01mm and 27.12% for trabecular thickness. In the case where measurements yield negative values or when the root means square error approaches zero, the coefficient of variance becomes high and discordant. For this reason, the error measurements for trabecular bone pattern factor and structure model index have been omitted. This also explains why the coefficient of variation is high for trabecular separation and trabecular thickness.

15 Results

15.1 Animal Weight

Over the course of the experimental period, all animals groups showed a significant increase in weight ($p<0.01$). At day 30 however, the weights of the group receiving vibration alone, were significantly less than natural growth, but this group still had an overall increase in weight.

15.2 Quantitative Analysis

The mean and standard error for cartilage volume and the bone parameters for all study groups at different times are summarised in Table 2.

The mean for cartilage volume and bone parameters are represented graphically on line graphs in Tables 5-13 graph a.

The univariate ANOVA for cartilage volume and bone parameters are represented graphically on box plots in Tables 5-13 graph b.

The post hoc comparisons of changes in cartilage volume and bone parameters are summarised for each group in Table 3, and each time point in Table 4. For the post hoc comparisons, the mean difference is significant at 0.01 level, where $p<0.01$.

15.2.1 Changes in Total Cartilage Volume

The mandibular condylar cartilage volume measurements were significantly different between the four groups ($p<0.05$), between days ($p<0.05$) and for the interaction of group-by-day ($p<0.01$).

Post hoc comparison showed there was a significant increase in mandibular condylar cartilage volume associated with normal growth from baseline control to day 30 and day 7 to day 30 ($p<0.01$). In the presence of vibration only, there was a significant increase in mandibular condylar cartilage volume from baseline, peaking at day 21 ($p<0.01$), followed by a significant decrease from day 21 to day 30 ($p<0.01$). For the functional appliance group, there was a significant overall decrease in mandibular condylar cartilage volume from day 0 to day 30, with the decrease from day 21 to day 30 also being significant ($p<0.01$). In the functional appliance with vibration group, there was a significant increase in mandibular condylar cartilage volume from day 0 to a peak at day 7, followed by a significant decrease at day 21 that was maintained until day 30 ($p<0.01$). (Table 5 Graphs c-f)

At day 7, the mandibular condylar cartilage volume in the functional appliance group was significantly less than all the other groups and the mandibular condylar cartilage volume in the functional appliance with vibration group was significantly greater than that seen in normal growth ($p<0.01$). At day 21, the mandibular condylar cartilage volume in the vibration only group was significantly greater than all other groups ($p<0.01$), and the mandibular condylar cartilage volume in the functional appliance with vibration group was significantly less than that of normal growth ($p<0.01$). At day 30, the mandibular condylar cartilage volume in natural growth was significantly higher than the three other groups ($p<0.01$). (Table 5 Graphs g-i)

15.2.2 Changes in Bone parameters

The bone variables with significant group differences were BS ($p<0.001$), BS/BV ($p<0.001$), BS/TV ($p<0.001$), Tb.Pf ($p<0.001$), SMI ($p=0.002$), Tb.Th, ($p<0.001$), Tb.N ($p<0.001$), Tb.Sp ($p<0.001$). The other bone variables, TV, BV, BV/TV, and TS showed no statistically significant differences.

Multivariate ANOVA, using Wilks' Lambda, showed statistically significant values for the bone parameters for group ($p<0.001$), day ($p=0.004$) and the interaction between group by day ($p<0.000$).

15.2.2.1 Bone Surface (BS)

The post hoc comparison of the BS showed that with normal growth, vibration only or functional appliance with vibration, there was no statistically significant change between time points within each group. In the functional appliance only group, there was a significant overall decrease in BS from baseline to the end of the experimental period ($p<0.01$). (Table 6 Graphs c-f)

At all time points, there was no statistically significant difference between normal growth and vibration only groups. Whereas as, at all time points the functional appliance only group had significantly less bone surface compared to that of normal growth ($p<0.01$). Although the bone surface of the functional appliance with vibration group was significantly less than that of normal growth at all time points, it was consistently significantly greater than the functional appliance only group over time ($p<0.01$). (Table 6 Graphs g-i)

15.2.2.2 Bone Surface to Bone Volume Ratio (BS/BV)

There was an overall significant decrease ($P<0.01$) in BS/BV in all groups during the time of the experiment. (Table 7 Graphs c-f)

At all time points there was no statistically significant difference between normal growth and vibration only. However, the BS/BV in the functional appliance group was significantly less compared to normal growth ($p<0.01$). At day 21, the BS/BV in the functional appliance with vibration group was not significantly different to normal growth but was significantly greater than in the functional appliance only group. Although the BS/BV of the functional appliance with vibration group was significantly less than that of normal growth at days 7 and 30, it was significantly greater than the functional appliance only group at day 30 ($p<0.01$) and marginally significant at day 7 ($p=0.019$). (Table 7 Graphs g-i)

15.2.2.3 Bone Surface density (BS/TV)

There was no significant change in BS/TV associated with normal growth, the presence of vibration only and in functional loading with vibration. For the functional appliance only group, there was a significant decrease in the BS/TV from baseline to day 7, day 21 and day 30 and from day 7 to 21 ($p<0.01$). (Table 8 Graphs c-f)

At all time points, there was no statistically significant difference in BS/TV between normal growth and vibration only groups. At all time points, the functional appliance only group had significantly less BS/TV compared to that of normal growth ($p<0.01$). Although the BS/TV of the functional appliance with vibration group was significantly less than that of normal growth at all time points, it was consistently significantly greater than the functional appliance only group over time ($p<0.01$). (Table 8 Graphs g-i)

15.2.2.4 Trabecular Bone Pattern Factor (Tb.Pf)

There was a significant decrease in Tb.Pf associated with normal growth from day 0 to both day 21 and day 30 ($p<0.01$). In the presence of vibration only there was a significant decrease in the Tb.Pf from day 0 to day 30 ($p<0.01$). In the functional appliance group, the Tb.Pf remained equably constant over the experimental duration showing no statistically significant changes between any time points. In the functional appliance with vibration group, there was a significant decrease in the Tb.Pf from baseline to day 7, remaining constant thereafter. (Table 9 Graphs c-f)

At all time points, there was no statistically significant difference between normal growth and vibration only groups. There were no statistically significant differences in the Tb.Pf between groups at day 7. At days 21 and 30, the functional appliance only group had a significantly greater Tb.Pf compared to that of normal growth ($p<0.01$). The Tb.Pf in the functional appliance with vibration group was not significantly different to that of normal growth at all time points, and was significantly less than the functional appliance only group at day 21 ($p<0.01$). (Table 9 Graphs g-i)

15.2.2.5 Structure Model Index (SMI)

There was no significant change in SMI associated with normal growth, vibration only or functional appliance only. There was a significant decrease in SMI in the functional appliance with vibration group, from the baseline to day 21 ($p<0.01$). (Table 10 Graphs c-f)

The only significant differences between groups were seen at day 21 where the SMI associated with normal growth and functional appliance with vibration were significantly less than the functional appliance group ($p<0.01$). (Table 10 Graphs g-i)

15.2.2.6 Trabecular Thickness (Tb.Th)

There was a significant increase in Tb.Th from baseline to the end of the experimental period associated with the use of a functional appliance with vibration or without vibration ($p<0.01$). The Tb.Th remained within a constant range in normal growth and with vibration only. (Table 11 Graphs c-f)

There was no significant difference between the Tb.Th in normal growth and vibration alone at any time point. The Tb.Th in the functional appliance only group is significantly greater than that in normal growth at days 7, 21 and 30; and is significantly greater than functional appliance with vibration at days 21 and 30 ($p<0.01$). The Tb.Th in the functional appliance with vibration group was not significantly different to that seen in normal growth at day 21 and day 30. (Table 11 Graphs g-i)

15.2.2.7 Trabecular Number (Tb.N)

There was a significant increase ($p<0.01$) in Tb.N from baseline until day 21 associated with natural growth, after which time the trabecular number stabilised. In the presence of vibration only, there was a significant increase in Tb.N from baseline to the end of the experimental period ($p<0.01$). In the functional appliance group, there was a significant decrease in trabecular number across the experimental period ($p<0.01$) whereas the Tb.N did not significantly change between any time point when vibration was added. (Table 12 Graphs c-f)

At all time points there was no significant difference in Tb.N between the normal growth trend and vibration only. At all time points the functional appliance only, significantly reduced the trabecular number compared to that seen in normal growth ($p<0.01$). When vibration was added to the functional appliance, the Tb.N was significantly greater than the Tb.N in the functional appliance only group, approaching the values of normal growth trend ($p<0.01$). (Table 12 Graphs g-i)

15.2.2.8 Trabecular Separation (Tb.Sp)

There was no significant change in Tb.Sp associated with normal growth, vibration only and functional appliance with vibration. The functional appliance only, induced an increase in Tb.Sp in the condylar bone at the resorptive front, peaking at day 21, followed by a significant decrease at day 30 ($p<0.01$). (Table 13 Graphs c-f)

The Tb.Sp in the functional appliance only group was significantly greater than all other groups ($p<0.01$), with the Tb.Sp in the functional appliance with vibration falling to values comparable to that of natural growth. (Table 13 Graphs g-i)

15.2.3 Qualitative Changes

15.2.3.1 Normal Growth

The gross morphology of the mandibular condyle appeared consistent during natural growth over the experimental duration, with the surface anatomy being smooth and well defined. (Figure 5)

Microscopically, the cartilage appeared intact and consistent in thickness during the experimental period. (Figure 6)

15.2.3.2 Vibration only

The gross morphology of the mandibular condyle with vibration only appeared consistent throughout the experimental period and comparable to the morphology of the untreated animals. (Figure 5)

Microscopically, the cartilage was intact at all time points. A thicker layer of cartilage, indicated by more profound staining by the gadolinium chloride, was observed at day 7 and further at day 21, followed by thinning observed at day 30. This was consistent with the decrease in cartilage volume measured quantitatively. (Figure 7)

15.2.3.3 Functional appliance only

The gross morphology of the condyle in animals receiving functional appliance therapy alone changed over the experimental period starting by day 7. This was seen as flattening superiorly with the condyle becoming narrower as it elongated in the posterior superior direction, as seen on the medial and lateral 3D images. (Figure 5) Over time the anterior surface of the condyle appeared rough and undulated, whereas the posterior surface remained smooth and intact. (Figure 10) There was a close relationship between the condyle and the fossa.

At the microscopic level at day 7, mild anterior condylar resorption and glenoid fossa resorption were observed in one fifth of the animals. By days 21 and 30, all of the animals showed signs of condylar resorption of increasing severity, and one third and two third of animals showed signs of glenoid fossa resorption by day 21 and day 30, respectively. Loss of condylar cartilage integrity adjacent to the areas of resorption was observed in all animals by 7 days and persisted for the remaining time points in the experiment. (Figure 8)

At all time points during the experiment, a relatively radiolucent area between the intact bone and cartilage at the posterior medial aspect of the condyle was observed in several of the samples, perhaps indicating the deposition of chondroid matrix as a result of chondrogenesis at this site. (Figure 11)

15.2.3.4 Functional appliance with vibration

The gross morphology of the condyle in animals receiving functional appliance with vibration changed over the experimental period in the same manner as the functional appliance alone group

as seen by flattening superiorly and elongation in the superior, posterior direction on the lateral and medial 3D images, starting by day 7. (Figure 5) Over time, the anterior surface of the condyle appeared roughened and undulating, whereas the posterior surface remained smooth and intact. (Figure 10)

As seen in the functional appliance only group, mild anterior condylar resorption and glenoid fossa resorption were observed microscopically in one fifth of the animals at day 7. The condylar cartilage however remained intact at this time point and appeared thick, as indicated by the profound gadolinium stain. All animals at days 21 and 30 showed a loss of condylar cartilage integrity and signs of condylar resorption of increasing severity at the anterior aspect of the condyle. An increasing number of animals displayed signs of glenoid fossa resorption as the experiment progressed to day 21 and further on to day 30. (Figure 9)

At all time points during the experiment, a relatively radiolucent area between bone and intact cartilage at the posterior medial aspect of the condyle was observed in several of the samples, perhaps indicating the deposition of new bone precursors by chondrocytes at this site. (Figure 11)

16 Discussion

The mandibular condylar cartilage is a unique type of articular cartilage, capable of adaptive responses to external stimuli throughout life. The adaptive nature of the mandibular condylar cartilage is of interest in the field of orthodontics, in that it may contribute to the overall response to functional appliance treatment used as an orthopaedic means of correcting Class II mandibular retrognathic skeletal patterns during the peak pubertal growth period.

High-frequency, low-magnitude stimuli have been reported extensively in the literature to exert a positive effect on bone quality. Preliminary in vitro experiments [65,66] on cultured chondrocytes have concluded that vibration may also be useful in maintaining chondrocyte function under adverse

conditions and during cartilage regeneration, by activating favourable intracellular pathways. Recent independent studies using micro-CT have shown that functional appliances in adult rats, [34] and high-frequency, low-magnitude mechanical stimulation in adult mice,[28] positively enhance endochondral ossification in the mandibular condyles of the respective animals. Using 130 juvenile female Sprague-Dawley rats we tested the hypothesis that mechanical vibration may enhance orthopaedic treatment related to the adaptive growth of the mandibular condyle.

16.1 Study design

16.1.1 Animal Selection and Housing

Small animal research using rats is appropriate for initial studies investigating new treatment modalities. Large numbers of animals can be used proving relatively economical compared to large animal work. The use of rats in this investigation made it feasible to observe the interactions between the experimental variables and growth, at short time intervals, over a relatively short experimental duration. In particular, Sprague-Dawley rats have been used extensively to investigate the effects of functional appliances on the rat condyle [2,13,35-42,44-48,67-72], and vibration has produced anabolic effects in the bone of this species[33]. Therefore, Sprague-Dawley rats were appropriate for investigating these treatment variables concomitantly. As the peak pubertal growth in rats occurs between post-natal days 31.5 to 135, the experiment was started when the rats were five weeks of age to ensure that the peak pubertal growth was included in the experimental period. One animal died following functional appliance placement. Post mortem examination revealed this was associated with the aspiration of blood derived from the oral cavity. Animals receiving functional appliance therapy were housed two to a cage to facilitate thorough post surgical monitoring, whereas all the other animals were housed four to a cage. Consistency in the numbers of animals per cage across groups would have been preferable, however was not considered economically

beneficially. All animals significantly gained weight over the experimental duration and therefore the housing distribution of the animals was inconsequential.

16.1.2 Appliance Design

Different functional appliance designs have been used to achieve mandibular protrusion in rats. Designing an appropriate functional appliance to achieve adequate and continuous mandibular repositioning has proved difficult due to the anatomy and masticatory physiology of the rat. A ten millimetre edentulous space exists between the molars and incisors, and the upper and lower molars do not interdigitation in one particular position [73]. This, along with the anatomy of the temporomandibular joint allows a large degree of lateral mandibular movements, and mouth opening of at least one centimetre [74]. Therefore, the aim of a functional appliance is to hold the mandible forward without the jaw deviating to one side or back into retrusion, and without causing impairment of the animals feeding ability [75]. The design should also facilitate ease of placement and consistency in mandibular protrusion in order to increase the reliability of the study [75]. The normal distance between the upper and lower incisors in the sagittal plane when the mandible is closed normally is six millimetres [74]. This was used to gauge the extent of mandibular protrusion achieved by the functional appliance in each animal.

The most common design used in the literature involves [38,39] the placement of an inclined plane over the upper incisors, that provides a surface for the lower incisors to contact to hold the lower jaw forward. Owing to the ability of the rats to open their mouths in excess of one centimetre, past experiments have reported the mandible slipping back into functional retrusion [57,58]. The addition of a lower component to the functional appliance design has been used and described by Xiong *et al.* [76]. One anticipated concern with this appliance was the large amount of protrusion achieved that may predispose to unwanted lateral excursion. In addition, this particular design appeared to impair the animals feeding ability, seen by a significant reduction in body weight of ‘about 10%’ in the first

week after functional appliance placement. This persisted until the end of the second week and normalised by the third week of the experiment. With respect to our investigation, criteria set by the Animal Care and Ethics Committee stipulated that a loss in animal weight of 10% would warrant intervention (for example, special feeding or removal of the appliance) and a loss of 15% would necessitate euthanasia of the animal. Fortunately, the need for this did not arise and all of the animals were considered healthy at the end of the experiment.

To overcome the abovementioned difficulties, a new functional appliance design was used involving the placement of upper and lower paediatric strip crowns on the incisor teeth. This design proved to be successful in achieving adequate and continuous mandibular protrusion (seen in the change in incisor relationship at the time of placement and on the post-mortem radiographs), without causing impairment of the animals' ability to feed (seen by daily consumption of all the food supplied and the gradual weight gain immediately following functional appliance placement). No animals adopted a retruded mandibular position following appliance placement. Only one upper crown of one of the appliances was lost during the experiment. This animal was excluded from the study.

16.1.3 Vibration

The administration of high-frequency, low-magnitude mechanical stimuli of 30Hz and 0.3g respectively, for 20 minutes per day was chosen based on previous studies. This vibration protocol has been proven effective in the long bones of adult sheep [50,55,56] and rats [51,53] and has been used safely and effectively in human studies [52,54]. Experiments using C3H mice investigating the effect of vibration on cranial bone healing [27] and the mandibular condyle [28] have also shown that vibration delivered at 30Hz and 0.3g for 20 minutes per day for 28days produces significantly positive results. Sprague-Dawley rats have responded positively to other vibration regimes [33].

The effectiveness of whole body vibration has been studied in humans by testing the degree to which high-frequency, low-magnitude mechanical stimuli are transmitted to the skeleton, using

transcutaneous bone pins connected to accelerometers. At a frequency of 25Hz, the transmissibility of the stimulus at the hip and spine was 80%. No studies have been conducted assessing the transmissibility of mechanical stimuli to the bones of small animals using this method. However Ozcivici *et al.* [32] used micro-CT and bone morphometric measurements to gauge the transmissibility of high-frequency oscillations on trabecular bone of long limbs in response to loading and Sriram *et al.* [28] found vibration had an effect on the condyles of adult mice. Based on the variability in bone quality recorded between the experimental groups in our study, it appeared that mechanical stimuli administered at 30Hz and 0.3g for 20 minutes a day, for 30 days, was transmitted to the condyles of the Sprague-Dawley rats. In order to ensure the maximum transmissibility to the skeleton of the rats in this investigation, only one cage at a time was placed on the vibration platforms.

The rats were observed while on the vibration platforms and no untoward responses or behaviours were noted. On the contrary, the time on the vibration platform appeared to be enjoyed by the animals.

16.1.4 Experimental Duration

The length of the experiment was based on previous studies that have investigated the effects of functional appliances on the expression of markers of chondrogenesis and endochondral ossification, influential in natural growth. Studies investigating the expression of SOX9 [44], Type II collagen, parathyroid hormone related peptide (PTHrP) [42], Indian hedgehog (Ihh) [71], Runx2 / core bonding factor alpha (Cbfa1) [72], integrins [77], collagen type X [13,36], cell cycle genes [67], and insulin-like growth factor (IGF) [70] have all assessed changes over a 30 day period. In addition, changes in bone and cartilage of the mandibular condyle in response to vibration also occur within this time frame [28]. Hence an experimental duration of 30 days was regarded appropriate for this investigation and proved adequate in revealing changes at the condyle in response to mandibular protrusion using micro-CT.

The sacrifice time points in the abovementioned histological experiments were 3, 7, 14, 21 and 30 days. As it takes longer to see changes radiographically, the time points 7, 21 and 30 were considered adequate in assessing changes over time using micro-CT.

Chayanupatkul *et al.* [68] have investigated the effect of early and late functional appliance removal in Sprague-Dawley rats whereby early removal was considered to be 30 days. For this reason, the appliances were kept in place for the entire duration of the experiment.

16.2 Image analysis

16.2.1 Condylar Cartilage

The use of the Gaussian filter, enhanced image visualisation by removing image noise. In addition, image visualisation was improved by the use of gadolinium chloride that subsequently facilitated the segmentation process. Gadolinium staining has be shown to be an effective way of enhancing the contrast of cartilage on micro-CT scans [59]. The uptake of the Gadolinium chloride stain determines the ease of segmentation by creating a differential in grey values between cartilage and underlying bone. The stain was most effective when the cartilage was thick, increasing the accuracy and ease of segmentation in these samples. It appeared that the gadolinium chloride was not entirely specific for cartilage, often also staining other structures in the mandible. Therefore, the initial selection of grey scale values in the region growing step, resulted in the inclusion of these structures into the region of interest. Elimination of the areas beyond the anatomically defined region of the condylar cartilage was subsequently achieved by the use of interactive editing tools. The interactive editing tools were also employed when additions to the region of interest were required, for example, in the case of thin cartilage or voids in the cartilage following region growing. This ensured accurate and repeatable representation of the condylar cartilage. The technical complexity of this measuring technique required a high degree of operator expertise to ensure optimal use of the software, in order to achieve measurement standardisation and minimisation of measurement error. It was

therefore appropriate for the measurements of condylar cartilage volume to be made by one operator.

16.2.2 Bone Morphometric Analysis

X-ray microtomographic scans of resolution less than 10µm are reported in the literature to be adequate to obtain bone morphometric data from trabecular bone [60-62]. Hence the resolution of 6.8µm was justified in this study and proved to yield adequate, useful data. The use of a lower resolutions in the vicinity of 2µm, have also produced good results [28] and may be a factor in reducing the error of measure in this type of analysis.

Bone morphometric analysis from the micro-CT scans was achieved successfully using CT Analyser software (Skyscan™; CTAn Version 1.10.1.0). The region of interest was consistently extracted from the centre of the condyle, directly beneath the condylar cartilage in intact bone. As morphometric analysis is performed on binarised images, the threshold was interactively set by a single operator using visual criteria to minimise noise and maximise visibility of bone components.

In light of the different states of bone activity in the condyle in response to the functional appliances, morphometric measurements at the anterior and posterior regions of the condyle may be an interesting extension to this investigation. A comparison of the bone quality between these two regions may further the understanding of the type of bone modelling taking place in response to the functional appliance and determine the effect of vibration, in this process.

16.3 Results

16.3.1 Animal weights

All animal groups significantly gained weight over the course of the experiment. At the end of the experiment there was no significant difference between the groups with functional appliances and natural growth, therefore it can be concluded that the functional appliance did not interfere with

the ability of the animals to feed. Interestingly, the vibration only group weighed significantly less at day 30 when compared to natural growth despite still having an overall increase in weight over the experimental duration. Although not significant, the weight of the rats with the functional appliance together with vibration was less than the animals with the functional appliance alone. Whole body vibration devices are marketed to suggest they promote weight loss or decrease in fat[78]. There is no evidence to support this directly, however studies show that whole body vibration modulates energy expenditure that may result in alterations in body composition. Although the evidence correlating whole body vibration with weight loss is inconclusive [78], it may be an explanation as to why the rats receiving only vibration weighed significantly less than the untreated animals.

16.3.2 Qualitative Analysis

Gross morphological examination using the 3D micro-CT visualisation, revealed changes in condylar morphology in the functional appliance groups, with and without vibration, that were not observed during normal growth or with vibration alone. The condyle appeared to elongate in a posterior direction and flatten along its superior surface as seen from the medial and lateral aspects on the 3D images. The observed changes are consistent with findings from functional appliance studies in both animals [5,6,12,14,16,79] and humans [17,18,80-82] and are believed to contribute to the correction of the Class II malocclusion. Histologically, the changes in morphology have been associated with an increase in cellular response in the proliferative zone of the mandibular condylar cartilage at the posterior regions of the condyle in response to functional protrusion, prior to endochondral ossification [11,13,14]. This adaptive change has been documented in humans using MRI scans [17,18] in response to Herbst appliance treatment.

In addition to successfully representing the condyle in 3D, micro-CT permitted high resolution slice by slice visualisation of the condyles in three planes of space enabling radiographic analysis not possible using conventional radiography, magnetic resonance imaging or low resolution

conventional computed tomography. Examination of the sectional micro-CT images of the condyles revealed intact cartilage and bone at the posterior aspect of the condyles in the functional appliance groups with and without vibration. Interestingly, in these animals a narrow radiolucent band at the posterior-medial part of the condyle between the intact condylar cartilage and bone was observed on the micro-CT images. This band may represent the products of chondrogenesis that are deposited prior to endochondral ossification, indicative of favourable bone modelling at the posterior part of the condyle during functional protrusion in the rat model.

In contrast, bone resorption at the anterior region of the condyle together with a loss of integrity of the mandibular condylar cartilage was observed in the same animals with intact posterior cartilage and bone. Glenoid fossa resorption was also noted. (Figure 12) The major direct cause of mandibular condylar cartilage breakdown and subsequent bone resorption is mechanical overloading [83] which may account for the mild to extreme breakdown of condylar cartilage and bone resorption at the anterior aspect of the condyle observed in our study. It has been suggested that such break down is associated with the effect of the new functional appliance design that potentially increased protrusion of the mandible, resulting in overloading at the anterior aspect of the condyle and fossa. Sheer loading of the condylar cartilage, plays an important role in its breakdown whereby the cartilage is sheered to adapt to the incongruent articular surfaces, together with a decline in joint lubrication [84]. During such loading, mechanoreceptors predominantly on the mature chondrocytes instigate an increase in metabolic activity and activation of pathological processes that may lead to cartilage degradation. Matrix metalloproteinases and aggrecanases mediate the cartilage breakdown by targeting collagen and proteoglycans [84]. Recently, Shirakura *et al.* [85] have demonstrated Hif-1α activation in overloaded mature chondrocytes in the rat temporomandibular joint. Hif-1α causes repression of osteoprotegrin expression, thereby favouring osteoclastogenesis, leading to bone resorption. In addition, Hif-1α binds to the hypoxia response element in the human vascular endothelial growth factor (VEGF) promoter resulting in an increased expression of VEGF in

mature chondrocytes [86,87]. Under excessive loading, VEGF is capable of osteoclast differentiation and recruitment thereby controlling osteoclastic bone resorption [88,89]. Shirakura *et al.* [85] also found that the increase in Hif-1α associated with condylar cartilage breakdown was paralleled by an increase in tartrate resistant acid phosphatase (TRAP) positive cell numbers, supporting the notion of concomitant bone resorption. In our study, we observed an increasing severity of condylar cartilage breakdown and bone resorption over the course of the experimental period. If our findings are indicative of pathologic resorption, this trend is consistent with the findings of Shirakura *et al.* [85] who stated that the degree of degeneration of the condylar cartilage was in proportion to the duration of overloading. The response of the rat TMJ to loading has been visualised for the first time using micro-CT imaging. Immunohistochemistry would be useful for further analysis of the samples in order to characterise the nature of the cartilage breakdown and bone resorption.

Given the presence of resorption at the anterior condyle, and the apparent endochondral bone formation at the posterior condyle, it is appears two opposite physiological processes are occurring simultaneously at different locations of the condyle. This would account for the apparent gross 'remodelling' of the condyle and is consistent with the smooth appearance of the posterior surface of the condyle, as opposed to the roughened undulating appearance anteriorly, as seen on the 3D micro-CT visualisation. (Figure 10)

The response of the glenoid fossa to functional appliance therapy has been extensively reported in the literature [1,5,6,12,16-18,80,90]. Radiographic and histological investigations using monkeys [1,5,6,12,16,90] have documented continuous deposition of bone along the anterior border of the postglenoid spine, and resorption along the posterior border of the postglenoid spine of the glenoid fossa. This culminates in anterior repositioning of the fossa after continuous forward positioning of the mandible, thereby contributing to Class II correction. A histological study using rats found that forward positioning of the mandible leads to new bone formation at the posterior aspect of the

glenoid fossa in response to the direction of forward pull [38]. Anterior-inferior relocation of the glenoid fossa observed on MRI scans in response to Herbst treatment in humans has been reported [17,18,80]. Based on such literature, the resorption in the glenoid fossa observed in this study may be associated, in part, with physiological adaption in response to functional protrusion. However no study has investigated the effects of TMJ overloading on the integrity of the glenoid fossa, and therefore, further histological investigations would be required to clarify the type of bone resorption seen at this site.

Given a longer experimental duration, restoration of the integrity of the mandibular condylar cartilage and bone in both the condyle and fossa may have occurred with or without removal of the appliance, through biological repair processes integral with bone modelling. Shirakura *et al.* [85] noted in their study that the osteo-arthritic like lesions under investigation decreased after the removal of the overloading appliances.

Finally, the changes reported in the morphology of the condyle and glenoid fossa pertain only to their respective time points in the study and cannot be extrapolated to indicate long-term changes that may favour Class II correction. Long-term data derived from Pancherz *et al.* [80,91] shows that the direction of condylar growth resumes a more vertical direction and the glenoid fossa reverts back to a posterior direction following the removal of the functional appliance. A longer experimental duration would be required to assess such patterns of relapse and stability, with early and late appliance removal at days 30 and 44 respectively, as suggested by Chayanupaktul *et al.* [68].

16.3.3 Quantitative Analysis

Quantitative analysis measured the volume of the cartilage and the quality of the bone in the condyle. This analysis shows the independent and interactive behaviours of the cartilage and bone at the different experimental time points in the presence of the different experimental regimens.

16.3.3.1 Functional Appliance Only

The adaptive nature of the mandibular condylar cartilage is thought to play an important role in the changes associated with orthopaedic Class II correction. Previous studies [1,11-14,16-18] have documented that the mandibular condylar cartilage initially increases in thickness in response to functional appliance therapy, followed by a return to a thickness comparable to age matched controls except at the posterior region. Subsequent to this, the thickness of the cartilage becomes indistinguishable to the age matched controls. The condylar cartilage volume in this investigation significantly decreased from the start to the end of the experimental period, however, this was not due to variations in thickness as observed in previous studies but rather due to breakdown of the cartilage at the anterior condyle in response to mechanical overloading at this site. The volume recorded therefore represents the remaining intact cartilage predominantly at the posterior surface of the condyle.

The bone morphometric parameters recorded, collectively indicate deterioration of the trabecular bone in the condyle in response to functional appliance therapy compared to the values recorded for normal growth. The significant decrease in Tb.N was mirrored by a significant increase in Tb.Sp indicating that as some trabeculae break down in response to the applied loading, the distance between the remaining trabeculae increases. The increase in Tb.Th of the remaining trabeculae was due to the bone adapting to the applied load by depositing bone on the existing trabeculae. No change was seen in the Tb.Pf however this was significantly greater than the values for Tb.Pf associated with normal growth. Thus, the connectivity of the trabecular lattices in the animals treated with functional appliances was relatively inferior to the bone of the untreated age matched animals. The structure model index (SMI) indicates the relative presence of rods and plates in trabecular bone. A plate-like trabecular structure (indicated by values approaching 0) reflects healthy bone of sound quality, whereas bone with a rod-like trabecular structure (indicated by values approaching 3) is less connected and of inferior quality. Although the SMI values in the functional appliance only group did not change significantly over the experimental period, they

empirically represented a more rod-like trabecular structure and were significantly less than the values recorded for natural growth. The empirical values seen in natural growth indicated a plate like trabecular structure. Therefore, the SMI in the animals treated with the functional appliance alone indicates less connected trabecular bone of inferior quality compared to the trabeculae associated with natural growth. The significant decrease in BS, BS/TV and BS/BV is connotative of an overall loss of complexity of the trabecular structure. All of the values recorded for the bone morphometric parameters in the functional appliance group varied significantly to the values recorded for normal growth, indicative of relatively poorer bone. These findings are contrary to those of Xiong *et al.* [76] who observed signs of new bone formation using micro-CT and bone morphometry. This is likely to be due to the mechanical overloading in this study resulting in adverse effects in the bone.

It is therefore apparent that mechanical overloading of the TMJ with a mandibular protrusive appliance causes a loss in mandibular condylar cartilage integrity at the anterior aspect of the condyle as indicated quantitatively by a decrease in mandibular condylar cartilage volume. Bone resorption occurs simultaneously adjacent to the area of cartilage breakdown. Examination of the bone adjacent to the resorptive front shows a significant reduction in bone quality associated with loading by the functional appliance.

Closer examination between days 21 to day 30 in the functional appliance group warrants consideration. It appeared that values for the bone morphometric parameters between these two time points changed in favour of improved bone quality. Most importantly there were significant increases in both Tb.Th ($p<0.001$) and Tb.N ($p<0.001$), and a significant decrease in Tb.Sp ($p=0.006$). There were marginal increases in BS/TV and BS, and decreases in Tb.Pf and SMI. Collectively, it appears that bone quality improved between these two time points, a change that may represent the initiation of reparative biological processes.

In addition, the mandibular condylar cartilage volume decreased between days 21 and 30. In light of the cartilage breakdown at the anterior aspect of the condyles of the animals treated with the functional appliance alone, the volumetric measurements represent the remaining intact cartilage at the posterior aspect of the condyle. Hence, the decrease in cartilage volume can be assimilated to thinning of the cartilage at this site, and could therefore be associated with ensuing endochondral ossification. This is consistent with the radiolucent band between the cartilage and bone visualised on the micro-CT images, and is the anticipated response to forward mandibular positioning, as evidenced by previous functional appliance studies [1,11-14,16-18] .

16.3.3.2 Vibration Only

In response to vibration alone, the mandibular condylar cartilage volume decreased with a concomitant increase in bone quality as endochondral ossification ensues. The bone parameters of particular interest in this process are, trabecular number (Tb.N), trabecular thickness (Tb.Th), trabecular separation (Tb.Sp) and trabecular pattern factor (Tb.Pf). The significant increase in the trabecular number signifies an increase in bone quantity, with the thickness of the original and new trabeculae remaining the same signifying maintenance of the bone quality. The spacing between the trabeculae did not change indicating accord in the trabecular spatial organisation over time. Tb.Pf is a relative inverse index of connectivity of trabecular bone. The significant decrease in Tb.Pf observed in the vibration only group in this study represented a well connected spongy lattice of increasing trabecular connectivity. Although the cartilage volume was significantly less than in normal growth at the end of the experimental period, the bone parameters in the vibration only group were not significantly different to those of natural growth. These findings differ to those of Sriram *et al.* [28] who conducted a similar experiment on adult mice and found significant differences in the bone morphometric values between the vibrated and untreated animals. The difference in findings may be due to growth of the rats in the current study, whereby the morphometric measurements in the control group reflect endochondral ossification associated with normal growth. Had the duration of

the experiment been longer, it is probable that the values for Tb.N, BS, Tb.Sp and Tb.N in the vibration group could have become more representative of increasing bone quality and endochondral ossification, given such a dramatic decrease in the condylar cartilage volume. This would be consistent with the notion that as endochondral ossification ensues, the cartilage thins, based on the documented findings from previous studies [1,11-14,16-18].

16.3.3.3 Functional Appliance with Vibration

The aim of this investigation was to examine the effect of vibration on the rat condyle during mandibular protrusion using a functional appliance through analysis of the condylar cartilage volume and bone quality. It was hypothesised that the vibration would potentiate the effects of functional appliance treatment, thereby increasing the efficiency of Class II correction. In the event of mandibular condylar cartilage breakdown and bone resorption at the anterior condyle due to the functional appliances, this hypothesis remains unresolved. The effect of the vibration in the presence of condylar cartilage breakdown and bone resorption, resulting from overloading, subsequently became of interest in this study. The findings are reported below.

The mandibular condylar cartilage responded differently in the functional appliance groups with and without vibration. Although both groups exhibited loss of condylar cartilage integrity by the end of the experimental period, as visualised on the micro-CT scans, this occurred early (by day 7) without vibration and later (at day 21) with vibration. The quantitative measurements of the cartilage volume reflect these findings. Thus it appeared that the vibration prolonged the breakdown of the mandibular condylar cartilage under load in this experiment. Limited research has been devoted to the effect of vibration on cartilage with most studies being in vitro assessments of chondrocytes. However, these preliminary studies [65,66] have concluded that vibration may also be useful in maintaining chondrocyte function under adverse conditions and during cartilage regeneration, by activating favourable intracellular pathways.

The bone responded differently in the functional appliance groups with and without vibration, as evidenced by the bone morphometric measurements. Without vibration, the functional appliance resulted in relative deterioration in trabecular bone quality. In contrast, in the presence of vibration, the bone morphometric measurements collectively indicated trabecular adaption to the applied load without deterioration in trabecular bone quality.

Bone adaption in response to the applied load in the presence of vibration, was indicated by an increase in trabecular thickness, signifying the deposition of new bone on the existing trabeculae to enable attenuation of the applied load. There was also a significant decrease in SMI and Tb.Pf connotative of a more connected trabecular structure and better bone quality, despite the mechanical overloading.

A general observation was the similarity in the temporal pattern of bone adaption in the functional appliance groups with and without vibration across the experimental period. This can be seen clearly on the line graphs for the bone morphometric variables, except for Tb.Sp and SMI. (Tables 5-13 Graphs a). For example, the Tb.Pf in both functional appliance groups decreased from the start of the experiment to day 7, then increased at day 21, followed by a tapering-off and decrease in the vibration and no vibration group respectively. This general trend tended to be opposite to the trend seen in the groups without functional appliances.

Despite the similar trend seen in bone adaption between the functional appliance groups, the defining difference between the functional appliance groups with and without vibration over the course of the experiment was the degree of bone quality. Representation of the data on the line graphs for each bone variable shows that, the line representing the functional appliance group with vibration (i) lay between the line of normal growth, and the line representing functional appliance only and (ii) lay closer to the line representing normal growth. Upon closer examination, the values for Tb.Pf, SMI, Tb.Th, Tb.Sp and Tb.N in the functional appliance group with vibration were

significantly different compared to the functional appliance group without vibration, indicative of better bone quality. However these variables were not significantly different to values associated with normal growth. It can therefore be concluded that where functional appliances were used, vibration enhanced the bone quality, with the degree of bone quality remaining comparable to that of natural growth.

The complexity of the bone significantly reduced with the functional appliance, even in the presence of vibration. This was evidenced BS, BS/BV and BS/TV values falling significantly below the values seen in natural growth at day 30. Interestingly however, when the functional appliance groups were compared, the complexity of the bone with vibration was significantly greater than without vibration. It can therefore be concluded that, although the complexity of the bone decreases significantly in both functional appliance groups, this was less drastic in the presence of vibration.

Vibration accompanying functional appliance therapy appeared to preserve bone quality compared to functional appliance therapy without the vibration, which resulted in deterioration of bone quality. Vibration appeared to maintain the bone within physiological parameters, comparable to normal growth. This may be due to the response of bone at the cellular level whereby bone cells can sense high frequency oscillations and can orchestrate a structural response. The way in which bone responds to its mechanical environment is through the lacuna-canalicular network[92]. This is a network in bone comprised of copious osteocytes that maintain cellular communications with other osteocytes, osteoblasts and bone lining cells via gap junctions. This morphological arrangement facilitates mechanosensation and mechanotransduction, whereby cells are able to convert a physical force into a biochemical, cellular response [92,93]. Mechanical strain, induces deformation of the bone and flow of interstitial fluid through the lacuno-canalicular network [92,94]. This fluid flow at the osteocyte membrane generates fluid sheer stresses that influence the cell wall processes of the

mechanosensitive osteocytes. This occurs via integrins, and reorganisation of the cytoskeleton in turn induces a change in cell metabolic activity [92].

Functional appliances in humans are widely used and accepted [95]. As well as being used for Class II correction, intra-oral mandibular repositioning appliances have been used successfully in pathological states to unload the joint, easing conditions such as juvenile chronic arthritis[96],and aiding in the correction of growth disturbances of the mandible [97]. Previous functional appliance studies have not reported the finding of bone resorption in the condyle and glenoid fossa, as seen in this study. However, appliances specifically designed to load the TMJ have found similar results [85]. It is therefore likely, that although the new appliance design used in this investigation was successful in achieving continuous forward positioning of the mandible, it may have induced loading at the anterior aspect of the joint resulting in the loss of cartilage integrity and bone resorption. This was able to be seen with a high degree of image resolution using micro-CT. Based on MRI and conventional radiography, physiological joint remodelling has been reported to favour Class II correction in humans [17,18,80,82]. However, MRI and conventional radiography only produce low resolution images. A new imaging technique, limited cone-beam computed tomography, has been recently developed and has been used successfully for 3D imaging of the TMJ with a high degree of accuracy [98]. Limited cone-beam computed tomography may be useful in more accurate determination of the response of the human TMJ to mandibular advancement.

17 Conclusions

Based on the results of this study which qualitatively and quantitatively analysed the effect of vibration on bone and cartilage remodelling in the mandibular condyle during functional protrusion in growing rats, the following conclusions have been made:

- High-frequency, low-magnitude mechanical stimuli for a period of 30 days results in decreased condylar cartilage volume, and maintenance of trabecular bone tissue in juvenile rats
- Functional appliance caused mandibular condylar cartilage breakdown and adjacent bone resorption at the anterior aspect of the condyle
    - In the absence of vibration the functional appliances causes deterioration of trabecular bone adjacent to the resorptive front
    - In the presence of vibration the trabecular bone adjacent to the resorptive front is maintained within physiological parameters comparable to natural growth despite the loading incurred by the functional appliance. This may support the role of high-frequency, low-magnitude mechanical stimuli in pathological conditions such as osteoporosis.
- The bone and cartilage at the posterior aspect of the condyle remains intact during the functional appliance therapy and shows signs of chondrogenesis and endochondral ossification in response to the functional load. This is manifest by a change in gross morphology that favours Class II correction.

18 References

1. Woodside DG, Metaxas, A., Altuna, G. The influence of functional appliance therapy on glenoid fossa remodelling. Am J Orthod Dentofacial Orthop 1987;92:181-198.
2. Rabie AB, She, T.T., Hagg, U. Functional appliance therapy accelerates and enhances condylar growth. Am J Orthod Dentofacial Orthop. 2003;123:40-48.
3. Shen G, Darendeliler, M. The Adaptive remodelling of condylar cartilage – A transition from Chrondrogenesis to Osteogenesis. Journal of Dental Research 2005;84.
4. Hinton RJ, Carlson, D.S. Regulation of growth in mandibular condylar cartilage. Seminars in Orthodontics 2005;11:209-218.
5. Breitner C. Bone changes resulting from experimental orthodontic treatment. Am J Orthod 1940;26:521-547.
6. Breitner C. Further investigations of bone changes resulting from experimental orthodontic treatment. Am J Orthod 1941;27:605-632.
7. Adams C, Meikle M, Norwick K, Turpin D. Dentofacial remodelling produced by intermaxillary forces in the *Macaca mulatta*. Archives of Oral Biology 1972;17:1519-1534.
8. Baume L, Derichsweiler H. Is the condylar growth centre responsive to orthodontic therapy? Oral Surgery Oral Medicine and Oral Pathology 1961;14:347-362.
9. Hiniker J, Ramfjord S. Anterior displacement of the mandible in adult rhesus monkeys. J Prosthet Dent. 1966 16:503-512.
10. Meikle M. The effect of a class II intermaxillary force on the dentofacial complex in the adult *Macaca mulatta* monkey. Am J Orthod 1970;58:323-340.
11. Stockli PW, Willert, H.G. TMJ reaction to anterior displacement of mandible. Am J Orthod 1971;60:142-154.
12. Voudouris JC, Woodside, D.G., Altuna, G., Angelopoulos, G., Bourque, P.J., Lacouture, C.Y., Kuftinec, M.M. Condyle-fossa modifications and muscle interactions during Herbst treatment, Part 2. Results and conclusions. Am J Orthod Dentofacial Orthop. 2003;124:13-29.
13. Shen G, Zhao, Z., Kaluarachchi, K., Rabie, B.A. Expression of type X collagen and capillary endothelium in condylar cartilage during osteogenic transition--a comparison between adaptive remodelling and natural growth. Eur J Orthod 2006;28:210-216.
14. McNamara JA, Carlson D.S. Quantitative analysis of temporomandibular joint adaptations to protrusive function. Am J Orthod 1979;79.
15. McNamara JAJ, Bryan, F.A. Long-term mandibular adaptations to protrusive function: An experimental study in Macaca Mulatta. Am J Orthod Dentofac Orthop 1987;92:98-108.
16. Peterson J, McNamara J. Temporomandibular joint adaptions associated with Herbst appliance treatment in juvenille rhesus monkeys. Sem Orthod 2003;9:12-25.
17. Ruf S, Pancherz, H. Temporomandibular joint growth adaptation in Herbst treatment. A prospective magnetic resonance imaging and cephalometric roentgenographic study. Eur J Orthod 1998;20:375-388.
18. Ruf S, Pancherz, H. Temporomandibular joint remodelling in adolescence and young adults during Herbst treatment: a retrospective longitudinal magnetic resonance imaging and cephalometric radiographic investigation. Am J Orthod Dentofacial Orthop. 1999;115:607-618.
19. Wolff J. Das Gesetz der Transformation der Knochen 1892.
20. Qin YX, Rubin CT, McLeod KJ. Nonlinear dependence of loading intensity and cycle number in the maintenance of bone mass and morphology. Journal of Orthopaedic Research 1998;16:482-489.
21. Rubin CT. Skeletal strain and the functional significance of bone architecture. Calcified Tissue International 1984;36 Suppl 1:S11-18.
22. Rubin CT, Lanyon LE. Regulation of bone mass by mechanical strain magnitude. Calcified Tissue International 1985;37:411-417.

23. Fritton SP, McLeod KJ, Rubin CT. Quantifying the strain history of bone: spatial uniformity and self-similarity of low-magnitude strains. Journal of Biomechanics 2000;33:317-325.
24. Rubin CT, Lanyon LE. Limb mechanics as a function of speed and gait: a study of functional strains in the radius and tibia of horse and dog. Journal of Experimental Biology 1982;101:187-211.
25. Fritton JC, Rubin CT, Qin YX, McLeod KJ. Whole-body vibration in the skeleton: development of a resonance-based testing device. Annals of Biomedical Engineering 1997;25:831-839.
26. Rubin C, Pope M, Fritton JC, Magnusson M, Hansson T, McLeod K et al. Transmissibility of 15-hertz to 35-hertz vibrations to the human hip and lumbar spine: determining the physiologic feasibility of delivering low-level anabolic mechanical stimuli to skeletal regions at greatest risk of fracture because of osteoporosis. Spine 2003;28:2621-2627.
27. Omar H, Shen G, Jones AS, Zoellner H, Petocz P, Darendeliler MA. Effect of low magnitude and high frequency mechanical stimuli on defects healing in cranial bones. Journal of Oral & Maxillofacial Surgery 2008;66:1104-1111.
28. Sriram D, Jones, A., Alatli-Burt, I., Petocz, P., Darendeliler, M.A. The effects of low magnitude, high frequency mechanical stimuli on adaptive remodeling of condylar cartilage and bony tissue. A Micro-CT study. Journal of Dental Research 2009.
29. Xie L, Jacobson JM, Choi ES, Busa B, Donahue LR, Miller LM et al. Low-level mechanical vibrations can influence bone resorption and bone formation in the growing skeleton. Bone 2006;39:1059-1066.
30. Xie L, Rubin C, Judex S, Xie L, Rubin C, Judex S. Enhancement of the adolescent murine musculoskeletal system using low-level mechanical vibrations. Journal of Applied Physiology 2008;104:1056-1062.
31. Garman R, Gaudette G, Donahue LR, Rubin C, Judex S, Garman R et al. Low-level accelerations applied in the absence of weight bearing can enhance trabecular bone formation. Journal of Orthopaedic Research 2007;25:732-740.
32. Ozcivici E, Garman R, Judex S, Ozcivici E, Garman R, Judex S. High-frequency oscillatory motions enhance the simulated mechanical properties of non-weight bearing trabecular bone. Journal of Biomechanics 2007;40:3404-3411.
33. Rubin C, Xu G, Judex S. The anabolic activity of bone tissue, suppressed by disuse, is normalized by brief exposure to extremely low-magnitude mechanical stimuli. FASEB Journal 2001;15:2225-2229.
34. Xiong H, Rabie A, Hagg U. Neovascularisation and mandibular condylar bone remodelling in adult rats under mechanical strain. Frontiers in Bioscience 20005;10:74-82.
35. Shen G, Rabie, B., Hagg, U. Neovascularisation in the TMJ in response to mandibular protrusion. Clin J Dent Res 2003;6:28-38.
36. Shen G, Rabie, A.B., Zhao, Z.H., Kaluarachchi, K. Forward deviation of the mandibular condyle enhances endochondral ossification of condylar cartilage indicated by increased expression of type X collagen. Arch Oral Biol. . 2006;51:315-324.
37. Shen G, Hagg U, Rabie A, Kaluarachchi K. Identification of temporal pattern of mandibular condylar growth: a molecular and biochemical experiment. Orthod Craniofacial Res 2005;8:114-122.
38. Rabie AB, Zhao, Z., Shen, G., Hagg, E.U., Robinson, W. Osteogenesis in the glenoid fossa in response to mandibular advancement Am J Orthod Dentofacial Orthop 2001;119:390-400.
39. Rabie AB, Leung, F.Y., Chayanupatkul, A., Hagg, U. The correlation between neovascularization and bone formation in the condyle during forward mandibular positioning. Angle Orthod. 2002;72:431-438.
40. Rabie AB, Hagg, U. Factors regulating mandibular condylar growth. Am J Orthod Dentofacial Orthop 2002;122:401-409.
41. Rabie AB, Wong, L., Tsai, M. Replicating mesenchymal cells in the condyle and the glenoid fossa during mandibular forward positioning. Am J Orthod Dentofacial Orthop. 2003;123:49-57.

42. Rabie AB, Tang, G.H., Xiong, H., Hagg, U. PTHrp regulates chondrocyte matuation in condylar cartilage. J Dent Res 2003;82:627-631.
43. Rabie AB, Xiong, H., Hagg, U. Forward mandibular positioning enhances condylar adaptation in adult rats. Eur J Orthod. 2004;26:353-358.
44. Rabie AB, She TT, Harley VR, Rabie ABM. Forward mandibular positioning up-regulates SOX9 and type II collagen expression in the glenoid fossa. Journal of Dental Research 2003;82:725-730.
45. Rabie AB, Shum L, Chayanupatkul A, Rabie ABM, Shum L, Chayanupatkul A. VEGF and bone formation in the glenoid fossa during forward mandibular positioning. American Journal of Orthodontics & Dentofacial Orthopedics 2002;122:202-209.
46. Rabie AB, Hagg, U, Tang G. Cbfa1 couples chondorcyte maturation and endochondral ossification in the rat mandibular condylar cartilage. Archives of Oral Biology 2004;49:109-118.
47. Rabie AB, Tsai MJ, Hagg U, Du X, Chou BW, Rabie ABM et al. The correlation of replicating cells and osteogenesis in the condyle during stepwise advancement. Angle Orthodontist 2003;73:457-465.
48. Rabie AB, Wong L, Hagg U, Rabie ABM, Wong L, Hagg U. Correlation of replicating cells and osteogenesis in the glenoid fossa during stepwise advancement. American Journal of Orthodontics & Dentofacial Orthopedics 2003;123:521-526.
49. Luder H. Post natal development, ageing and degeneration of the TMJ in humans monkeys and rats. In: J M, editor. Craniofacial growth series. Michigan Ann Arbor Centre for Human Growth and development; University of Michigan 1993.
50. Rubin C, Turner AS, Muller R, Mittra E, McLeod K, Lin W et al. Quantity and quality of trabecular bone in the femur are enhanced by a strongly anabolic, noninvasive mechanical intervention. Journal of Bone & Mineral Research 2002;17:349-357.
51. Flieger J, Karachalios T, Khaldi L, Raptou P, Lyritis G. Mechanical stimulation in the form of vibration prevents postmenopausal bone loss in ovariectomized rats. Calcified Tissue International 1998;63:510-514.
52. Gilsanz V, Wren TA, Sanchez M, Dorey F, Judex S, Rubin C et al. Low-level, high-frequency mechanical signals enhance musculoskeletal development of young women with low BMD. Journal of Bone & Mineral Research 2006;21:1464-1474.
53. Oxlund BS, Ortoft G, Andreassen TT, Oxlund H. Low-intensity, high-frequency vibration appears to prevent the decrease in strength of the femur and tibia associated with ovariectomy of adult rats. Bone 2003;32:69-77.
54. Rubin C, Recker R, Cullen D, Ryaby J, McCabe J, McLeod K et al. Prevention of postmenopausal bone loss by a low-magnitude, high-frequency mechanical stimuli: a clinical trial assessing compliance, efficacy, and safety. Journal of Bone & Mineral Research 2004;19:343-351.
55. Rubin C, Turner AS, Bain S, Mallinckrodt C, McLeod K. Anabolism. Low mechanical signals strengthen long bones. Nature 2001;412:603-604.
56. Rubin C, Turner AS, Mallinckrodt C, Jerome C, McLeod K, Bain S. Mechanical strain, induced noninvasively in the high-frequency domain, is anabolic to cancellous bone, but not cortical bone. Bone 2002;30:445-452.
57. Barley G. The effects of combined glucosamine sulfte and chondroitin sulfate supplements on condylar cartilage remodelling during functional appliance therapy. A micro-CT study. Orthodontics. Sydney: University of Sydney 2008.
58. Tan A. The effects of combined glucosamine sulfate and chondroitin sulfate supplements on condylar cartilage during functional appliance therapy. A micro CT Study. Orthodontics. Sydney: University of Sydney; 2008.
59. Cockman MD, Blanton, C.A., Chmielewski, P.A., Dong, L., Dufresne, T.E., Hookfin, E.B., Karb, M.J., Liu, S., Wehmeyer, K.R. Quantitative imaging of protegoglycan in cartilage using a gadolinium probe and microCT. Osteoarthritis & Cartilage. 2006;14:210-214.

60. Ito M. Assessment of bone quality using micro-computed tomography (micro-CT) and synchrotron micro CT. Journal of Bone and Mineral Res 2005;23(suppl):114-121.
61. Chappard D, Retailleau-Gaborit N, Legrand E, Basle MF, Audran M. Comparison Insight Bone Measurements by Histomorphometry and micro-CT. Journal of Bone and Mineral Res 2005;20:1177-1184.
62. Jiang Y, Zhao, J., White, D.L., Genant, H.K. Micro CT and Micro MR imaging of 3D architecture of animal skeleton. J Musculoskelet Neuronal Interact. 2000;1:45-41.
63. Parfitt A, Drezner M, Glorieux F, Kanis J, Malluche H, Meunier P et al. Bone Histomorphometry: Standardisation of nomenclature, symbols and units. Journal of Bone and Mineral Res 1987;2:595-610.
64. Hahn M, Vogel M, Pompesius-Kempa M, Delling G. Trabecular bone pattern factor - a new parameter for simple quantification of bone microarchitecture. Bone 1992;13:327-330.
65. Liu J, Sekiya I, Asai K, Tada T, Kato T, Matsui N. Biosynthetic response of cultured articular chondrocytes to mechanical vibration. Research in Experimental Medicine 2001;200:183-193.
66. Yamazaki S, Banes AJ, Weinhold PS, Tsuzaki M, Kawakami M, Minchew JT et al. Vibratory loading decreases extracellular matrix and matrix metalloproteinase gene expression in rabbit annulus cells. Spine Journal: Official Journal of the North American Spine Society 2002;2:415-420.
67. Al-kalaly A, Wu C, Wong R, Rabie A. The assessment of cell cycle genes in the rat mandibular condyle. Archives of Oral Biology 2009;54:470-478.
68. Chayanupatkul A, Rabie, A.B., Hagg ,U. Temporomandibular response to early and late removal of bite-jumping devices. Eur J Orthod. 2003;25:465-470.
69. Dai J, Rabie A. VEGF: an essential mediator of both angiogenesis and endochondral ossification. J Dent Res 2007;86:937-950.
70. Hajjar D, Santos, M.F., Kimura, E.T. Propulsive appliance stimulates the synthesis of insulin-like growth factors I and II in the mandibular condylar cartilage of young rats. Archives of Oral Biology 2003;48:635-642.
71. Tang GH, Rabie AB, Hagg U, Rabie ABM. Indian hedgehog: a mechanotransduction mediator in condylar cartilage. Journal of Dental Research 2004;83:434-438.
72. Tang GH, Rabie AB, Rabie ABM. Runx2 regulates endochondral ossification in condyle during mandibular advancement. Journal of Dental Research 2005;84:166-171.
73. Siegel M, Mooney M. Appropriate animal models for craniofacial biology. Cleft Palate Journal 1990;27:18-25.
74. Hiiemae KM, Ardran, G.M. A cinefluorgraphic study of mandibular movement during feeding in the rat (rattus norvegicus). Journal of Zoology 1968;154:139-154.
75. Tsolakis A, Spyropoulos, M. An Appliance designed for experimental mandibular hyperpropulsion in rats. Eur J Orthod 1997;19:1-7.
76. Xiong H, Hagg, U., Tang, G.H., Rabie, A.B., Robinson, W. The effect of continuous bite-jumping in adult rats: a morphological study. Angle Orthod. 2004;74:86-92.
77. Marques MR, Hajjar D, Franchini KG, Moriscot AS, Santos MF, Marques MR et al. Mandibular appliance modulates condylar growth through integrins. Journal of Dental Research 2008;87:153-158.
78. Prisby R, Lafage-Proust M, Malaval L, Belli A, Vico L. Effects of whole body vibration on the skeleton and other organ systems in man and animal models: What we know and what we need to know. Ageing Research Reviews 2008;7:319-329.
79. Charlier JP, Petrovic, A., Herrmann–Stutzmann, J. Effects of mandibular hyperpropulsion on the pre chondroblastic zone of young rat condyle. Am J Orthod 1969:71-74.
80. Pancherz H, Fisher S. Amount and direction of temporomandibular joint growth changes in Herbst treatment: a cephalometric long term investigation. Angle Orthod. 2003;73:493-501.
81. Pancherz H, Littmann C. Somatic maturity and manibular morphological changes during Herbst treatment. Inf Orthod Keiferorthop 1988;20:455-470.

82. Paulsen H. Morphological changes of the TMJ condyles of 100 patients treated with the Herbst appliance in the period of puberty to adulthood: A long-term radiographic study. Eur J Orthod 1997;19:657-668.
83. Tanaka E, Detamore M, Mecuri L. Degenerative disorders of the temporomandibular joint; etiology, diagnosis, and treatment. J Dent Res 2008;87:296-307.
84. Kuroda S, Tanimoto K, Izawa T, Fujihara S, Koolstra J, Tanaka E. Biomechanical and biocehmical characteristics of the mandibular condylar cartilage. Osteoarthr Cart 2009;17:1408-1415.
85. Shirakura M, Tanimoto K, Eguchi H, Miyauchi M, Nakamura H, Hiyama K et al. Activation of the hypoxia-inducible factor 1 in overloaded temporomandibular joint and induction of osteoclastogenesis. Biochem Biophys Res Com 2010;393:800-805.
86. Forsythe J, Jiang B, Iyer N, Agani F, Leung S, Koos R et al. Activation of vascular endothelial growth factor gene transcription by hypoxia-inducible factor 1. Mol. Cel. Biol 1996;16:4604-4613.
87. Pufe T, Lemke A, Kurz B, Petersen W, Tillmann B, Grodzinsky A et al. Mechanical overload induces VEGF in cartilage discs via hypoxia-inducible factor. Am J Pathol 2004;164:185-192.
88. Engsig M, Chen T, Vu T, Pedersen A, Thirkidsen B, Lund L et al. MMP9 and VEGF are essential for osteoclast recruitment into developing long bones. J Cell Biol 2000;151:879-889.
89. Niida S, Kaku H, Amano H, Yoshida H, Kataoka H, Nishikawa S et al. VEGF can substitue for macrophase CSF in the support of osteoclastic bone resorption. J Exp Med 1999;190:293-298.
90. Hinton R, McNamara JJ. Temporal bone adaptations in response to protrusive function in juvenile and young adult rhesus monkeys (*Macaca mulatta)*. Eur J Orthod 1984;6:155-174.
91. Pancherz H, Littmann C. Mandibular morphology and position in Herbst treatment. A cpehalometric analysis of changes to the end of growth. Inf Orthod Keiferorthop 1989;21.
92. Burger EH, Klein-Nulend J. Mechanotransduction in bone--role of the lacuno-canalicular network. FASEB Journal 1999;13 Suppl:S101-112.
93. Robling A, Castilli A, Turner C. Biomechanical and molecular regulation of bone remodeling. Annual Review of Biomedical Engineering 2006;8:455-498.
94. Cowin SC, Moss-Salentijn L, Moss ML. Candidates for the mechanosensory system in bone. Journal of Biomechanical Engineering 1991;113:191-197.
95. Proffit WR, Fields, H.W., editors. Contemporary orthodontics. 4th ed. : St Louis: Mosby; 2007.
96. Pedersen T, Gronhoj J, Melsen B, Herlin T. Condylar condition and mandibular growth during early functional treatment of children with juvenile chronic arthritis. European Journal of Orthod 1995;17:385-394.
97. Melsen B, Bjerregaard J, Bundgaard M. The effect of treatment with functional appliance on a pathological growth pattern of the condyle. American Journal of Orthodontics & Dentofacial Orthopedics 1986;90:503-512.
98. Ikeda K, Kawamura A. Assessment of optimal condylar position with limited con-beam computed tomography. American Journal of Orthodontics & Dentofacial Orthopedics 2009;135:495-501.
99. Baccetti T, Franchi L, Toth LR, McNamara JA, Jr. Treatment timing for Twin-block therapy. American Journal of Orthodontics & Dentofacial Orthopedics 2000;118:159-170.

List of Figures

Figure 1: Functional appliance achieving mandibular protrusion

Figure 2: Study Design

Figure 3: Condylar cartilage rendered into a three dimensional image with the segmented cartilage

Figure 4: Segmentation of bone for bone morphometric analysis using CTAnalyzser

Figure 5: Gross morphological changes of the condyle from baseline at day 0, to day 30 for natural growth, vibration, functional appliance, and functional appliance with vibration

Figure 6: Microscopic condylar changes with normal growth (x-z imaging plane)

Figure 7: Microscopic condylar changes with vibration alone (x-z imaging plane)

Figure 8: Microscopic condylar changes with functional appliance alone (x-z imaging plane)

Figure 9: Microscopic condylar changes with functional appliance together with vibration (x-z imaging plane)

Figure 10: Surface changes to the condyle with functional appliance treatment

Figure 11: Endochondral ossification at posterior condyle with functional appliance, with and without vibration

Figure 12: Severe condylar and glenoid fossa resorption seen with functional appliance

List of Tables

Table 1: Bone parameters from CT Analyzer (SkyScan™, *Aartselaar, Belgium*)

Table 2: Mean and standard error for mandibular condylar cartilage volume and bone parameters for each group at each time point

Table 3: Post hoc comparisons of changes in cartilage volume and bone parameters between groups at each time point

Table 4: Post hoc comparisons of changes in cartilage volume and bone parameters between time points for each group

Table 5: Graphs for mandibular condylar cartilage volume

Table 6: Graphs for bone surface

Table 7: Graphs for bone surface to volume ratio

Table 8: Graphs for bone surface density

Table 9: Graphs for trabecular bone pattern factor

Table 10: Graphs for structure model index

Table 11: Graphs for trabecular thickness

Table 12: Graphs for trabecular number

Table 13: Graphs for trabecular separation

Figures

Figure 1: Functional appliance achieving mandibular protrusion

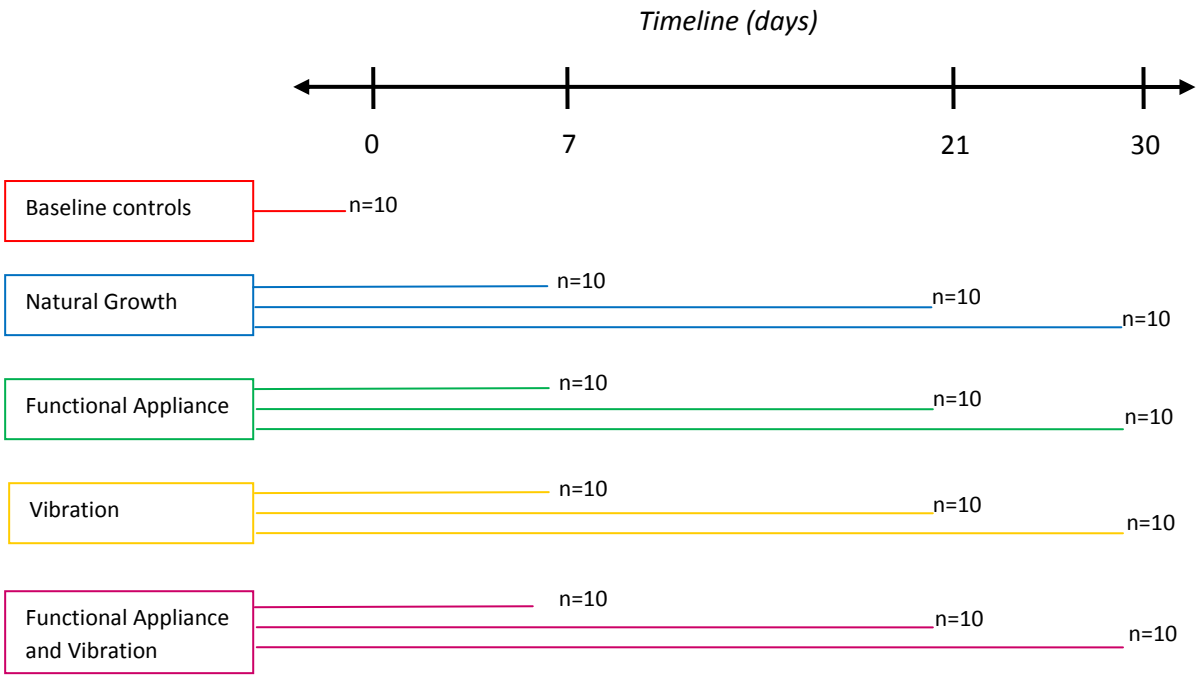

Figure 2: Experimental timeline

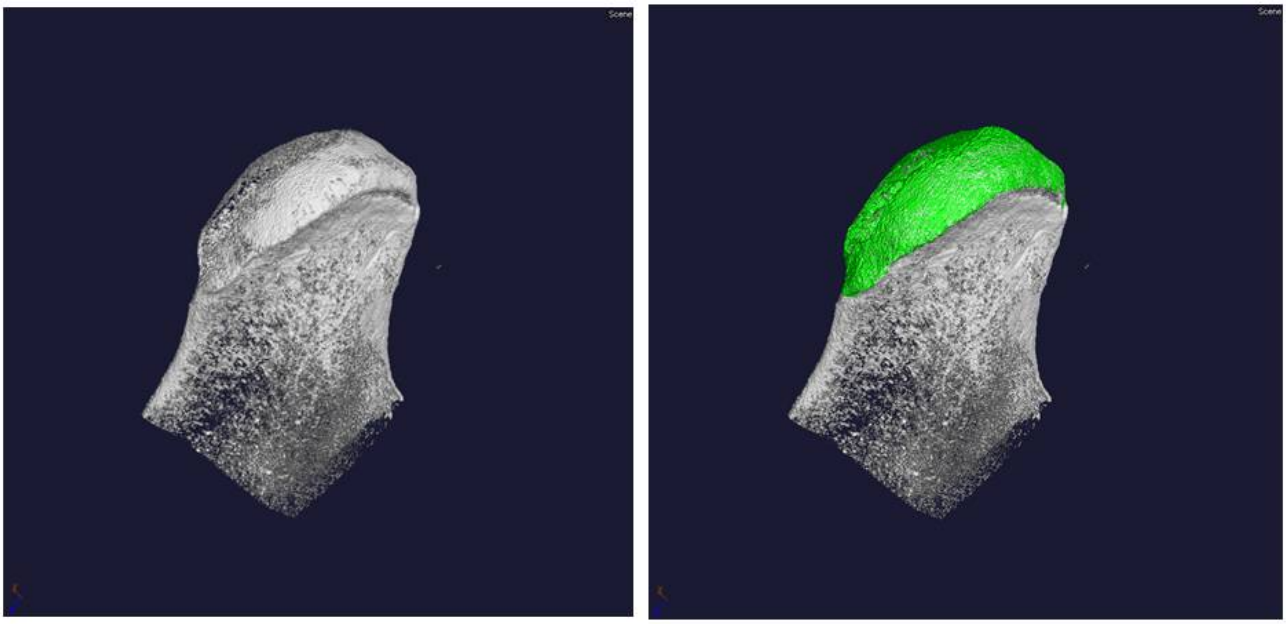

Figure 3: Condylar process rendered into a three dimensional image with the segmented cartilage (green)

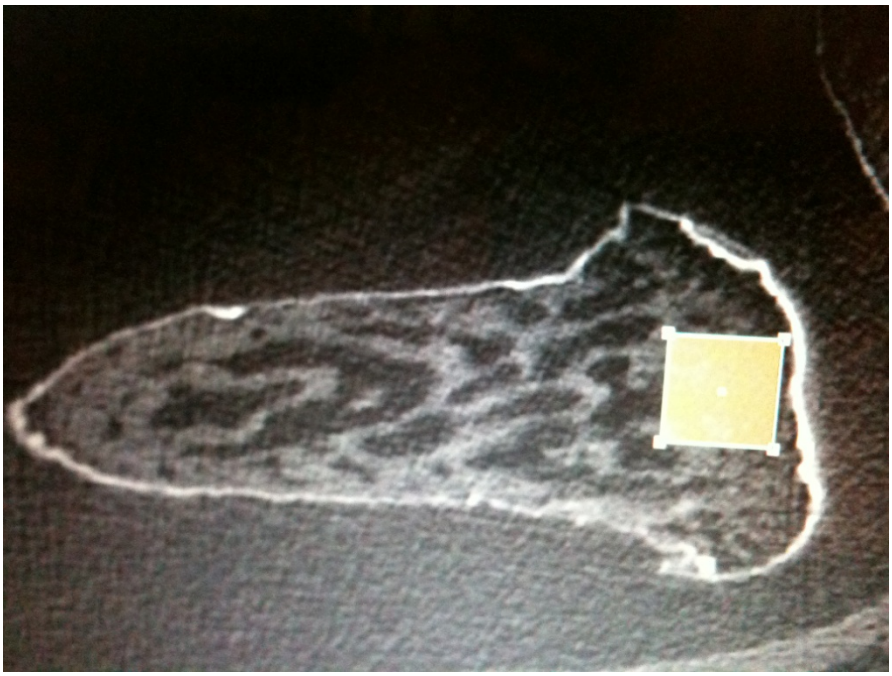

Figure 4: Segmentation of bone for bone morphometric analysis

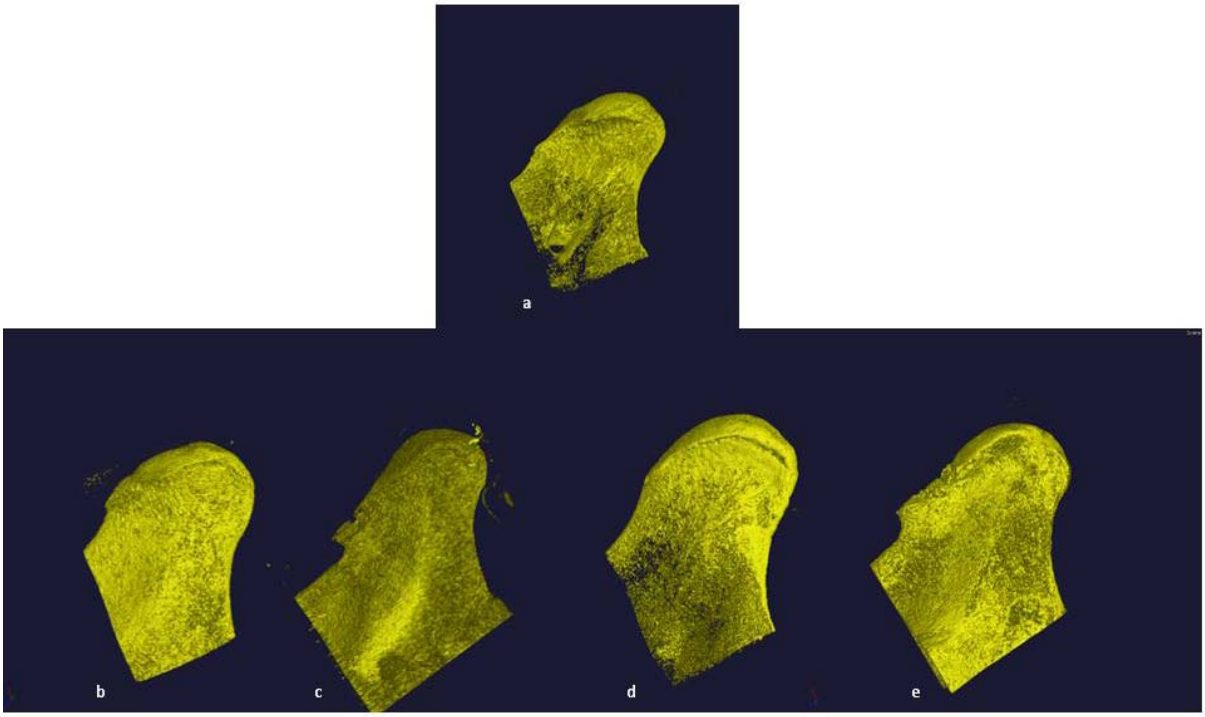

Figure 5: Gross morphological changes of the condyle from (a) baseline at day 0 (b) natural growth at day 30 (c) vibration at day 30 (d) functional appliance at day 30 and (e) functional appliance with vibration at day 30

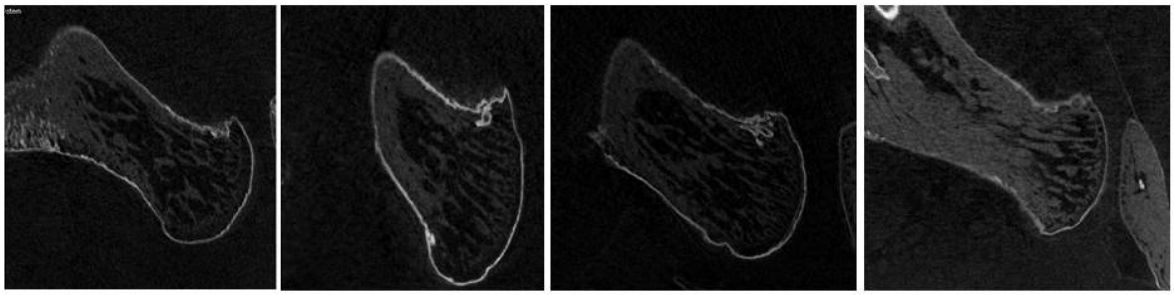

Day 0 Day 7 Day 21 Day 30

Figure 6: Condylar cartilage and bone. Natural growth. x-z micro-CT imaging plane

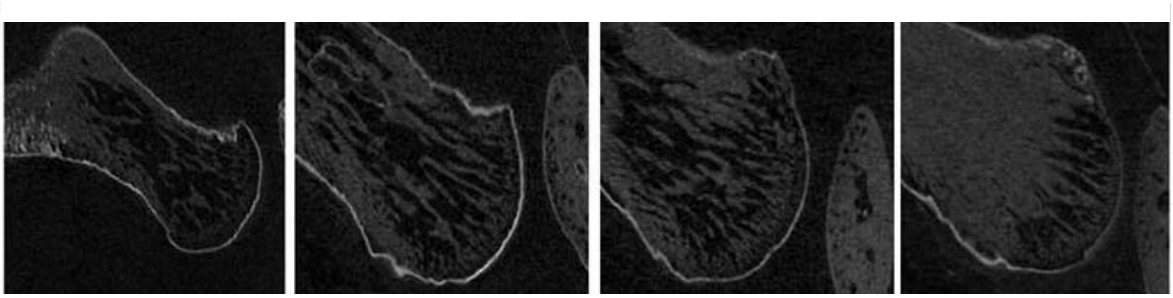

Day 0 Day 7 Day 21 Day 30

Figure 7: Thinning of condylar cartilage with vibrayion Natural growth. x-z micro-CT imaging plane

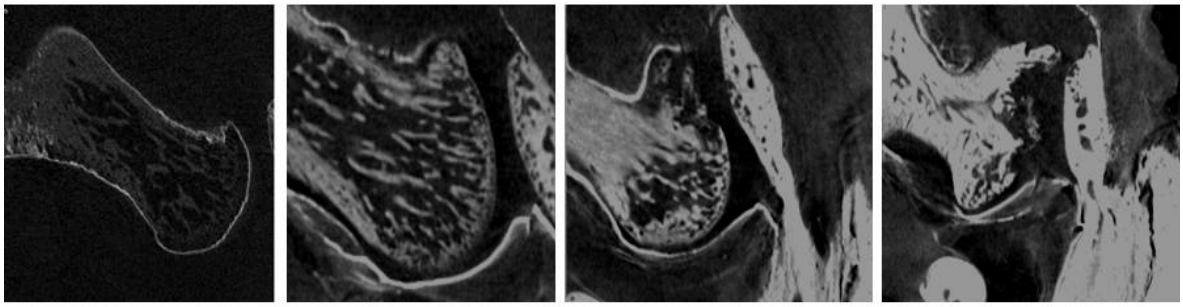

Day 0 Day 7 Day 21 Day 30

Figure 8: Condylar cartilage breakdown and anterior condylar resorption with functional appliance only. x-z micro-CT imaging plane

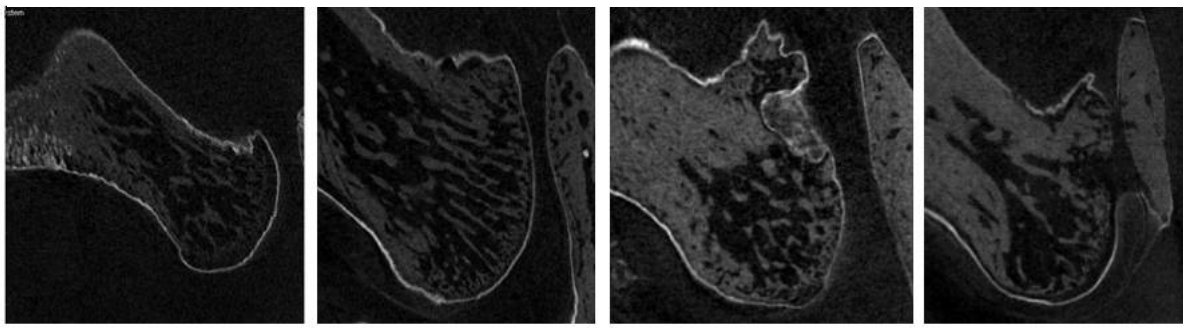

Day 0 Day 7 Day 21 Day 30

Figure 9: Condylar cartilage breakdown and anterior condylar resorption with functional appliance and vibration. x-z micro-CT imaging plane

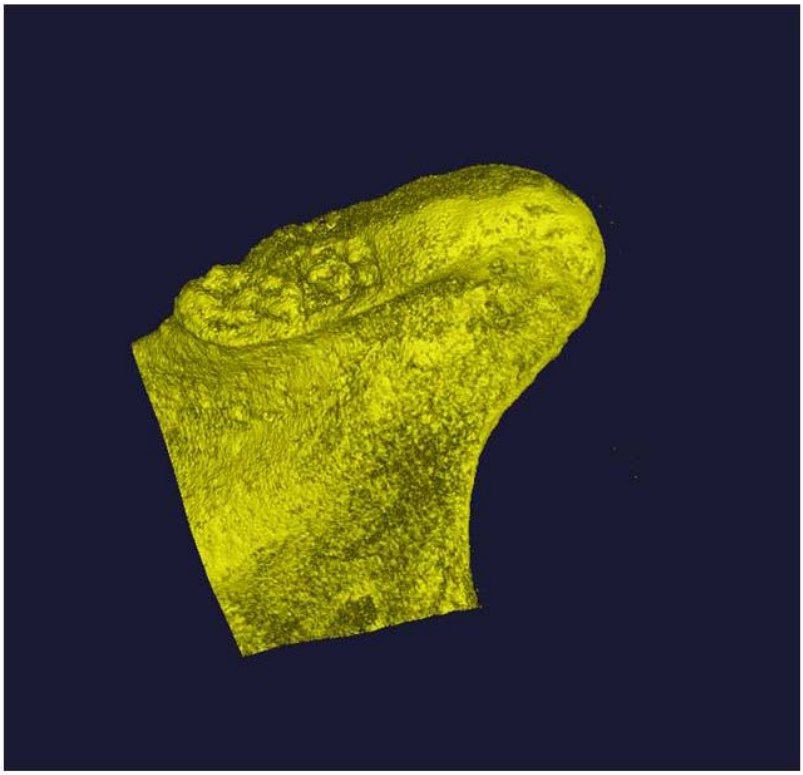

Figure 10: Surface changes to condyle with functional appliance treatment

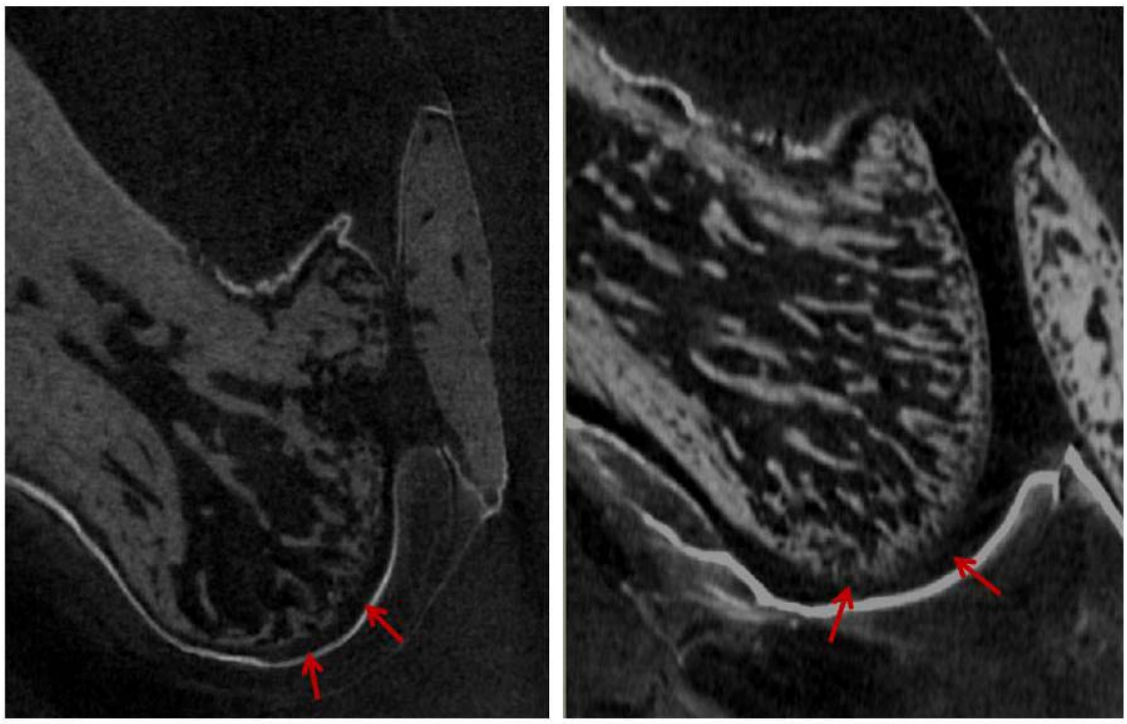

Figure 11: Endochondral ossification in functional appliance with vibration (left) and functional appliance alone (right) indicated by the red arrows.

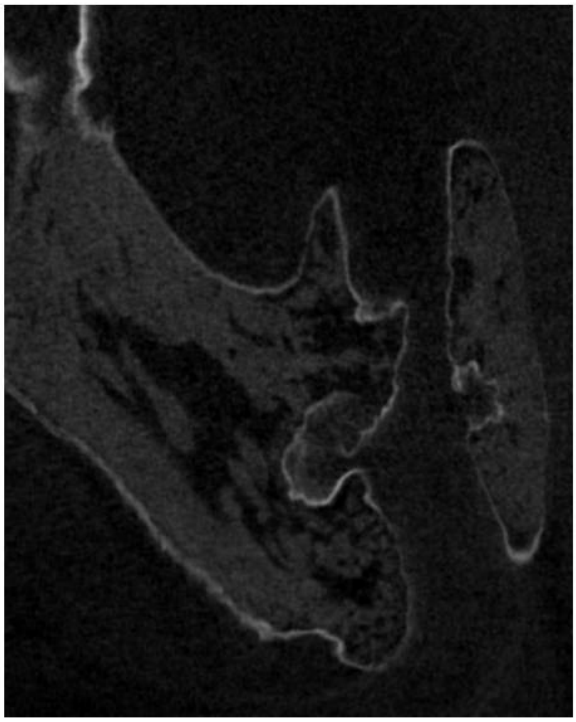

Figure 12: Severe condylar and glenoid fossa resorption associated with functional appliance

Tables

3D Morphometric Parameters	**Abbreviation** **Bone ASBMR[63]**	**Units**
Tissue volume	TV	mm^3
Bone volume	BV	mm^3
Percent bone volume	BV/TV	%
Tissue surface	TS	mm^2
Bone Surface	BS	mm^2
Bone surface / bone volume ratio	BS/BV	mm^{-1}
Bone surface density	BS/TV	mm^{-1}
Trabecular thickness	Tb.Th	mm
Trabecular number	Tb.N	mm^{-1}
Structure model index	SMI	(none)
Trabecular bone pattern factor	Tb.Pf	mm^{-1}
Trabecular separation	Tb.Sp	mm

Table 1 3D Bone Morphometric Parameters generated by Skyscan CT Analyser software

Table 2 Mean and Standard Error (SE) for mandibular condylar cartilage volume and bone parameters for each group at each time point.

Group	Time (days)	MCCVol voxel x10^4		BS mm^2		BS/BV mm^{-1}		BS/TV mm^{-1}		Tb.Th mm		Tb.N mm^{-1}		SMI		Tb.Sp mm		Tb.Pf mm^{-1}	
		Mean	SE	Mean	SE	Mean	SE	Mean	SE	Mean	SE	Mean	SE	Mean	SE	Mean	SE	Mean	SE
0 BLC	0	61.106	2.492	2.934	0.178	150.470	6.687	34.463	1.836	0.033	0.004	7.114	0.531	1.192	0.250	0.066	0.009	18.992	5.765
1 NG	7	65.780	2.492	3.281	0.178	120.635	6.687	38.090	1.836	0.037	0.004	8.649	0.531	1.513	0.250	0.065	0.009	1.838	5.765
	21	69.023	2.492	3.417	0.178	104.364	6.687	39.100	1.836	0.041	0.004	9.229	0.531	1.119	0.250	0.064	0.009	-12.255	5.765
	30	75.120	2.492	3.284	0.178	118.007	6.687	38.658	1.836	0.038	0.004	8.703	0.531	1.305	0.250	0.067	0.009	-7.612	5.765
2 FA	7	52.897	2.627	1.910	0.188	67.060	7.049	22.327	1.935	0.069	0.004	5.899	0.560	1.530	0.264	0.105	0.009	11.887	6.076
	21	61.680	2.492	1.176	0.188	62.189	7.049	12.743	1.935	0.077	0.004	3.054	0.560	2.244	0.264	0.179	0.009	23.460	6.076
	30	46.972	2.492	1.379	0.178	47.504	6.687	15.761	1.836	0.105	0.004	3.729	0.531	1.910	0.250	0.144	0.009	14.692	5.765
3 V	7	73.270	2.627	3.087	0.178	136.559	6.687	36.024	1.836	0.035	0.004	7.674	0.531	1.791	0.250	0.067	0.009	11.830	5.765
	21	79.985	2.492	3.438	0.178	113.152	6.687	39.007	1.836	0.039	0.004	8.922	0.531	1.473	0.250	0.061	0.009	0.951	5.765
	30	52.936	2.492	3.461	0.178	109.524	6.687	40.167	1.836	0.039	0.004	9.515	0.531	1.180	0.250	0/061	0.009	-6.227	5.765
4 FA+V	7	79.152	2.492	2.613	0.178	80.098	6.687	29.987	1.836	0.050	0.004	7.587	0.531	1.022	0.250	0.090	0.009	-6.094	5.765
	21	53.980	2.627	2.371	0.188	102.841	7.049	27.721	1.935	0.047	0.004	6.890	0.560	0.861	0.264	0.086	0.009	-1.285	6.076
	30	53.289	2.627	2.282	0.188	91.273	7.049	29.580	1.935	0.051	0.004	7.085	0.560	1.192	0.264	0.094	0.009	-0.358	6.076

BLC= Baseline controls; NG= Natural Growth; FA= Functional Appliance; V= Vibration; FA+V= Functional Appliance with Vibration; MCCVol = Mandibular condylar cartilage volume (1voxel = 6.8μm^3 = 3.1x$10^{-7}$$mm^{)}$; BS=Bone Surface; BS/BV=bone surface to volume ratio; BS/TV=bone surface density; Tb.Th=Trabecular thickness; Tb.N=Trabecular Number; SMI=Structure model index; Tb.Sp.=Trabecular separation; Tb.Pf=trabecular bone pattern factor

Table 3 Post hoc comparisons of changes in cartilage volume and bone parameters between groups at each time poin

Time Point	Compared Groups		MCCVol voxel x10^4		BS mm^2		BS/BV mm^{-1}		BS/TV mm^{-1}		Tb.Th mm		Tb.N mm^{-1}		SMI		Tb.Sp mm		Tb.Pf mm^{-1}	
			Dif	Sig.	Dif	Sig.	Dif	Sig.	Dif	Sig.	Dif	Sig.	Dif	Sig.	Dif	Sig.	Dif	Sig.	Dif	Sig.
Day 7	1	2	12.883*	.001	1.371*	<.001	63.574*	<.001	15.763*	<.001	-.032*	<.001	2.750*	.001	-.017	.962	-.041*	.002	-10.049	.233
		3	-7.490	.041	.195	.441	-15.925	.095	2.066	.428	.002	.677	.975	.197	-.279	.432	-.002	.861	-9.992	.223
		4	-13.372*	<.001	.668*	.009	40.537*	<.001	8.103*	.002	-.013*	.012	1.063	.160	.491	.168	-.025*	.041	7.931	.333
	2	3	-20.373*	<.001	-1.176*	<.001	-79.499*	<.001	-13.697*	<.001	.034*	<.001	-1.775*	.023	-.262	.473	.038*	.003	.057	.995
		4	-26.255*	<.001	-.703*	.008	-23.038*	.019	-7.660*	.005	.019*	<.001	-1.687*	.031	.508	.165	.015	.219	17.980	.034
	3	4	-5.882	.107	.474	.062	56.461*	<.001	6.037	.022	-.015*	.004	.088	.907	.770	.032	-.023	.062	17.923*	.030
Day 21	1	2	7.343	.039	2.241*	<.001	42.175*	<.001	26.358*	<.001	-.036*	<.001	6.176*	<.001	-1.126*	.002	-.115*	<.001	-35.715*	<.001
		3	-10.962*	.002	-.022	.932	-8.788	.355	.094	.971	.002	.744	.308	.683	-.355	.318	.003	.787	-6.029	.461
		4	15.043*	<.001	1.045*	<.001	1.524	.876	11.379*	<.001	-.006	.281	2.340*	.003	.257	.480	-.022	.076	-10.970	.193
	2	3	-18.306*	<.001	-2.262*	<.001	-50.963*	<.001	-26.264*	<.001	.039*	<.001	-5.868*	<.001	.771*	.036	.118*	<.001	22.509*	.008
		4	7.700	.036	-1.195*	<.001	-40.652*	<.001	-14.978*	<.001	.031*	<.001	-3.836*	<.001	1.383*	<.001	.092*	<.001	24.745*	.005
	3	4	26.005*	<.001	1.067*	<.001	10.311	.291	11.286*	<.001	-.007	.164	2.032*	.010	.612	.095	-.026*	.042	2.236	.790
Day 30	1	2	28.148*	<.001	1.905*	<.001	70.502*	<.001	22.897*	<.001	-.066*	<.001	4.974*	<.001	-.605	.090	-.077*	<.001	-22.304*	.007
		3	22.184*	<.001	-.178	.482	8.483	.372	-1.509	.562	.000	.944	-.812	.282	.125	.726	.006	.651	-1.385	.865
		4	21.831*	<.001	1.002*	<.001	26.734*	.007	9.078*	.001	-.013*	.016	1.617*	.038	.112	.758	-.028*	.029	-7.254	.388
	2	3	-5.964	.093	-2.083*	<.001	-62.020*	<.001	-24.406*	<.001	.066*	<.001	-5.786*	<.001	.729	.042	.082*	<.001	20.919*	.012
		4	-6.317	.084	-.903*	.001	-43.768*	<.001	-13.819*	<.001	.054*	<.001	-3.357*	<.001	.717	.051	.049*	<.001	15.050	.075
	3	4	-.353	.922	1.180*	<.001	18.251	.063	10.587*	<.001	-.012*	.019	2.430*	.002	-.012	.974	-.033*	.009	-5.869	.485

* the mean difference is significant at 0.01 level (p<0.01); Dif = difference; Sig. = Significance
1= Natural Growth; 2=Functional Appliance; 3=Vibration; 4=Functional Appliance with Vibration; MCCVol = Mandibular condylar cartilage volume (1voxel = 6.8µm^3 = 3.1x$10^{-7}$$mm^{)}$; BS=Bone Surface; BS/BV=bone surface to volume ratio; BS/TV=bone surface density; Tb.Th=Trabecular thickness; Tb.N=Trabecular Number; SMI=Structure model index; Tb.Sp.=Trabecular separation; Tb.Pf=trabecular bone pattern factor

Table 4 Post hoc comparisons of changes in cartilage volume and bone parameters between time points for each group

Group	Compared Time Points (days)		MCCVol voxel x10^4		BS mm^2		BS/BV mm^{-1}		BS/TV mm^{-1}		Tb.Th mm		Tb.N mm^{-1}		SMI		Tb.Sp mm		Tb.Pf mm^{-1}	
			Dif	Sig	Dif	Sig	Dif	Sig	Dif	Sig	Dif	Sig	Dif	Sig	Dif	Sig	Dif	Sig	Dif	Sig
Group 1	0	7	-4.674	.187	-.347	.171	29.836*	.002	-3.627	.165	-.004	.430	-1.535	.043	.399	.261	.001	.919	17.154	.038
		21	-7.917*	.027	-.482	.058	46.106*	<.001	-4.637	.077	-.008	.105	-2.116*	.006	.794	.027	.002	.859	31.247*	<.001
		30	-14.014*	<.001	-.349	.168	32.464*	.001	-4.195	.109	-.006	.261	-1.589	.037	.607	.089	-.001	.995	26.604*	.001
	7	21	-3.243	.359	-.136	.591	16.270	.088	-1.011	.698	-.004	.401	-.580	.442	.394	.268	.001	.940	14.093	.087
		30	-9.340*	.009	-.003	.992	2.628	.782	-.568	.827	-.002	.736	-.054	.943	.208	.558	-.002	.874	9.449	.249
	21	30	-6.097	.086	.133	.598	-13.642	.152	.442	.865	.003	.614	.527	.485	-.186	.599	-.003	.815	-4.643	.570
Group 2	0	7	8.209	.025	1.024*	<.001	93.410*	<.001	12.136*	<.001	-.036*	<.001	1.215	.118	.382	.295	-.039*	.002	7.105	.398
		21	-.574	.871	1.758*	<.001	88.281*	<.001	21.720*	<.001	-.045*	<.001	4.060*	<.001	-.332	.362	-.113*	<.001	-4.468	.595
		30	14.134*	<.001	1.556*	<.001	102.966*	<.001	18.702*	<.001	-.072*	<.001	3.385*	<.001	.002	.995	-.077*	<.001	4.299	.599
	7	21	-8.783*	.017	.734*	.007	-5.129	.608	9.584*	.001	-.009	.098	2.846*	<.001	-.262	.473	-.073*	<.001	-11.573	.181
		30	5.925	.105	.532	.042	9.556	.327	6.566	.015	-.036*	<.001	2.171*	.006	-.380	.298	-.038*	.003	-2.806	.738
	21	30	14.708*	<.001	-.202	.435	14.685	.134	-3.018	.260	-.027*	<.001	-.675	.384	.335	.359	.035*	.006	8.768	.297
Group 3	0	7	-12.164*	.001	-.152	.547	13.911	.144	-1.561	.549	-.002	.709	-.561	.457	.121	.734	-.001	.942	7.162	.382
		21	-18.879*	<.001	-.504	.048	37.318*	<.001	-4.544	.083	-.007	.194	-1.808	.018	.439	.217	.005	.655	18.040	.029
		30	8.170	.022	-.527	.038	40.946*	<.001	-5.704	.030	-.006	.233	-2.401*	.002	.732	.041	.005	.692	25.218*	.002
	7	21	-6.715	.066	-.352	.165	23.407	.015	-2.983	.253	-.005	.353	-1.247	.100	.318	.371	-.038*	.003	10.878	.185
		30	20.334*	<.001	-.375	.139	27.035*	.005	-4.144	.133	-.004	.411	-1.841	.016	.611	.087	.006	.639	18.056	.029
	21	30	27.050*	<.001	-.023	.927	3.628	.702	-1.161	.656	.001	.914	-.593	.431	.293	.409	-.001	.960	7.178	.380
Group 4	0	7	-18.046*	<.001	.322	.204	70.372*	<.001	4.476	.087	-.017*	.001	-.473	.531	.890	.013	-.024	.052	25.085*	.003
		21	7.126	.051	.563	.031	47.630*	<.001	6.742	.013	-.014*	.009	.224	.772	1.051*	.005	-.020	.108	20.276	.017
		30	7.817*	.033	.653	.013	59.197*	<.001	4.883	.070	-.018*	.001	.029	.917	.720	.050	-.028	.025	19.349	.023
	7	21	25.172*	<.001	.241	.352	-22.743	.021	2.266	.397	.003	.558	.697	.369	.161	.659	.004	.771	-4.809	.567
		30	25.863*	<.001	.331	.203	-11.175	.253	.406	.879	-.002	.769	.501	.518	-.171	.640	-.004	.722	-5.736	.495
	21	30	.691	.853	.090	.736	11.568	.248	-1.859	.498	-.005	.039	-.196	.805	-.331	.376	-.008	.529	-.927	.914

* the mean difference is significant at 0.01 level (p<0.01); 1= Natural Growth; 2=Functional Appliance; 3=Vibration; 4=Functional Appliance with Vibration; MCCVol = Mandibular condylar cartilage volume (1voxel = 6.8µm^3 = 3.1x$10^{-7}$$mm^{)}$; BS=Bone Surface; BS/BV=bone surface to volume ratio; BS/TV=bone surface density; Tb.Th=Trabecular thickness; Tb.N=Trabecular Number; SMI=Structure model index; Tb.Sp.=Trabecular separation; Tb.Pf=trabecular bone pattern factor

Table 5 Graphs for Mandibular Condylar cartilage Volume (Voxel $\times 10^4$)

Line-graph of mean mandibular condylar cartilage volume

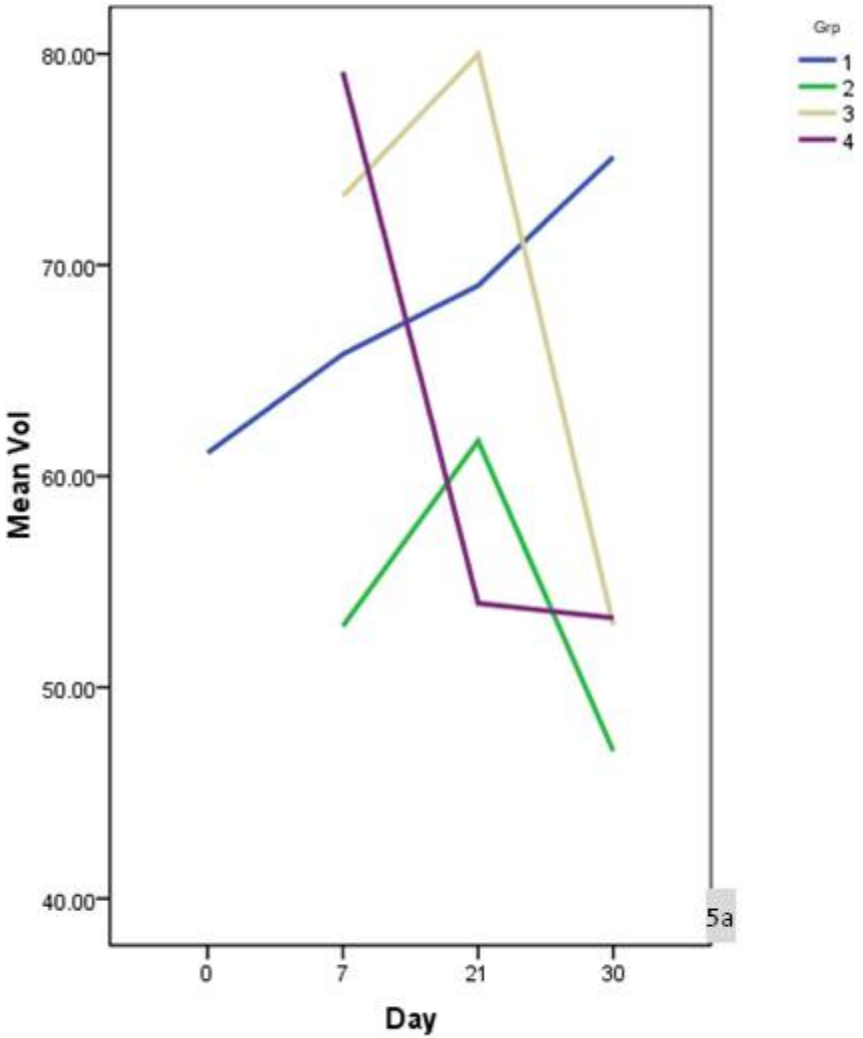

5a

Box plot of univariate ANOVA for mandibular condylar cartilage volume

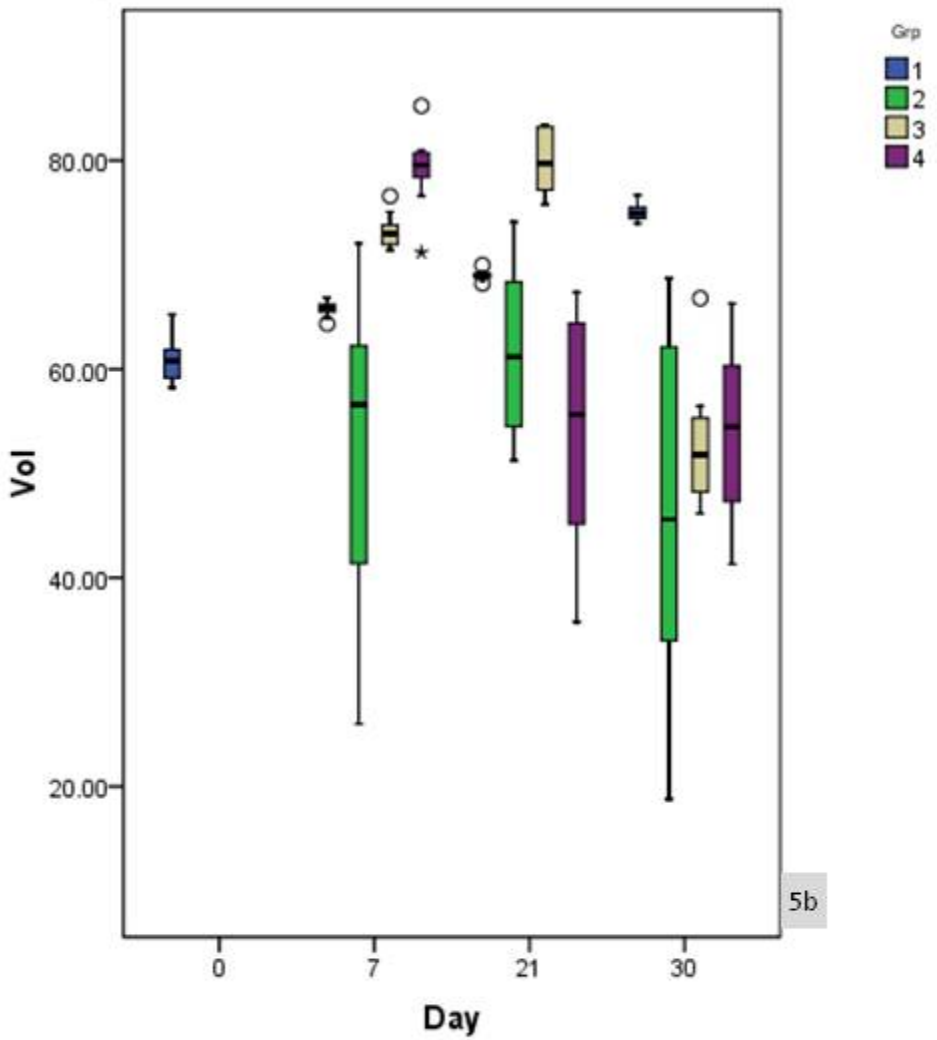

5b

Post-hoc comparisons of changes in mandibular condylar cartilage volume between time points for each group

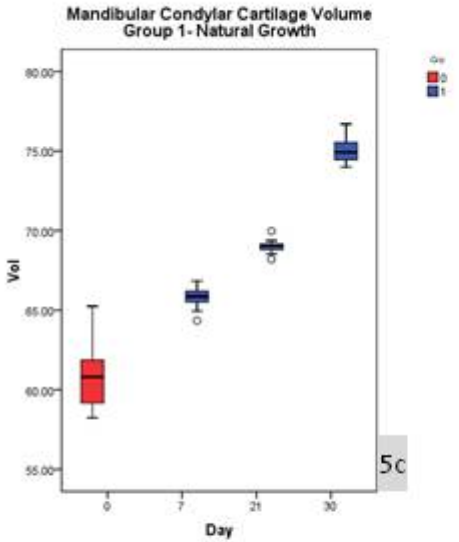

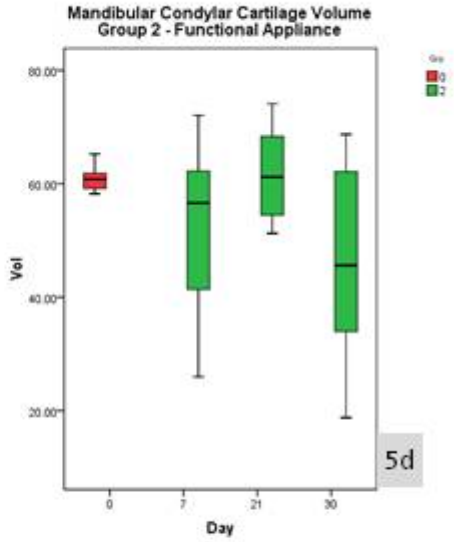

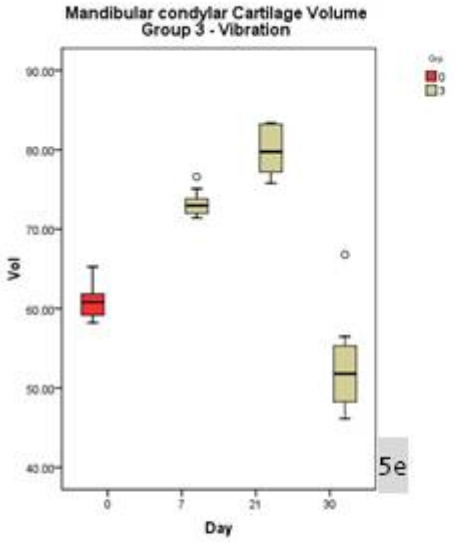

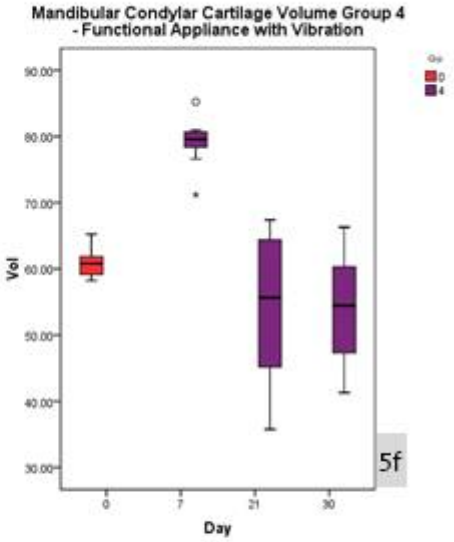

Post-hoc comparisons of changes in mandibular condylar cartilage volume between groups at each time point

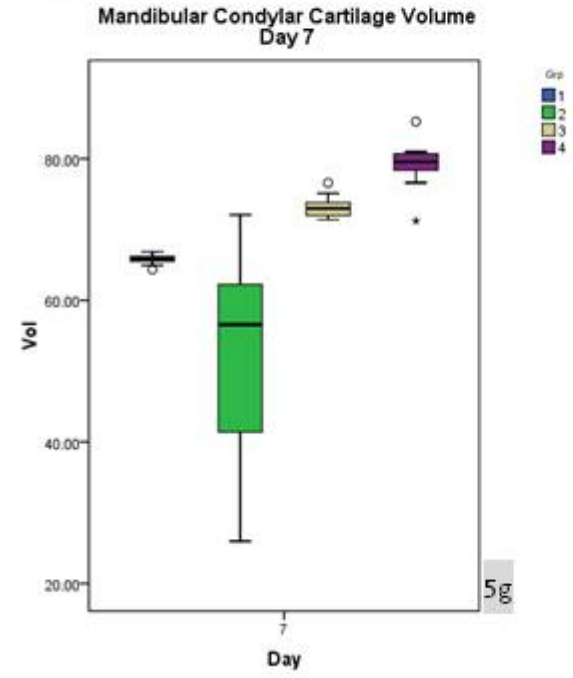

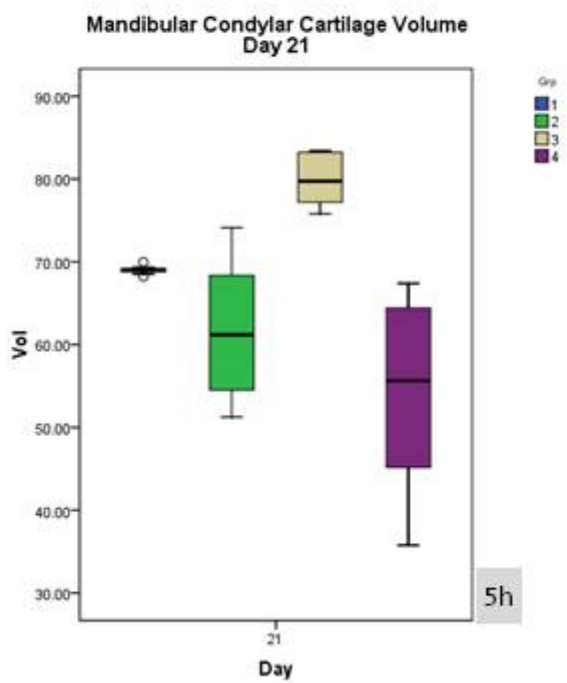

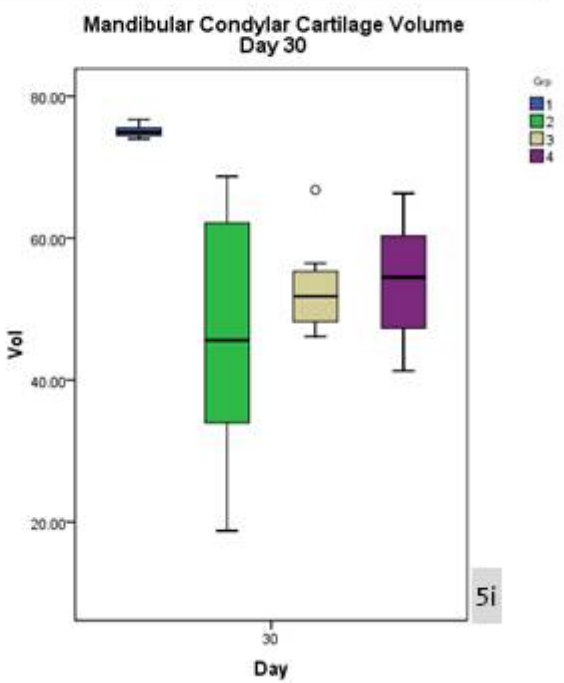

Table 6 Graphs for Bone Surface (BS mm²)

Line-graph of mean bone surface

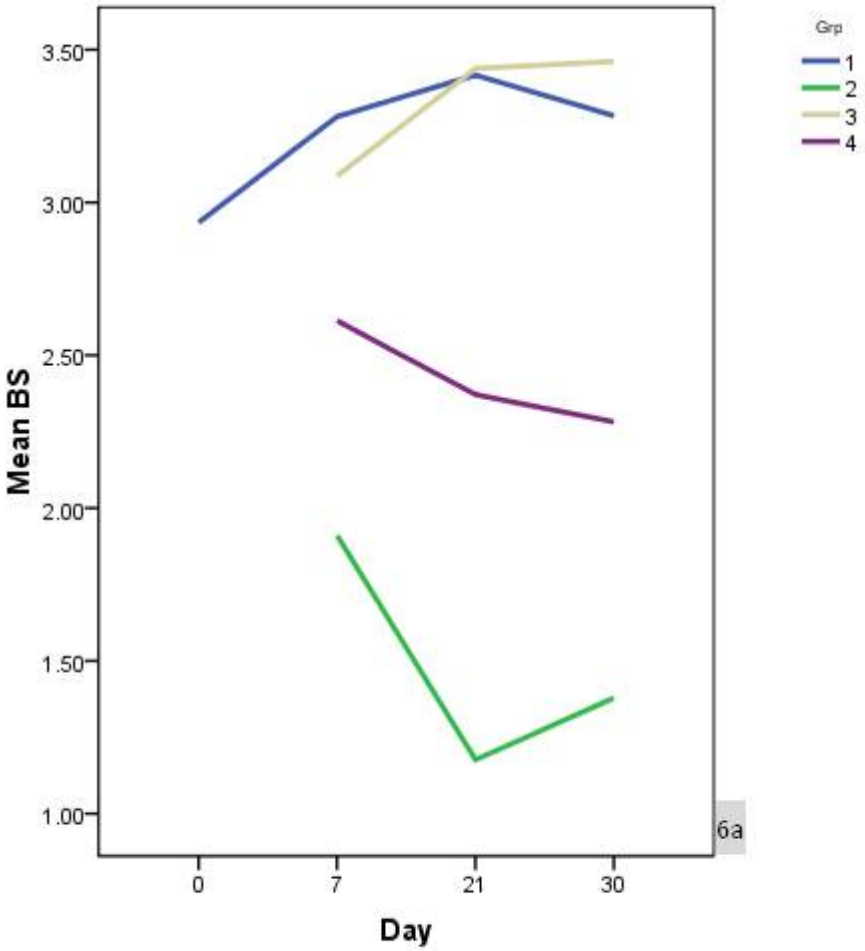

Box plot of univariate ANOVA for bone surface

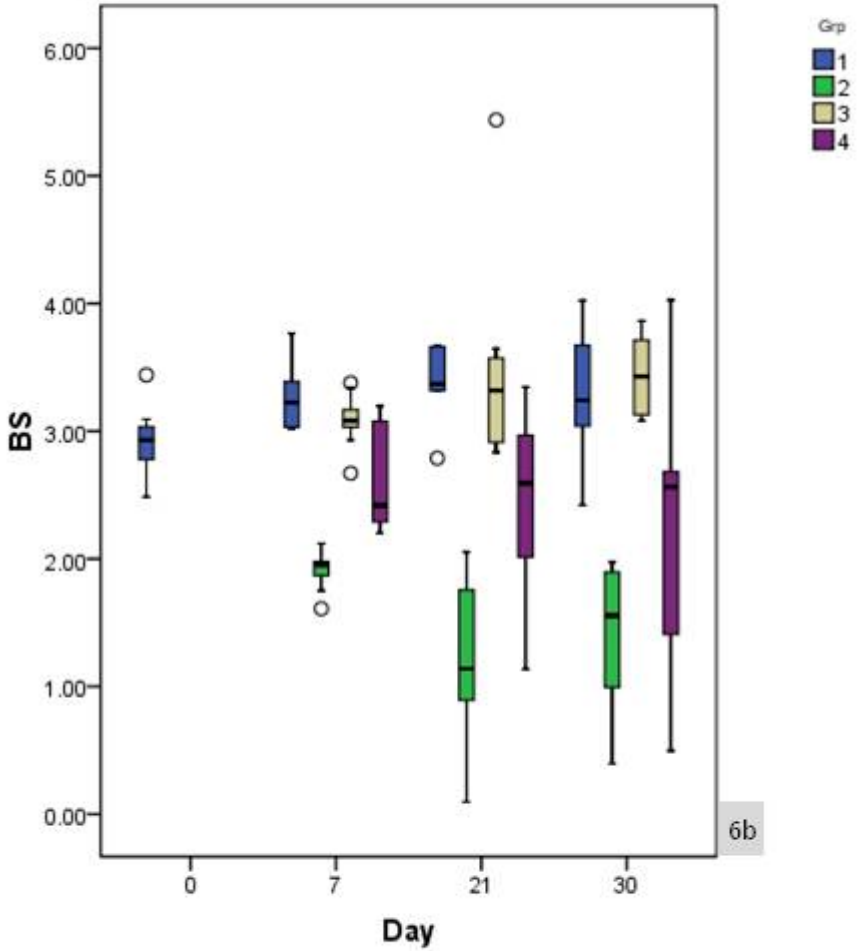

Post-hoc comparisons of changes in bone surface between time points for each group

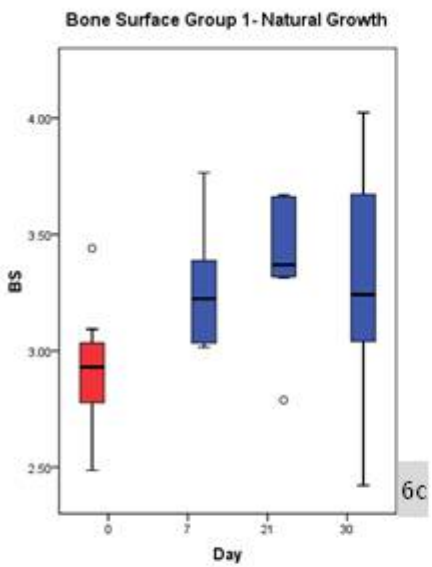

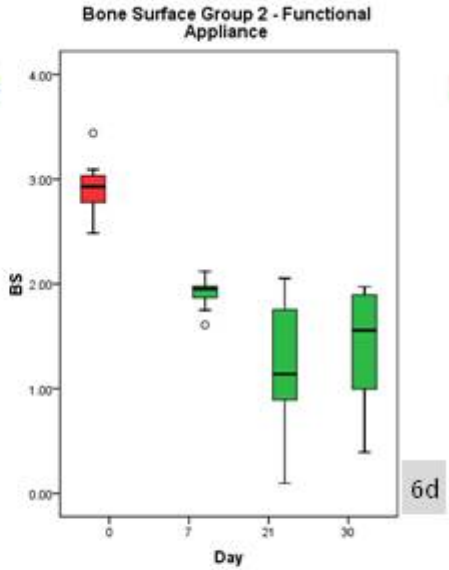

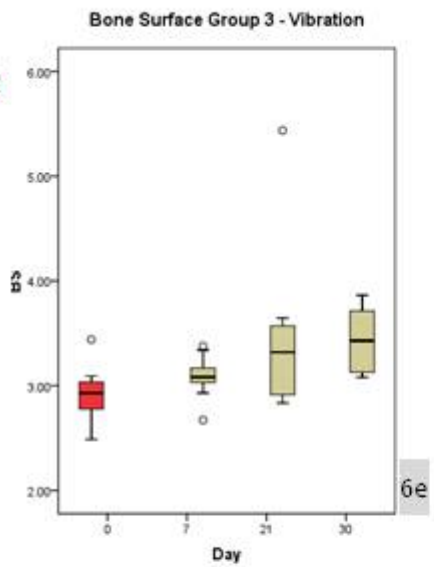

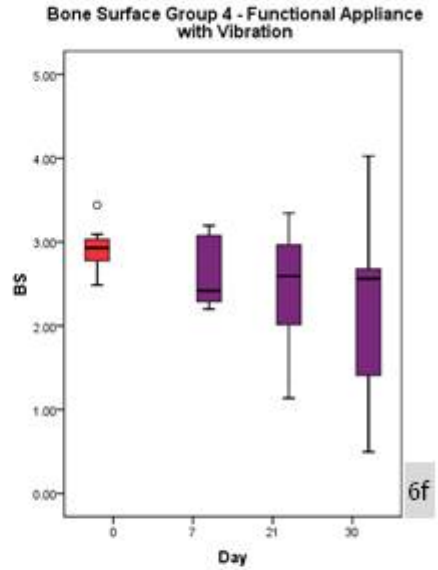

Post-hoc comparisons of changes in bone surface between groups at each time point

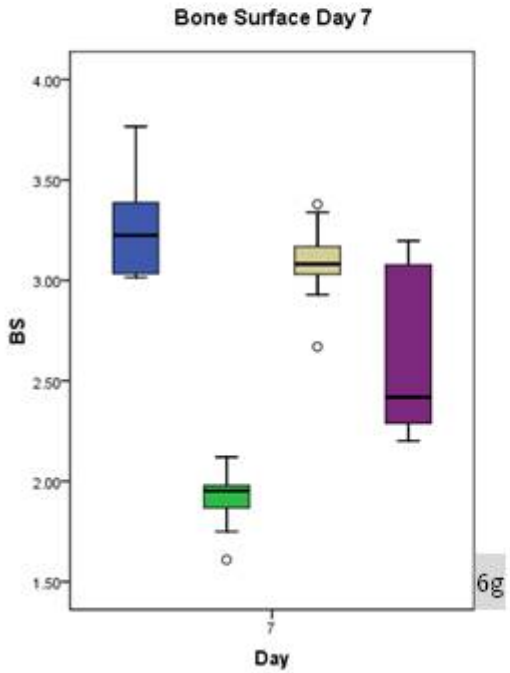

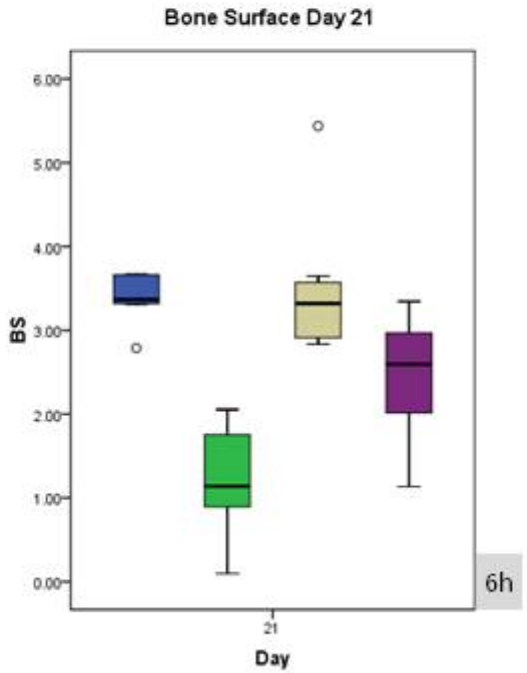

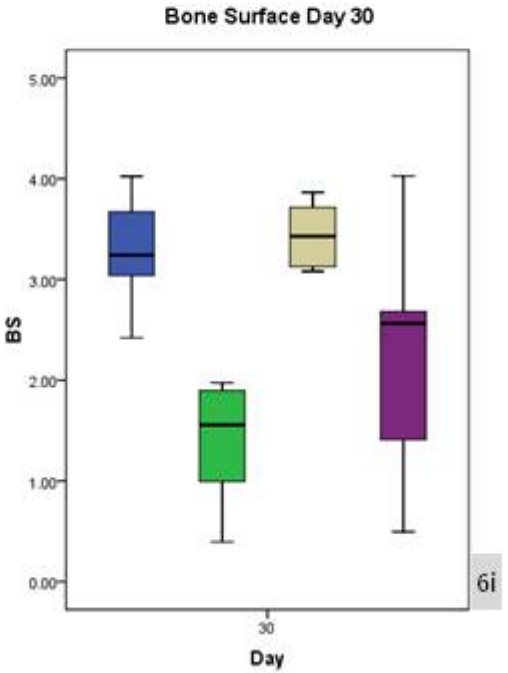

Table 7 Graphs for Bone Surface to Bone Volume ratio (BS/BV mm^{-1})

Line-graph of mean bone surface to volume ratio

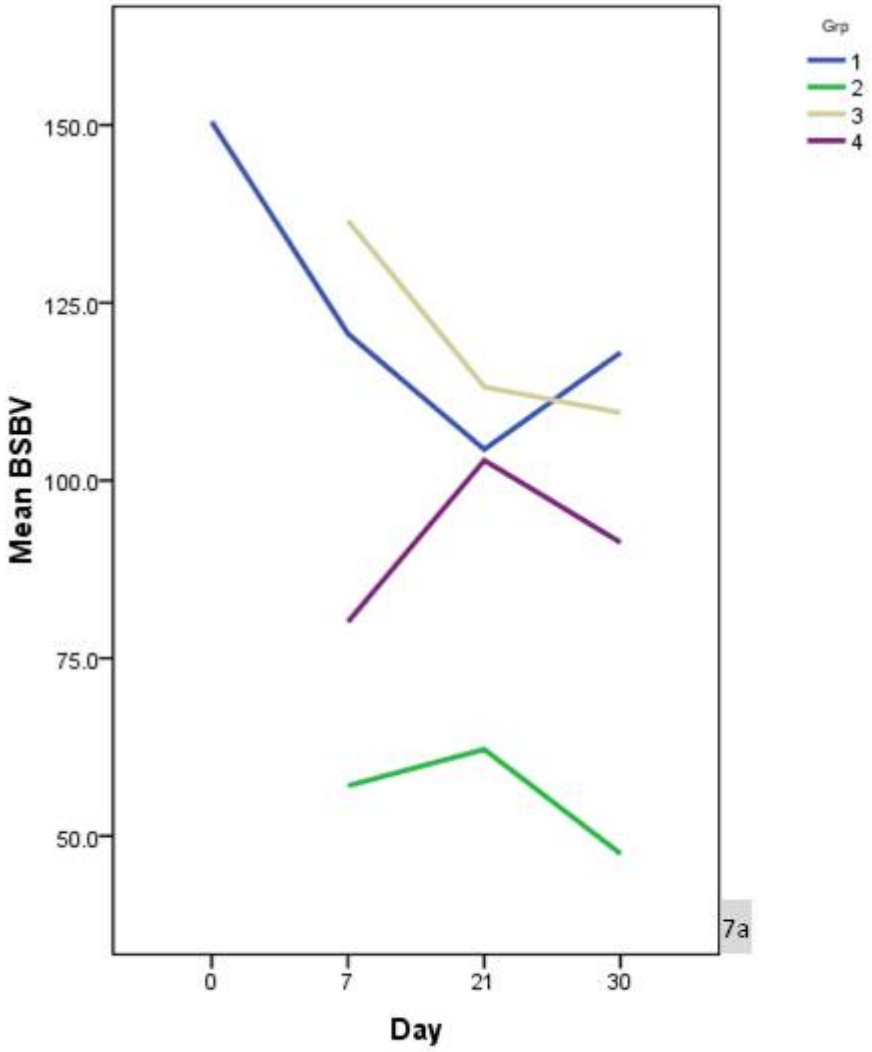

Box plot of univariate ANOVA for bone surface to bone volume ratio

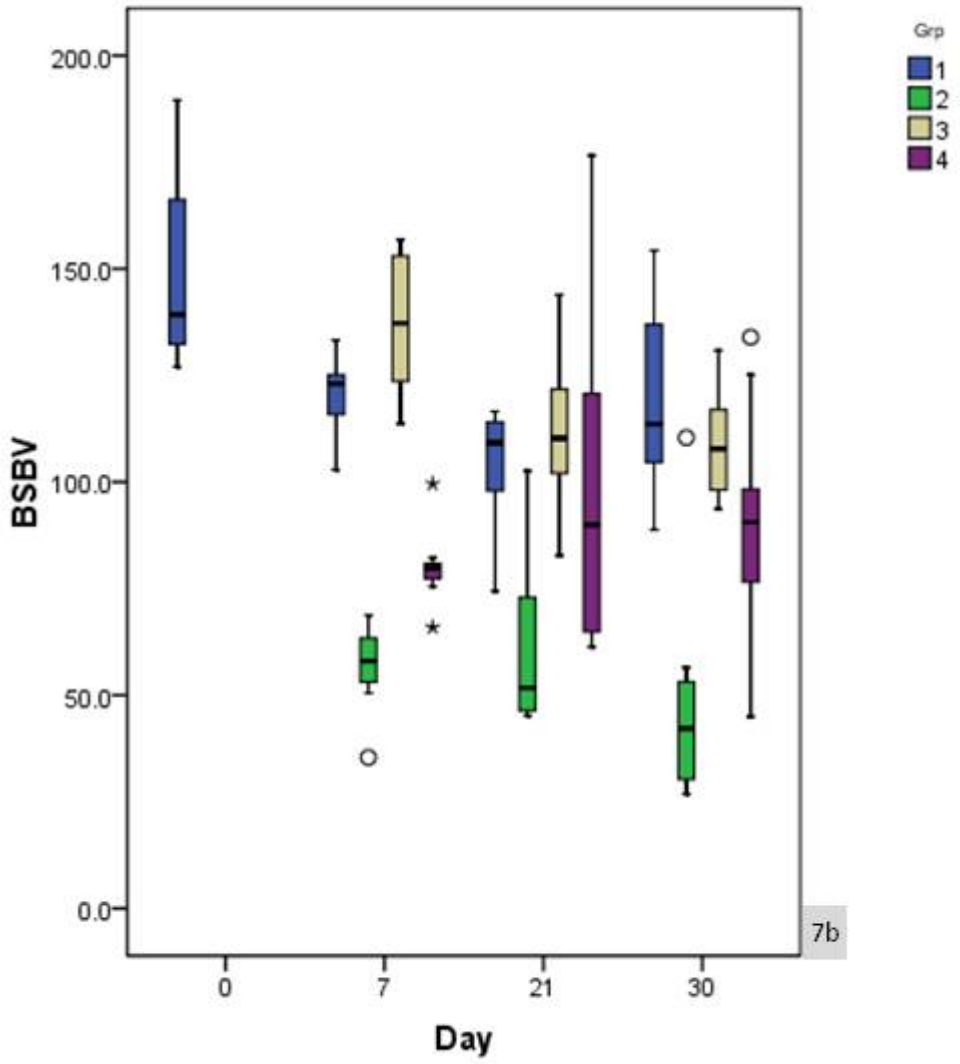

Post-hoc comparisons of changes in bone surface to bone volume ratio between time points for each group

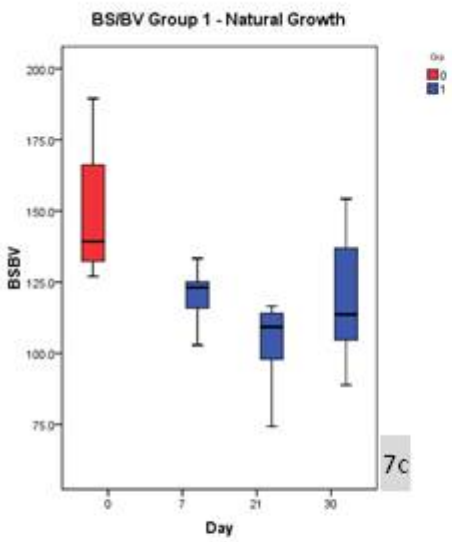

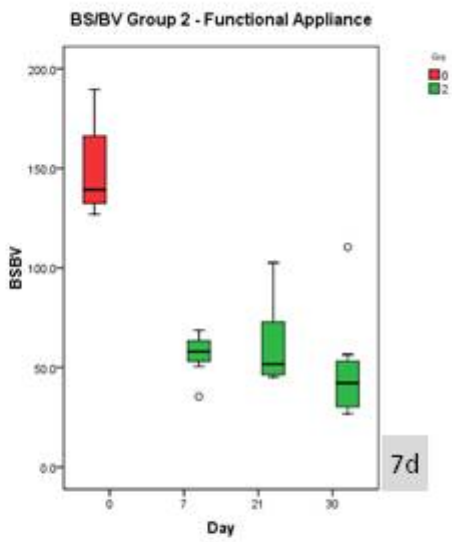

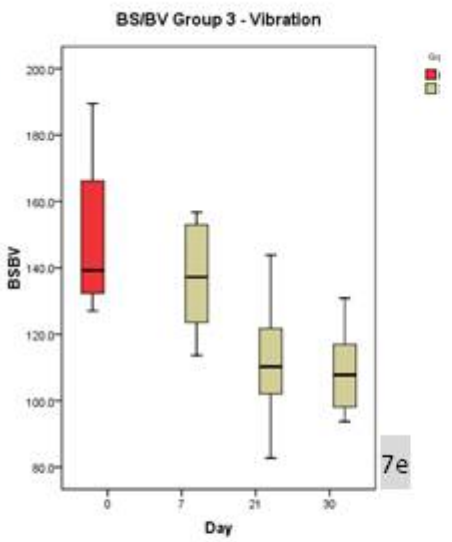

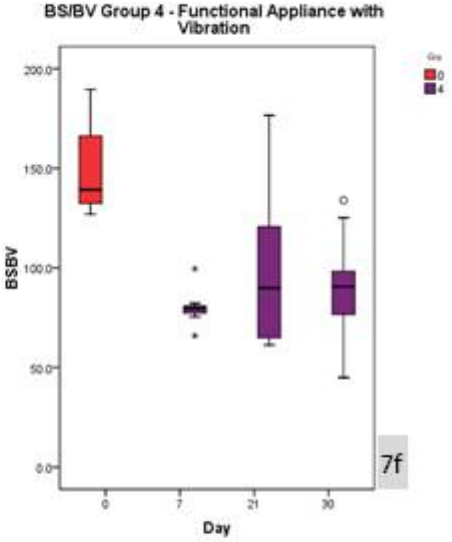

Post-hoc comparisons of changes in bone surface to bone volume ratio between groups at each time point

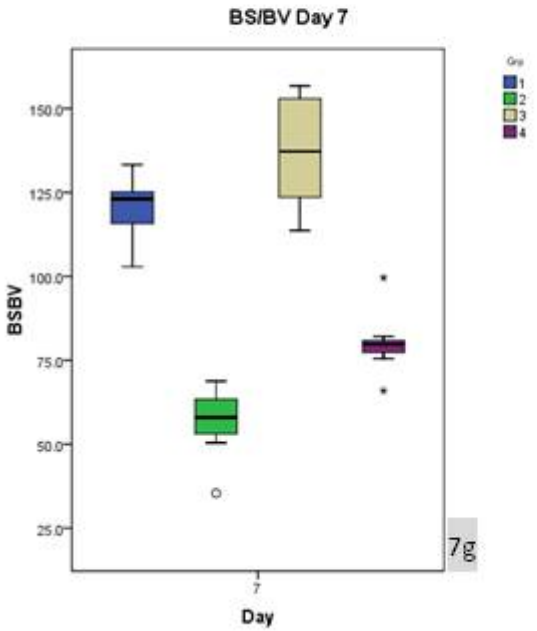

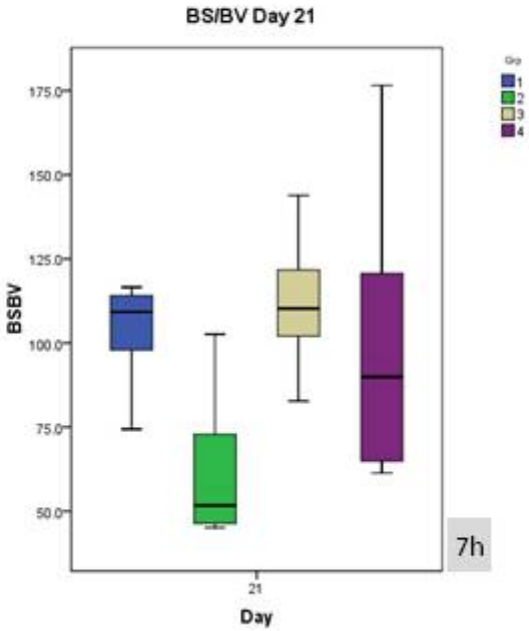

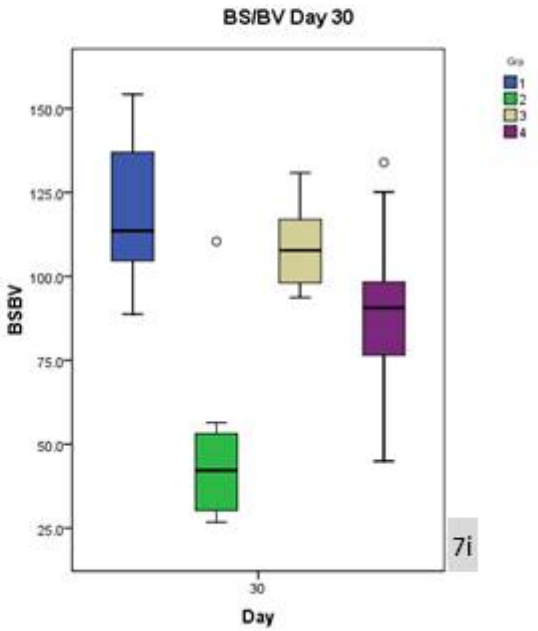

Table 8 Graphs for Bone Surface density (BS/TV mm^{-1})

Line-graph of mean bone surface density

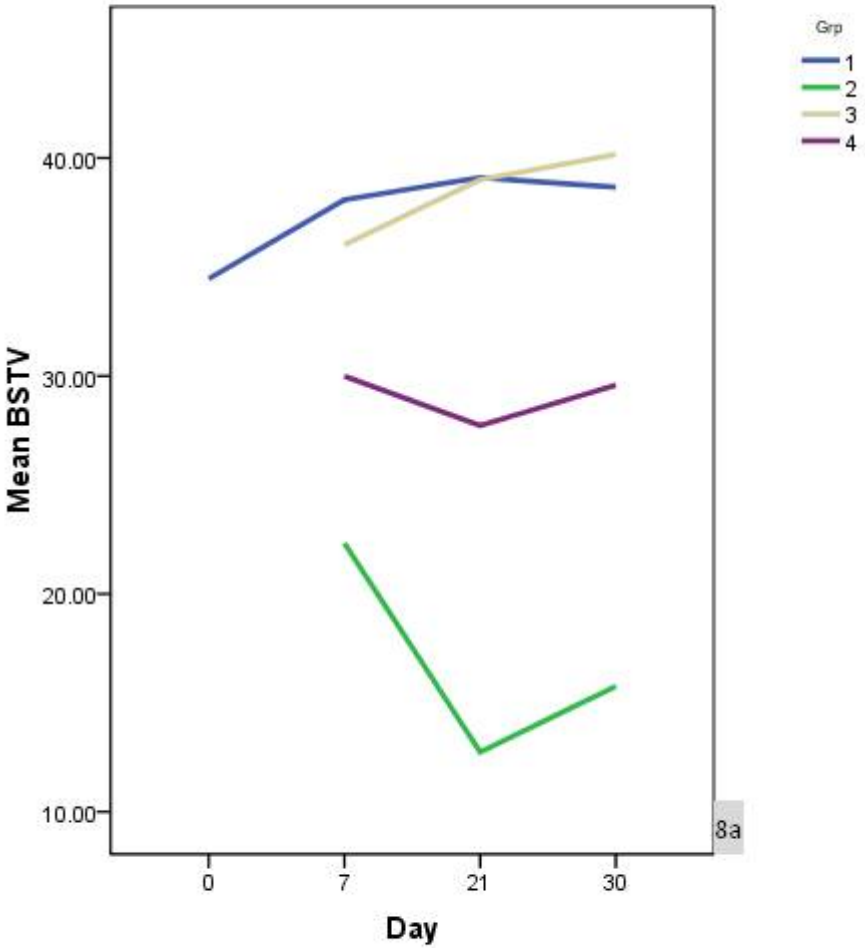

Box plot of univariate ANOVA for bone surface density

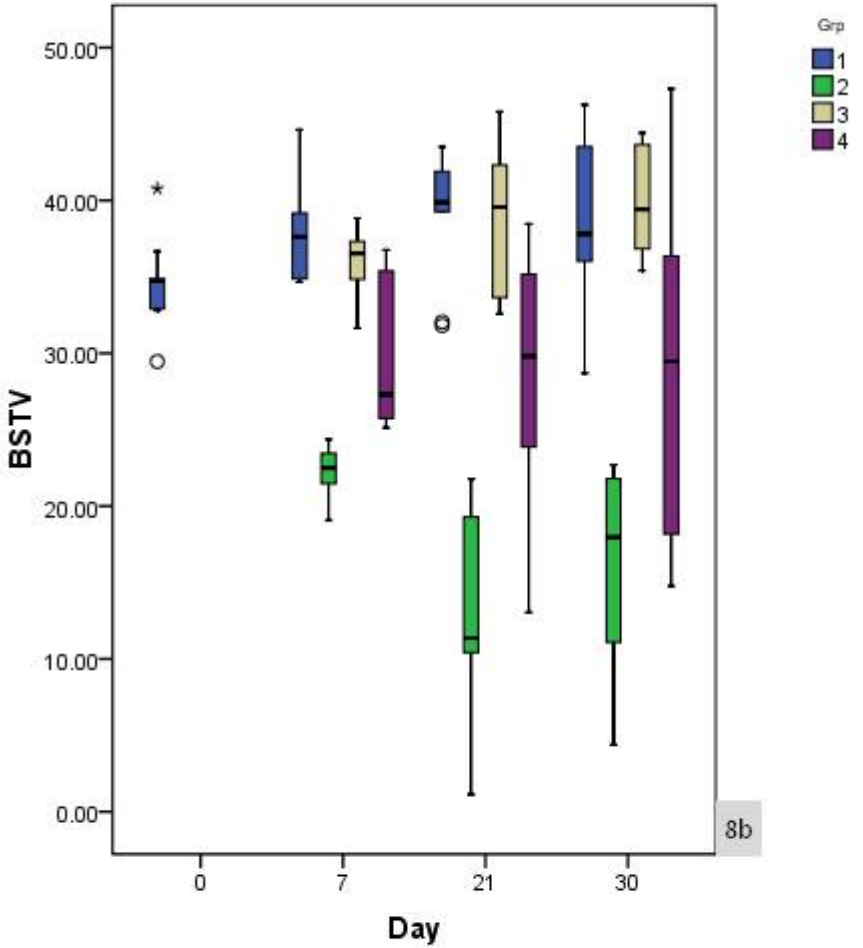

Post-hoc comparisons of changes in bone surface density between time points for each group

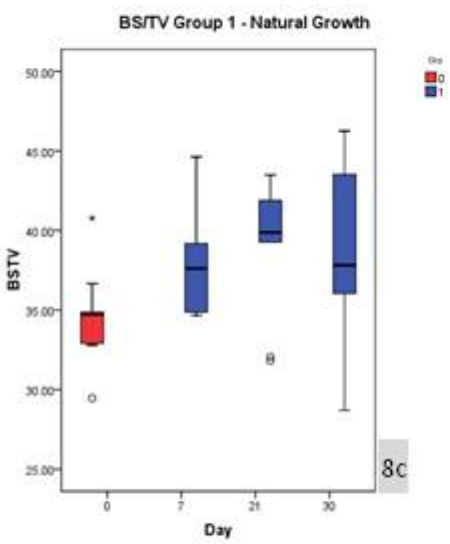

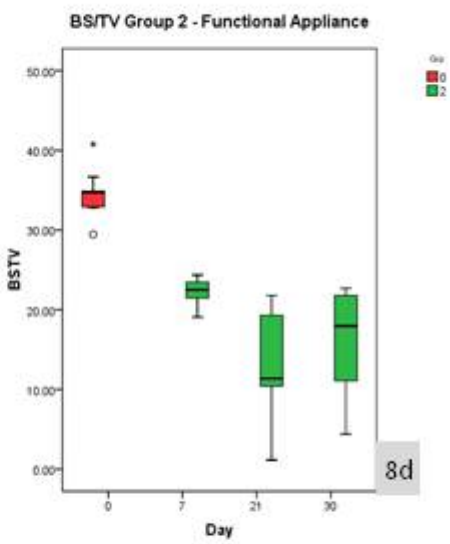

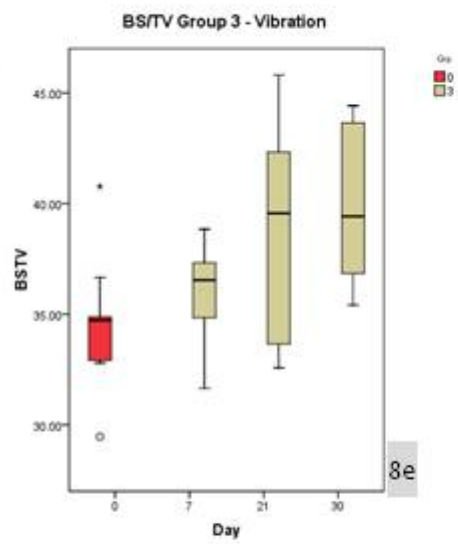

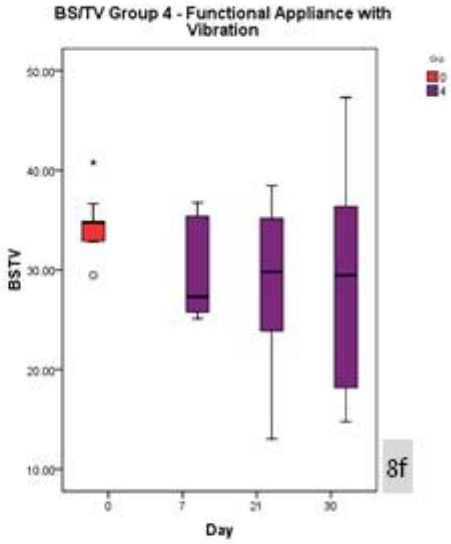

Post-hoc comparisons of changes in bone surface density between groups at each time point

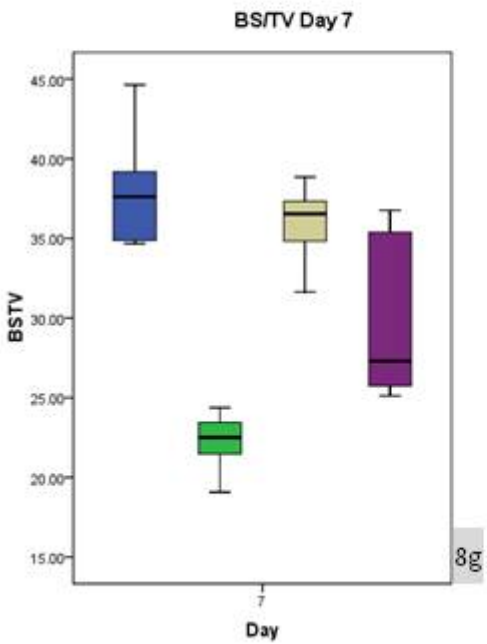

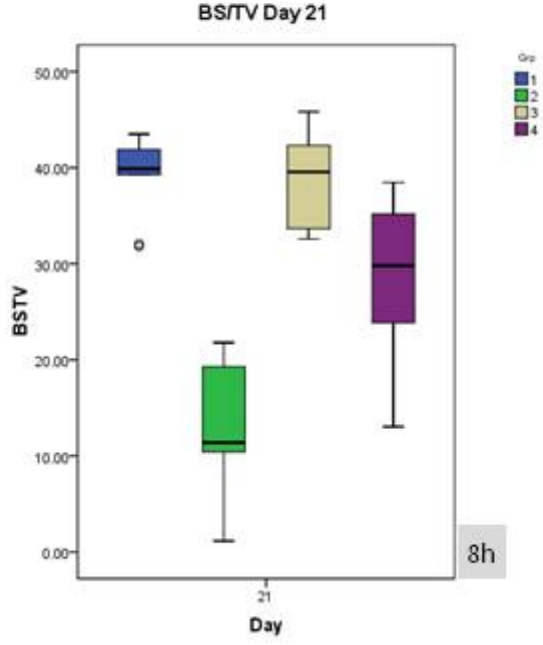

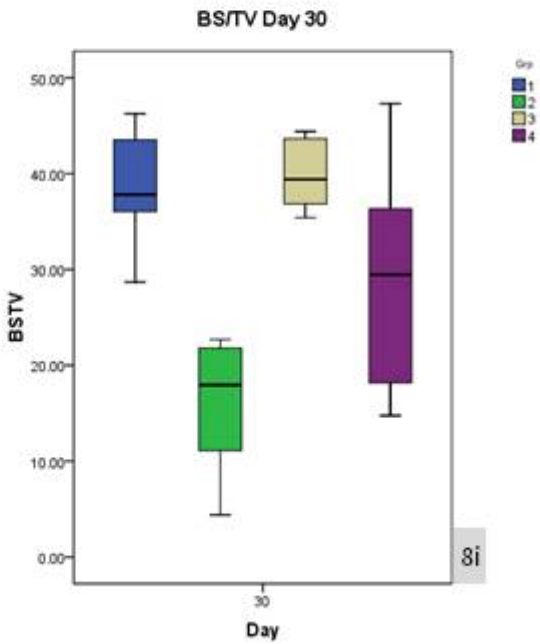

Table 9 Graphs for Trabecular Bone Pattern Factor (Tb.Pf mm^{-1})

Line-graph of mean trabecular bone pattern factor

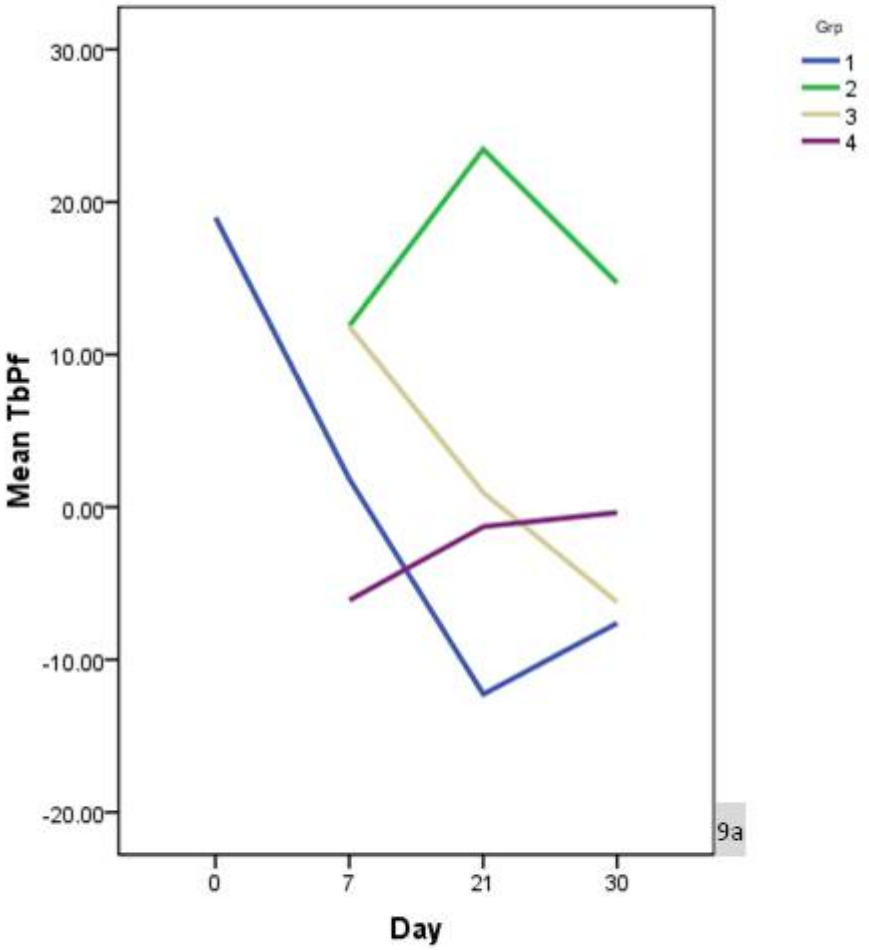

9a

Box plot of univariate ANOVA for mean trabecular bone pattern factor

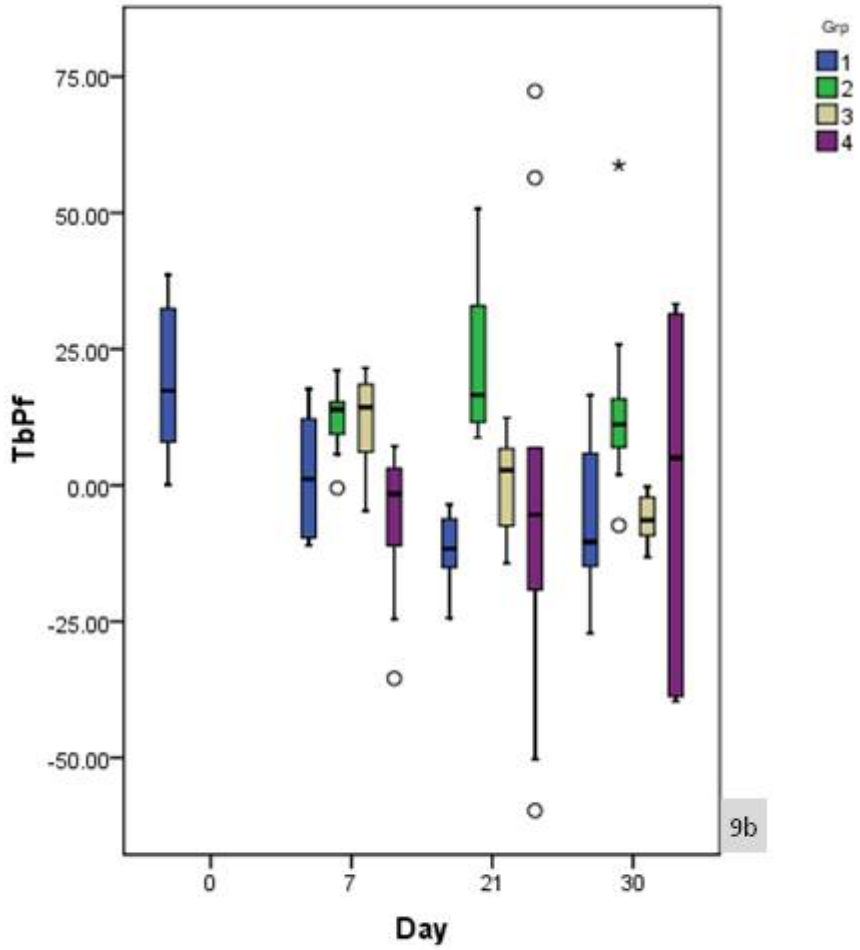

9b

Post-hoc comparisons of changes in trabecular bone pattern factor between time points for each group

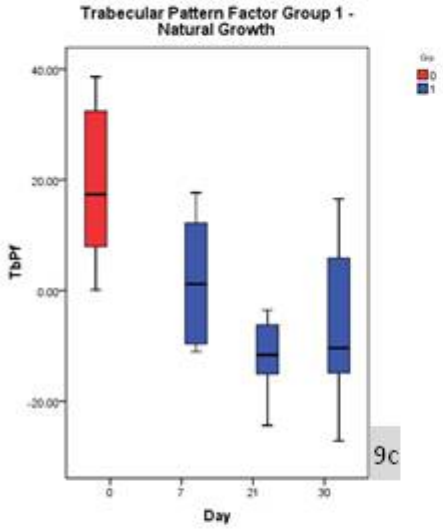

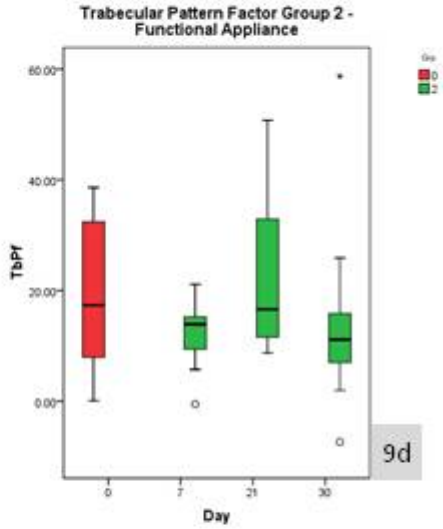

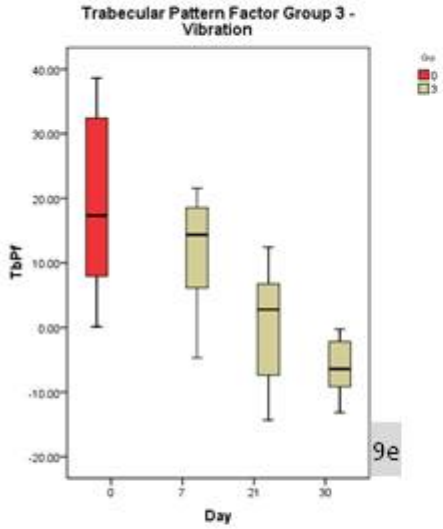

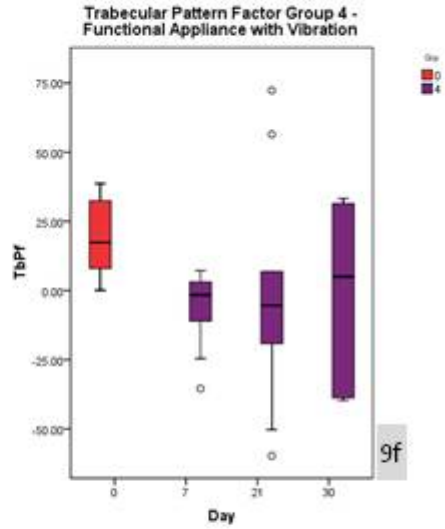

Post-hoc comparisons of changes in trabecular bone pattern factor between groups at each time point

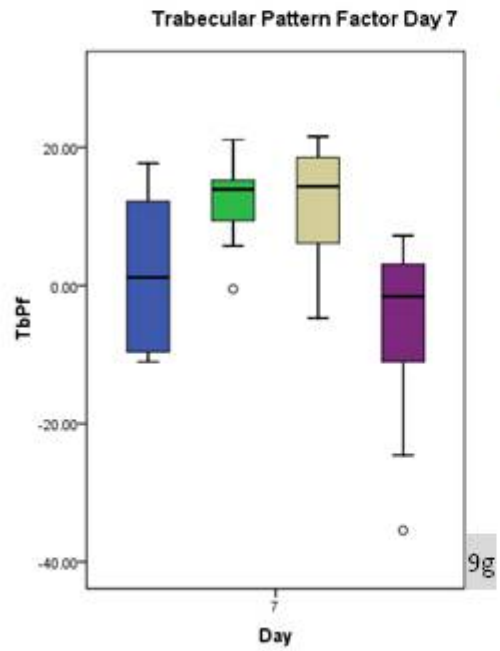

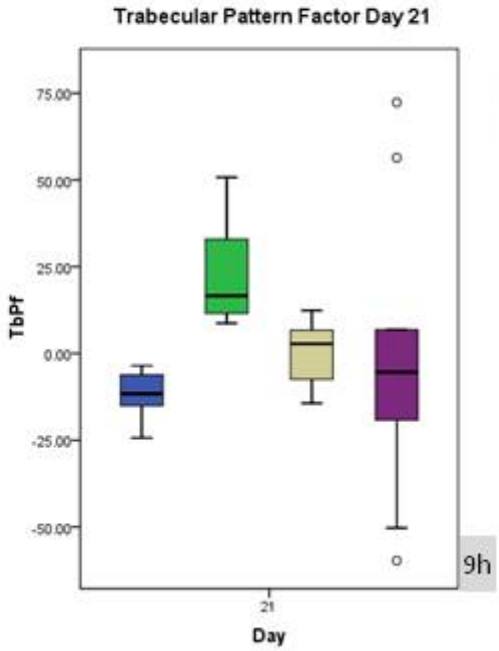

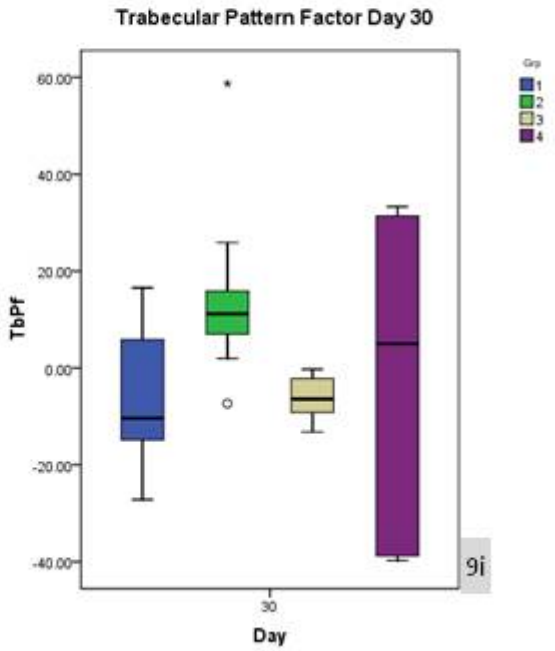

Table 10 Graphs for Structure Model Index (SMI)

Line-graph of mean structure model index

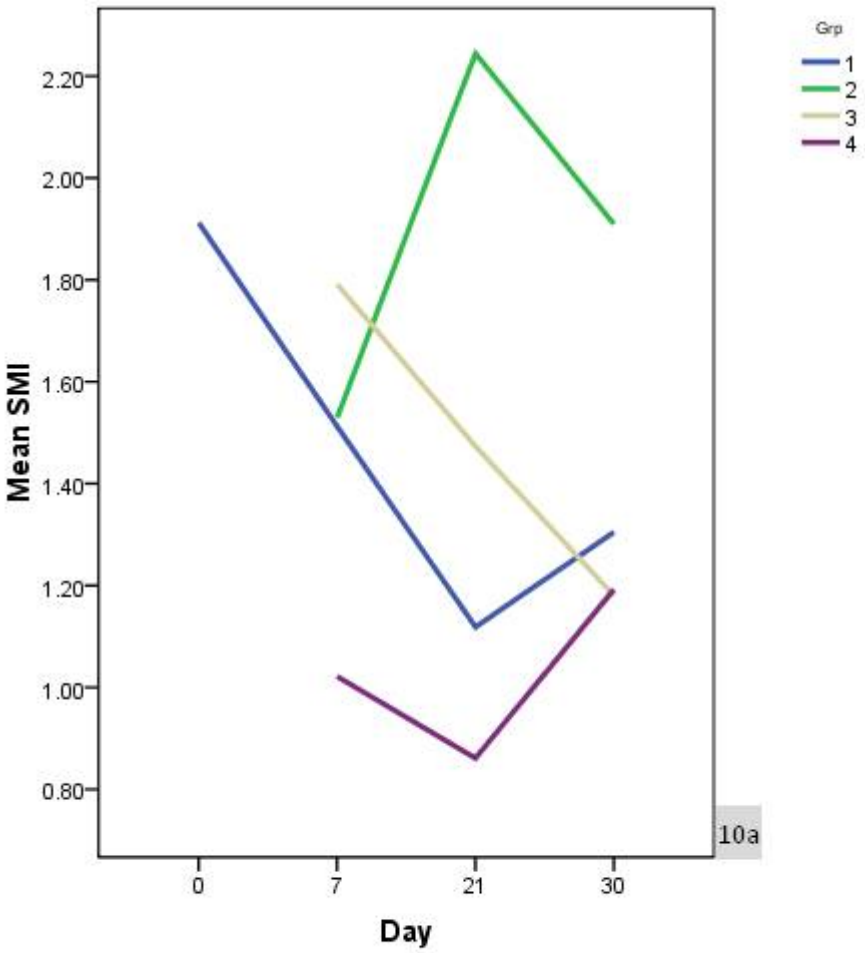

10a

Box plot of univariate ANOVA for structure model index

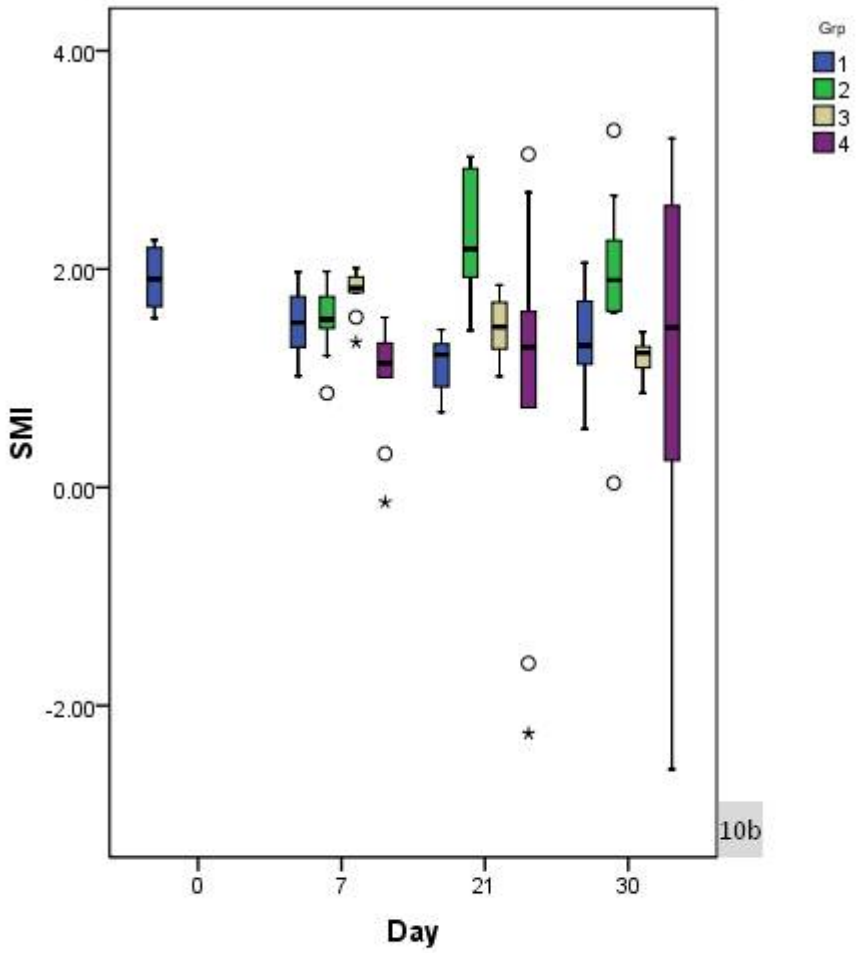

10b

Post-hoc comparisons of changes in structure model index between time points for each group

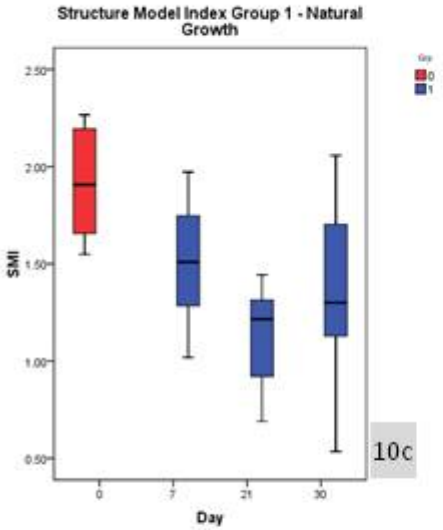

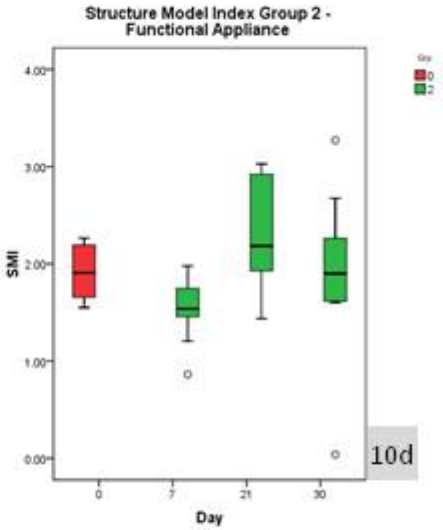

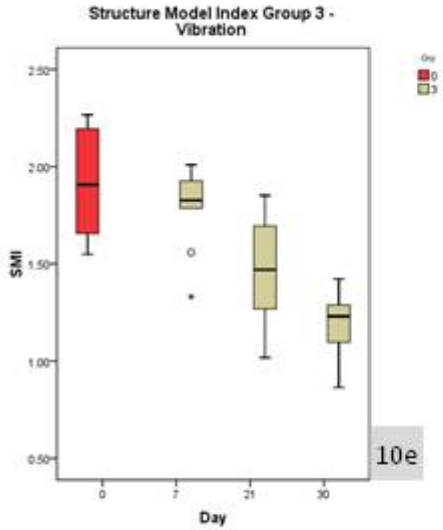

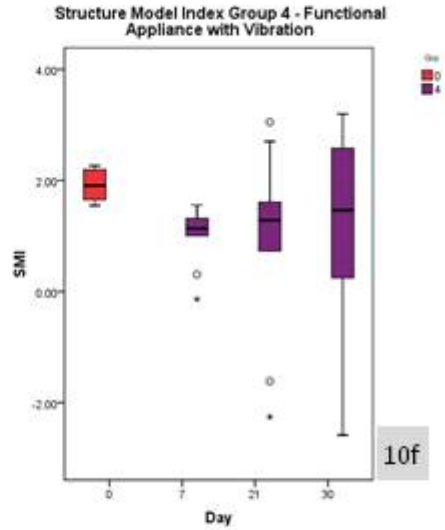

Post-hoc comparisons of changes in structure model index between groups at each time point

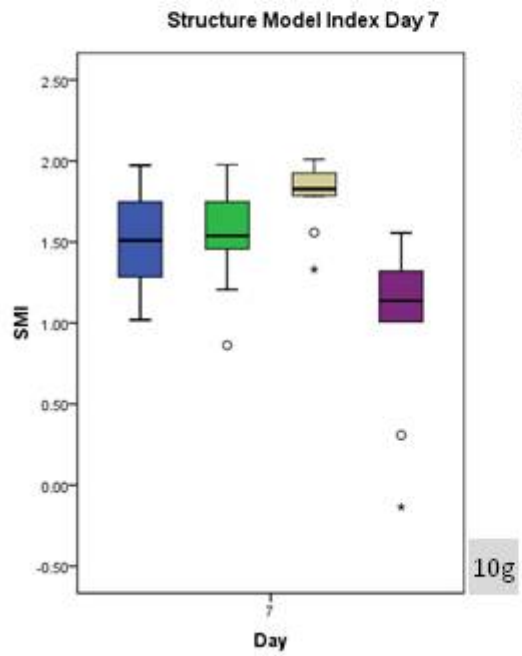

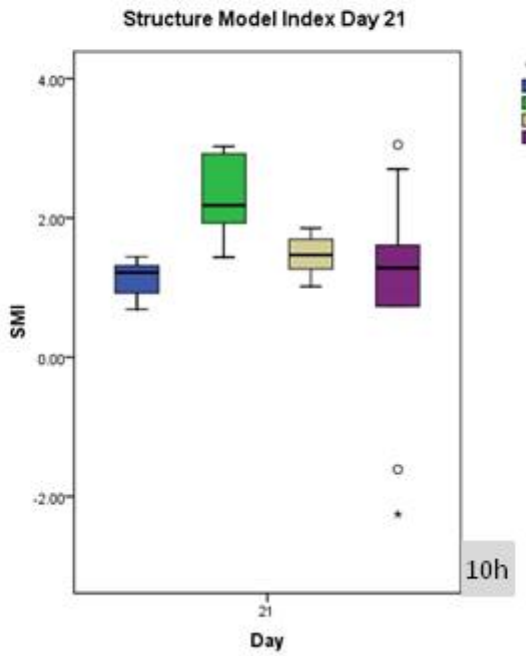

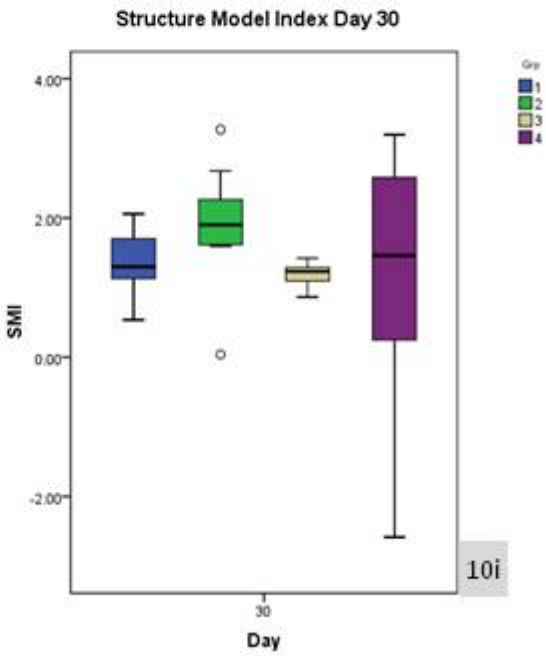

Table 11 Graphs for Trabecular Thickness (Tb.Th mm)

Line-graph of mean trabecular thickness

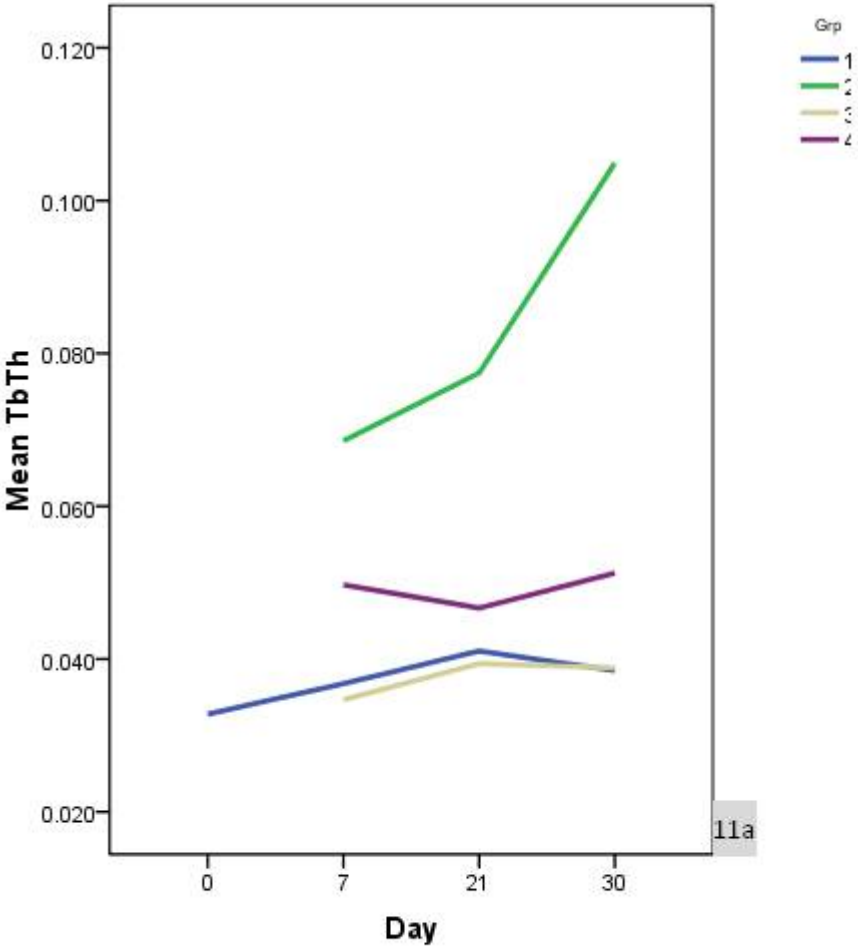

Box plot of univariate ANOVA for trabecular thickness

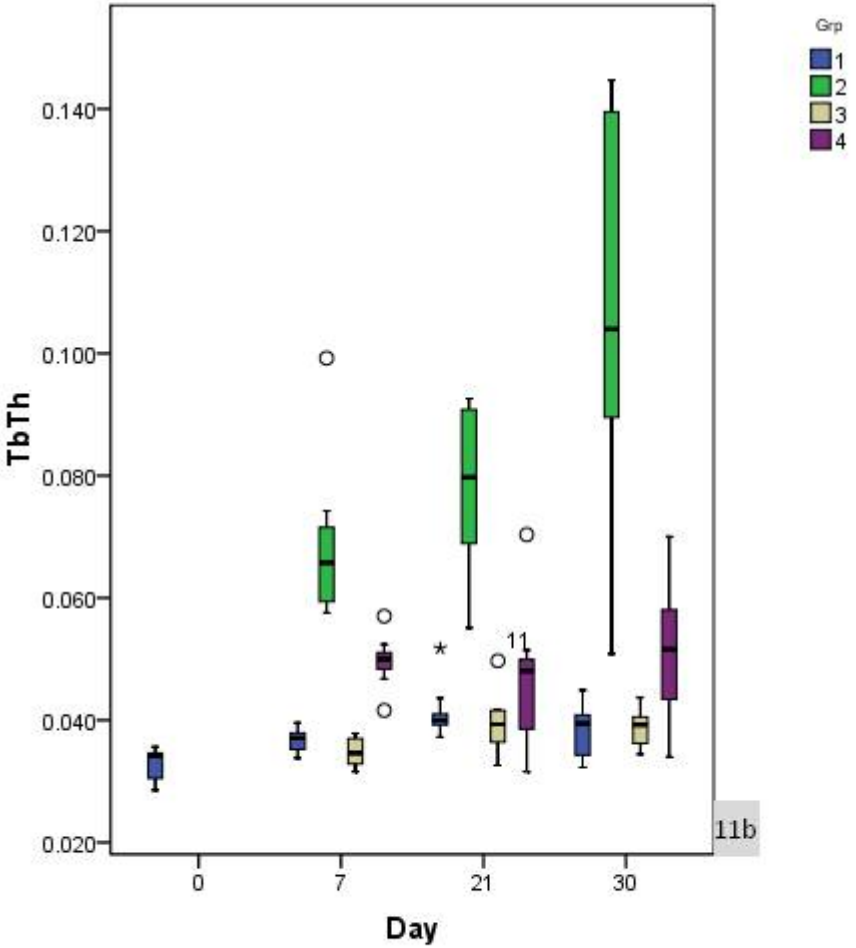

Post-hoc comparisons of changes in trabecular thickness between time points for each group

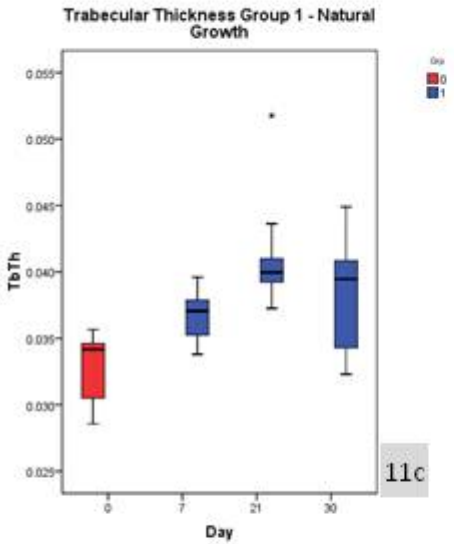

11c

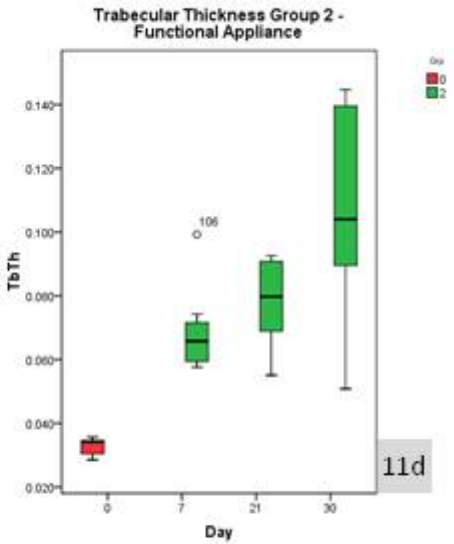

11d

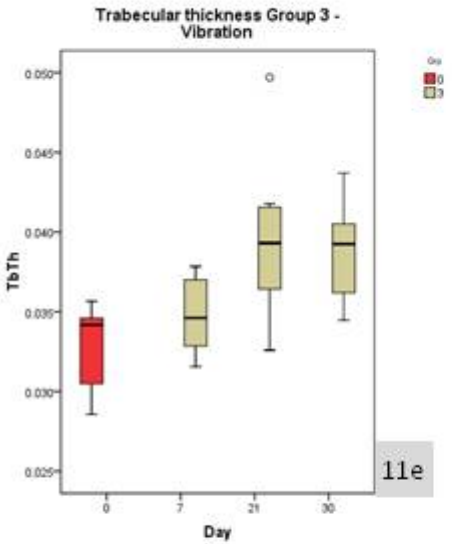

11e

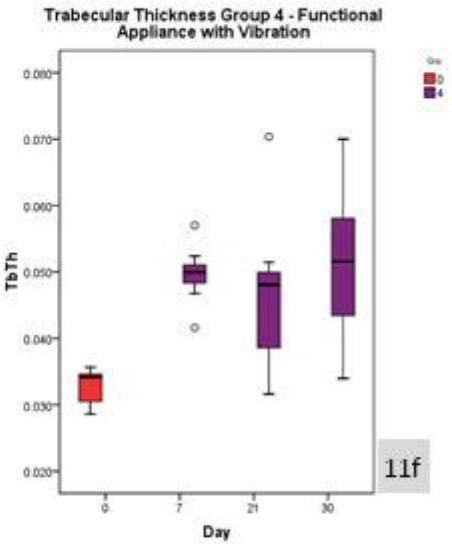

11f

Post-hoc comparisons of changes in trabecular thickness between groups at each time point

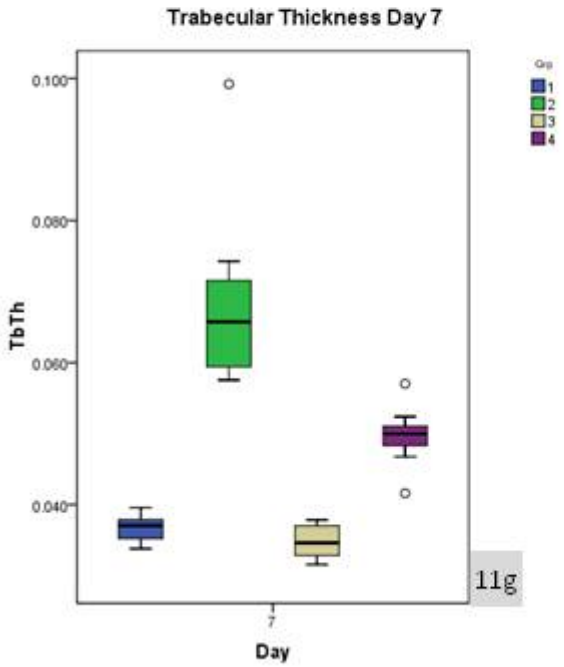

11g

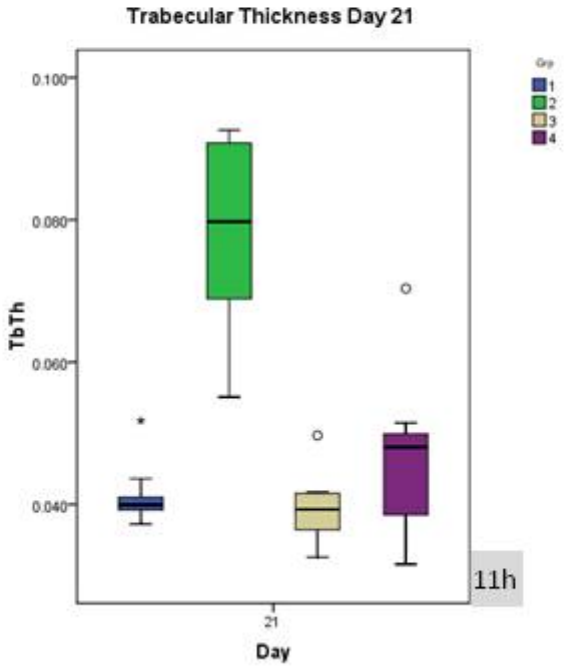

11h

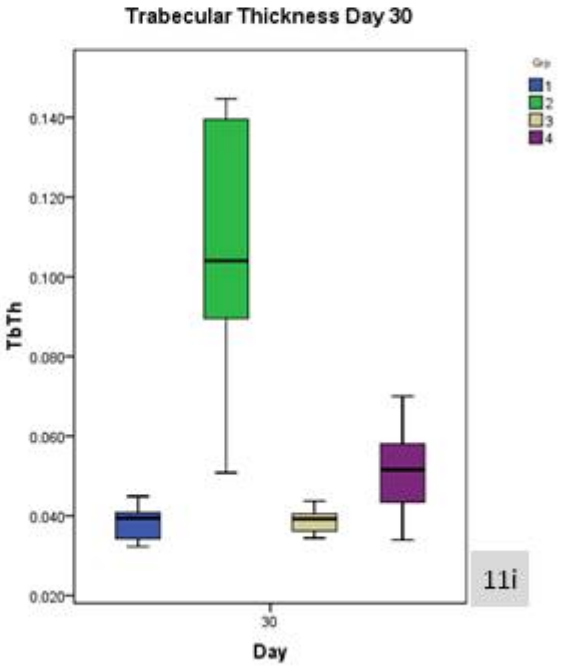

11i

Table 12 Graphs for Trabecular Number (Tb.N mm^{-1})

Line-graph of mean trabecular number

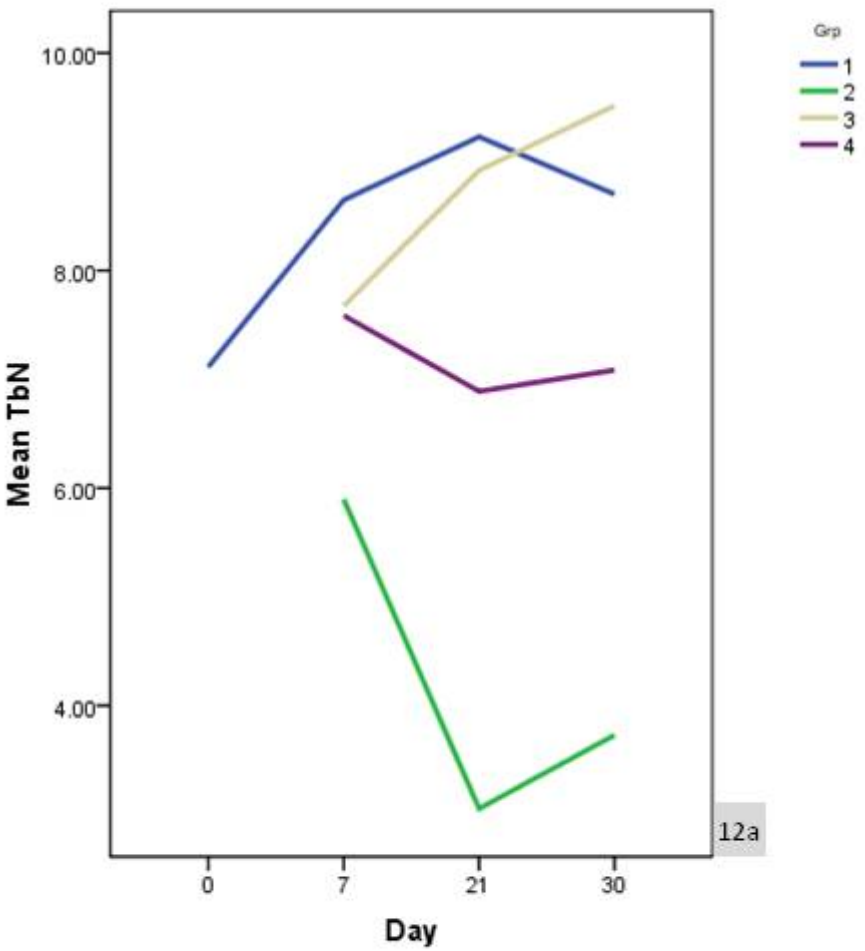

12a

Box plot of univariate ANOVA trabecular number

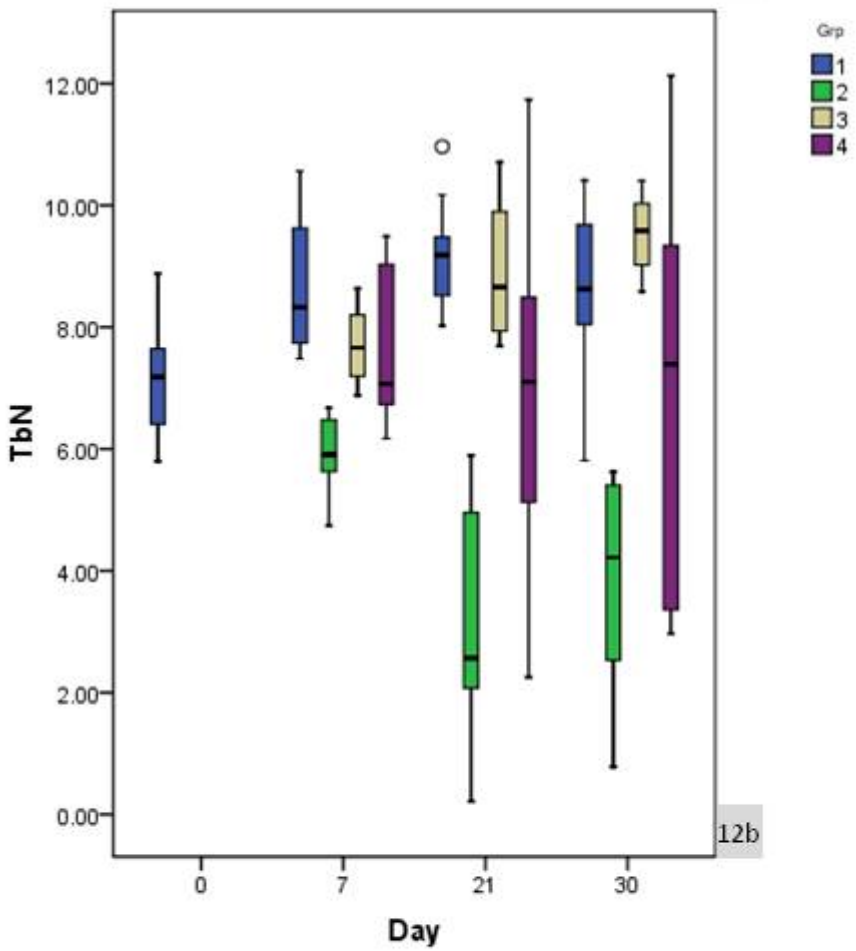

12b

Post-hoc comparisons of changes in trabecular number between time points for each group

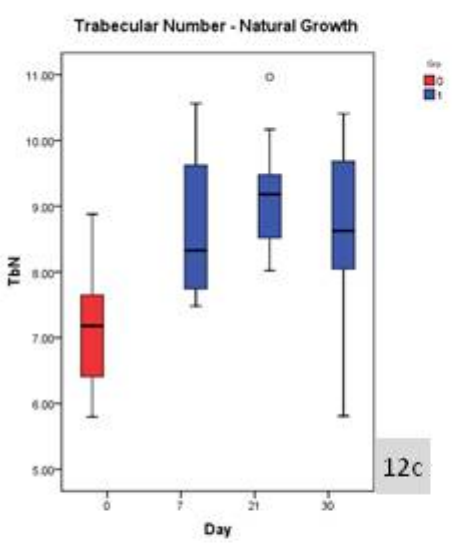

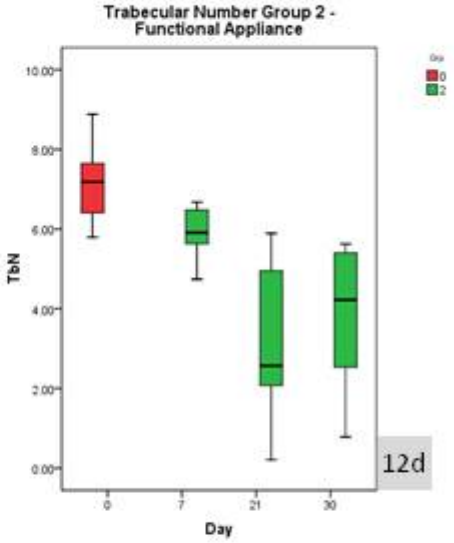

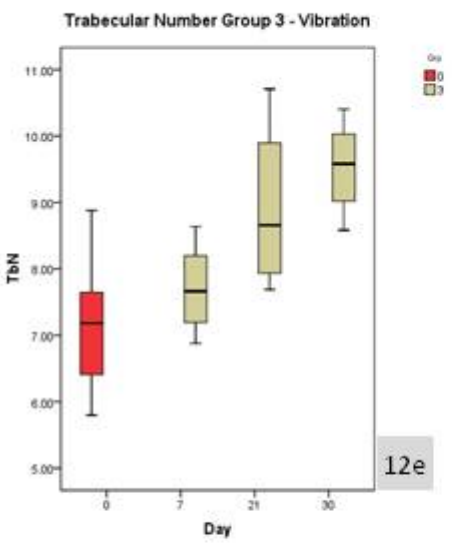

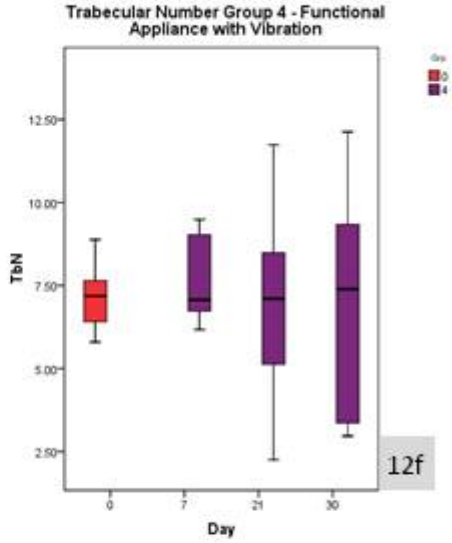

Post-hoc comparisons of changes in trabecular number between groups at each time point

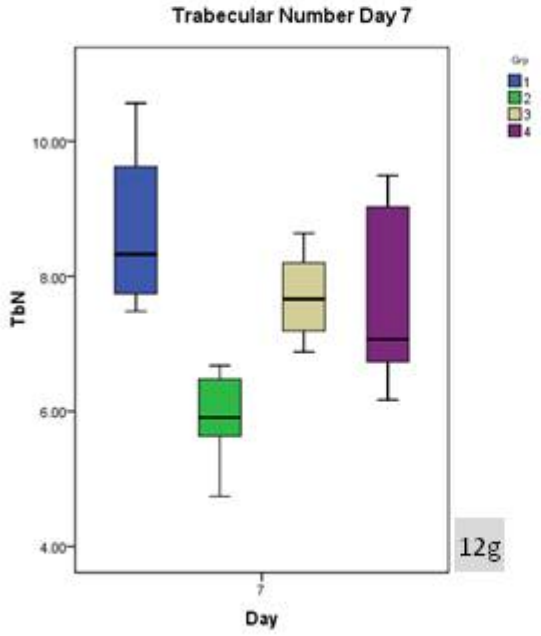

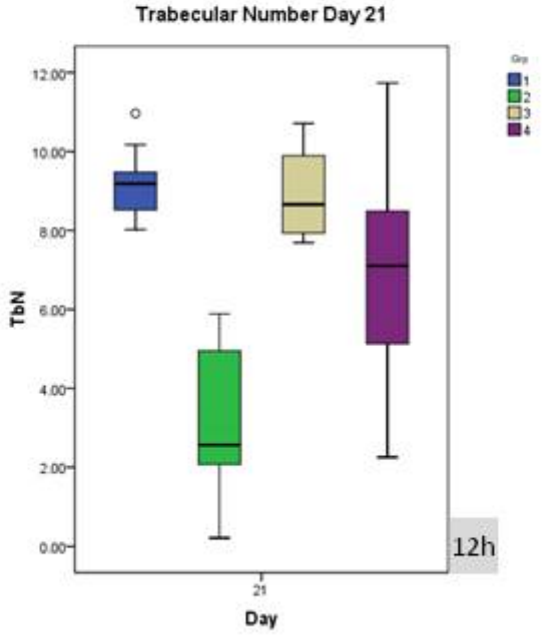

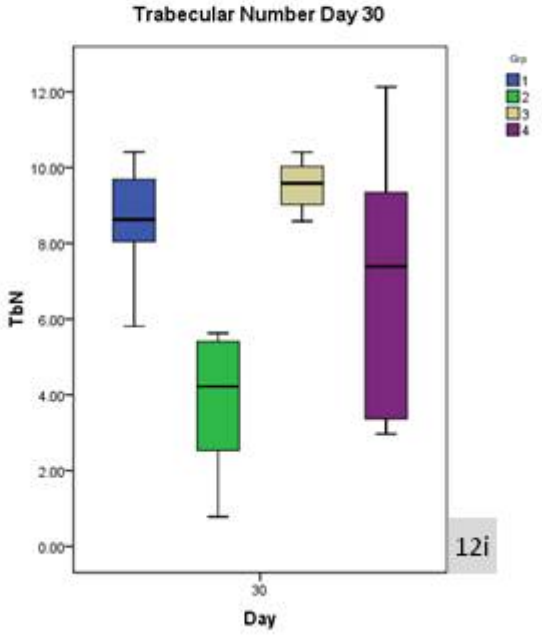

Table 13 Graphs for Trabecular Separation (Tb.Sp mm)

Line-graph of mean trabecular separation

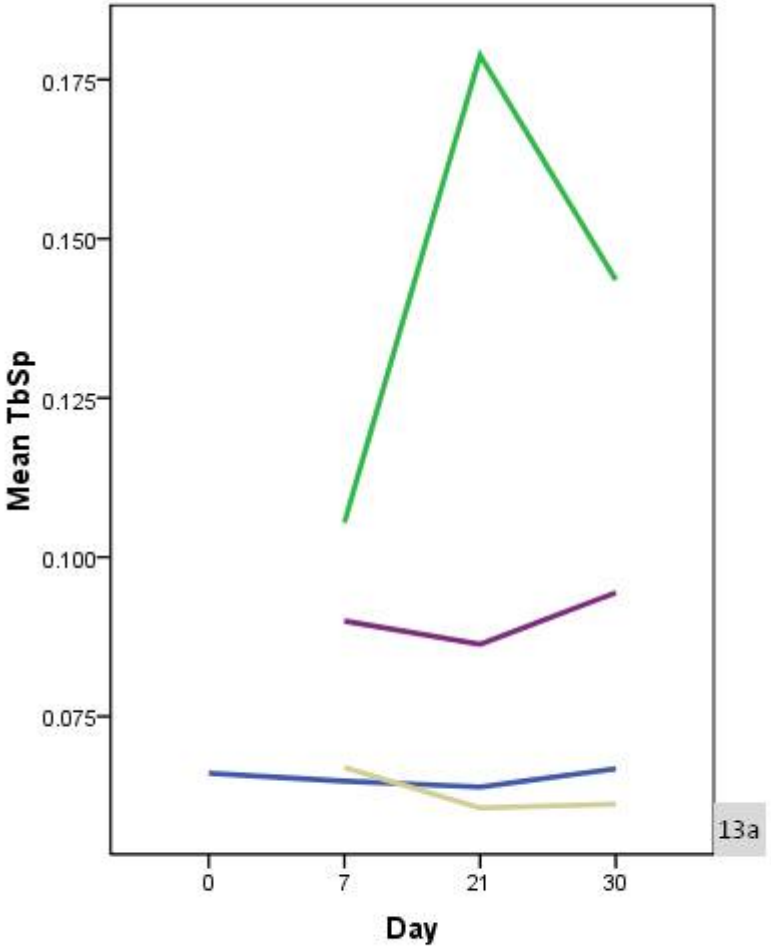

Box plot of univariate ANOVA for trabecular separation

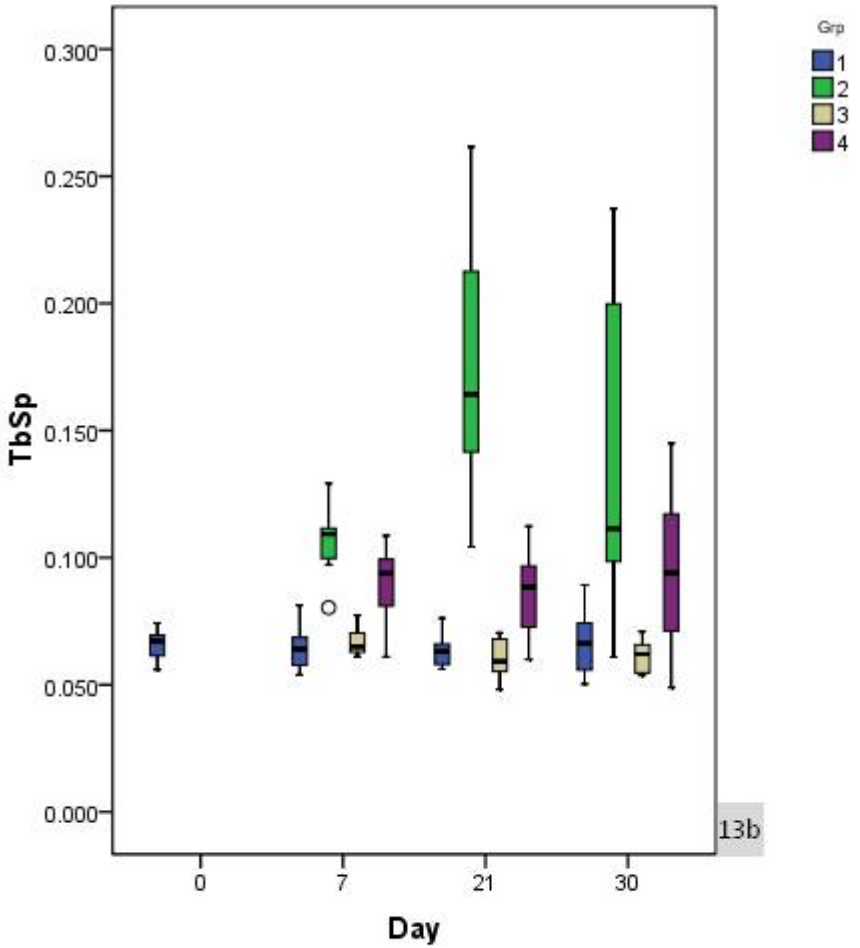

Post-hoc comparisons of changes in trabecular separation between time points for each group

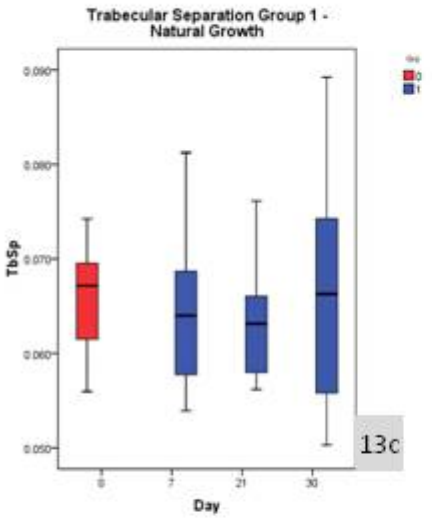

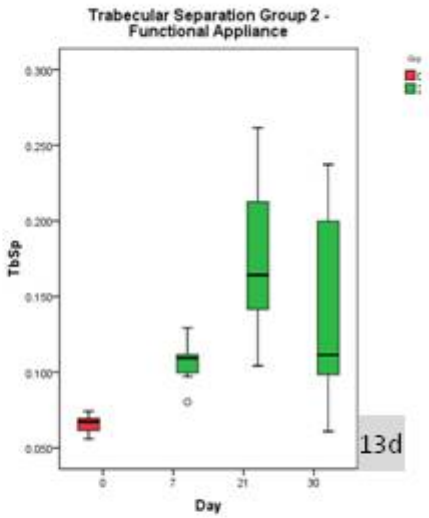

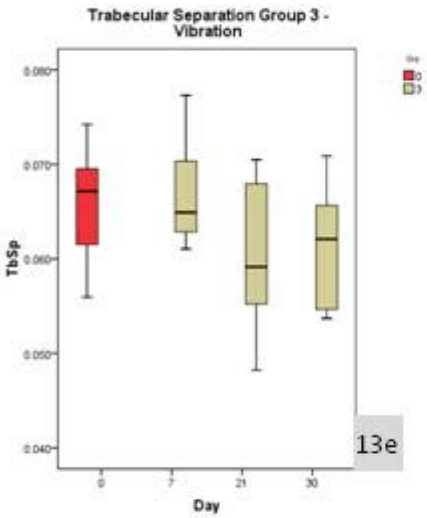

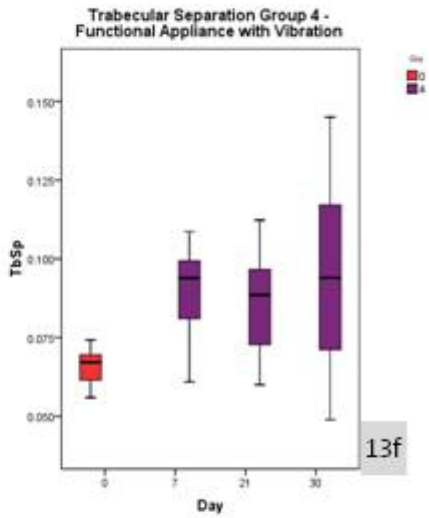

Post-hoc comparisons of changes in trabecular separation between groups at each time point

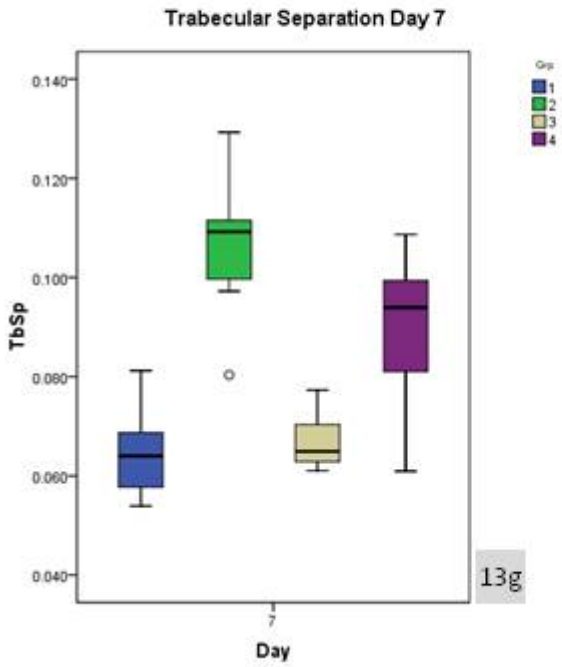

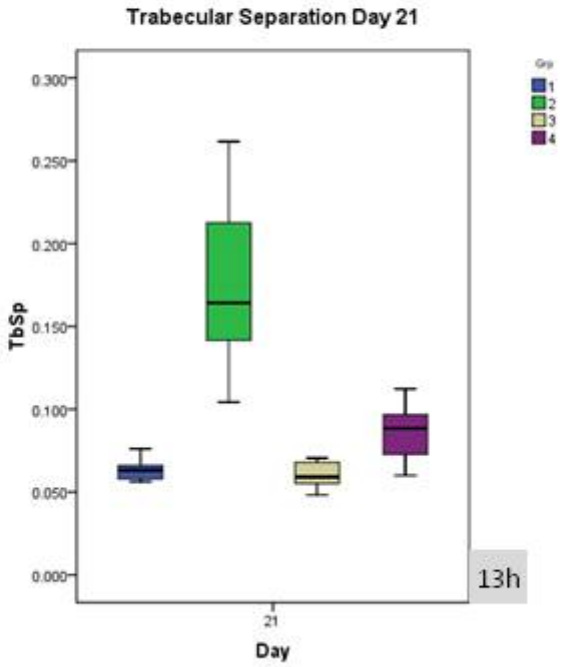

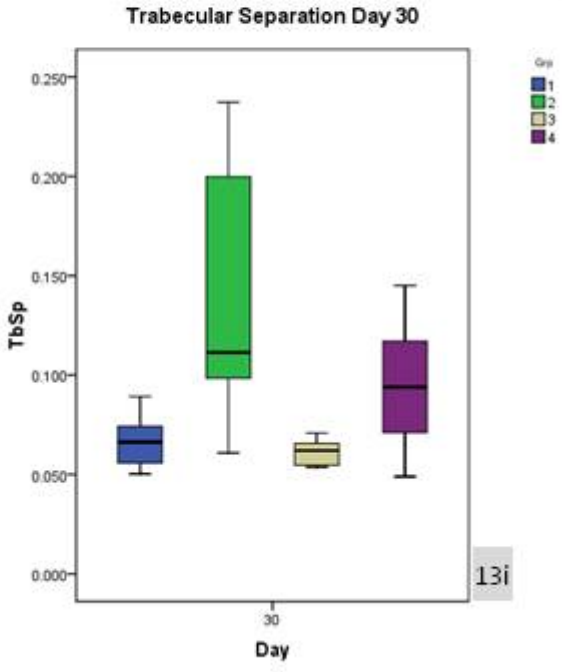

19 Appendix One Literature Review

19.1 Appendix 1a

Histological section of mandibular condylar cartilage. (Adopted from Shen and Darendeliler 2005[1])

19.2

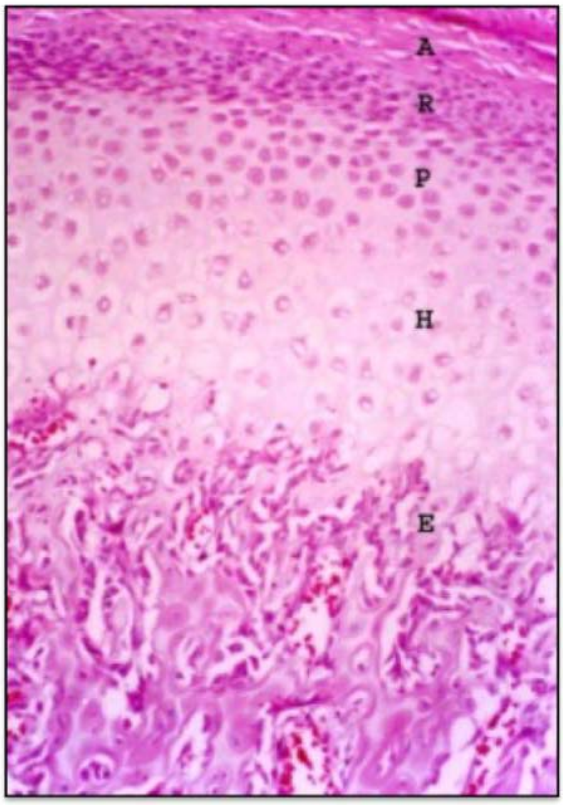

Appendix 1b

Flow-chart of appositional endochondral ossification and the growth factors involved during normal growth and mandibular anterior positioning

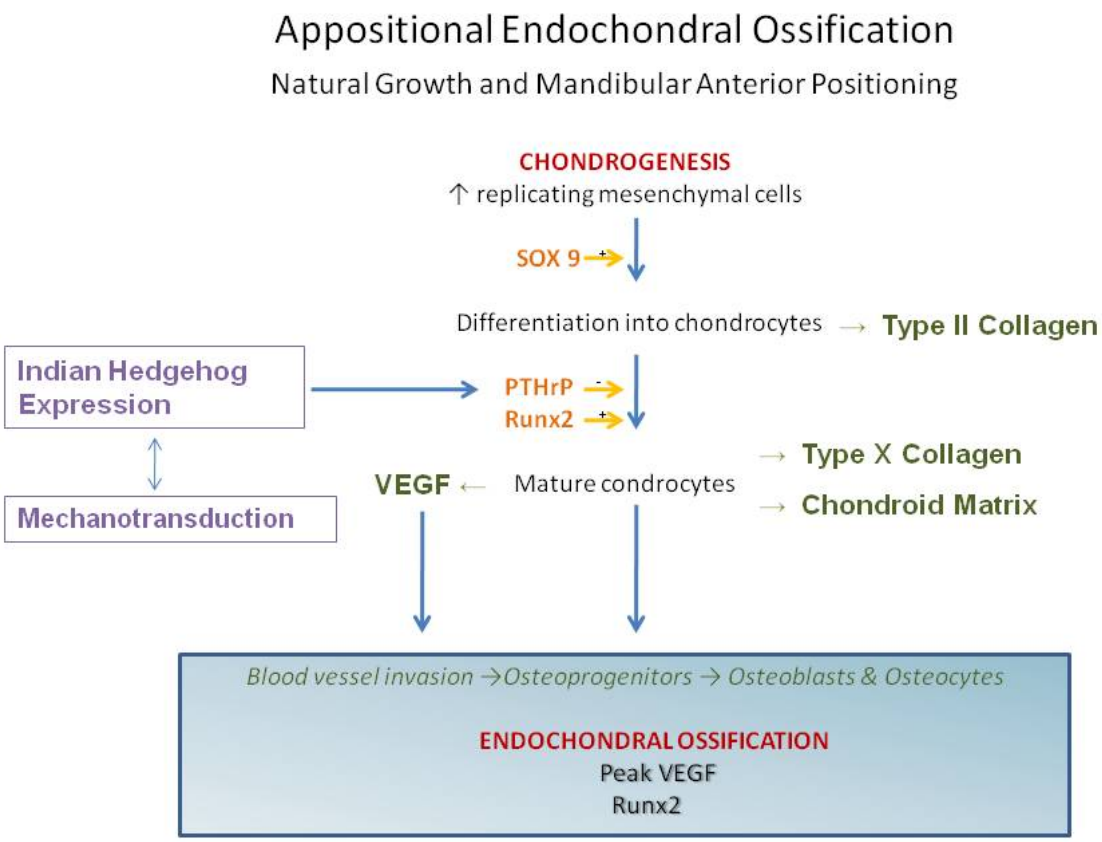

19.3 Appendix 1c

Summary of Studies on mandibular protrusion in rats and factors that control condylar growth and adaption

Author	Aim	Method	Conclusion
Rabie *etal.*[2]	To identify and quantify the temporal sequence of replicating mesenchymal cells during natural growth and mandibular advancement	150, 35 day old female Sprague-Dawley rats; functional appliances were fitted; 60 day duration; time points 3,7,14,21,30,33,37,44,51,60 days; immunohistochemistry (IHC)	The number of mesenchymal cells is genetically controlled and may account for individual response to orthopaedic treatment; up-regulation of mesenchymal cells is seen with mandibular protrusion
Rabie *et al.*[3]	To investigate the temporal expression of SOX9 and collagen II in the glenoid fossa with mandibular protrusion	80, 35 day old female Sprague Dawley rats; functional appliances fitted; duration 17 days; time points 1,3,5,7,9,11,14,17 days; IHC	Chondroid bone formation in the glenoid fossa in response to forward mandibular positioning is regulated by molecular markers indicative of endochondral ossification
Rabie *et al.*[4]	To quantitatively assess the temporal pattern of expression of SOX9, and type II collagen during mandibular protrusion	165, 35 day old female Sprague Dawley rats; 60 day duration; time points 3,7,14,21,30,33,37,44,51,60 days; IHC;	The accelerated and enhanced expression of SOX9 and collagen II during mandibular protrusion compared with natural growth indicates acceleration and enhancement of condylar growth with mandibular protrusion
Rabie *et al.*[5]	To investigate the potential role of PTHrP in natural condylar growth and during mandibular protrusion	100, 35 day old, female Sprague-Dawley rats; functional appliances; 30 day duration; time points 3, 7, 14, 21, 30; IHC;	Higher levels of PTHrP in the mandibular protrusion group was associated with a decreased rate of chondrocyte maturation implicating PTHrp in mandibular adaption to protrusion.
Tang *et al* [6]	To find out whether Ihh is a functional factor that mediates condylar growth in response to mandibular advancement	100, 35 day old, female Sprague-Dawley rats; functional appliances; 30 day duration; time points 3, 7, 14, 21, 30; IHC	Mandibular advancement triggered Ihh expression in condylar cartilage and therefore Ihh acts as a mediator in mechanotransduction that converts mechanical signals resulting from anterior mandibular displacement to stimulate cellular proliferation in condylar cartilage.
Marques *et al.*[7]	To determine if the force applied to the condyle with protrusion appliances exerts its effect on the condylar cartilage via integrins	56, 28 day old, male Wistar rats; 30 day duration; time points 3, 5, 7, 9, 11, 15, 30 days; IHC	Integrins participate in mechanotransduction in response to mandibular protrusion in rats
Tang *et al.*[8]	To determine whether Runx2 (Cbfa-1) is responsible for signalling chondrocyte maturation and endochondral ossification in the condyle during mandibular protrusion	100, 35 day old, female Sprague-Dawley rats; functional appliances; 30 day duration; time points 3, 7, 14, 21, 30; IHC	Runx2 expression is increased in response to mandibular protrusion and results in an expansion of collagen X. Therefore, Runx2 mediates chondrocyte terminal maturation and endochondral

			ossification in the mandibular condyle in response to mandibular advancement
Hajjar *et al.*	To verify the mRNA and protein expression of IGF-I and IGF-II in the condyle during mandibular protrusion	70, 21 day old male Wistar rats; 15 day experimental duration; functional appliance; time points 3, 5, 7, 9, 11, 13, 15; IHC	IGFI and II were both expressed more during functional protrusion and therefore can be implicated in functional adaption of the mandibular condyle
Rabie *et al.*[9]	To identify the temporal sequence of cellular changes in the glenoid fossa and to quantify the amount of bone formation in response to mandibular advancement	100, 35 day old, female Sprague Dawley rats; functional appliances; 30 day duration; time points 3, 7, 14, 21, 30; IHC	Bone formation significantly increased in response to the functional appliance; mandibular protrusion resulted in osteoprogenitor cells being oriented in the direction of pull
Rabie *et al.*[10]	To identify the relationship between vascularisation and bone formation in the glenoid fossa during natural growth and functional appliance therapy	150, 35 day old, female Sprague-Dawley rats; 60 day duration; time points 3,7,14,21,30,33,37,44,51,60 days; IHC	Forward mandibular positioning resulted in significant increases in vascularisation and new bone formation in the glenoid fossa indicated by an increased expression of VEGF
Shen *et al.* [11]	To investigate the expression of type X collagen during natural growth and mandibular protrusion	100, 35 day old, female Sprague Dawley rats; functional appliances; 30 day duration; time points 3, 7, 14, 21, 30; IHC	The temporal expression of collagen X in mandibular protrusion and natural growth is the same. Therefore bite jumping enhances adaptive remodelling of the condyle but does not acceleration bone formation; thinning of the mandibular condylar cartilage with mandibular protrusion occurs as ossification ensues
Shen *et al.*[12]	To evaluate condylar endochondral ossification by monitoring the temporal and spatial expression of type X collagen in forward mandibular positioning and natural growth	100, 35 day old, female Sprague Dawley rats; functional appliances; 30 day duration; time points 3, 7, 14, 21, 30; IHC	Forward mandibular position results in enhanced maturation of condylar chondrocytes resulting in increased synthesis of collagen X.
Rabie *et al.*[13]	To investigate the temporal pattern of expression of VEGF and new bone formation in the condyle during forward mandibular positioning	150, 35 day old, female Sprague-Dawley rats; 60 day duration; time points 3,7,14,21,30,33,37,44,51,60 days; IHC	Mandibular advancement solicited a sequence of events that resulted in significant increase in both vascularisation and mandibular formation resulting enhanced condylar growth
Chayanupatkul *et al.* [14]	To monitor the amount of bone formed after early and late appliance removal, and compare it to natural growth	130, 35 day old, female, Sprague-Dawley rats; functional appliances. Early removal = 30 days; late removal = 44 days; duration 60 days; time pints 3,7,14,21,30,33,37,44,60	Early appliance removal results in sub-normal growth of the posterior condyle but not the glenoid fossa; increasing the amount of time of mandibular advancement secures normal levels of mandibular growth in the post treatment period.

19.4 Appendix 1d

Functional Appliances - Randomised Control Trials

Author & Year	Aims / Objectives	Experimental design	Results and conclusions
RCT			
Webster 1996 Otago[15]	RCT 42 patients Criteria; Class II div 1 Ages 11.53, 11.70 and 11.70 yrs for Frankel, Activator and control groups respectively.	Frankel 18mths Harvold activator 18 mths Control	0.44^0,0.75^0 , 0.66^0 change in B point with Frankel, Activator and control respectively Although mandibular length increased significantly in treatment group, when compared to controls there was no evidence of treatment success.
Tulloch 1997 University of North Carolina [16]	RCT 166 patients Criteria ≥ 7mm overjet. Aged 9.9 yrs (7.7-12.4)	Bionator Headgear or Control. Duration 15mths	HG: 0.92mm change on A point, 0.15mm on B point. Bionator: 0.11mm Δ A-point, 1.07mm Δ B-point. Control: 0.26mm Δ A-point, 0.43mm B-point. Headgear had greater effect on maxilla, Bionator had greater effect on mandible. Differences between treatment and control groups were small.
Keeling 1998 University of Florida [17]	RCT 249 patients Criteria: Class II molars including subdivisions. Aged 9.6yrs ± 0.8yr	Bionator or Headgear and Plate or Control Treatment continued until Class I achieved or two years of Tx.	No difference between groups on Maxillary changes. Bionator and Headgear both significantly affected anterior mandibular growth over controls. Similar skeletal response between HG and Bionator, they did not affect maxillary growth but both enhanced mandibular anterior growth. More dental response with headgear, however more relapse in dental with headgear group.
Ghafari 1998 University of Pennsylvania [18]	*RCT* 63 patients. Criteria: Class II molars, ANB $>4.5^0$ Aged 7yr 4mo- 13yr 4mo.	Frankel Headgear (Straight pull) No controls Duration: Neutrocclusion of Class I achieved.	HG: -3.14^0 Δ on A-point, -0.55^0 in B point. Frankel: 0.15^0Δ on A-point, 1.44^0 in B-point. Headgear has a distalising effect on the maxilla and the molars. Frankel affects the forward growth of the mandible and proclination of lower incisors.
O'Brien 2003 University of Manchester (*Multi-centre Study*)[19]	*RCT* 174 patients. Aged 8-10yrs Criteria: Class II div I	Twin Block Control Duration 15 mths	TB: 0.57mm Δ on A-point, 3.52mm Δ on B-point Control: 1.45mm Δ on A point, 2.52 Δ on B point. Functional appliance treatment does not influence Class II pattern to a clinically significant degree.

19.5 Appendix 1e

Additional findings from the investigation by Fritton et al.[20] regarding Strain History from section 5.2.1.5.2

In addition to the findings discussed in 5.2.1.5.2, the results also showed that the 5 second spectra averaged over 12 hours for each bone illustrates that the average strain over a day is quite low in magnitude. The strain magnitude was seen to exhibit a power-law relationship with the frequency, that is, $1/f^{\alpha}$, where α is a constant and different in each animal and represented as the slope on the strain-frequency graph.

An unexpected finding in this study was that the recorded strain magnitudes exhibited similar characteristics on different time scales, a concept known as 'self similarity' [20]. A self similar object is exactly or approximately similar to a part of itself, or in other words, each part of the whole object is a reduced size copy of the whole [21]. In this study, the strain-time graph looks similar across 2 minutes as it does across 20 seconds and across 3 seconds. The property of self similarity along with the power-law relationship between strain magnitude and load frequency suggests that strain dynamics in bone may reflect a self-organised critical system. This is a dynamic system that has evolved into a barely stable state and depends on weak interactions of many small events, typically demonstrating the 1/f type distribution and is seen in many other physiological systems such as body sway, eyeball motion, speech, blood pressure and heart rate.

McLeod *et al.* in 1998 [22] hypothesised that bone exhibited the property of self similarity and described a paradigm shift in bone development and adaption from the telelogic theory to the dystelelogic theory. The telelogic paradigm is an assumption that states the skeleton has adopted the most optimal design as part of the evolutionary concept and consequently bone was likened to that of an engineering material. The dynamic nature of bone which inherently makes it different from a static engineering material is cause for rejection of this paradigm. The new paradigm of

skeletal morphology and adaption is consistent with current advances in theoretical biology which suggest that the process of development can occur 'without a plan' that is in a dysteleologic manner with special focus on the ability of organisms to self organise. Formerly growth, development and attainment of complexity were thought to be driven genetically towards attainment of optimal structure. Under the new paradigm, the process of self organisation is believed to be governed by epigenetic factors occurring at the microscopic cellular level whereby morphological complexity is spontaneously attainted in response to repetitive application of simple rules of organisation. At the microscopic level, the assembly process is dominated by small but persistent stimuli. The persistent environmental stimuli are therefore influential at the cellular level in developing the macroscopic form of the skeletal structure. McLeod [22] highlights that persistent physical stresses can take the form of dynamic mechanical stresses, hydrodynamic stresses and electrochemical stresses.

19.6 Appendix 1f

Bone Morphometric Parameters (Adopted from Skyscan N.V., Aartselaar, Belgium)

Morphometric parameters are calculated by CT-analyser either in direct 3D based on a surface-rendered volume model, or in 2D from individual binarised crossection images.

All calculations are performed over a selected region called the region of interest. Consistent and accurate selection of the regions or volumes of interest is fundamentally important to obtaining accurate and meaningful data.

Parameter names follow two alternative nomenclatures, “General Scientific” or “Bone ASBMR”, the latter based on Parfitt *et al.* [23] Parfitt’s paper proposed a system of symbols for bone histomorphometry, and the principles of Parfitt’s system are applied here to both the Bone (ASBMR) and the General Scientific parameter names.

Within Skyscan CT-analyser four alternative dimensional units are selectable: mm, µm, inch or pixel.

Nomenclature	General Scientific	Bone ASBMR
Parameter name	Total VOI volume	Tissue Volume
Parameter symbol	TV	TV
Unit	mm3	mm3

Total volume of the volume-of-interest (VOI). The 3D volume measurement is based on the marching cubes volume model of the VOI. Please note that in the case of Bone ASBMR nomenclature, the word “tissue” simply refers to the volume of interest. It does not mean any kind of recognition of any particular density range as biological tissue, soft, hard or otherwise.

Nomenclature	General Scientific	Bone ASBMR
Parameter name	Object volume	Bone volume
Parameter symbol	Obj.V	BV
Unit	mm3	mm3

Total volume of binarised objects within the VOI. The 3D volume measurement is based on the marching cubes volume model of the binarised objects within the VOI.

Nomenclature	General Scientific	Bone ASBMR
Parameter name	Percent object volume	Percent bone volume
Parameter symbol	Obj.V/TV	BV/TV
Unit	%	%

The proportion of the VOI occupied by binarised solid objects. This parameter is only relevant if the studied volume is fully contained within a well-defined biphasic region of solid and space, such as a trabecular bone region, and does not for example extend into or beyond the boundary of the object – such as the cortical boundary of a bone sample. The meaningfulness of measured percent volume depends on the criteria applied in selecting the volume of interest. Where the ROI / VOI boundaries are loosely drawn in the surrounding space around an object for instance, then % object volume has no meaning.

Nomenclature	General Scientific	Bone ASBMR
Parameter name	VOI surface	Tissue surface
Parameter symbol	TS	TS
Unit	mm2	mm2

The surface area of the volume of interest, measured in 3D (Marching cubes method).

Nomenclature	General Scientific	Bone ASBMR
Parameter name	Object surface	Bone surface
Parameter symbol	Obj.S	BS
Unit	mm2	mm2

The surface area of all the solid objects within the VOI, measured in 3D (Marching cubes method).

Nomenclature	General Scientific	Bone ASBMR
Parameter name	Object surface / volume ratio	Bone surface / volume ratio
Parameter symbol	Obj.S/Obj.V	BS/BV
Unit	mm-1	mm-1

The ratio of solid surface to volume measured in 3D within the VOI. Surface to volume ratio or "specific surface" is a useful basic parameter for characterising the thickness and complexity of structures.

Nomenclature	General Scientific	Bone ASBMR
Parameter name	Object surface density	Bone surface density
Parameter symbol	Obj.S/TV	BS/TV
Unit	mm-1	mm-1

The ratio of surface area to total volume measured as described above in 3D, within the VOI.

Nomenclature	General Scientific	Bone ASBMR
Parameter name	Fragmentation index	Trabecular bone pattern factor
Parameter symbol	Fr.I	Tb.Pf
Unit	mm-1	mm-1

This is an inverse index of connectivity, which was developed and defined by Hahn *et al.*[24] for application to trabecular bone. It was applied by these authors originally to 2D images of trabecular bone, and calculates an index of relative convexity or concavity of the total bone surface, on the principle that concavity indicates connectivity (and the presence of "nodes"), and convexity indicates isolated disconnected structures (struts). Tb.Pf is calculated in 3D, by comparing volume and surface of binarised solid before and after a single voxel image dilation. It is defined:

$$Tb.Pf = \left(\frac{S_1 - S_2}{V_1 - V_2} \right)$$

Where S and V are solid surface and volume, and the subscript numbers 1 and 2 indicate before and after image dilation.

Where structural / trabecular connectedness results in enclosed marrow spaces, then dilation of trabecular surfaces will contract the surface. By contrast, open ends or nodes will have their surface expanded by surface dilation. As a result, lower Tb.Pf signifies better connected trabecular lattices while higher Tb.Pf means a more disconnected trabecular structure. A prevalence of enclosed cavities and concave surfaces can push Tb.Pf to negative values – as with the structure model index (SMI) – see below. This parameter Tb.Pf or fragmentation index is best considered as a relative index for comparing different scanned objects; its absolute value does not have much meaning.

Nomenclature	General Scientific	Bone ASBMR
Parameter name	Structure model index	Structure model index
Parameter symbol	SMI	SMI
Unit	(none)	(none)

Structure model index indicates the relative prevalence of rods and plates in a 3D structure such as trabecular bone. SMI involves a measurement of surface convexity. This parameter is of importance in osteoporotic degradation of trabecular bone which is characterised by a transition from plate-like to rod-like architecture. An ideal plate, cylinder and sphere have SMI values of 0, 3 and 4 respectively.

The calculation of SMI is based on dilation of the 3D voxel model, that is, artificially adding one voxel thickness to all binarised object surfaces (Hildebrand *et al.* 1997b). This is also the basis of the Tb.Pf parameter (see above) which explains why changes in both parameters correlate very closely with each other. SMI is derived as follows:

$$SMI = 6x \ (\underline{S'xV} \ / \ S^2)$$

where S is the object surface area before dilation and S' is the change in surface area caused by dilation. V is the initial, undilated object volume.

It should be noted that concave surfaces of enclosed cavities represent negative convexity to the SMI parameter, since dilation of an enclosed space will reduce surface area causing S' to be negative. Therefore regions of bone containing a prevalence of enclosed cavities – such as regions with relative volume above 50% – can have negative SMI values. As a consequence, the SMI parameter is sensitive to relative volume, and this can accentuate differences between experimental groups in the measured SMI value.

Nomenclature	General Scientific	Bone ASBMR
Parameter name	Structure thickness	Trabecular thickness
Parameter symbol	St.Th	Tb.Th
Unit	mm	mm

With 3D image analysis by micro-CT a true 3D thickness can be measured which is model-independent. Local thickness for a point in solid is defined by Hildebrand and Ruegsegger (1997a) as the diameter of the largest sphere which fulfils two conditions:

the sphere encloses the point (but the point is not necessarily the centre of the sphere);

the sphere is entirely bounded within the solid surfaces.

The key advantage of the local thickness measurement is that the bias from the 3D orientation of the structure is kept to a minimum[25].

Distance transform methods described by Remy and Thiel[26] are the basis for the implementation by CT-analyser of local thickness measurement. The method starts with a "skeletonisation" identifying

the medial axes of all structures. Then the "sphere-fitting" local thickness measurement is made for all the voxels lying along this axis.

Histomorphometrists typically measure a single mean value of bone Tb.Th from a trabecular bone site. However a trabecular bone volume – or any complex biphasic object region – can also be characterised by a distribution of thicknesses. CT-analyser outputs a histogram of thickness (and separation also) with an interval of two pixels. Thickness distribution is a powerful method for characterising the shape of a complex structure.

Nomenclature	General Scientific	Bone ASBMR
Parameter name	Structure linear density	Trabecular number
Parameter symbol	St.Li.Dn	Tb.N
Unit	mm-1	mm-1

Structure linear density or trabecular number implies the number of traversals across a trabecular or solid structure made per unit length on a random linear path through the VOI.

Again the complexities of model dependence associated with 2D measurements are eliminated by true 3D calculation of St.Li.Dn / Tb.N from 3D micro-CT images. This parameter is measured in CT-analyser in 3D by application of the equation for the parallel plate model (fractional volume/thickness), but using a direct 3D measurement of thickness. Note that the optional stereology analysis (not included in this report) includes measurements of thickness, separation and number/linear density based on the mean intercept length (MIL) analysis which represents an alternative basis for these architectural measurements.

Furthermore, another alternative definition of trabecular number, based on 3D measurements of the spacing of trabeculae, is:

$$Tb.N = \frac{1}{(Tb.Th + Tb.Sp)}$$

Since both Tb.Th and Tb.Sp are measured in 3D by sphere-fitting, this latter equation could be considered a calculation directly from a 3D-measured trabecular spacing.

Nomenclature	General Scientific	Bone ASBMR
Parameter name	Structure separation	Trabecular separation
Parameter symbol	Sr.Sp	Tb.Sp
Unit	mm	mm

Trabecular separation is essentially the thickness of the spaces as defined by binarisation within the VOI. Skyscan CT-analyser software measures Tb.Sp directly and model-independently in 3D by the same method used to measure trabecular thickness (see above), just applied to the space rather than the solid voxels.

20 Appendix 2 Manuscript

20.1 Appendix 2a

Whole body vibration (Juvent®™ *Inc, New Jersy, USA)* platforms with the rats in cages

20.2 Appendix 2b

Dynamic Weighing Scales (OHAUS™ Explorer® Proanalytical Precision Balance, *Victoria Australia*)

20.3

20.4

20.5

20.6 Appendix 2c

Post mortem photographs and radiographs

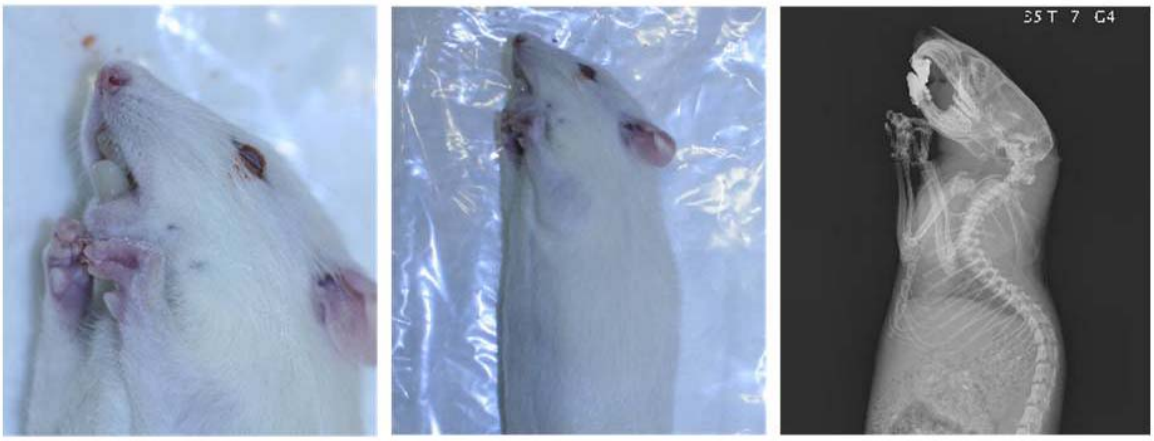

20.7 Appendix 2d

Specimens following preparation

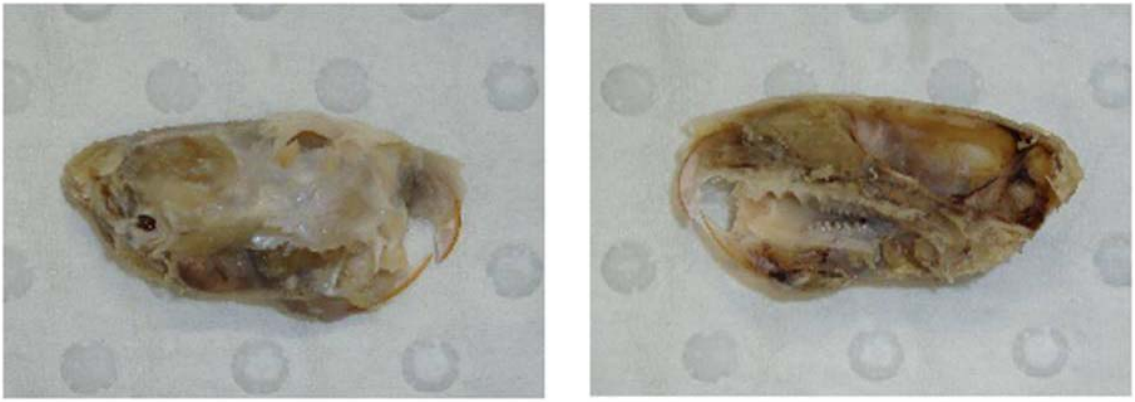

20.8

20.9 Appendix 2e

Scyscan 1172 X-ray microtomograph (SkyScan, *Aartselaar, Belgium*); Jig for the specimen; specimen in the Skyscan

20.10

20.11 Appendix 2f – description of box plot

With respect to the box plot, the bottom and top of the box represent the 25th and 75th percentiles respectively, with the box therefore containing the middle 50% of the results. The line inside the box shows the 50th percentile, or median and the ends of the whiskers represent the maximum and minimum values. The box plot also indicates which observations, if any, are outliers.

21.1 Appendix References

1. Shen G, Darendeliler, M. The Adaptive remodelling of condylar cartilage – A transition from Chrondrogenesis to Osteogenesis. Journal of Dental Research 2005;84.
2. Rabie AB, Wong, L., Tsai, M. Replicating mesenchymal cells in the condyle and the glenoid fossa during mandibular forward positioning. Am J Orthod Dentofacial Orthop. 2003;123:49-57.
3. Rabie AB, She TT, Harley VR, Rabie ABM. Forward mandibular positioning up-regulates SOX9 and type II collagen expression in the glenoid fossa. Journal of Dental Research 2003;82:725-730.
4. Rabie AB, Hagg, U. Factors regulating mandibular condylar growth. Am J Orthod Dentofacial Orthop 2002;122:401-409.
5. Rabie AB, Tang, G.H., Xiong, H., Hagg, U. PTHrp regulates chondrocyte matuation in condylar cartilage. J Dent Res 2003;82:627-631.
6. Tang GH, Rabie AB, Hagg U, Rabie ABM. Indian hedgehog: a mechanotransduction mediator in condylar cartilage. Journal of Dental Research 2004;83:434-438.
7. Marques MR, Hajjar D, Franchini KG, Moriscot AS, Santos MF, Marques MR et al. Mandibular appliance modulates condylar growth through integrins. Journal of Dental Research 2008;87:153-158.
8. Tang GH, Rabie AB, Rabie ABM. Runx2 regulates endochondral ossification in condyle during mandibular advancement. Journal of Dental Research 2005;84:166-171.
9. Rabie AB, Zhao, Z., Shen, G., Hagg, E.U., Robinson, W. Osteogenesis in the glenoid fossa in response to mandibular advancement Am J Orthod Dentofacial Orthop 2001;119:390-400.
10. Rabie AB, Shum L, Chayanupatkul A, Rabie ABM, Shum L, Chayanupatkul A. VEGF and bone formation in the glenoid fossa during forward mandibular positioning. American Journal of Orthodontics & Dentofacial Orthopedics 2002;122:202-209.
11. Shen G, Zhao, Z., Kaluarachchi, K., Rabie, B.A. Expression of type X collagen and capillary endothelium in condylar cartilage during osteogenic transition--a comparison between adaptive remodelling and natural growth. Eur J Orthod 2006;28:210-216.
12. Shen G, Rabie, A.B., Zhao, Z.H., Kaluarachchi, K. Forward deviation of the mandibular condyle enhances endochondral ossification of condylar cartilage indicated by increased expression of type X collagen. Arch Oral Biol. . 2006;51:315-324.
13. Rabie AB, Leung, F.Y., Chayanupatkul, A., Hagg, U. The correlation between neovascularization and bone formation in the condyle during forward mandibular positioning. Angle Orthod. 2002;72:431-438.
14. Chayanupatkul A, Rabie, A.B., Hagg ,U. Temporomandibular response to early and late removal of bite-jumping devices. Eur J Orthod. 2003;25:465-470.
15. Webster T, Harkness, M., Herbison, P. Associations between changes in selevted facial dimensions and the outcome of orthodontic treatment. Am J Orthod Dentofacial Orthop 1996;110:46-53.
16. Tulloch JF, Phillips, C., Koch, G., Proffit, W.R. The effect of early intervention on skeletal pattern in Class II malocclusion: a randomized clinical trial. Am J Orthod Dentofacial Orthop. 1997;111:391-400.
17. Keeling SD, Wheeler, T.T., King, G.J. Anteroposterior skeletal and dental changes after early Class II treatment with bionators and headgear. Am J Orthod Dentofacial Orthop 1998;113.
18. Ghafari J, Schofer, F.S., Hunt-Jacobsson, U. Headgear versus functional regulator in the ealy treatment of Class II, Division I malocclusion: a randomized clinical study Am J Orthod Dentofacial Orthop 1998;113:51-61.
19. O'Brien K, Wright J, Conboy F, Chadwick S, Connolly I, Cook P et al. Effectiveness of early treatment with the Twin-block appliance: a multi-center, randomized, controlled trial. Part 1: dental and skeletal effects Am J Orthod Dentofacial Orthop 2003;124:234-243.

20. Fritton SP, McLeod KJ, Rubin CT. Quantifying the strain history of bone: spatial uniformity and self-similarity of low-magnitude strains. Journal of Biomechanics 2000;33:317-325.
21. Mandelbrot B. The Fractal Geometry of Nature: Freeman and Company; 1982.
22. McLeod KJ, Rubin CT, Otter MW, Qin YX. Skeletal cell stresses and bone adaptation. American Journal of the Medical Sciences 1998;316:176-183.
23. Parfitt A, Drezner M, Glorieux F, Kanis J, Malluche H, Meunier P et al. Bone Histomorphometry: Standardisation of nomenclature, symbols and units. Journal of Bone and Mineral Res 1987;2:595-610.
24. Hahn M, Vogel M, Pompesius-Kempa M, Delling G. Trabecular bone pattern factor - a new parameter for simple quantification of bone microarchitecture. Bone 1992;13:327-330.
25. Ulrich D, Rietbergen Bv, Laib A, Rüegsegger P. The ability of three-dimensional structural indices to reflect mechanical aspects of trabecular bone. Bone 1999;25:55-60.
26. Remy E, Thiel E. Medial axis for chamfer distances: computing look-up tables and neighbourhoods in 2D or 3D.
. Pattern Recognition Letters 2002;23:649-661.

21.2 Future Directions

Whilst conclusive results have been reached from this study, further investigations on this topic may include:

- Histological examination of the left condyles to determine the true nature of the resorption at the anterior aspects of the condyle and the possibility of new bone formation at the posterior condyle represented by the radiopaque band seen on the micro-CT images
- Histological examination of the bone resorption in the glenoid fossa
- Repetition of the experiment of longer duration to assess the possibility of repair of the areas of resorption with and without FA removal over time and the pattern of relapse and stability following functional appliance removal
- Cephalometric radiographic examination of the entire mandible to further clarify the change in condylar morphology and the impact this may have on supplementary mandibular lengthening in response to the functional appliance and therefore class II correction. The experimental protocol could be adopted from previous studies [15,99]
- Examination of the bone quality using morphometric analysis in the anterior and posterior part of the condyle to determine if there is a difference in bone quality closer to and further from the site of resorption. This may clarify the nature of the resorption at the anterior aspect of the condyle and the likelihood of bone formation at the posterior aspect of the condyle where the cartilage remained intact.
- Repeat the experiment altering the design of the functional appliance to less protrusive position to decrease loading of the TMJ in order to examine the effect of functional appliance therapy with vibration in the absence of severe bone resorption